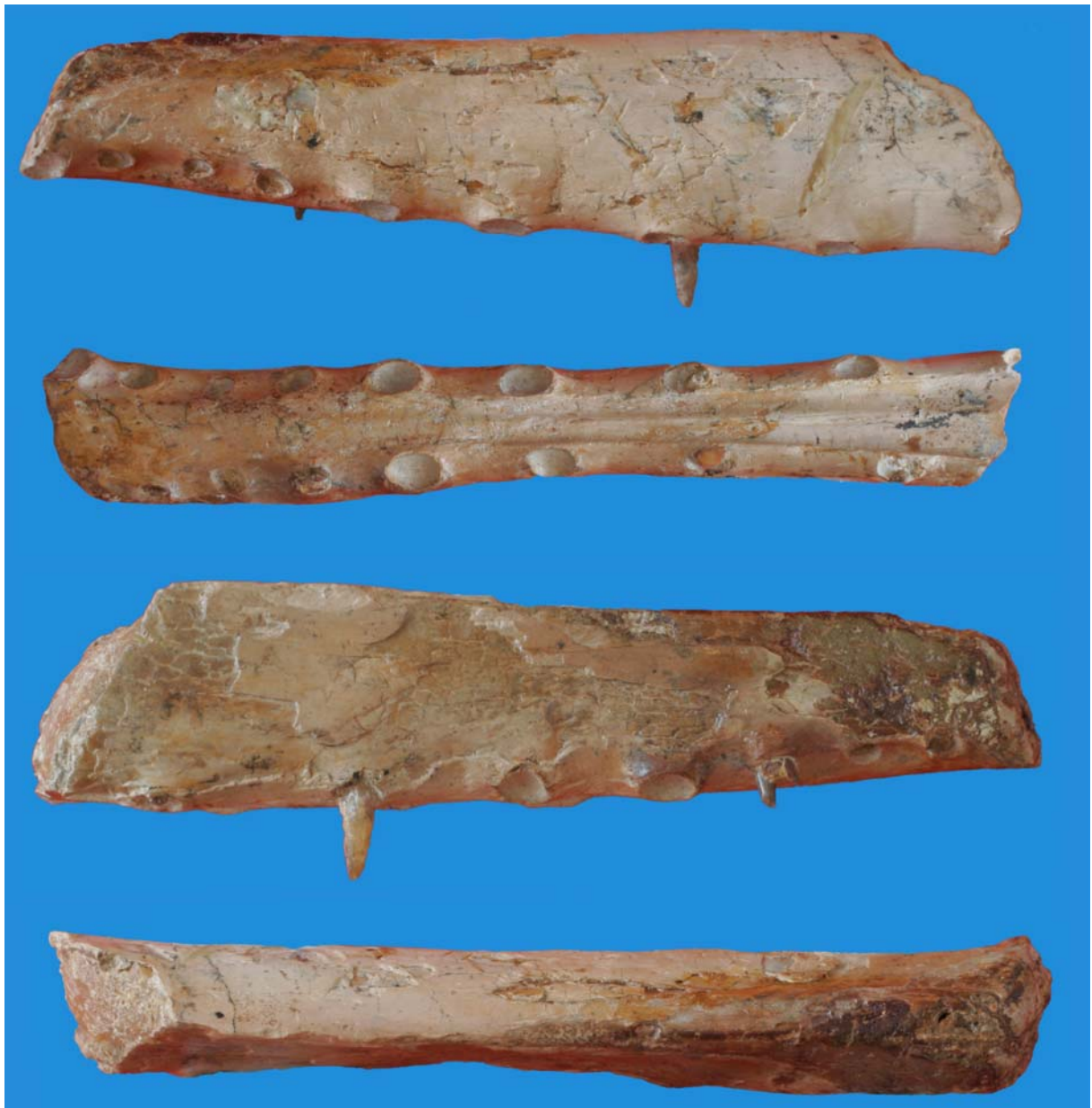


**Toothed pterosaurs from the Santana Formation
(Cretaceous; Aptian–Albian) of northeastern Brazil.
A reappraisal on the basis of newly described
material**

André J. Veldmeijer



Courtesy of the BSP, Munich (photographs by A. 't Hooft)

Toothed pterosaurs from the Santana Formation (Cretaceous; Aptian-Albian) of northeastern Brazil. A reappraisal on the basis of newly described material

Tand-pterosauriërs uit de Santana Formatie (Krijt; Aptian-Albian) van noordoost Brazilië. Een herwaardering op basis van nieuw beschreven materiaal

(met een samenvatting in het Nederlands)

Proefschrift

ter verkrijging van de graad van doctor aan de Universiteit Utrecht
op gezag van de Rector Magnificus, Prof. dr. W.H. Gispen,
ingevolge het besluit van het College voor Promoties
in het openbaar het verdedigen
op maandag 30 januari 2006 des middags te 2.30 uur

door

André Jacques Veldmeijer
geboren op 13 april 1969
te Vlissingen

promoter: Prof. dr. J.W.F. Reumer
Faculty of Geosciences,
Utrecht University
Utrecht, The Netherlands
&
Natuurhistorisch Museum Rotterdam
Rotterdam, The Netherlands

co-promotor: Dr. J. de Vos
Conservator Fossiele Macrovertebraten
Nationaal Natuurhistorisch Museum – Naturalis
Leiden, The Netherlands

In honour of my parents:

Antje Veldmeijer-Wagt (1940-1988)

Marten Veldmeijer

Contents

1.	Introduction	10
1.1.	Appendix	154
1.1.1.	Figures and plates	154
2.	Description of <i>Coloborhynchus spielbergi</i> sp. nov. (Pterodactyloidea) from the Albian (Lower Cretaceous) of Brazil	12
2.1.	Introduction	12
2.2.	Material	12
2.2.1.	Description of nodules	13
2.2.2.	Description of the preservation after preparation	13
2.3.	Abbreviations	15
2.3.1.	Institutions	15
2.3.2.	Figures	15
2.4.	Systematic palaeontology, description and comparison	17
2.4.1.	Cranial skeleton	18
2.4.2.	Axial skeleton	30
2.4.3.	Pectoral girdle and forelimb	33
2.4.4.	Pelvic girdle and hind limb	37
2.5.	Discussion and conclusion	39
2.6.	Reconstruction	43
2.7.	Appendix	156
2.7.1.	Measurements	156
2.7.2.	Figures and plates	163
2.7.3.	Scanning a pterosaur skull; supplement to the description of <i>Coloborhynchus spielbergi</i> in Scripta Geologica, 2003, 125: 37–139	200
3.	Pterosaurs from the Lower Cretaceous of Brazil in the Stuttgart Collection (and supplement)	46
3.1.	Introduction	46
3.2.	Abbreviations	46
3.3.	Systematic palaeontology, description and comparison	46
3.3.1.	Mandible SMNS 56994	47
3.3.2.	Isolated humeri SMNS 55407, 55408, 55409, 55883	49
3.3.3.	Isolated ulnae and radii SMNS 55410, 55411, 55413, 82001	53
3.3.4.	Associated humerus and ulna/radius SMNS 81976	56
3.3.5.	Phalanges of wing finger SMNS 55412, 55415	57
3.3.6.	Partial front extremity SMNS 80437	58
3.4.	Concluding remarks	59
3.5.	Appendix	204
3.5.1.	Measurements	204
3.5.2.	Figures and plates	205
4.	Description of two pterosaurs (Pterodactyloidea) mandibles from the Lower Cretaceous Santana Formation, Brazil	61
4.1.	Introduction	61
4.2.	Abbreviations	61
4.3.	Systematic palaeontology, description and comparison SAO 251093	61

4.3.1.	General	62
4.3.2.	Description	62
4.3.3.	Comparison and discussion	63
4.4.	Systematic palaeontology, description and comparison SAO 200602	65
4.4.1.	General	65
4.4.2.	Description	65
4.4.3.	Comparison and discussion	67
4.5.	Appendix	216
4.5.1.	Measurements	216
4.5.2.	Figures and plates	217
5.	Preliminary description of a skull and wing of a Brazilian Cretaceous (Santana Formation; Aptian–Albian) pterosaur (Pterodactyloidea) in the collection of the AMNH	70
5.1.	Introduction	70
5.2.	Abbreviations	70
5.3.	Preservation	70
5.4.	Systematic palaeontology and description	71
5.4.1.	Cranial skeleton	72
5.4.2.	Post–cranial skeleton	73
5.5.	Comparison and discussion	73
5.6.	Appendix	230
5.6.1.	Measurements	230
5.6.2.	Figures and plates	232
6.	Description of pterosaurian (Pterodactyloidea) remains from the Lower Cretaceous of Brazil in various German collections	75
6.1.	Introduction	75
6.2.	Abbreviations	75
6.3.	The <i>Brasileodactylus</i> mandible SMNS 55414	75
6.3.1.	Preservation	75
6.3.2.	Systematic palaeontology and description	76
6.3.3.	Comparison and discussion	77
6.4.	The partial skeleton of <i>Brasileodactylus</i> in the Munich collection	78
6.4.1.	Preservation	78
6.4.2.	Systematic palaeontology, description and comparison	79
6.5.	Final remarks	89
6.6.	Appendix	236
6.6.1.	Measurements	236
6.6.2.	Figures and plates	238
7.	Updating the toothed taxa	91
7.1.	<i>Brasileodactylus</i> (Pterosauria, Pterodactyloidea, Anhangueridae); an update	91
7.1.1.	Introduction	91
7.1.2.	The known specimens	91
7.1.3.	Diastemae	95
7.2.	<i>Coloborhynchus</i> from the Lower Cretaceous Santana Formation, Brazil (Pterosauria, Pterodactyloidea, Anhangueridae); an update	95
7.2.1.	Introduction	95

7.2.2.	The known specimens	95
7.2.3.	Diastemae	100
7.3.	<i>Anhanguera</i> from the Lower Cretaceous Santana Formation, Brazil (Pterosauria, Pterodactyloidea, Anhangueridae); an update	100
7.3.1.	Introduction	100
7.3.2.	The known specimens	100
7.3.3.	Diastemae	103
7.4.	<i>Criorhynchus</i> from the Lower Cretaceous Santana Formation, Brazil (Pterosauria, Pterodactyloidea, Anhangueridae); an update	103
7.4.1.	Introduction	103
7.4.2.	The known specimens	104
7.4.3.	Diastemae	105
7.5.	Discussion	106
7.6.	Appendix	254
7.6.1.	Figures and plates	254
8.	Final remarks	108
8.1.	Ornithocheiridae versus Anhangueridae	108
8.2.	The <i>Brasileodactylus</i> -problem	108
8.3.	Appendix	268
8.3.1.	Figures and plates	268
9.	Acknowledgements	110
10.	Cited literature	111
11.	General appendix	117
11.1.	Additional data chapter 7	117
11.1.1.	Measurements dentition	117
11.1.2.	Individual graphs dentition taxon <i>Brasileodactylus</i>	124
11.1.3.	Individual graphs dentition taxon <i>Coloborhynchus</i>	130
11.1.4.	Individual graphs dentition taxon <i>Anhanguera</i>	140
11.1.5.	Individual graphs dentition taxon <i>Criorhynchus</i>	144
12.	Notes	147
	Samenvatting	149
	Summary	150
	Curriculum Vitae	151
	Appendices to the chapters:	
	Chapter 1	153
	Chapter 2	155
	Chapter 3	203
	Chapter 4	215
	Chapter 5	229
	Chapter 6	235
	Chapter 7	253
	Chapter 8	267

1. Introduction

Campos & Kellner (1985b) related that references to flying reptiles from Brazil (not from the Araripe Basin) were made as early as the 19th century, but the first find from Chapada do Araripe was described as late as the 1970s (Price, 1971, post-cranial remains of *Araripesaurus castilhoi*). Wellnhofer (1977) published the description of a phalanx of a wing finger of a pterosaur from the Santana Formation and named it *Araripedactylus dehmi*. Since then, much has been published on the pterosaurs from Brazil, and there has been an increasing interest in the material from this area, resulting in an increase in scientific interest in pterosaurs in general.

The plateau of the Araripe Basin, in northeast Brazil on the boundaries of Piauí, Ceará and Pernambuco (figure 1.1) was already famous for its well preserved fossils, especially fish (e.g. Maisey, 1991), long before the area became the most important source of Cretaceous pterosaur fossils. At present, it is the most important area for Cretaceous pterosaurs globally, although an increasing number of finds are reported from China (e.g. Lü & Ji, 2005; Wang & Lü, 2001 and Wang & Zhou, 2003). Some of the Brazilian material is severely compacted (Crato Formation; Frey & Martill, 1994; Frey *et al.*, 2003a, b; Sayão & Kellner, 2000) and preserved on a laminated limestone comparable to that of Solnhofen. (The type locality of most, if not all, pterosaur fossils from the Araripe Basin is uncertain, because no systematic, scientifically based excavations or even surveys have been done in this area. In stead, the fossils are obtained from the local people. For the geological setting of the Araripe Basin, the reader is referred to Beurlen (1971), De Buissonjé (1980); Kellner & Tomida (2000); Martill *et al.* (1993); Maisey (1991); Pons *et al.* (1990); Wellnhofer (1977, 1985) and Wellnhofer *et al.* (1983). Fossils in nodules are typical for the Rornualdo Member of the Santana Formation [Martill, pers. com.]).

However, many pterosaur fossils from Brazil are preserved as three-dimensional parts of skeletons (e.g. De Buissonjé, 1980; Campos & Kellner, 1985a, b, 1997; Dalla Vecchia, 1993; Dalla Vecchia & Ligabue, 1993; Fastnacht, 2001; Kellner, 1984, 1995a, 1996a; Kellner & Campos, 1989, 1994; Kellner & Hasegawa, 1993; Leonardi & Borgomanero, 1985, 1987; Martill & Frey, 1999; Price, 1971; Veldmeijer, 2002; Wellnhofer, 1977, 1985, 1987, 1991b; Wellnhofer & Kellner, 1991; Wellnhofer *et al.*, 1983), or almost complete skeletons (Kellner & Tomida, 2000; Veldmeijer, 2003a; Wellnhofer, 1985, 1991b). Apart from descriptions palaeobiological studies of Brazilian pterosaurs include those of Bennett (1990, functional morphology; 1992, sexual dimorphism; 1993, ontogeny), Campos *et al.*, (1984, soft tissue), Frey & Martill (1998, ontogeny), Frey *et al.*, 2003c; Kellner (1994a, soft tissue; 1994b, paleoecology; 1995b, 1996b, phylogeny; 1996c, soft tissue), Kellner & Tomida (1996, phylogeny), Martill & Frey (1998, diversity), Martill & Unwin (1989, soft tissue) and Wellnhofer (1988, functional morphology).

The increasing interest however, has not lead to much more clarity in the systematics of the prehistoric animals. The Brazilian toothed taxa are linked with the pterosaurs from the Cambridge Greensands, Cambridge, England, which include two type species (*Coloborhynchus* and *Criorhynchus*). The material however, is extremely fragmented and the systematics is much complicated and discussed (see Unwin, 2001 for an exhaustive list of publications concerning this material). Even the most recent evaluation (*ibidem*) does not enlighten the situation much.

The material presented here (*Coloborhynchus* in chapter 2; *Criorhynchus* in chapter 3; *Thalassodromeus* and *Anhanguera* in chapter 4; *Brasileodactylus* in chapter 5 and 6) not always proved to be a new species (only in the case of *Coloborhynchus*, a new species could be assigned). Nevertheless, the evaluation of this previously unpublished material as well as

the first hand study of most of the published fossils, has resulted, not only in alternative systematics, differing from the systematics advocated by Kellner (for example Kellner & Tomida, 2000) and Unwin (for example Unwin, 2001), but also in the creation of more detailed diagnoses. Does this however mean that problems have been solved now? Far from that. It is striking that systematic palaeontology is often based on very small pieces (the material from the Cambridge Greensands is particularly notorious, but quite a few holotypes from Brazil are only small fragments too whereas almost complete specimens are hitherto unpublished), partially prepared specimens (*Th. sethi* for example), specimens collected over long period of time (again *Th. sethi*) and so forth. Fossils, seemingly belonging to already existing taxa cannot rely on much interest even though these specimens might be much more complete than the holotypes. This is unfortunate, as the present work shows, because not only will it result in more detailed and reliable diagnoses (which, in turn, will increase the reliability of the phylogenetic studies), but also statistic studies increase in reliability.

For obvious reasons, first hand study of material is inevitable. But despite the fact that material in collections should be available for study, this is unfortunately not always the case, either because of unwillingness of people in charge or some other, often unclear reason (for instance closed down institutes or institutes which do not exist [yet]). Fortunately, some institutes already started to put their collection on the worldwide web, including pictures (AMNH New York) but these pictures are in low resolution. There is another major problem attached to the material from Chapada do Araripe. All material, as far as I am aware, has been obtained through fossil dealers. This means that valuable information on the site and stratigraphy and so on has been lost.¹ Furthermore, the production of fake fossils has become regular practice (see also Martill, 1993). For pterosaurs in particular this means that specimens, apparently complete, are in fact composites. If the owner is lucky, he/she knows what belongs to what, but unfortunately most of the time nobody knows (anymore). Not only the Brazilian fossil hunters are guilty of this kind of practice (the creation of composite skeletons) but well known preparators in Europe do not hesitate to create their fossils. Although sometimes they say the specimen is a composite, important details on what exactly was put together, lacks.

The present work presents descriptions of new material from Brazil of most toothed taxa (*Criorhynchus*, *Coloborhynchus*, *Anhanguera* and *Brasileodactylus*). Most of the chapters in this work have been published previously as papers in various journals; the reader is therefore requested to refer to the original papers, rather than the edited chapters herein. In the present work, the papers have been inserted largely intact. However, if necessary alterations had to be made, this is either done by means of endnotes, or indicated in an endnote but altered in the text proper. Minor alterations such as corrections of grammar have not been indicated; references have been unified in one section 'Cited literature'. Furthermore, the layout of the various different papers have been abandoned in order to unify them in this work. Joining the papers also resulted in inclusion of a list of abbreviations in each chapter because of the use of different abbreviations in various papers. No references to figures in other chapters are made.

2. Description of *Coloborhynchus spielbergi* sp. nov. (Pterodactyloidea) from the Albian (Lower Cretaceous) of Brazil²

2.1. Introduction

The description and classification of a Brazilian Cretaceous pterosaur (Santana Formation of the Chapada do Araripe) in the collection of the Nationaal Natuurhistorisch Museum, Leiden (RGM), The Netherlands, focuses on the presentation of new information because general anatomical features of this specimen agree with earlier descriptions (Campos & Kellner, 1985b; Fastnacht, 2001; Kellner, 1996a; Kellner & Tomida, 2000; Veldmeijer, 2002; Wellhofer, 1985; 1991b). Consequently, previously described features not considered in the present text may still be indicated in the figures (marked * in the list of abbreviations). Extra attention is given to parts with higher diagnostic value.

The comparison focuses on the differences rather than similarities with toothed taxa from the Cretaceous of Brazil, excluding non-Brazilian pterosaurs such as Dsungaripterids (Martill *et al.*, 2000) and edentulous pterosaurs such as Tapejarids (Wellhofer & Kellner, 1991). The one exception is the type species *Coloborhynchus clavirostris* Owen, 1874, from England. Although *Criorhynchus* originated from England as well, Fastnacht (2001) considered the material too fragmented, and consequently no clear distinction could be made between the British *Cr. simus* and the Brazilian *Cr. mesembrinus*. Therefore, the comparison will be focussed on *Cr. mesembrinus*. The problems with the England Greensand material is well known (Kellner & Tomida, 2000; Lee, 1994; Unwin, 2001; Wellhofer, 1978). However, *Criorhynchus* is not unambiguously accepted and Unwin (2001) regarded it as a synonym of *Ornithocheirus*.

The Leiden specimen is one of few near complete skeletons from Brazil that are prepared in three dimensions. Furthermore, as already pointed out (Veldmeijer, 1998), the specimen is classified in a genus (*Coloborhynchus*) that was unknown from the record of Brazil until recently.

2.2. Material

The fossil was obtained by the RGM. The specimen was still in the matrix of calcareous nodules when offered to the museum (figure 2.1 & 2.2). In order to determine the completeness of the specimen, X-rays were made by Dr. Ph.J. Hoedemaker in cooperation with the Academisch Ziekenhuis Leiden in January 1993. Dr P.H. de Buissonjé (1993) made an internal report in which he gave a provisional evaluation of the fossil on the basis of these X-rays (figure 2.2) as well as external observations of the nodules. The specimen was taken to Leonhardt & Partner, a German institute of palaeontological preparation, in early 1993. The process of preparation was documented photographically and the fossil was prepared in three dimensions, despite the recommendations of De Buissonjé (*ibidem*) to perform the preparation in half relief, mechanically.

There were a total of 11 nodules, which had horizontal measurements of 85 by 90 cm (De Buissonjé, 1993). The X-ray photographs did not reveal exactly which part of the skeleton is on top of the other. Due to the lack of information regarding the type locality and original excavation, there is no information on the stratigraphy and it is uncertain which side faced down.

2.2.1. Description of nodules

The following description uses the drawing of the X-ray as the reference orientation (figure 2.2). The mandible was disconnected from the skull but the two were embedded closely together and the articulation areas were still very closely associated. The skull lies on its lateral side, whereas the mandible is orientated in a ventral aspect. The cervical vertebrae, easily recognisable by their size and shape show their left lateral sides with their anterior orientated towards the skull. Their position in the nodules, allowing some distortion, was natural. The notarium was dislocated relative to the eighth cervical vertebra and the scapulocoracoids. Only two of the free dorsal vertebrae were not visible on the X-rays. One is visible between the rami of the mandible and another close to the left radius. The difference in size on the drawing and X-ray was due to the distance of the specific nodules to the X-ray machine. As the nodules were not level, thicker parts were closer to the machinery and appear larger. The lateroventral aspect of the pelvis shows on top and the right lateral aspect is directed towards the right femur. This right femur was easily recognised due to the incomplete head. The position of both femora was changed over 180° relative to the pelvis. Both tibiae were severely dislocated in comparison with the femora. The left scapulocoracoid is left of the cervical vertebrae; reorientated the bone to the right was the right scapulocoracoid. They were still in their original positions although reorientated onto an anterior aspect. The left humerus was still close to the left scapulocoracoid. The sternum was possibly situated beneath the cervical vertebrae, based on the small piece of bone visible, which in that case would have been the cristospine. De Buissonjé (1993) suspected that the bone that lay close to the mandible and the left radius was the sternum but it was too thin to be shown clearly on the X-rays. The left ulna was still in the neighbourhood of the humerus but at the other side of the skull. It was positioned in such a way that there was a sharp bend between the humerus and ulna. The left ulna was totally disconnected from the radius. The left proximal syncarpal was embedded at the end of the left ulna and was more or less in its natural position. One of the claws was situated at some distance of this syncarpal.

2.2.2. Description of the preservation after preparation

In general, the state of preservation is typical of fossils from this region. The skeleton is over 60% complete (table 2.1) and some parts of the skeleton, notably the pelvis and sternum, are unique in their state of preservation. No uncrushed and/or incomplete or three-dimensionally prepared and complete pelvises from Brazil have been published apart from the study of Kellner & Tomida (2000). Two-dimensional, crushed and/or incomplete pelvises were discussed by Frey & Martill (1994, they used another pelvis for comparison); Wellnhofer (1988, 1991b) and Bennett (1990). The present sternum is one of the first nearly complete specimens to be described from Brazil. Small portions are missing from the one published by Kellner & Tomida (2000).

The skull was embedded in four nodules and has suffered a great deal from the fossilisation process. Parts of the skull, especially on the left side, have been restored. The left maxilla has been restored from three quarters of the premaxillary sagittal crest until the end of the quadrate. A small piece of the right maxilla has been restored. The palate is incompletely preserved but pieces of the pterygoid have survived although dislocated slightly dorsally. The right frontal has been compressed slightly in a ventral direction, whereas the left side was not. No serious displacement of the right lacrimal has occurred and this side has also a complete jugal. The left jugal is less well preserved, with only the dorsal part of the lacrimal process and the dorsalmost part of the postorbital process surviving. The maxillar process of the right

jugal is broken behind the centrum and is attached to the medial aspect of this part of the bone, posterior to the break. The left as well as the right pterygoid are incomplete and dislocated. Little remains of the palatine. The left quadrate has been restored entirely. The right quadrate is preserved; the restoration of the left element, seen from a ventral position, continues into the right element. Consequently, the medial margin of the condyloid process cannot be determined. The restoration obscures the fusion between the quadrate and the basisphenoid. The lamella, seen from a medial position, is not complete at the medial (inner) side of the quadrate. The right prootic is still in place, whereas the left one is lost.

The mandible has been prepared from one concretion, which was broken into six fragments. It is largely uncrushed although some restoration work was necessary. The left retroarticular process and the right surangular have been partially restored. Most of the teeth are still visible although some have been broken just above the alveolus. A cross-section has been made of the part of the mandible between the seventh and ninth tooth. The seventh tooth on the right side has been sectioned lengthwise due to this cross-section. The cross-section allows the study of the interior of both the tooth and mandible. The mandible has been remodelled at the point where the cross-section has been made. The left articular has been partly restored, but the right one is original. The transverse ridge at the retroarticular process of the left articular has been restored almost completely, but the right one is only partly restored. The surangular has been restored on both sides; the left one is almost complete, apart for a small fragment medially. Half of the right surangular has been restored in its medial aspect and both restorations continue dorsally. The sutures of the angular are not observed at the right lateral aspect of the mandible. Parts of the sutures on the left lateral aspect are identified.

The seventh cervical vertebra is in good condition despite some minor restorations. The features of the eighth cervical vertebra are distinguished although the preservation is inferior to the seventh. The capitulum and tuberculum of the rib still articulate with the vertebra and the sutures are visible. The postzygapophysis is either missing (left side) or has been restored (right side).

The notarium is well preserved, although not complete. The distal parts of the transverse processes consist of a light brown homogeneous matrix, which is possibly the same as reported for other pterosaurs of the Santana Formation (Wellnhofer *et al.*, 1983). A chemical, rather than mechanical, preparation would probably have revealed more of the features of the notarium (*cf.* Wellnhofer *et al.*, 1983). The space between the centra of the coalesced notarial vertebrae has not been freed from matrix entirely. A large part of the caudal aspect of the notarium is lacking but has been restored. All dorsal vertebrae display some damage. Most of them lack the tips of their transverse processes and some display incompleteness of the anterior cotyle and/or posterior condyle.

The sternum is only slightly malformed. The right side of the plate has an almost horizontally extending lateral side, whereas it should be extending smoothly like the left side. The right coracoid facet is incomplete. The dorsal aspect is still partially covered with matrix, which was probably done to avoid damage to the thin and fragile plate.

Both scapulocoracoids are in good condition. The left part of the shoulder girdle is prepared out of one nodule and the right part out of two. Consequently, the right scapulocoracoid has a fracture on the proximal part near to the articular surface of the coracoid with the sternum, which has been partly reconstructed. The anterior aspect of the left scapulocoracoid, opposite the glenoid fossa, is damaged.

The left humerus, the only one preserved, as with the other bones of the front extremities, has been preserved almost completely. It was embedded in two nodules. The dorsal aspect displays crushing of the distal part. Smaller fractures occur at the rim of the

incomplete deltopectoral crest. The left radius is complete except for some minor restorations. The left ulna is prepared out of two nodules and badly fragmented. It is restored in several places. The bone wall is broken in many pieces and glued with epoxy resin. Furthermore, a part of the anterior aspect is crushed; the area towards the proximal aspect is damaged. A crack starts in the middle of the bone and extends distally. It has a length of 70 mm. The worst damage occurs where the distal articular surface has been restored almost entirely. This restoration continues onto the posterior aspect for one quarter of the length of the bone. Minor restorations occur on the proximal articulation area.

The left proximal syncarpal is completely preserved and in excellent condition without any reconstruction. Three claws are preserved of which one is complete. The other two lack their tips. The smallest claw has been restored partly on one side.

The pelvis was embedded in one big nodule, together with the anterior part of the skull. The bone is exceptionally well preserved. One small part of the right anterior blade of the ilium and the caudal part of the synsacrum are missing. The left side is complete.

Both femora are prepared out of two different pieces of concretion. The femoral head of the right femur has been reconstructed partially, but the distal end is almost complete save some minor damage. The femoral head of the left femur is complete, but the distal end has been reconstructed.

Both tibiae are preserved, but have suffered severely from the fossilisation process. Many small restorations have been made of which the partial restoration of the proximal articular surface of the left tibia is the largest. Other parts, like the distal articular surface of the right tibia, are incomplete, but have not been reconstructed. The situation with the distal articular surface of the left tibia is comparable though more intact.

2.3. Abbreviations

2.3.1. Institutions

AMNH	American Museum of Natural History, New York, USA.
BMNH	The Natural History Museum, London, England.
BSP	Bayerische Staatssammlung für Paläontologie und historische Geologie, Munich, Germany.
CB	Borgomanero Collection, Italy.
CCSRL	Centro Studi e Ricerche Ligabue, Venice, Italy.
LINHM	Long Island Natural History Museum, Long Island, USA.
MN	Museu Nacional, Rio de Janeiro, Brazil.
NSM	National Science Museum, Tokyo, Japan
RGM	Naturalis (Nationaal Natuurhistorisch Museum), Leiden, The Netherlands.
SAO	Sammlung Oberli, St. Gallen, Switzerland (includes one specimen on exhibition in the Natural Museum, St. Gallen).
SM	Sedgwick Museum, Cambridge.
SMNK	Staatliches Museum für Naturkunde, Karlsruhe, Germany.
SMNS	Staatliches Museum für Naturkunde, Stuttgart, Germany.
UvA	Geological Institute of the University of Amsterdam, The Netherlands.

2.3.2. Figures

a.	articular	n.s.	neural spine
ac.	acetabulum	*nas.	nasal

ad.fos.	adductor fossa	nas.fen.	nasoantorbital fenestra
ang.	angular	not.	notarium
*art.f.f.	articular facet fibula	*o.cond.	occipital condyle
b.il.	anterior blade of the ilium	o.f.	obturator foramen
b.o.	basioccipital	o.sag.ri.	occipital sagittal ridge
b.sph.	basisphenoid	op.	opisthotic
b.t.	biceps tubercle	or.	orbit
c.	centrum	*ov.fos.	oval fossa
c.f.	coracoid facet	p.t.f.	posttemporal fenestra
c.s.	cristospine	pal.	palatine
cap.	capitulum	pal.sag.r.	palatinal sagittal ridge
cap.cot.	capitular cotyle	par.	parietal
cer.	cervical vertebra	par.cr.	parietal crest
ch.	choanae	pat.sul.	patellar sulcus
co.	cotyle	pel.	pelvis
cr.q.op.	cranioquadrate opening	pl.	plate
*d.a.s.	distal articulation surface	po.ac.il.	postacetabular process of the illium
del.cr.	deltopectoral crest	po.fr.	postfrontal
den.	dentary	po.or.	postorbital
den.sag.cr.	dentary sagittal crest	po.z.	postzygapophysis
den.sag.gr.	dentary sagittal groove	pop.fos.	popliteal fossa
dep.	depression	post.tub.	posterior tuberosity
dors.	dorsal vertebra	pr.max.	premaxilla
dt.	dentine	*pr.pub.art.	prepubic articulation
duc.lac.	ductus lacrimalis	pr.sag.cr.	premaxillary sagittal crest
en.	enamel	pr.a.	prearticular
ex.o.	exoccipital	*pr.fr.	prefrontal
fem.	femur	pr.z.	prezygapophysis
for.	foramen	*pro.	prootic
for.mag.	foramen magnum	pt.	pterygoid
fr.	frontal	pub.	pubis
f.t.	fourth trochanter	pulp.	pulp cavity
g.t.	greater trochanter	q.	quadrate
h.	head	q.j.	quadratojugal
hum.	humerus	r.	ridge
in.sul.	intercondylar sulcus	ra.	radius
in.fos.	intertrochanteric fossa	rib.	rib articulation
in.os.mem.	interosseus membrane	s.p.	sacral process
in.pr.for.	interprocessal foramina	s.t.f.	subtemporal fenestra
in.pt.vac.	interpterygoid vacuity	sc.	scapula
in.sep.	interorbital septum	sc.art.	scapular articulation
is.	ischium	sk.	skull
is.fen.	ischiopubic fenestra	spl.	splenial
j.	jugal	sq.	squamosal
l.t.f.	lower temporal fenestra	st.	stop in wrist
lac.	lacrimal	ste.	sternum
lac.fos.	lacrimal fossa	sul.	sulcus
lam.	lamella	sup.n.p.	supraneural plate
lat.cond.	lateral condyle		

lat.cot.	lateral cotyle	sup.o.	supraoccipital
lat.ep.	lateral epicondyle	sup.pr.	supracondylar process
mand.	mandible	sur.	surangular
max.	maxilla	sut.	suture
mec.fos.	Meckelian fossa	syn.	syncarpal
med.cond.	medial condyle	sym.	symphysis
med.cot.	medial cotyle	t.p.	transverse process
med.ep.	medial epicondyle	tib.	tibia
n.	neck	tr.	trochlea
n.c.	neural canal	tr.cot.	trochlear cotyle
		ul.	ulna
		v.for.	vagus foramen

2.4. Systematic palaeontology, description and comparison

Order Pterosauria Kaup, 1834
 Suborder Pterodactyloidea Plieninger, 1901
 Family Anhangueridae Campos & Kellner, 1985b
 Genus *Coloborhynchus* Owen, 1874

Type species: *Coloborhynchus clavirostris* Owen, 1874.

Diagnosis of type specimen (Fastnacht, 2001: 24, modified after Lee, 1994: 756): "Medial depression on the anterior margin of the upper jaw. Flattened anterior margin of the premaxilla triangular. Pair of teeth projecting anteriorly from the blunt anterior margin of the upper jaw at a significant elevation above the palate relative to subsequent teeth. Medial crest on the upper jaw rises from the tip of the snout. Upper jaw laterally expanded in a spoon-shape in dorsal view from the second to the fourth pair of alveoli. Lower jaw with medial crest rising from its anterior end. Lower jaw laterally expanded in a spoon-shape from the first to the third pair of alveoli. Second and third pair of alveoli of the upper and lower jaw enlarged to other alveoli."

Coloborhynchus spielbergi sp. nov.

Etymology: *spielbergi*, in honour of Steven Spielberg, the director of the three Jurassic Park movies in which dinosaurs and pterosaurs were animated.

Holotype: RGM 401 880, consisting of skull, mandible, seventh and eighth cervical vertebrae, notarium, left and right scapulocoracoid, sternum, left humerus, left ulna, left radius, left proximal syncarpal, a third phalanx, three claws, seven dorsals, five pieces of rib, pelvis, both femora and tibiae and fragments of ceratobranchialia.

Locus typicus: Unknown. Chapada do Araripe (northeast Brazil).

Stratum typicum: Typical calcareous nodule of the Rornualdo Member (Albian), Santana Formation (Aptian–Albian) of the Araripe Basin.

Diagnosis: Ill-defined, almost absent (lowest and shallowest of all *Coloborhynchus* species) palatinal ridge and corresponding mandibular groove; mandibular groove not extending onto spoon-shaped expansion; slight, almost absent, venterolaterally extending teeth-bearing

maxillae; large premaxillary sagittal crest, in ratio length–total length skull, which extends dorsally from the anterior aspect until the anterior border of the nasoantorbital fenestra; strongly medial bended rami; sternum with rounded triangular posterior plate of which the length is as long as the width.

2.4.1. Cranial skeleton (figures 2.3–2.8; tables 2.2–2.7)

Skull

The skull is elongated and slender (figures 2.3–2.5; table 2.2–2.4). It is lightly built with many openings, which is a characteristic of pterosaurs, with the nasoantorbital fenestra being the biggest. The skull has a large premaxillary sagittal crest in front of the nasoantorbital fenestra. Anteriorly, the skull expands, resulting in a spoon-shaped, expanded anterior part. The anterior aspect is flat and contains two alveoli, which are situated stronger dorsally relative to the subsequent alveoli. The skull has 18 alveoli on each side, which are increasingly wider spaced in a posterior direction. Because both maxillae are incomplete, it is not clear whether this is the original number or not. The skull displays a very high degree of co-ossification and can therefore be regarded as an adult, perhaps even an older animal as suggested by various post-cranial bones (see below).

Premaxilla (pr.max.)

The dorsally thin and ventrally widening premaxillary sagittal crest (pr.sag.cr.) extends dorsally, after its start at the anterior aspect (figures 2.3A–G, 2.4A, C, E, I). It continues with a strong convex dorsal margin to the nasoantorbital fenestra (nas.fen.) where it ends immediately anterior to this fenestra. The anteriormost edge of the dorsal margin is slightly concave. The crest is asymmetrical because the anterior half is less steep relative to the posterior half. The posterior margin of the crest does not extend laterally. The anterior edges extend laterally towards the base and form a triangular anterior aspect. A network of small grooves, mainly less than 1 mm wide, is visible at the crest (figure 2.3G). The grooves occur only on the crest. A patchy brown–yellow colouring is visible in the grooves and in their proximity. A few small holes with diameters of 1 mm or less insert obliquely into the crest.

Comparison: *Coloborhynchus clavirostris* Owen, 1874 (figure 2.5A) has a depression in the anterior aspect, ventral to the teeth. The anterior aspect in *Co. spielbergi* is only partially complete; it is uncertain whether the aspect has a depression and, if so, where it is placed. The palatal ridge in *Co. clavirostris* is more strongly developed and the anterior spoon-shaped expansion is more robust and square, instead of the rounded expansion in *Co. spielbergi*. The premaxillary sagittal crest is robuster at its base.

Comparison with the holotype of *Brasileodactylus araripensis* Kellner, 1984, is not possible because it is only the anterior part of the mandible, but another specimen (MN 4797–V; figure 2.5B), includes the anterior part of the skull (Sayão & Kellner, 2000) and demonstrates that the main difference is the complete absence of a sagittal crest. Furthermore, the snout is not blunt.

Comparison with *Cearadactylus atrox* Leonardi & Borgomanero, 1985 (figure 2.5C) is hindered by the incomplete preparation of the type specimen of this species. However, the premaxilla in *Ce. atrox* as well as in *Cearadactylus? ligabuei* Dalla Vecchia, 1993 (figure 2.5D), lacks a sagittal crest. Neither of the two specimens have a flat anterior aspect. This latter also has a wide gap between rostrum and mandible.

In *Anhanguera blittersdorffi* Campos & Kellner, 1985b (MN 4805–V; figure 2.5E), the premaxillary crest does not start at the anteriormost aspect, but more posteriorly and ends almost at the anterior border of the nasoantorbital fenestra. However, the crest does not extend as far posteriorly in the referred specimen, n. 40 Pz–DBAV–UERJ; Kellner & Tomida, 2000: 104, figure 62). Lee (1994) and Fastnacht (2001) remarked that the crest in *An. blittersdorffi* (MN 4805–V) is thin, even at its base. However, Lee must have concluded this on the basis of the published drawings of the skull and was misled by the way the crest was drawn, because two thin lines mark the dorsal extension of the crest and not the base (Campos & Kellner, 1985b). The construction is the same as with other, comparable crests, viz. continuously increasing in width ventrally. Anteriorly, the jaw is expanded, but in *Co. spielbergi* this expansion is markedly robust. The anterior aspect of *An. blittersdorffi* is not blunt and the first pair of alveoli are not positioned dorsally relative to the subsequent alveoli.

The holotype of *Coloborhynchus araripensis* (Wellnhofer, 1985) (BSP 1982 I 89; figure 2.5F) lacks the anterior part and braincase. However, another specimen of this taxon (SAO 16494; figure 2.5G, see Veldmeijer *et al.*, in review) shows that the premaxillary crest starts at the anterior aspect and initially extends concave, after which it continues convex towards the nasoantorbital fenestra. It ends more posteriorly to this fenestra and is nearly as large as in *Co. spielbergi*. The ratio between the height and length of the crest is largest in a referred specimen of *Co. araripensis*, MN 4735–V (not illustrated; Kellner & Tomida, 2000: 104, figure 62), but it is large in SAO 16494 and *Criorhynchus mesembrinus* (Wellnhofer, 1987; BSP 1987 I 46; figure 2.5J) relative to the skull length (table 2.4). The anterior tip is bent slightly upwards in *Co. araripensis* (SAO 16494), but not in the referred specimen (MN 4735–V). The crest of this latter specimen forms the highest point of the skull.

The premaxilla in the holotype of *Anhanguera santanae* (Wellnhofer, 1985) (BSP 1982 I 90; figure 2.5H) is concave and extends steeply in a posterior direction, contrasting with the straight, more horizontal shapes in *Co. spielbergi* and *An. santanae* (AMNH 22555; figure 2.5I). However, the holotype of *An. santanae* (BSP 1982 I 90) might not have had a crest (see below); but if there was one it did not extend until close to the anterior limit of the nasoantorbital fenestra, contrasting with both *Co. spielbergi* and *An. santanae* (AMNH 22555). The premaxillary crest in the latter specimen is comparable to that of *An. blittersdorffi* (MN 4805–V) and differs in few respects from *Co. spielbergi*. First, the crest does not start at the anterior aspect and secondly, the crest is substantially smaller, also relative to *An. blittersdorffi* (MN 4805–V) (table 2.4), which might be due to the non-adult stage of growth. The anterior expansion is less relative to *Co. spielbergi* and the anterior aspect is not blunt, but rather flattened dorsoventrally. There is not a pair of more dorsally situated alveoli. The tip of the jaw is turned upwards more severely.

Comparison with the type specimen of *Criorhynchus* is seriously hindered by that the fragment being the small anteriormost part of the upper jaw. *Criorhynchus mesembrinus* (BSP 1987 I 46) has a large premaxillary crest which is symmetrical in the sagittal plane. Compared with *Co. spielbergi*, the crest is smaller in length (relative to skull length), but higher (relative to the crests length; table 2.4). The jaw, only slightly bent upwards, has an elongated triangular, flat anterior aspect with a small, shallow, medial depression slightly dorsal to the front teeth. These teeth are not placed substantially more dorsal relative to the subsequent teeth, as seen in *Co. spielbergi*.³ The anterior part is not expanded.

The holotype of *Coloborhynchus robustus* (Wellnhofer, 1987) (BSP 1987 I 47) lacks a skull but the anterodorsal aspect of the premaxillary crest in another specimen, *Co. robustus* (SMNK 2302 PAL; figure 2.5K), starts concave and extends, more dorsally, convex against the almost convex anterodorsal border as in *Co. spielbergi*. The base suggests a more robust crest. Furthermore, the triangular anterior aspect in *Co. robustus* (SMNK 2302 PAL) is flat

and almost completely filled with the first pair of alveoli, leaving little space dorsal to the teeth. A depression is situated dorsal to these alveoli. The morphology of the anterior aspect in *Co. spielbergi* is unclear due to its damaged state. The spoon-shaped expansion of the skull starts at the fourth alveolar pair in *Co. spielbergi* and at the fifth in *Co. robustus* (SMNK 2302 PAL), and is robuster in the latter. The preserved anterior part is more elongate, corresponding with the more elongated symphysis of the mandible.

The crest in *Coloborhynchus piscator* (Kellner & Tomida, 2000) (figure 2.5L) starts well before the anterior border of the nasoantorbital fenestra. The anterodorsal border is strongly concave and extends slightly dorsally. This condition is seen in the referred specimen of *An. blittersdorffi* (n. 40 Pz-DBAV-UERJ, Kellner & Tomida, 2000: 104, figure 62) and also *An. santanae* (AMNH 22555). *Coloborhynchus piscator* is a juvenile and the crest is likely not fully-grown yet; immaturity may also explain the relatively small length and height (table 2.4). The anterior aspect is flat, but smaller relative to *Co. spielbergi*, *Co. araripensis* and *Co. robustus*.

Maxilla (max.)

The lateroventral border of the skull is straight, but the anterior portion is bent slightly upwards, starting approximately at the posterior beginning of the spoon-shaped expansion (figures 2.3B–D, 2.4C, E, G). Seen in ventral view, the maxilla extends far posteriorly, but the exact posterior course cannot be determined. It continues at least medially and ventrally to the maxillary process of the jugal. The lateral teeth-bearing parts of the maxilla are slightly ventrally raised relative to the palatine (pal.). This is not seen within the teeth-bearing part of the premaxilla; however, the suture is not visible, so the boundary between these two bones cannot be determined. From a lateral perspective, the maxilla forms the anterior and ventral edges of the nasoantorbital fenestra and meets the premaxilla dorsally.

A small fragment of bone 71 mm long is separated from the skull. The fragment is broken into two connected pieces, though displaced. Only the lateral bone wall is preserved. One tooth remains, which is broken at the alveolar border.

Comparison: The inclined ventral border of the anterior part of the maxilla distinguishes *Ce. atrox* (figure 3C) from *Co. spielbergi*. The alveolar margin of the maxilla in *Ce.? ligabuei* (figure 2.5D) is also recessed, although it starts more posteriorly (at the fifth alveolus) relative to *Ce. atrox* and is shorter, ending at the eighth.

Ventrally, the teeth-bearing maxilla in *An. blittersdorffi* (figure 2.5E) protrudes relative to the palatine, which is also seen in *Co. araripensis* (figures 2.5F, G). However, the maxilla in *An. santanae* (figures 2.5H, I), protrudes less relative to *An. blittersdorffi* and *Co. araripensis*, but still more than in *Co. spielbergi*. Furthermore, *An. blittersdorffi* has a more distinct palatal ridge.

Alveoli 5–7 are positioned in a concavity in *Co. robustus* (SMNK 2302 PAL; figure 2.5K). These concavities are best visible from ventrally and are clearly less prominent than in *Cearadactylus*. Such concavities are absent in *Co. spielbergi*.

Dentition

The alveoli are orientated lateroventrally except for the anteriormost pair, which is orientated anteriorly (figures 2.3D–F, 2.4G, I; table 2.3). The presence of the front alveoli has been proven using CT-scan (figure 2.3F; the arrow points to the alveoli⁴). The first seven pairs of alveoli are positioned lateroventrally and the teeth are pointing slightly anteriorly. They have a posteromedial curvature. Alveoli 13–15 of the right side are positioned

lateroventrally and the teeth have a posteromedial curvature too. There is some doubt as to the precise orientation of some teeth, especially for those posterior to tooth eight on the left side, due to poor preservation. On the right side 18 alveoli are present. Due to the reconstruction of the maxilla posterior to tooth 18 on the right side, it is unclear whether there were more teeth or not; only the anterior nine teeth survived on the left side. The size of the first alveolus is uncertain, but the third is probably the largest. The second and fourth alveoli are smaller than the third one. Two smaller alveoli of comparable size follow the fourth tooth. The description is based on the measurements taken at the right side, except for the measurements of the fifth and sixth alveoli, which are based on the measurements taken at the left side. Alveolus 7 and 8 are larger than the two foregoing alveoli, but smaller than the third. Alveolus 9 on the left side is large and comparable to alveolus 2. Alveoli 10–15 are of similar size and the average size is one third of the third alveolus. The last three alveoli (16–18) are the smallest. The diastemae pattern shows a continuous increase in width posteriorly and is slightly more erratic than the pattern of the mandible. The wide diastema between tooth 15 and 16 on the right side is probably a result of restoration. Most probably, there was an alveolus, which would result in at least 19 teeth on one half of the skull.

Comparison: The second to fourth alveoli in *Co. clavirostris* are far more laterally placed relative to the subsequent teeth and relative to these alveoli in *Co. spielbergi*. The alveolar size of *B. cf. araripensis* (MN 4797–V) varies less, but the pattern is comparable.

The number of alveoli in *Ce. atrox* is less (30–32 against at least 36 in *Co. spielbergi*), but the number of teeth in *Ce.? ligabuei*, at least 22 in each side, exceeds the number in *Co. spielbergi*. *Cearadactylus? ligabuei* has a first pair at the anterior aspect that are positioned slightly more dorsal relative to the subsequent alveoli. The second pair is transitional, being placed anteroventrally, resembling *Anhanguera*.

Anhanguera blittersdorffi (MN 4805–V) has 52 alveoli, which exceeds the number in *Co. spielbergi* markedly. The largest pair of alveoli in *An. blittersdorffi* (MN 4805–V) is the tenth and the alveolar pattern is less erratic relative to *Co. spielbergi*. However, the third tooth of the referred specimen of *An. blittersdorffi* (n. 40 Pz–DBAV–UERJ) is, as in *Co. spielbergi*, the largest, but the alveolar pattern is far less erratic relative to the holotype and *Co. spielbergi*. The number of alveoli is less than is seen in the holotype (44 in total).

The number of alveoli in *Co. araripensis* (SAO 16494) is 36, which is the minimal number in *Co. spielbergi*. The dentition pattern is less erratic and the position of the alveoli two to six is stronger anteroventrally.

An. santanae has a less distinct variation in alveolar size. The number of alveoli is estimated (both skulls are incomplete) at 40 (Wellnhofer, 1991b).

The dentition in *Cr. mesembrinus* (BSP 1987 I 46) lacks distinct variation in alveolar size and the position of the alveoli is, in general, less laterally and there are less alveoli than *Co. spielbergi* (14 in each side; contra Wellnhofer, 1987). The number of teeth in *Co. robustus* is not known. However, the pattern is comparable to the new species, although the second and third alveoli in *Co. robustus* are the largest against the third, fourth and ninth in *Co. spielbergi*.

The number of teeth in *Co. piscator* is 40 (observed on the cast) and the dentition pattern is comparable to *Co. spielbergi*, although there are differences between the seventh, eighth and ninth alveolus. These are of comparable size in *Co. spielbergi* and vary distinctly in *Co. piscator*.

Frontal (fr.)

The suture medial between the left and right frontal is well developed and forms a shallow ridge. Seen from posterior, the suture continues far between the two parietals (figures 2.3C, 2.4E, F).

Comparison: The frontoparietal crest is more strongly developed in the holotype of *An. blittersdorffi* (figure 2.5E) and *Co. araripensis* (figures 2.5G) than *Co. spielbergi*. The crest in *An. santanae* (figures 2.5H, I) is longer and slightly more distinct. It is weak in *Co. piscator* (figure 2.5L) and comparable to *Co. spielbergi*.

Parietal (par.)

The left and right parietals fuse posterior to the suture of the frontal and dorsal to the lower temporal fenestra (figures 2.3A–C, 2.4A–F).

Comparison: The parietal in *Co. spielbergi* is more strongly concave than that of *An. santanae* (figures 2.5H, I). The short and blunt parietal crest (par.cr.) seen in *Cr. mesembrinus* (BSP 1987 I 46; figure 2.5J) is nearly absent in *Co. spielbergi*.

Lacrima (lac.)

The posterior edge of the lacrimal forms a curve that points into the orbit (figures 2.3A–C, 2.4B, D, F). An opening, the lacrimal fossa (lac.fos.), is situated in the middle of the lacrimal and is bean-shaped, with its recess anteriorly. From here a ridge extends concavely towards the orbit (or.), separating the lacrimal from the lacrimal process. At the end of this ridge is a small opening, interpreted as the ductus lacrimalis (duc.lac.).

Comparison: The lacrimal process in *An. blittersdorffi* (figure 2.5E) is comparatively small and long, and the lacrimal fossa is somewhat larger. The small fossa posteroventral to the lacrimal fossa is not seen in *Co. spielbergi*.

Assuming that the lacrimal is complete in *Co. spielbergi*, it is shorter compared to *Co. araripensis* (figure 2.5G) but the process that points into the orbit is more massive. *Coloborhynchus araripensis* has a small fossa dorsal to the larger lacrimal fossa.

Criorhynchus mesembrinus (BSP 1987 I 46; figure 2.5J) lacks a lacrimal with a process that points into the orbit. The lacrimal fossa in *Co. piscator* (figure 2.5L) is larger and the process pointing into the orbit is substantially smaller.

Postfrontal (po.fr.)

The postfrontal forms the posterodorsal edge of the orbit, and is sandwiched between the frontal and the postorbital (figures 2.3B, C, 2.4D, F). The postfrontal is arched slightly posteroventrally towards the inner side of the orbit.

Comparison: According to Kellner & Tomida (2000) the presence of this bone is uncertain in *Co. piscator* (figure 2.5L).

Postorbital (po.or.)

The postorbital is a triradiate bone of which the rays extend anteroventrally (the jugal process), posteroventrally (the squamosal process) and dorsally (the frontal process) (figures 2.3A–C, 2.4B, C, F). The postorbital closes the orbit posteriorly and the lower temporal fenestra dorsally.

Comparison: The jugal process of the postorbital in *An. blittersdorffi* (figure 2.5E) extends more laterally, giving the skull, seen in dorsal view, a somewhat broader appearance.

Jugal, quadratojugal (j., q.j.)

The processes of the triradiate jugal extend dorsally (lacrimal process), posterodorsally (postorbital process) and anterodorsally (maxillar process) (figures 2.3B, C, 2.4D, F). The quadratojugal is sandwiched between the jugal and the quadrate (q.).

Comparison: The maxillar process of the jugal in *Co. piscator* (figure 2.5L) is extremely long and slender in contrast to the short and robust process in *Co. spielbergi*.

Squamosal (sq.)

The squamosal consists of three rays, the parietal, postorbital and otic processes that originate in the broad, well developed centrum (figures 2.3A–D, 2.4B, D, H). The centrum is twisted diagonally posteroventrally to anterodorsally. Seen in ventral view, the otic process overlaps the quadrate. The otic process broadens anteriorly, with its largest width at two-thirds of the length of the ventral aspect of the centrum of the squamosal. Beyond this point the angle of the squamosal changes and the bone continues anterolaterally. The squamosal lies against the opistotic and the supraoccipital, and forms the junction between the opistotic, the quadrate, the parietal and the postorbital.

Comparison: The edge of the otic process is sharper and extends more strongly dorsally in *Co. spielbergi* and *An. santanae* (AMNH 22555) relative to *An. santanae* (BSP 1982 I 90).

Palatine (pal.)

The palatine is in contact with the maxilla laterally, but the exact borders, both anteriorly and posteriorly, cannot be determined (figures 2.3D, 2.4G). The palatine is recessed slightly relative to the palatine. Posteriorly, the palatine limits the choanae (ch.). More anteriorly, it has a small and low sagittal ridge (pal.sag.r.) that has its counterpart on the mandible. This ridge is most obvious between teeth 5 and 10. Posterior to tooth 10, the ridge disappears.

Comparison: Comparison with the palatal region of *Ce. atrox* is not possible. But the palatine of *Ce.? ligabuei* (figure 2.5D) has a clear sagittal ridge extending far anteriorly and extend laterally at the posterior expansion.

Anhanguera blittersdorffi (figure 2.5E) has a distinct palatal sagittal ridge, extending to the anterior border of the choanae. In the referred specimen, it extends anteriorly until the expansion, and fades between the fourth and fifth alveolus.

Coloborhynchus araripensis (figures 2.5F, G) has a ridge at the palatine, but this is far less distinct relative to *Cr. mesembrinus* (BSP 1987 I 46; figure 2.5J) and *An. blittersdorffi* (figure 2.5E). It is still stronger relative to *Co. spielbergi*.

The palatal ridge is most obvious between tooth 6 and 11 in *An. santanae* (AMNH 22555, figure 2.5I) and between tooth 5 and 10 in *Co. spielbergi*. Although none of the specimens have a strongly developed palatal sagittal ridge, the ridge of *Co. spielbergi* is weakest.

In *Cr. mesembrinus* (BSP 1987 I 46; figure 2.5J) the "palate is elevated to a high medial ridge fitting into a corresponding deep sulcus on the mandibular symphysis" (Wellnhofer, 1987: 179), contrasting with the almost absent ridge in *Co. spielbergi*. No palatal sagittal ridge can be observed in *Co. robustus* (SMNK 2302 PAL; figure 2.5K), which is probably

due to only the anterior part being preserved. A depressed medial area evolves between the eighth and ninth left alveolar pair in this species. If *Co. robustus* had a palatal ridge, it did not extend far anteriorly. The distinction between the depressed medial area and teeth-bearing maxillae is more distinct relative to *Co. spielbergi*.

Pterygoid (pt.)

The pterygoid is triangular (figures 2.3C, D, 2.4E, G). The interpterygoid vacuity (in.pt.vac.) is comparatively large. Both pterygoids are firmly united with the quadrate, posterolateral to the vacuity.

Comparison: The pterygoid in *An. blittersdorffi* (figure 2.5E) has a distinct foramen, which is not seen in *Co. spielbergi*. *Coloborhynchus araripensis* (figures 2.5F, G) has a small process at the pterygoid that is directed towards the subtemporal fenestra (s.t.f.), which cannot be observed in *Co. spielbergi*.

Quadrate (q.)

The anterior aspect of the quadrate is directed anteroventrally and lies ventral to the quadratojugal and the jugal (figures 2.3B, D, 2.4D, H). Seen from a ventral aspect, the quadrate is a thin, bar-like bone with the, damaged, condyloid process situated anteriorly. Parts of the fragile, thin, bony lamella (lam.) are still in place in the anterior corner of the cranioquadrate opening (cr.q.op.). The lamella is situated at the inner side of the quadrate, starts at the side of the basisphenoid and extends more than halfway along the posterior extending process of the quadrate. A foramen is situated in the anteromedial corner.

Comparison: The foramen in the anteromedial corner, at the junction with the basisphenoid, is absent in *An. blittersdorffi* (figure 2.5E), *Co. araripensis* (figure 2.5G) and *Cr. mesembrinus* (BSP 1987 I 46; figure 2.5J). The reconstructed width of the skull of *Co. spielbergi* is larger relative to the other taxa discussed herein, except *Cr. mesembrinus* (table 2.4).

Basisphenoid, interorbital septum (b.sph., in.sep.)

The basisphenoid is orientated anteroventrally and narrows posteriorly, where it is in contact with the basioccipital (b.o.), and penetrates this bone between the left and right vagus foramen (v.for.) (figures 2.3D, 2.4H, J). Anteriorly, the basisphenoid limits the interpterygoid vacuity. The interorbital septum lies dorsal to the basisphenoid inside the braincase and is a dorsally-trending, small bony plate that forms a small elliptical opening against the back wall of the braincase.

Comparison: Posteriorly, the lateral expansion of the basisphenoid in *An. blittersdorffi* (figure 2.4E) is more abrupt and stronger than in *Co. spielbergi*. In the holotype of *An. blittersdorffi* (MN 4805-V) the bone is not completely fused with the quadrate anteriorly, in contrast to the referred specimen (n. 40 Pz-DBAV-UERJ, Kellner & Tomida, 2000: 104, figure 62) and *Co. spielbergi*. The lateral expansion of the basisphenoid is anteriorly and posteriorly stronger in *Cr. mesembrinus* (figure 2.5J).

Basioccipital, opisthotic, exoccipital (b.o., op., ex.o.)

The complete borders between these three bones cannot be determined, due to the very high degree of ossification obliterating the sutures (figures 2.3D, 2.4H). However, small parts

of the sutures between the basisphenoid, basioccipital and exoccipital are still visible, and the entire posterodorsal suture of the opisthotic can be traced. Morphologically these bones are comparable to those of previously described taxa.

Supraoccipital (sup.o.)

Posteroventrally, the skull is closed by the supraoccipital, the element that forms the dorsal margin of the posttemporal fenestra (p.t.f.) and foramen magnum (for.mag.) (figure 2.3D, 2.4H). The posterior of the supraoccipital joins the parietal, which is overlapped by the parietal process of the squamosal. Posteriorly, the supraoccipital has a medial and strongly developed, bulb shaped protrusion that extends anteroventrally into a ridge (o.sag.ri.) that fades towards the foramen magnum. At both sides of the ridge are posteromedially orientated pneumatic foramina.

Comparison: The holotype of *An. blittersdorffi* (figure 2.5E) has a strongly developed occipital sagittal ridge which is even stronger developed in the referred specimen. The occipital region in the latter is wider relative to the holotype as well as to *Co. spielbergi*.

The occipital sagittal ridge in *Cr. mesembrinus* (BSP 1987 I 46; figure 2.5J) is distinctly robuster than that of *Co. spielbergi*. The posteroventral aspects of the skull in *Co. araripensis* (SAO 16494; figure 2.5G), *An. santanae* (BSP 1982 I 90; figure 2.5H) and *Co. piscator* (figure 2.5L) are steeper relative to *Co. spielbergi* and *An. santanae* (AMNH 22555; figure 2.5I). The occipital sagittal ridge in *Co. piscator* is weaker.

Skull openings

The shape of many of the skull openings at the ventral aspect cannot be determined because of the fragmented nature of the Leiden skull (figures 2.3A–D, 2.4A, F, J). The skull openings of others specimens are also poorly preserved.

Comparison: The interpterygoid vacuity in *Co. spielbergi* is wider relative to that of *An. blittersdorffi* (figure 2.5E) and *Co. araripensis* (figures 2.5F, G). The lower temporal fenestra in *An. blittersdorffi* (figure 2.5E) is more oblong. The orbit in *Co. araripensis* (figure 2.5G) is slightly wider and the orbit in *Cr. mesembrinus* (BSP 1987 I 46; figure 2.5J) is more elliptical, contrasting with the oval orbit in *Co. spielbergi*. The ratio of the length of the nasoantorbital fenestra to length of the skull is lowest in *Co. araripensis*. This ratio in other taxa varies by only a few percent (table 2.4).

Mandible

The morphology of the mandible is comparable to those of the known toothed pterosaurs except for the presence of crests (absent in some taxa) (figures 2.6–2.8; tables 2.5–2.7). The mandible is long and slender with a comparatively short symphysis and diverging rami. The rami display a strong posteromedial bending of the posterior half. Anteriorly, the jaw has a dentary sagittal crest, which is substantially smaller than the premaxillary sagittal crest. The length of the lower jaw is substantially larger than that of other species discussed herein. However, comparison with other taxa are limited because most mandibles are incomplete and/or only partially prepared.

Dentary (den.)

In medial view, the dentary starts immediately posterior to the last alveolus and forms the dorsal border of the Meckelian fossa (mec.fos.) (figures 2.6A, B, D, E, G, H, 2.7A, B, D, E, G, H). The left and right dentaries meet each other anteromedially, forming the symphysis. In dorsal view, there is a shallow ill-defined dentary sagittal groove (den.sag.gr.). Towards the anterior spoon-shaped expansion, this groove widens and disappears. The teeth-bearing lateral edges protrude relative to the medial area. The dentary sagittal crest starts at the cross-sectioned area, probably between alveolus seven and nine, and narrows ventrally continuously, ending in a ventralmost border 3 mm thick. The posterior view of the cross-section (figure 2.6J, 2.7J) demonstrates the strengthening of the ventral inner side of the crest.

Comparison: The dentary of *B. araripensis* (MN 4804–V; figure 2.8A) lacks a sagittal crest and is spoon-shaped expanded, but less distinct than in *Co. spielbergi*. The dentary sagittal groove, which is defined sharply, is continuous to almost the anterior aspect, contrasting with the weak and short groove in *Co. spielbergi*.

The dorsal border up to the sixth alveolus inclines in a ventral direction in *Ce. atrox* (figure 2.8C) and there is no dentary sagittal crest. The dentary is spatulate and more expanded than the premaxilla (Leonardi & Borgomanero, 1985).

The mandible of *An. blittersdorffi* (n. 40 Pz–DBAV–UERJ, Kellner & Tomida, 2000: 104, figure 62) is proportionally narrower than that of *Co. spielbergi* with a smaller dentary sagittal crest (table 2.7). The configuration of the dorsal aspect (recessed medial area having a sagittal groove flanked by ridges) is comparable to *An. santanae* and the two other *Anhanguera* mandibles (see below), but differs from *Co. spielbergi*, which has an ill-defined dentary groove that is situated in the recessed medial area. The teeth-bearing edges are less clearly raised and separated from this medial area in *Co. spielbergi*. The dentary configuration in *An. blittersdorffi* is probably only seen in *Anhanguera* sp. indet.⁵ The rami in *An. blittersdorffi* diverge straight and posterolaterally instead of with a posteromedial bending as seen in *Co. spielbergi*.

Wellnhofer (1985) mentioned a coronoid in *Co. araripensis* (BSP 1982 I 89; figure 2.8D), which is not observed in *Co. spielbergi*. However, this might be due to the high co-ossification of the latter. The rami in *Co. araripensis* (BSP 1982 I 89) are less strongly curved.

The reconstruction of the proportionally narrower mandible of *An. santanae* (BSP 1982 I 90; figure 2.8E), is without a crest (Wellnhofer, 1985, 1991b). The anterior part, starting roughly 50 mm anterior to the symphysis, is missing in the holotype. Only the retroarticular process is preserved in *An. santanae* (AMNH 22555). Although the reconstruction of the skull was altered later (Wellnhofer, 1991b), Kellner & Tomida (2000) made no attempt to reconstruct the mandible. However, the reconstructions are hypothetical and there is no evidence for the presence of the crest or its position. If there was a crest, it is unlikely that it was placed posterior to the anterior aspect, allowing an analogy with *An. blittersdorffi* (n. 40 Pz–DBAV–UERJ, Kellner & Tomida, 2000: 104, figure 62) on the basis of the comparable position of the premaxillary sagittal crests (which has the dentary sagittal crest starting at the anterior aspect). Seen from a dorsal perspective, the teeth-bearing borders in *An. santanae* are raised relative to the medial part. Medial to this recessed area is a dentary sagittal groove that is flanked by two parallel running, slightly raised ridges as seen in *An. blittersdorffi* (see above). The cross-section of the symphyseal part is, as in the *Anhanguera* sp., rounded trapezoid, unlike the section of this region in *Co. spielbergi*.

The mandible of *Cr. mesembrinus* (figure 2.8F, G) is proportionally smaller and the crest is shorter, albeit markedly deeper. The anterior aspect has a small depression

mediodorsal to the two front teeth. The anterior part is almost not expanded. The sagittal groove is deep and posteriorly widening. The curvature of the rami is less.

The anterior margin of the mandible in the holotype of *Co. robustus* (figure 2.8H) is blunt and "forms an angle of c. 50° with the upper edge of the jaw" (Wellnhofer, 1987: 182). The anterior margin of *Co. spielbergi* is also blunt, and the dentary sagittal crest is far smoother and longer, but less deep relative to *Co. robustus*. The dorsal aspect of the spoon-shaped anterior part is slightly concave in *Co. robustus* against slightly convex in *Co. spielbergi*. The dentary sagittal groove in *Co. robustus*, especially SMNK 2302 PAL (figure 2.8I), is clearly defined and comparatively deep, which contrasts sharply with the ill-defined groove in *Co. spielbergi*. It extends further anteriorly in *Co. robustus*, until the anterior expanded part, widens posteriorly, starting approximately between the ninth and tenth alveolus. This groove differs from the dentary groove in *Anhanguera*, having no flanking ridges and extending further anteriorly. In *Co. robustus* (BSP 1987 I 47), the symphysis starts at the tenth alveolus. This is with the twelfth in *Co. spielbergi*, which results in a longer and therefore more slender appearance of the lower jaw of *Co. robustus*.

Proportionally, the mandible of *Co. piscator* (figure 2.8J) is narrower and the crest shorter but deeper. The anterior tip in *Co. piscator* is curved upwards, and the rami are less strongly curved, unlike *Co. spielbergi*.

The proportions of the mandibles in the *Anhanguera* sp. indet.⁶ (figures 2.8K, L) are comparable and differ from *Co. spielbergi* mainly because they have a shorter, but deeper, crest. The different dentary sagittal groove was discussed above.

Dentition

The teeth are still preserved although most are incomplete (figures 2.6G–J, 2.7G–J; table 2.6). The left side of the jaw contains 16 teeth, which is also the number of teeth on the right side (excluding the putative tooth numbered 15a', see below). They are distributed over the anterior half of the mandible. The alveoli are orientated laterodorsally and the two alveoli at the anterior aspect anteriorly. They are elliptic with their long axis longitudinally (except the first pair which are circular). Alveoli two to seven are orientated laterodorsally and slightly anteriorly. The teeth are curved posteromedially (based on the complete second and third on the left side and the third tooth on the right). The remaining alveoli are positioned dorsally and the teeth are curved posteromedially as well. The first and second alveoli are of comparable size, but smaller than the third. The description is based on the measurements taken at the left side. Alveoli 4–6, all of comparable size, are smaller than alveoli 1–3. Alveoli 7–8 are of comparable size to each other and are larger than alveoli 1, 2, 4–6 but smaller than alveolus 3. Alveoli 9–16 are of comparable size to 4–6. The alveoli are widely spaced although the first six less widely than the following (an average of 7 mm against an average of 29 mm). There is a continuous increase, save some small fluctuations, in the size of the diastemae. Alveolus 16 of the right ramus is orientated more medially than all other alveoli whereas the putative alveolus posterior to alveolus 16 and numbered 15a', is orientated laterally. The expansion at this place on the lateral aspect is likely due to the root of the tooth in his alveolus, although the tooth itself is not preserved.

Tooth 7 of the right side is sectioned longitudinally, which provides a good view of the interior of the tooth (figures 2.6J(i), 2.7J). The lateral aspect of the tooth extends convexly into the alveolus. The medial aspect extends with a concave curvature until the alveolar margin, where it has its largest diameter (6.5 mm compared to 1.7 mm at the dorsalmost point, measured lateromedially) and continues almost straight into the alveolus. The diameter of the tooth decreases continuously ventrally. The tooth ends in a sharp edge. The large, oval

space inside is the pulp cavity (pulp.). A small layer, comparable to enamel (en.), is observed between the alveolar margin and the dentine (dt.). This layer is continuous onto the crown, where it is very thin (less than 1 mm). The root is firmly embedded in the jaw by means of large quantities of small bony transverse joins. These joins form small compartments that serve as a base for the tooth. This structure is only present in the surroundings of the tooth; the rest of the jaw is hollow with a structure of bony transverse bars.

Comparison: The second to sixth alveoli are positioned more laterally in *B. araripensis* (MN 4804–V). The first pair of alveoli is placed more anteriorly. The differences in alveolar size are far less relative to *Co. spielbergi*.

The number of alveoli in *Ce. atrox* is smaller (28 against 32 in *Co. spielbergi*). At least 42 alveoli occur in *An. blittersdorffi* (n. 40 Pz–DBAV–UERJ), which is a substantially larger number relative to *Co. spielbergi* (32). The third alveolus is the biggest and the alveolar size decreases from the seventh alveolus continuously in size, against the large ninth alveolus in *Co. spielbergi*. The pattern is less erratic and generally the alveoli are substantially smaller. The pattern of diastema size is more regular than in *Co. spielbergi* and size decreases from alveoli 10–11 onwards.

The alveoli in *Cr. mesembrinus* are set at the anterior and lateral edge, and face dorsally rather than laterodorsally as seen in *Co. spielbergi*. The alveoli are all comparable in size and twelve teeth are observed at both sides.

The pattern of dentition of the two *Co. robustus* specimens are comparable but the ninth alveolus in *Co. spielbergi* is of approximately the same size as the third. In the holotype of *Co. robustus* (BSP 1987 I 47) this is the eighth (although this alveolus is still substantially smaller). Alveoli 6 and 7 in *Co. robustus* (SMNK 2302 PAL) are slightly larger than alveoli 5 and 8, but still substantially smaller relative to the third alveolus. Furthermore, the increase in size of the diastemae is more severe in the latter specimen. In this, the holotype of *Co. robustus* and *Co. spielbergi* are more comparable. The former specimen also differs from *Co. spielbergi* by the large differences in measurement ratios (table 2.7). Both animals are fully-grown but have a different number of teeth (18 against 15). Kellner & Tomida (2000: 118) mistakenly mentioned a "(height between the dorsal margin of the mandible and the ventral part of the sagittal crest)" of 760 mm. The depth of the crest measures 76 mm.

The alveoli in *Co. piscator* are more numerous, 38 against 32 in *Co. spielbergi*. The mandibular teeth in *Co. piscator* are generally larger than the teeth in the upper jaw, which is the other way around in *Co. spielbergi*. The variation in alveolar size is larger in *Co. piscator*. The pattern of diastemae size shows a distinct difference. The alveoli are increasingly less widely spaced from approximately halfway the dentition in *Co. piscator*, whereas the alveoli in *Co. spielbergi* are continuously wider spaced posteriorly, save a minor decrease between the last four alveoli.

The *Anhanguera* sp. has 38 teeth. The dentition pattern in the *Anhanguera* sp. is comparable to *An. blittersdorffi* although measurements are slightly greater and the graph is slightly more erratic. The pattern still contrasts with *Co. spielbergi* for reasons explained with *An. blittersdorffi*. The diastemae variation also differs from *Co. spielbergi* in the same way as the variation differs between *An. blittersdorffi* and *Co. spielbergi*.

Surangular, angular (sur., ang.)

The surangular extends further posteriorly than the cotyles and ends in a overhanging ridge dorsal to the cotyles (figures 2.6A–E, G, H, 2.7A–E, G, H). The anterior aspect is orientated medially with a curve and ends in a sharp edge. Seen from a medial perspective,

the anterior part ends in a sharp edge pointing anteroventrally. The exact position of the angular cannot be determined.

Prearticular (pr.a.)

Seen from a medial perspective, the left ramus has an element between the articular (a.), the Meckelian fossa, the splenial and the angular that is interpreted as the prearticular (figures 2.6B–E, 2.7B, E). Posteriorly, the prearticular forms the edge of the retroarticular process. It confines the ventral sides of the surangular and the adductor fossa (ad.fos.), and forms a ridge at the latter. The prearticular is in contact with the angular dorsally.

Splenial (spl.)

The dorsal side of the splenial is confined by the dentary (figures 2.6B, E, 2.7B, E). Seen from a medial perspective, the splenial continues anteriorly to the Meckelian fossa and forms its posterior border. Posteriorly, the splenial forms the anteroventral border of the adductor fossa.

Comparison: The splenial in *Co. araripensis* (BSP 1982 I 89) has several small pneumatic foramina, absent in *Co. spielbergi*.

Retroarticular process

The retroarticular process forms an edge with the mandible of 40° and is orientated posteroventrally (figures 2.6C, D, 2.7C, F). The articular is relatively long and small in comparison with the ramus. It narrows posteriorly, and consists of the lateral and medial cotyle (lat.cot., med.cot., respectively) that is separated by a distinct posterolaterally and anteromedially orientated ridge. A large pneumatic foramen (for.) is situated posteroventrally to the medial cotyle.

Comparison: The holotype of *B. araripensis* retains the anterior part of the retroarticular process, but a more complete specimen⁷ shows that the rami and especially the retroarticular process are, seen from dorsal, less strongly inclined. The mandible in *B. araripensis* has smaller dimensions overall.

Comparison of the mandible with *Co. araripensis* (BSP 1982 I 89: figure 2.8D) indicates a more elongated articular relative to *Co. spielbergi* and the dorsal aspect of the articular is less steep and pointed. The articular in *Cr. mesembrinus* (BSP 1987 I 46: figure 2.8F) is even shorter.

?Ceratobranchials

A piece of slender bone is still attached to the matrix (figure 2.6K, 2.7K). The cross-section is circular, but one end of the bone is curved and flatter than the other extremity. Another piece (not illustrated) is a thin, almost straight fragment with an oval cross-section. It is slightly bent, which becomes even clearer when it is connected with another part of the bone that is completely freed from the matrix (not illustrated).

Comparison: Comparison of these fragments reveals a strong resemblance and they are regarded as possible pieces of ceratobranchialia. The shape and size suggests that the bone is a piece of ceratobranchialia of the hyoid apparatus (Wellnhofer, 1985⁸).

2.4.2. Axial skeleton (figures 2.9–2.21; tables 2.8–2.13)

Cervical vertebrae

The seventh and eighth cervical vertebrae (the last two before the notarium; figure 2.9A–L; table 2.8) are similar to those described by previous authors (Wellnhofer, 1991b; Kellner & Tomida, 2000). However, the eighth cervical vertebra has pieces of the rib fused (figure 2.9G–L).

Comparison: Comparison with the cervicals of other taxa from Brazil is limited by the paucity of data. The seventh and eighth cervical in *An. santanae* (AMNH 22555; figure 2.10) and *Co. spielbergi* are, apart from slight biometrical differences (the cervicals in *An. santanae* are overall smaller), similar despite the fact that the neural spine of the eighth cervical of the new species has a more convex anterior border and its prezygapophysis is comparatively more robust.

The cervical vertebrae in *Co. piscator* are, besides the size "essentially the same as in *Anhanguera santanae* (AMNH 22555)" (Kellner & Tomida, 2000: 34). However, the cervicals of *Co. piscator* (not illustrated) are longer and higher relative to *Co. spielbergi*. In contrast, the width over the pre- and postzygapophyses is larger in the latter species. Kellner & Tomida (2000) remarked that there is no fusion of the centra of the eighth and ninth cervical vertebrae, contrasting with the fused situation in *An. santanae* (AMNH 22555; contra the addition of 'apparently' by Kellner & Tomida, 2000: 34, because it is clearly visible that the centrum and neural arch of the eighth and ninth cervicals are completely co-ossified) and *Co. spielbergi*.

Notarium

The notarium consists of six vertebrae, which are firmly fused by their centra (c.), zygapophyses and neural spines (figures 2.11, 2.12; table 2.9). The neural spines form a stout supraneural plate (sup.n.p.). The posterior half of this plate expands laterally, starting dorsal to the fourth vertebra and obtains its largest width dorsal to the fifth vertebra, which results in a stouter part. The scapular articulation (sc.art.) is situated at this bulbous part, which is in the middle of the supraneural plate, dorsoventrally, and posterodorsal to the fifth vertebra. The surfaces are oval and saddle-shaped. A large foramen is situated immediately posterior to the scapular articulation.

A ridge characterises the sutures between the centra. The sutures between the third and fourth, fourth and fifth, and fifth and sixth notarial vertebrae are even more distinct, and marked by a distinct bulging of the articular areas. Comparatively large foramina are visible between the centra.

The first vertebra of the notarium is the last cervical (number nine) and is firmly fused with the following notarial dorsals. The rounded triangular neural canal (n.c.) is flanked by pneumatic foramina immediately ventral to the prezygapophyses (pr.z.). The cotyle (co.) of this vertebra is elliptical of shape and directed slightly anteroventrally. The part of the supraneural plate that belongs to this vertebra is thicker in comparison to the rest.

The transverse processes (t.p.) of the first three notarial dorsals are thick and their distal extremities narrow strongly relative to the transverse processes of the fourth dorsal. The transverse processes of the third and fourth notarial dorsals are situated slightly more posteriorly relative to the other vertebrae. The transverse processes of the last dorsal is orientated more anteriorly than the others, and the relatively big and flat transverse process is orientated slightly laterally, relative to the previous ones. The articular area for the rib (rib.) is

oval, convex and orientated anteroventrally. The small part of the neural canal that is to distinguish from the damaged posterior aspect suggests a triangular shape.

Comparison: Few notaria from Brazil have been described (Frey & Martill, 1994; Wellnhofer *et al.*, 1983). The notarium in *Santanadactylus brasiliensis* De Buisonjé, 1980 (figure 2.13) is included in this genus on the basis of its size (Wellnhofer *et al.*, 1983). The notarium is composed of five vertebrae because Wellnhofer *et al.* (1983) concluded that the first notarial vertebra, *i.e.*, the last cervical, does not take part in the notarium, in contrast with *Co. spielbergi*. The scapular articulation is situated dorsal to the fourth notarial dorsal, the same as in *Co. spielbergi*. The neural spines of the vertebrae in *Co. spielbergi* form a stout supraneural plate, but the neural spines in *S. brasiliensis* are not completely fused.

Anhanguera santanae (AMNH 22555) lacks a notarium. Another specimen of *An. santanae* (BSP 1982 I 91) lacks a co-ossified notarium too (Wellnhofer, 1985, 1991b), as well as the juvenile *Co. piscator*. The scapular articulation, however, is situated at the fourth notarial dorsal in *An. santanae* (AMNH 22555) as well as in *Co. spielbergi*.

The notarium in *Arthurdactylus conandoylei* Frey & Martill, 1994, is characterised by "three fused neural spines, two of them serving as attachment site for the very broad scapulae" (Frey & Martill, 1994: 395).

Dorsals

There are seven isolated dorsals (number 6–12), which are similar in morphology (figure 2.14; table 2.10). Therefore, the morphology of the sixth dorsal, which is the first free dorsal, is described in detail and the subsequent dorsals are discussed by focussing on the differences with the sixth dorsal.

The neural spine (n.s.) of the sixth dorsal is high and slender, occupying 40% of the total height. The dorsal edge is slightly convex. The prezygapophyses, which are situated slightly ventrally relative to the postzygapophyses (po.z), point anterodorsally, but less so than the postzygapophyses. The prezygapophyses are located anterodorsally relative to the transverse processes. The area dorsal to the prezygapophyses and ventral to the neural canal is slightly sunken. The depressed area ventral and lateroventral to the postzygapophyses is large, but less deep relative to the seventh cervical. The comparatively large neural canal is circular and the bottom of the neural canal is deeply dented. The ventral aspects of the transverse processes extend concave towards the centrum and taper laterally. The lateralmost extremities point slightly ventrally. The articulation surface with the rib is slightly oval with its pointed aspect orientated posteriorly and slightly posterodorsally. The elongated slender centrum has laterally expanding cotyles and condyles. The ventral aspect of the centrum is concave longitudinally and convex transversely. The condyle is convex and elliptical of shape. Seen from posteriorly, it partially obscures the neural canal. The cotyle is concave and bean-shaped, and the ventral and lateral edges are distinct swollen. The areas lateral to the neural canal taper ventrally. The dorsal margin of the cotyle changes into these areas lateral to the canal.

Dorsals seven to 12 differ from the sixth dorsal in having a more posterodorsal orientation of the posterior aspect of their neural spine. The prezygapophyses are situated slightly ventral to the transverse processes and are less close together. The area between these prezygapophyses is less deeply sunken. The postzygapophyses are less close together as well. The condyle is smaller laterodorsally as well as dorsoventrally. The centra are less elongated, but slightly more concave in sagittal plane.

Comparison: Unfortunately, no detailed comparison is possible with the dorsals in *An. santanae* (AMNH 22555) due to their damaged state. Wellnhofer (1991b) counted 13 dorsals

in *An. santanae* (AMNH 22555). If this number is correct, it differs from the new species (12 dorsals). The comparison with another specimen of *An. santanae* (BSP 1982 I 91) suggests a high degree of resemblance. *Coloborhynchus spielbergi* has seven dorsals in total (12 with the dorsals of the notarium included and 16 when the dorsals of the pelvis are also counted). The only preserved, first five dorsals in *Co. piscator* are not fused into a notarium (see above).

Synsacrum

The synsacrum consist of at least six, but possibly seven, vertebrae, which are fused with their centra and zygapophyses (figure 2.15, 2.16; table 2.11). The vertebrae are sacrals, characterised by the fused neural spines (though the spine of the first is not fused to the others), and the short, broad and fused transverse processes—sacral ribs (s.p.) which are firmly fused to the pelvic girdle. It is unclear whether there is a seventh vertebra (caudal vertebra?) due to the damaged state of the posterior part of the synsacrum.

The sacral processes increase in width continuously towards the pelvic girdle. The oval openings between the subsequent processes decrease in size posteriorly. The length, *i.e.*, the transverse measurement, of the processes is largest in the anteriormost of these vertebrae. The length of the processes of the subsequent vertebrae decreases continuously. The first sacral shows both prezygapophyses as well as an incomplete cotyle. The width of the centrum of the first vertebra is largest, whereas the width of the subsequent centra decreases. The dorsal extremities of the neural spines of the last five sacrals are fused with their dorsalmost edges, forming a dorsoventrally small, supraneural plate, with large oval interprocessal foramina (in.pr.for.) between the individual neural spines.

Comparison: The neural spines of the different sacrals are not fused in *An. santanae* (AMNH 22555; figure 2.17A) (Wellnhofer, 1988, 1991b), but the fusion of the sacral processes with the pelvic girdle is equally complete. The synsacrum in AMNH 22555 consists of five sacrals.

In the partially preserved pterodactyloid pelvis AMNH 22569 (Bennett, 1990) (figure 2.17B) the number of fused vertebrae is nine, but only five are sacrals. Though the centra are fused, the neural spines are broken and the presence of a supraneural plate in AMNH 22569 cannot be confirmed.

The unfused state of the sacral processes is one of the obvious differences between the badly preserved synsacrum in *Art. conandoylei* (figure 2.17C) and *Co. spielbergi*, besides the lack of a supraneural plate in the former. Furthermore, the openings between the sacral processes are larger in *Art. conandoylei*.

Co. piscator (figure 2.17D) possibly has five sacrals, against six in *Co. spielbergi*. The sacrals of *Co. piscator* are not fused, neither with their centra nor with their spines. The openings between the sacral processes are larger. The transverse size difference between the anterior and posterior vertebrae is comparatively larger relative to *Co. spielbergi*.

Ribs

Four pieces of cervical rib (figure 2.18A; table 2.12) are preserved, of which three still bear, albeit only partly, the proximal articulation areas. The four pieces are identified as a cervical rib because the capitulum has a strong ventral orientation and the rib itself is comparatively broad. The shaft, arched dorsally and caudally, has a strong oval cross-section. The area between the capitulum and the tuberculum consists of very thin bone.

A small piece of hollow bone (figure 2.18B), highly oval and bent at one of the sides, is a piece of notarial rib (first right). The bending is orientated towards the proximal articular

surface. The bone is broken slightly proximal to the beginning of the bending. Its width is 11 mm and its preserved length 100 mm.

Comparison: The pieces of cervical rib are nearly identical to those of *An. santanae* (AMNH 22555) and *Co. piscator*. The notarial ribs are the first one noticed in these pterosaurs, but were reported by Bennett (2001) in *Pteranodon*.

Sternum

The sternum consists of a large, strongly developed anteroventral process and a large, thin posterior plate, which is slightly twisted in sagittal plane (figures 2.19–2.21; table 2.13). The cristospine extends strongly ventrally and anteriorly relative to the posterior plate (pl). Seen from a lateral position, the anterior part of the cristospine extends more horizontally than the posterior part, starting immediately anteroventrally of the coracoid facet (c.f.). Slightly posterior to this point the cristospine broadens, gaining its largest width halfway its length. The anterior aspect of the spine is orientated posterodorsally. The anteroventral aspect of the cristospine is slightly convex. The laterally sloping, anteroventral part ends at the lateral aspects of the cristospine in slightly swollen ridges. The cristospine is covered with muscle marks, most clearly visible at the anterior aspect.

The left anterior margin extends with a smooth concave curve towards the edge of the posterior plate and the anterolateral corner points anteriorly. The posterior plate is rounded triangular and in contact with the cristospine between the coracoid facets, which are anteriorly buttressed by stout, dorsally extending processes. These processes are separated from the facets by distinct swollen, lateral extending edges. The saddle-shaped coracoid facets are arranged symmetrically at the laterodorsal aspects and are orientated anteroventrally. A small sunken area posteromedial to the coracoid facets has a small foramen. A large foramen that opens into the body of the posterior plate is still partly filled with matrix.

Comparison: Although several unpublished sterna are known, only the sternum in *Co. piscator* (figure 2.21) has been published, of which the posterior plate is less complete than that described above, although the cristospine is better preserved. The overall measurements in *Co. spielbergi* are larger. The posterior plate in *Co. piscator* is more rectangular instead of rounded triangular. The ventral aspect of the cristospine is flatter in *Co. spielbergi* (against convex in *Co. piscator*), but the ridge at the anterior aspect of the cristospine, extending from left to right and from dorsal to ventral, is more prominent in *Co. piscator*. Furthermore, *Co. spielbergi* lacks the small processes on the anterior edge of the spine for the attachment of a supposedly cartilaginous extension, visible in *Co. piscator* (Kellner & Tomida, 2000).

2.4.3. Pectoral girdle and forelimb (figures 2.22–2.33; tables 2.14–2.20)

Scapulocoracoid

The scapula and coracoid are firmly co-ossified and form a scapulocoracoid (figure 2.22; table 2.14). The scapula is strong, thick and short, and the coracoid is much thinner and longer. The general morphology is well known and agrees well with previously described specimens (Kellner & Tomida, 2000; Wellnhofer, 1985, 1991b).

Comparison: The most important difference between the shoulder girdles in *An. santanae* (BSP 1982 I 91), *An. santanae* (AMNH 22555; figure 2.23B) and *Co. spielbergi* is that in the latter it is firmly co-ossified into a scapulocoracoid, whereas it is not co-ossified in the *Anhanguera* species. Similarly, scapula and coracoid in *Co. piscator* (figure 2.23C) share the same morphology as *Anhanguera*. However, the glenoid fossa in *Co. spielbergi* is deeper

and more pronounced, and the shaft of the scapula is narrower than in the aforementioned taxa. The larger Cretaceous Pterodactyloidea possess a large longitudinal foramen at the posterior aspect of the scapulocoracoid (De Buissonjé, 1980). Wellnhofer (1991b) noticed such a foramen in *S. brasilensis* (BSP 1987 I 65; figure 2.23A). Though such a foramen is also observed at the scapulocoracoid in *Co. spielbergi*, it is a shallow one. The glenoid fossae in *Co. spielbergi* and in *An. santanae* (AMNH 22555) have more prominent overhanging borders than is seen in *S. brasilensis*, and is more comparable to *Co. piscator*. The process at the anterior aspect of the coracoid is more prominent in *Co. spielbergi* than in *S. brasilensis* (BSP 1987 I 65) and *Co. piscator*. The supraneural plate articulation in *Co. spielbergi* is more circular when compared to the stronger elliptical surface in *S. brasilensis* (BSP 1987 I 65). The scapular shaft is curved more strongly in *S. brasilensis*.

The overall size is largest for *Co. spielbergi*. The length of the scapula is 38% of the total length of the scapulocoracoid. Despite the differences in measurements in various Cretaceous Brazilian pterosaurs, this ratio is always between roughly 35 and 40%. Also the length of the coracoid and the length of the scapulocoracoid are, as far as could be calculated, in comparable ratios, but larger than the ratio calculated for the scapula. This suggests that there is little space for variation in the ratios of the shoulder girdle.

Humerus

The humerus is a part of the post-cranial skeleton that has been commonly described (e.g. Kellner & Tomida, 2000; Veldmeijer, 2002; Wellnhofer, 1985, 1991b) and a detailed description is therefore not presented. It is a comparatively short, but robust bone (figures 2.24, 2.25; table 2.15; 2.18). It has a convex head, expanded distal end and a large deltopectoral crest.

The head (h.) is kidney-shaped and has a convex articular surface; a faint, shallow ridge separates the concave ventral area from the convex dorsal area. The posterior tuberosity (post.tub.) extends towards the head. It is a large expansion, relative to the head itself, but substantially smaller relative to the deltopectoral crest (del.cr.). The transition between the shaft and the tuberosity is fluent but a difference in angle is noticeable between the head and the tuberosity. A large pneumatic foramen is situated at the dorsal aspect and penetrates the bone distally.

Seen from a ventral position, the deltopectoral crest starts as a thin ridge proximally, but develops into a broad plane ventrodistally. The plane of the strongly developed crest is rough and shows large junctures for the attachment of powerful muscles. The deltopectoral crest is slightly turned inwards (i.e., in a proximal direction) and the rim is straight, but the crest is incomplete and damaged at the rim.

In the anteroposterior plane, the extension of the proximal end is stronger than that of the distal end. A scar proximal to the deltopectoral crest at roughly three quarters of the length is identified as the supracondylar process (sup.pr.). Slightly posterior to this process is a second muscle scar, which is less pronounced. The distal aspect is dominated by the large pneumatic foramen, flanked by the capitulum (cap.) anteriorly and by the trochlea (tr.) ventrally.

Comparison: The humerus of the Leiden *Coloborhynchus* is the largest to be described. The deltopectoral crest in *Co. spielbergi* extends directly from the head, in contrast to *S. brasilensis* (M 4894; figure 2.26A), in which the extension of the crest starts distal to the humeral head, giving it a constricted appearance.

The most important difference between the humeri of *Co. araripensis* (BSP 1982 I 89; figure 2.26B) and *Co. spielbergi* is that the "dünne proximale Rand dieses sehr kraftigen

Fortsatzes geht mit konkaver Linie vom Humeruskopf aus" (Wellnhofer, 1985: 120). The thicker rim in *Co. spielbergi* does not extend as strongly concave from the head. The straight ventral edge of the deltopectoral crest in *Co. spielbergi* differs from the situation in *Co. araripensis* (BSP 1982 I 89) and *S. pricei* (BSP 1980 I 43, AMNH 22552; figures 2.26D, E) (convex), and more closely resembles *S. brasiliensis*. However, the humerus of the Leiden specimen is damaged and little value can be credited to this feature. The middle portion of the deltopectoral crest is not bent inwards, *i.e.*, in posterior direction, as severely as in *S. brasiliensis*. The almost straight ventral margin of the proximal and middle portions of the deltopectoral crest was regarded by Kellner & Tomida (2000) as a possible apomorphy. The humeral head in *Santanadactylus* has a distinct ridge, which is absent in *Anhanguera*, but poorly defined in the Leiden *Coloborhynchus*. Kellner & Tomida (2000) suggested that this might be an ontogenetic feature developing towards maturity, as opposed to the view of Wellnhofer (1991b), who regarded this as a diagnostic feature in *Santanadactylus*. Due to the reclassification of *S. araripensis* as *Co. araripensis*⁹, this feature is seen in *Coloborhynchus* as well. The skeleton of the Leiden specimen displays a high degree of co-ossification and must be regarded as an adult, perhaps an older individual. Thus it is unlikely that the presence of a ridge is ontogenetic because this specimen lacks such a feature. Because of the degree of co-ossification it is suggested that the fusion of the epiphyses occurred very late in the ontogenetic sequence.

One humerus of *An. santanae* (AMNH 225525: figure 2.26C) is known. The humeral head is more comparable to that of *Co. spielbergi* than the humerus of *Santanadactylus*; the lack of a distinct ridge is most conspicuous. However, the proximal edge is more strongly concave and the deltopectoral crest is stronger turned inwards (*i.e.*, in a posterior direction). The posterior tuberosity is less strongly developed.

The humerus in *S. pricei* is substantially smaller than that of *Co. spielbergi* and the shaft has a stronger circular cross-section. The ratio of the smallest width of the shaft to length of the humerus is slightly higher (13% against 12% in *Co. spielbergi*). The proximal aspect shows a broad and short posterior tuberosity relative to *Co. spielbergi*. The head is set stronger dorsally.

The humerus in *Co. piscator* (figure 2.26F) is highly comparable to *Co. spielbergi*. The deltopectoral crest has a strongly concave rim and the crest is more strongly turned inwards.

Ulna

The ulna is a long and comparatively robust bone (figures 2.27, 2.28; tables 2.16, 2.18). The shaft is straight and the ends are expanded. It has an elliptical cross-section in the anteroposterior plane. No pneumatic foramen is observed, although the places where foramina are often situated (anterior aspect, close to the proximal articulation area) are damaged.

The proximal aspect is dominated by the cotyles, separated from each other by a ridge. Seen from the anterior, the biceps tubercle (b.t.) is strong developed and starts about 50 mm distal to the proximal aspect. It extends towards the trochlear cotyle (tr.cot.) at the proximal aspect. At the opposite side is a large, low protrusion, relative to the tubercle, which is the capitular cotyle (cap.cot.).

Seen from a ventral perspective, at approximately one third from the proximal aspect, a sharp ridge extends to the middle of the length of the bone. It has a smooth surface without roughness. It is tentatively suggested that this is an attachment for interosseus membrane (in.os.mem.) (see Bennett, 2001).

Comparison: The ulna is a comparatively featureless bone, which has a low diagnostic value (Veldmeijer, 2002), which is even further limited by the incompleteness of the Leiden specimen. Nevertheless, RGM 401 880 is the longest ulna from Brazil published so far.

The damaged distal end of *Co. spielbergi* hampers a detailed comparison with *Co. araripensis* (BSP 1982 I 89). The cross-section of the ulna of *Co. araripensis* is circular.

Differences with *S. pricei* are, besides the large size difference (the ulna of *S. pricei* is smaller), that the proximal end in *S. pricei* is less expanded, especially the side of the capitular cotyle. The shaft of the new species is less strongly bent and the cotyles at the proximal aspect are comparatively smaller.

The ulna in *An. santanae* (BSP 1982 I 90) shows a slight backward bending of the proximal end. The shaft has a circular cross-section, against elliptical in *Co. spielbergi*.

The ulna in *Co. piscator* is comparable. The "sharp ventral crest on the distal articulation of ulna" (Kellner & Tomida, 2000: 7), mentioned as a diagnostic feature, is not depicted and hence no comparison can be done.

Radius

The general morphology is similar to that of other described radii (Kellner & Tomida, 2000). The radius is the most slender bone of the ulna/radius complex (figures 2.29, 2.30; table 17, 18), having a diameter less than half of that of the ulna. The radius is slightly shorter than the ulna and the cross-section is strong elliptical. Both ends expand in venterodorsal plane. The radius lies close to the ulna.

Comparison: The radius is large relative to the compared specimens. The radii in *Co. araripensis* (BSP 1982 I 89) and *S. pricei* show few differences to each other and *Co. spielbergi*. The biceps tubercle in *Co. spielbergi* is stronger developed and the radius in *S. pricei* is far more circular in cross-section. The distal end in *S. pricei* is less expanded. The diameter is about half the diameter of the ulna.

The radius in *An. santanae* (BSP 1982 I 90) is very comparable to *Co. spielbergi*. The stop against bending (st.), however, is far more distinct in *Co. spielbergi*. The diameter in *An. santanae* (AMNH 22555) is larger than half the diameter of the ulna, but the measurements are made more closely to the distal end rather than the middle (= smallest width). The distal articulation surface in *Co. piscator* is less clearly defined and the stop is less pronounced. The ventral expansion is slightly stronger.

The ratio width-length of the radius varies substantially in various pterosaurs, whereas that of the ulnae does not. The biometric comparison of the humerus and ulna/radius of different Brazilian pterosaurs shows that the ratio length humerus to length ulna/radius (of the total length humerus/ulna/radius-complex; figure 2.18A) is comparable. Only the humerus in *Co. araripensis* (BSP 1982 I 89) is less than 40% of the total length. The different ratios in *Art. conandoylei* are due to the different measurements of the humerus (Frey & Martill, 1994). More obvious differences are observed in the ratios of the length of the scapula, humerus and ulna/radius relative to the total length of the bones (figure 2.18B). The relative length of the scapula in *Art. conandoylei* is shortest. In all but one species, *Co. piscator*, the scapula-humerus occupies about 50% of the total length of the scapula-humerus-ulna/radius, despite differences of the relative length of the scapula.

Carpus

Carpal bones are robust and commonly preserved. Their general morphology in *Co. spielbergi* agrees with published material (Kellner & Tomida, 2000; Wellnhofer, 1985,

1991b) (figures 2.31, 2.32; table 2.19). In RGM 401 880, the proximal syncarpal is completely co-ossified.

Comparison: The proximal syncarpal in *Co. spielbergi* shows more resemblance to *Co. araripensis* (BSP 1982 I 89; figure 2.32A) than to the various species of *Anhanguera*. In both *Co. spielbergi* and *Co. araripensis* the carpals are firmly fused.

The only preserved proximal syncarpal in a *Santanadactylus* is in *S. pricei* (AMNH 22552; figure 2.32B). The articular facet with the radius is responsible for an extension dorsal to the ulnar tubercle. Consequently, the tubercle is situated more strongly ventrally relative to *Co. spielbergi*. Furthermore, seen from a distal perspective, the syncarpal becomes distinct smaller in a ventral direction. Although this is also visible in *Co. spielbergi*, it is less strongly developed. The overall size of the syncarpal in *S. pricei* is smaller.

The syncarpal is not completely fused in *An. santanae* (figures 2.32C, D) and *Co. piscator* (figure 2.32E). The syncarpal is comparable with *An. santanae* although the articular facet for the ulna is more clearly defined in *Co. spielbergi* and *An. santanae* (BSP 1982 I 89), than in *An. santanae* (AMNH 22555).

Metacarpals, phalanges and unguals

Two bones lie close to each other; as preserved the smaller one is one third of the length of the larger one (figure 2.33A, B; table 2.20). This larger bone fragment is straight and circular in shape. These two bones may be the first and third metacarpalia (*cf.* Wellnhofer, 1991b). Between the two fragments are traces of another bone, now lost, interpreted as the second metacarpal. Another piece of bone, though not illustrated, is attached at the reverse of the matrix. Its inner side reveals the trabecular system.

A small complete bone is identified as the third phalanx of the third digit (figure 2.33B, table 2.20), based on the comparison with *S. pricei* (AMNH 22552). A small piece of the second phalanx still contact the proximal end. The bone has a slender shaft, but broadens rapidly towards the proximal and distal ends. The proximal end is the more strongly developed one. The shaft has a rounded square cross-section. Seen from a distal perspective, a shallow groove continues onto the anterior aspect.

None of the claws (figure 2.33C; table 2.20) can be assigned with certainty to a digit, which are not preserved. The curvature of the smallest claw is the strongest. A groove on both sides of the claw separates the flexor tubercles from the body. The flexor tubercles are comparatively shallow and most strongly developed in the smallest claw.

2.4.4. Pelvic girdle and hind limb (figures 2.15, 2.16, 2.34–2.37; tables 2.11, 2.21–2.22)

Pelvic girdle

The anterior blade of the ilium (b.il.) is long (half the length in sagittal plane) and extends anteriorly with a curvature in a dorsal direction (figures 2.15, 2.16; table 2.11). Posteriorly, it tapers, reaching its smallest width at the articulation with the synsacrum. The blade is triangular in cross-section of which the dorsal line declines medially with a slight concave course. The postacetabular process (po.ac.il.) develops dorsal to the anterior rim of the acetabulum (ac.), extends posteromedially–anterolaterally and reaches the highest point posterodorsal to the acetabulum. The dorsal border is convex. Ventrally, the postacetabular process is thickened posterodorsal to the acetabulum, where the ilium meets the ischium (is.). Sutures cannot be identified, but the vaguely swollen line indicates that the ilium forms the dorsal half of the acetabulum.

The pubis (pub.) and ischium form the posterolateral and posterior aspects of the pelvis. The pubis extends from the area anteroventral to the acetabulum, the united sacral rib and transverse process, in a concave line in posteroventral direction. The pubis has a small, distinct tubercle ventral to the acetabulum. The dorsal part of the pubis forms the anteroventral part of the acetabulum. The obturator foramen (o.f.) is located posteroventrally to the acetabulum in a slightly depressed area, which is created by the medial orientation of the posterior part of the pubis. The ventral aspect of the pubis, the articulation area for the prepubes, ends 55 mm ventral to the centrum of the acetabulum.

The ischium and pubis are partially fused and separated by an opening, the ischiopubic fenestra (is.fen.). Part of the suture between the ischium and pubis is visible posterodorsally and anteroventrally to the obturator foramen. No suture is visible in the acetabulum itself, but the swollen line indicates that the posteroventral part of the acetabulum consists of the ischium. The left and right ischia close the pelvis posteroventrally and establish a strong symphysis (sym). The ischia taper posteroventrally, making a stronger angle than the two pubes, which close the pelvis ventrally. The ischial symphysis is V-shaped (anteroventrally) and forms a flat surface.

Comparison: Four pterosaur pelvises have been described from the Santana Formation. For a comparison between the pelvises of *Art. conandoylei*, *An. santanae* (AMNH 22555) and AMNH 22569, see also Frey & Martill (1994). The pelvis of RGM 401 880 is larger relative to the compared specimens.

There are several distinct differences between the pelvis in *An. santanae* (AMNH 22555; 2.17A) and *Co. spielbergi*. The ventral connection of the left and right pubis of the pelvis is not seen in *An. santanae*. The ischium and pubis in *Co. spielbergi* form an ischiopubic plate, also seen in AMNH 22569 (figure 2.17B) and *Art. conandoylei* (figure 2.17C). The anterior blade of the ilium inclines more strongly medially in *An. santanae*.

Seen from a dorsal perspective, the reconstructed anterior blade of the ilium extends more strongly medially. The pelvis does not show an ischiopubic fenestra. It remains uncertain, despite the reconstructions of Bennett (1990) based on *Pteranodon* and of Frey & Martill (1994), whether the neural spines were fused into a supraneural plate. The "striking resemblance" observed by Bennett (1990: 81) between the Santana pelvis AMNH 22569 and that of *Pteranodon* (*cf.* Eaton, 1903, 1910) let Bennett to conclude that pelvises are non-diagnostic but this is likely a premature conclusion (*cf.* Frey & Martill, 1994). However, the pelvis AMNH 22569 is far more *Pteranodon*-like than any of the other pelvises.

The unfused state of the pelvis in *Co. piscator* (figure 2.17D) is in contrast with the firmly fused condition in *Co. spielbergi*. Furthermore, the ventral symphysis of the left and right pubis is not seen in *Co. piscator*, as is the ventral symphysis of the left and right ischium. The anterior border of the postacetabular process extends more strongly ventrally, which results in a flatter course of the ilium. Although Kellner & Tomida (2000) did not present measurements of the pelvis, it could be deduced from the illustration that the overall size of *Co. piscator* is smaller.¹⁰

Femur

The femur is a short, relative to the ulna/radius, and slender bone, which is slightly bent (figures 2.34, 2.35; table 2.21). The head is separated from the shaft by a constricted neck.

The constricted neck (n) extends into the greater trochanter (g.t.) at the lateral aspect of the femur. The proximal aspect of the strongly developed trochanter is slender relative to the femoral neck and shaft. Distally it widens to fuse with the shaft at 50 mm, measured from the proximal edge of the greater trochanter. The trochanter is flanked at the posterolateral and

anteromedial aspects by distinct, shallow grooves. The depression between the head and the trochanter is identified as an intertrochanteric fossa (in.fos.). Approximately in the centre, at the posterior aspect, is the fourth trochanter (f.t.) consisting of a well defined groove.

The lateral (lat.cond.) and medial (med.cond.) condyles are rounded protrusions at the distal end and posterior aspect. They are separated by a distinct intercondylar sulcus. The medial condyle is slightly more bulbous relative to the lateral condyle and extends further posterodistally. Small tubercles are situated laterodorsally to the lateral condyle (lat.ep.) and mediodorsally to the medial condyle (med.co.). Seen from a posterior perspective, the epicondyles are separated by a large, but shallow, oval depression (pop.fos.) relative to the length of the condyles.

Seen from an anterior perspective, the patellar sulcus (pat.sul.) at the distal end is shallow compared to the more distally situated intercondylar sulcus (in.sul.). The lateral side of this sulcus is well defined.

Comparison: Femora of pterosaurs are not often reported, but a detailed description was provided by Kellner & Tomida (2000) with which the general morphology compares well. The femur in *Co. piscator* is shorter than that of *Co. spielbergi*. The sulcus at the head is deeper and longer in *Co. spielbergi*, and the patellar sulcus and popliteal sulcus are more distinct, as well as the features at the distal aspect.

Tibia

The tibia is more slender than the femur and slightly bent (figures 2.36, 2.37; table 2.22). The damaged distal end expands posteriorly and laterally. The lateral expansion is stronger relative to the posterior expansion. The lateral and medial condyles are separated by a gentle intercondylar sulcus.

Comparison: Tibiae are seldom preserved and the described tibiae of *Co. piscator* are the only ones known from Brazil. The general morphology is however, highly comparable. The tibia of *Co. piscator* is shorter and the tuberosity at the posterior end lacks in *Co. spielbergi*.

2.5. Discussion and conclusion

The Leiden pterosaur is not classified as *Criorhynchus* because of the lack of expansion, the different configuration of the anterior aspect, the difference in mandibular groove and the different dentition pattern. The most obvious difference between *Co. spielbergi* and *Brasileodactylus* are the lack of crests, the different mandibular groove and the anterior expansion. *Cearadactylus* differs because of the lack of crests and the differences in teeth-bearing parts. *Santanadactylus* differs in size and in having a distinct ridge at the humeral head. Comparison with *Art. conandoylei* shows the size difference to be considerable and there are distinct differences in pelvis. *Coloborhynchus spielbergi* differs from *Anhanguera* mainly because of the morphology of the anterior part of the skull (blunt anterior aspect with teeth protruding and crest starting at the anterior aspect) and the configuration of the mandibular groove (the groove in *Anhanguera* is flanked by small ridges, in contrast to *Coloborhynchus*). The specimen (RGM 401 880) in the National Museum of Natural History, Leiden, The Netherlands, is regarded as *Coloborhynchus* because all the diagnostic features of the type genus are apparent (but see below). It is considered to be a new species, differing from *Co. clavirostris*, *Co. robustus*, *Co. araripensis* and *Co. piscator* in having markedly weaker (almost absent) mandibular groove and palatinal ridge. The mandibular groove does not extend onto the anterior expansion as seen in *Co. robustus*. The rami in *Co. spielbergi* are

distinctly bent. It is not clear if *Co. spielbergi* has a pterygoid process as seen in *Co. araripensis* due to the incompleteness of the palatal region in the RGM specimen. *Coloborhynchus spielbergi* and *Co. piscator* (the latter surely not fully-grown but the largest known specimen) differ in size and morphology of the sterna. Furthermore, the dentition of the lower jaw in *Co. piscator* (the anterior eighth) is larger than the dentition of the skull. This, however, might be due to its ontogenetic state.

The following remarks on Brazilian pterosaurs are made in the light of the systematic classification of the present pterosaur and the new insights gained from its study. According to Wellnhofer (1978), morphology of the sternum is diagnostic at the generic level. Because *Co. piscator* is a species of *Coloborhynchus* (see below), and the sternum of *Co. spielbergi* differs from that of *Co. piscator*, it is regarded as diagnostic at the species level.

Although post-cranial material is known to have a limited diagnostic value, humeri are often used to differentiate between pterosaurs, but their diagnostic value appears to be more limited than previously thought. Minor differences, as for instance the thickness of the proximal edge of the deltopectoral crest and its inward (*i.e.*, posterior direction) orientation, might be explained as individual variation (see also Veldmeijer, 2002).

The diagnosis of the type specimen of *Coloborhynchus* needs reviewing. The depression at the anterior aspect is not seen in *Co. araripensis*.¹¹ Differences between *Anhanguera* and *Coloborhynchus* are limited. The expansion in *Coloborhynchus* is robust, but in *Anhanguera* is slight. The premaxillary crest in fully-grown specimens of *Anhanguera* starts distinct posterior to the tip of the snout and extends to the anterior border of the nasoantorbital fenestra. The tip of the snout is dorsoventrally compressed, leaving no space for teeth anteriorly. Only one species can be definitely assigned to *Anhanguera* (*An. blittersdorffi*), whereas *An. santanae* (AMNH 22555) might be an immature stage of *Coloborhynchus* (see below).

All known species hitherto assigned to *Anhanguera* display an unfused state of the skeleton (see below) except *An. blittersdorffi* (Campos & Kellner, 1985b), which is only represented by cranial material. Possibly, the skull was first to fuse completely and perhaps early in the ontogeny of pterodactyloids (Kellner & Tomida, 2000). This makes it uncertain whether *An. blittersdorffi* was an adult with a completely fused skeleton, as seen in *Co. spielbergi*, or close to adulthood with still unfused post-cranial parts.

The lack of a notarium in *An. santanae* (AMNH 22555) was explained thus by Wellnhofer (1991b: 58): "Allerdings ist eine Tendenz hierzu [co-ossification of the first five dorsals] erkennbar, so daß nicht auszuschließen ist, daß bei weiterem Wachstum bzw. höherem Lebensalter des Individuums eine Verschmelzung dieser Wirbel eingetreten wäre." The holotype and another specimen of *An. santanae* (BSP 1982 I 90 and 1982 I 91) and the described specimen of *Co. piscator* all lack a co-ossified notarium. Further, the carpals of these specimens are unfused and in *Co. piscator* most bones are unfused throughout the skeleton; it is consequently regarded as juvenile (Kellner & Tomida, 2000). However, Wellnhofer (1985) initially used the incomplete fusion as a diagnostic feature for *Anhanguera* although he later regarded this feature as "ontogenetisch sehr spät einsetzenden Koossifizierung [...]" (Wellnhofer, 1991b: 99). It is generally accepted that incomplete fusion is ontogenetic rather than diagnostic, although the diagnosis of *Art. conandoylei* is based for the major part on the degree of fusion (Frey & Martill, 1994). Kellner & Tomida (2000) pointed out that these features are possibly ontogenetic. The number of fossilised juvenile pterosaurs is large, perhaps even more specimens than adult animals. Apparently, being adult did not mean that the animal already had a completely co-ossified skeleton – should we speak, instead, of fully-grown or not?

Bennett (1993, 1994) regarded *Anhanguera* as sub-adults of *Co. araripensis* on the basis of the unfused elements. Although *An. santanae* is represented by non-adult specimens, *An. blittersdorffi* is regarded as adult (but see above) and can therefore not be seen as a sub-adult of *Co. araripensis*.

The comparison of *Anhanguera* and *Co. spielbergi* shows, besides the difference in degree of co-ossification, few distinct differences apart from the shape and position of the premaxillary sagittal crest. It is possible that, in aging, bone accumulated on the crest, especially anteriorly. This would explain the more posterior start of the crest in many specimens. In these specimens then, the bone did not accumulate at that point because the animal was not yet full-grown. This might also explain the concavity at the anterodorsal border of many of the crests. If the animal accumulated bone at the crest during the growing process, this might result in: larger crests as the animal gets closer to being fully-grown, that is, the older it gets; a crest that, when the animal stopped growing, starts at the anteriormost aspect of the skull; and a flat anterior aspect from which teeth could possibly protrude, only seen in fully-grown animals and already in the not fully-grown *Co. piscator*.

The first prediction is confirmed by *Co. spielbergi*, a fully-grown animal, of which the premaxillary crest is largest (in percent of the length of the cranium) relative to the compared *Anhanguera* species. The second prediction is supported by differences in the position of the crests. The premaxillary crest in *An. santanae* (AMNH 22555) starts substantially posterior to the anterior aspect of the skull. The crest in another specimen, SMNK 1136 PAL, referred to by Frey & Martill (1994) as *Anhanguera* sp. has a crest that starts far more anteriorly relative to *An. santanae* (AMNH 22555). However, it does not start at the anteriormost edge of the skull as seen in *Coloborhynchus*.

The third prediction is supported by the two front teeth in *Anhanguera*, which often are already positioned dorsal to the imaginary line made by the rest of the teeth. This is apparent in *An. santanae* (AMNH 22555). It would take only slight alterations to create an anterior aspect as seen in *Coloborhynchus*. The anterior aspect in *Co. piscator* displays a high degree of similarity with *Co. robustus* (SMNK 2302 PAL). The dorsal margin therefore cannot be used as diagnostic feature, but might be ontogenetic.

Unfortunately, Kellner & Tomida (2000: 15) did not describe or illustrate the "texture of the bone surface" of the crests. However, there is no reason to believe that the crests were formerly covered with horny sheets as suggested by Kellner & Tomida (2000) nor extended with wattle-like structures. No trace of the supposed horny sheets is preserved despite the abundant records of the preservation of soft tissue from the Araripe basin. The crests display strong, well defined edges, in contrast to the crests of the skulls of those pterosaurs which did have soft tissue wattle-like extensions, like the Tapejaridae *indet.* in the collection of the Staatliches Museum für Naturkunde at Karlsruhe (Frey & Tischlinger, 2000; pers.obs.; Frey, pers. com.). Finally, no area of attachment can be detected at the crest. Suggestions for the texture of the surface, as described for the crests in *Co. spielbergi* (figure 2.3G), vary from copies of the internal trabecular system to the internal surface of the bony crests (Wellnhofer, pers. comm., on the basis of photographs) to the internal surface of very thin bone in which the outside, few tens of microns, has flaked away during preparation (Martill, pers. com., on the basis of photographs) rather than scars for the anchoring of sheets or soft tissue material. Mader & Kellner (1999) observed rugosities, meandering striations and shallow pits on the anterior part of the cranium of *Siroccopteryx moroccensis* Mader & Kellner, 1999. The description prohibits a comparison with the, in the present work described, condition. However, it seems not unlikely that the features are the same. Mader & Kellner (1999) interpreted the features as pathologic.

If we accept the theory on the creation of crests as a working hypothesis, it is tentatively suggested that the immature *An. santanae* might be young stages of *Coloborhynchus*, rather than *Santanadactylus* as suggested by Bennett (1993). The skull in *An. santanae* (BSP 1982 I 90) shows the posterior start of a crest. Because the anterior extension is not known, the crest cannot be used as diagnostic feature and the generic classification, as either *Anhanguera* or *Coloborhynchus*, is uncertain. Comparison of this specimen with *An. santanae* (AMNH 22555) shows some striking differences. The quadrate in AMNH 22555 is robuster, the lower temporal fenestra smaller, the nasal longer and wider, and the prefrontal extends less far posteriorly. The straight posteroventral back of the skull in *An. santanae* (BSP 1982 I 90) inclines more sharply, through which it has a higher appearance. The back of the skull in *Co. spielbergi* is more comparable to AMNH 22555 than to BSP 1982 I 90. Because the latter is the holotype, it can be questioned whether the classification of AMNH 22555 pterosaur as *An. santanae* is justifiable. The differences as explained are far less compared to the skull in *Co. spielbergi*. Though the skulls suggest close relationships, *Anhanguera* has a pointed snout, and a crest that does not start immediately anterior to the nasoantorbital fenestra and does not extend to the anterior aspect (but see above).

The reconstruction of the mandible in *An. santanae* (AMNH 22555) is not based on studied material because a complete mandible with associated skull is not known, but rather based on the assumptions that because the animal has a premaxillary sagittal crest it had a dentary sagittal crest as well and since the premaxillary crest starts more posteriorly, the dentary crest starts more posteriorly as well. Neither of these assumptions is necessarily true. On the contrary, there are strong indications that the dentary sagittal crest in *Anhanguera* did not start posteriorly at all (*An. blittersdorffi*, referred specimen Kellner & Tomida, 2000; Veldmeijer, pers.obs.¹²), which makes the mandible less easy to diagnose. Differences between the mandible in *Coloborhynchus* and *Anhanguera* include the configuration of the groove at the ventral aspect, which is flanked with tiny raised ridges in the latter.

From the above arguments, it may be that *An. piscator* should be classified as a species of *Coloborhynchus*. It is also relevant that the premaxillary crest in *An. piscator* runs all the way to the anterior aspect of the skull (contra Kellner & Tomida, 2000). Additional support is provided by the flat, though small, anterior aspect of the skull from which two teeth project that are positioned more dorsally relative to the subsequent teeth. It is beyond the scope of this work to discuss the classification of this specimen in detail but the large size alone (the juvenile specimen is as large as for instance the adult *Co. spielbergi*) points to a new, largest known species of the *Coloborhynchus* and is therefore referred to as *Co. piscator*.

Wellnhofer (1985) classified the remains of a large pterosaur (BSP 1982 I 89) as *Santanadactylus araripensis*. Kellner (1990) reclassified this material as *Anhanguera*, because, as stated by Kellner & Tomida (2000: 104): "the preserved dorsal portion of the premaxilla becomes gradually sharper toward the preserved rostral part of the skull, suggesting the presence of a sagittal crest rostral to the nasoantorbital fenestra." Apparently, the presence of a crest was the only reason for the reclassification of the specimen (Kellner & Tomida, 2000: 106; note that "Kellner (1990), [...], referred this taxon to *Anhanguera* (*A. araripensis*) as a member of the Anhangueridae, based on the dorsal margin of the premaxillary crest"). Neither, the presence of a crest nor the posterior start of a crest can be proven; consequently, the specimen cannot be referred to as *Anhanguera*. Conversely, the referred specimen has a crest, but the anterior aspect is distinctly different from *Anhanguera*. The resemblance between the holotype (BSP 1982 I 89), the referred specimen (MN 4735-V; see Kellner & Tomida, 2000) and a complete skull in the Oberli collection Switzerland (SAO 16494) has been pointed elsewhere.¹³ Consequently, *S. araripensis* is reclassified as

Coloborhynchus araripensis. In doing this, the suggestion that *S. araripensis* might be identical to *Brasileodactylus* (e.g. Wellnhofer, 1991b) can be rejected.

Tropeognathus robustus (Wellnhofer, 1987) was classified as *Anhanguera robustus* by Kellner & Campos (1989; see also Kellner & Tomida, 2000). However, Veldmeijer (1998), reclassified the mandible as *Co. robustus* on the basis of the comparison with *Co. spielbergi* and *Co. robustus* (SMNK 2302 PAL; see also Fastnacht, 2001).

Tropeognathus mesembrinus is distinct from all other *Coloborhynchus* and *Anhanguera* species. Though regarded as valid taxon by Kellner & Tomida (2000), a recent study by Fastnacht (2001) reclassified it as *Criorhynchus mesembrinus*.

Although ratios are helpful in pointing out differences they can only be used with reserve because pterosaurs display true allometry (Brower & Veinus, 1981) and there is still debate as to whether some specimens are juveniles, sub-adults or adults, so it is even more difficult to establish ratios for a specific species. Further, there are too few specimens of the same species that are determined in order to have a statistically reliable picture.

The reconstruction of the feeding habits and the method of collecting food proposed for crested pterosaurs may be an oversimplification, since all pterosaurs with crests are thought to have collected food in the same way (e.g., Wellnhofer, 1991a). Although this might be true if the position and size of crests is related to age, it is odd that so little attention has been given to changes in functional morphology relative to the position and form of the crests. Crests were probably multifunctional and, may have been a instrument for recognition and courtship display, for example.

The following is a list of toothed pterosaurs from the Santana Formation. For a list of the compared material, which includes non-Brazilian specimens, see the inventory numbers and publications in table 2.23.

Anhanguera blittersdorffi, *An. santanae*

Brasileodactylus araripensis

Cearadactylus atrox, *Ce.? ligabuei*

Coloborhynchus robustus, *Co. spielbergi*, *Co. araripensis*, *Co. piscator*

Santanadactylus brasiliensis, *S. pricei*, "*S.*" *spixi*

Criorhynchus mesembrinus

2.6. Reconstruction (figure 2.38)

The relation between different parts of the skeleton depends on variables such as age and species. However, in making a reliable reconstruction it is assumed that the ratios of related animals are comparable, so variables within species may not be adequately considered.

Figure 2.38 shows different possible shapes of the wings. The preservation of the scapulocoracoid, humerus, ulna/radius and syncarpal allows an estimation of the wingspan. The length of the scapula (table 2.14) is taken as a whole despite the angled position and, therefore, slightly smaller length in left lateral–right lateral plane. The humerus, ulna and radius are preserved in total length (tables 2.15–2.17) as is the proximal syncarpal (table 2.19). Furthermore, some length has to be taken into account for the cartilage. The length of the metacarpals and wing finger has to be reconstructed since these bones were not among those preserved.

The remains of *S. pricei*, *Co. piscator* and *Art. conandoylei* contain the fourth metacarpal and preserved humeri that are close in length to those of *Co. spielbergi* (except for *S. pricei*). The measurement of the proximal syncarpal is taken from Wellnhofer (1991b).

The length of the humerus in *S. pricei* is 167 mm and the length of the fourth metacarpal is 172 mm (*ibidem*). The length of the humerus in *Co. piscator* is 255 mm and the fourth metacarpal measures 256 mm (Kellner & Tomida, 2000). The length of the humerus in *Art. conandoylei* is 230 mm and the length of the metacarpal 227 mm (Frey & Martill, 1994). Consequently, it can be assumed that the length of the fourth metacarpal, the biggest of the metacarpalia, is only slightly smaller in length relative to the humerus and must have been about 285 mm.

The wing finger in *S. pricei* has a total length of at least 1,108 mm, divided over four digits with lengths of 372, 324, 252 and 160 mm, respectively (Wellnhofer, 1991b). The length of the humerus + ulna/radius (412 mm) and the length of the complete wing finger are in the ratio of 1:2.7. The wing finger in *Art. conandoylei* has a total length of 1,434 mm, divided over four digits with lengths of 445, 402, 312 and 275 mm, respectively (Frey & Martill, 1994). The length of the humerus + ulna/radius (542 mm) and the length of the complete wing finger are in the ratio of 1:2.6. The ratios calculated for the different pterosaurs are comparable. Therefore, a ratio of the length humerus + ulna/radius and the length of the complete wing finger of 1:2.6 is proposed for *Co. spielbergi*. The wing finger is reconstructed with a length of 2.6 x length humerus (290 mm) + length ulna/radius (410 mm). The total reconstructed length of the wing finger is 1,820 mm. The reconstructed span of one wing can be estimated by adding 130 (scapula) + 290 (humerus) + 410 (ulna) + 3 (carpal *An. santanae*) + 285 fourth metacarpal, reconstructed) + 1,820 (wing finger, reconstructed) mm, that is 2,938 mm. Allowing for some cartilage, the length of one wing, including the chest since the length of the scapula represents the circumference of the chest, might have been about 2,950 mm. The total wingspan is thus reconstructed at 5,900 mm.

The length of the animal, stretched from top to bottom, can be estimated by reference to the skeleton of *Co. piscator*, which includes the caudal vertebrae. The length of the skull in *Co. spielbergi* is 712 mm (table 2.2). The preserved cervical vertebrae (table 2.8), notarium (table 2.9), dorsals (table 2.10) and synsacrum (table 2.11) have a total length of 72 (seventh and eighth cervical) + 135 (notarium) + 135 (dorsals) + approximately 165 (synsacrum) = 507 mm.

Anhanguera santanae (AMNH 22555) has a complete neck, of which the length of the cervicals that are not preserved in *Co. spielbergi*, the first to sixth can be calculated as 223 mm (Wellnhofer, 1991b). The length of the seventh + eighth cervical (62.5 mm; *ibidem*) and the length of the first to sixth cervical, are in the ratio of 1:3.6.

Coloborhynchus piscator also has a complete preserved neck, of which the length of the cervicals that are not preserved in *Co. spielbergi*, are calculated at 218 mm (Kellner & Tomida, 2000). Assuming that the ratio between the height and length of the seventh cervical is 1:1.5, which is comparable to this ratio in *Co. spielbergi* (1:1.4) and *An. santanae* (AMNH 22555) (1:1.6), an estimated length of the seventh cervical in *Co. piscator* is 45 mm. The reconstructed length of the seventh + eighth cervical (45 + 28; Kellner & Tomida, 2000) and the length of the first up to and including sixth cervical are in the ratio of 1:3.0.

The length of the neck in *Co. spielbergi* is estimated to be 251 mm (76 [table 2.8]), if it is assumed a ratio that is the average of those calculated in *An. santanae* and *Co. piscator*. Allowing some cartilage it seems reasonable to estimate the length of the neck as at least 255 mm.

The eleven caudal vertebrae in *Co. piscator* have a total length of 164 mm although it is not certain whether this was the complete tail (Kellner & Tomida, 2000). It is uncertain whether *Co. spielbergi* had a comparable tail. However, because of the close relationship between *Coloborhynchus* and *Anhanguera*, it is assumed that *Co. spielbergi* possessed a comparable tail. The length of the tail and the reconstructed length of the first eight cervicals

of the neck in *Co. piscator* (see above) are in the ratio of 1:1.6. Assuming a comparable ratio in *Co. spielbergi*, the tail might have been 156.8 mm long. Allowing for some cartilage, a length of 160 mm is assumed. Consequently, the reconstructed length from the tip of the snout to the tip of the tail is estimated at $712 + 255 + 135 + 140$ (dorsals and cartilage) $+ 165 + 160 = 1,567$ mm. The wingspan and length does not take natural bendings of the skeleton into account.

3. Pterosaurs from the Lower Cretaceous of Brazil in the Stuttgart Collection¹⁴

3.1. Introduction

The Staatliches Museum für Naturkunde Stuttgart possesses various specimens of pterosaurs, Rhamphorhynchoids as well as Pterodactyloids, from Germany (Urlichs *et al.*, 1994; Ziegler, 1992). Besides these 'native' pterosaur fossils, the collection incorporates pterosaur remains from the Santana Formation, Brazil.

The material in the collection of the Stuttgart museum is obtained from various people. The mandible with the inventory number SMNS 56994 is obtained from C. Novaes Ferreira, Sao Paulo, Brazil (7–11–1990) by the Stiftung Stadt Stuttgart. The small nodule with the remnants of various arm bones, SMNS 80437, is a gift of W. Ludwig, Stuttgart (23–7–1996) and the humerus and radius with the inventory number SMNS 81976 is obtained from U. Seehuber (28–5–2001). The other bones are obtained in one transaction from a merchant in fossils, K.H. Frickhinger, but it is uncertain whether the bones belonged to one individual. Consequently, the bones are described separately.

The objective of the present work is to present a description and classification of the Brazilian pterosaur material in the collection. All bones are from the Cretaceous period, which precludes a designation as Rhamphorhynchoid pterosaurians.

3.2. Abbreviations

ad.fos.	adductor fossa	f.t.l.	first tooth left
ang.	angular	pn.for.	pneumatic foramen
art.	articular	hum.	humerus
b.t.	?biceps tubercle	i.cond.gr.	humeral intercondylar groove
cap.	humeral head	post.tub.	posterior tuberosity
cond.dors.	dorsal condyle	pre.art.	prearticular
cond.vent.	humeral ventral	ra.	radius
condyle		s.t.l.	second tooth left
cot.dors.	dorsal cotyle	scap.cor.	scapulocoracoideum
cot.lat.	lateral cotyle	su.	surangular
d.sag.cr.	dentary sagittal crest	sul.an.med.	sulcus anconaeus medialis
del.cr.	deltopectoral crest		(Wellnhofer, 1985: 121)
dent.	dentary	sup.pr.	supracondylar process
dent.ra.	dent for radius	ul.	ulna

3.3. Systematic palaeontology, description and comparison

Order Pterosauria Kaup, 1834
Suborder Pterodactyloidea Plieninger, 1901

The described bones are assigned to the suborder Pterodactyloidea. All described and mentioned Brazilian material is from the region of Chapada do Araripe, northeast Brazil, largely situated in the Province of Ceará; its horizon is the Santana Formation in the sense of the former Romualdo Member (Lower Cretaceous, Albian).

3.3.1. Mandible SMNS 56994 (figures 3.1, 3.2; table 3.1)

Family Anhangueridae Campos & Kellner, 1985b
Genus *Criorhynchus* (Owen, 1861)¹⁵

Diagnosis *Criorhynchus* according to Fastnacht (2001: 34): "[...] Lower jaw with mandibular crest on the symphysis. [...] lower jaw not expanded anteriorly"

Criorhynchus mesembrinus (Wellnhofer, 1987)
cf. *Criorhynchus mesembrinus* (Wellnhofer, 1987)

Holotype: Cranium and mandible BSP 1987 I 46, Bayerische Staatssammlung für Paläontologie und historische Geologie, Munich, Germany

Diagnosis *Tropeognathus mesembrinus* according to Wellnhofer (1987: 179): "*Tropeognathus* with high, rounded [...] smaller {than premaxillary sagittal crest} mandibular crest on the symphysis. [...] Deep groove on the mandibular symphysis. [...] lower jaws are not expanded anteriorly. Dentition with [...] 11 {sic} mandibular teeth in each side." Remark: between { } not in original.

Description

The mandible (figure 3.1, 3.2; table 3.1) is partially prepared from its calcareous matrix, exposing the lateral, anterior and ventral aspects completely and the dorsal aspect partially (only the dorsal aspects of the rami are exposed). The medial aspects of the rami are not visible due to the matrix still in place between them. The right retroarticular process is partially restored whereas the left one is restored completely. The ventral edge of the dentary sagittal crest lacks small pieces. The teeth of the anterior part are well preserved although some lack the buccal half. The smaller teeth more posterior (numbered 9–12) are missing, except tooth number 10 at the left side, which is still embedded in matrix.

The mandible shows a high degree of co-ossification and the lateral aspects are characterised by the relief of the attachment areas of the different bones of the mandible. The rami are bent slightly into medial direction. The posterior extremities, of which only the right one is preserved partially, is formed by the retroarticular process and expand strongly medially. Seen from posterior, the dorsal part of the retroarticular process shows a lateral cotyle (cot.lat) that occupies the entire lateromedial width without any internal divisions. The medial half of the lateral cotyle is less broad in dorsoventral plane, relative to the lateral part. The surangular (su.) forms strong dorsal boundaries of the lateral cotyle and overhangs especially the medial half. Seen from dorsal, the surangular commences at the mediodorsal aspect of the rami, at approximately 35 mm from the proximalmost border, and expands rapidly laterally, occupying the complete dorsal width of the rami at the posteriormost part.

The articular (art.) is reconstructed. The praearticular (pre.art.) forms the ventral border of the adductor fossa. The medial aspects of the rami are obscured by matrix, but seen from ventral, the posterior parts of the adductor fossa are still visible. The exact course of the praearticular cannot be established. The elongated angular (ang.) commences at the reconstructed parts at the posterior aspects, the exact posterior border cannot be established, and continues, at the right side, to slightly posterior to the tenth tooth. No suture can be traced anterior to this point. A shallow groove can be traced until slightly

anterior to the tenth tooth, followed by a piece of suture of the dentary (dent.). The dentary extends ventrally, forming a smoothly curved dentary sagittal crest (d.sag.cr.), which continues anteriorly to the anterior aspect of the mandible. The crest, which commences anterior to the symphysis, decreases in width continuously in ventral direction. Seen from lateral, a shale like pattern is to discern ventral to the first up to and including the fourth tooth at the right side. Seen from dorsal, the mandible continues in anterior direction without an increase in width. The measurements of the width vary from 21.0 mm (at the second pair of teeth) to 22.3 mm (at the third pair of teeth). The anterior aspect displays a shallow but distinct depression, venteromedial to the first pair of teeth.

The first pair of teeth is curved posterolingually and point anterodorsally. The second pair of teeth is curved posterolingually as well and the teeth point also anterodorsally, although less strongly anteriorly relative to the first pair of teeth. The following teeth, at least up to the eighth pair of teeth, display a comparable curving although less severe. They point dorsally rather than anterodorsally. The following teeth are not preserved, except the tenth tooth left. This tooth is substantially smaller¹⁶ and does not curve. The alveoli of the ninth up to the twelfth pair of teeth are elliptical and positioned with their long axis anteroposteriorly. The alveoli are positioned at the dorsal aspect of the rami. In contrast, the alveoli of the first eight pair of teeth, which are also elliptical of shape, are placed slightly lateromedially except for the first pair of alveoli, which is placed anterodorsally. The teeth show a continuous decrease in size, based on the measurements of the alveoli, with a continuous increase in diastema size.

Discussion

Few toothed pterosaurs are known from Brazil with dentary sagittal crests. *Criorhynchus mesembrinus* is published by Wellnhofer (1987) and renamed by Fastnacht (2001). *Coloborhynchus robustus* is also described by Wellnhofer (1987) and renamed by Veldmeijer (1998, see also Fastnacht, 2001). Veldmeijer (2003a) published the first *Coloborhynchus* with post-cranial material. Fossils, named as species of *Anhanguera* are described by Campos & Kellner (1985a, b), Kellner & Tomida (2000¹⁷) and Wellnhofer (1985, 1991b). Toothed species without a dentary sagittal crest are *Brasileodactylus* (Kellner, 1984), *Cearadactylus* (Leonardi & Borgomanero, 1985; Dalla Vecchia, 1993). Possibly, *Santanadactylus*, as published by Wellnhofer (1985, 1991b) lacks a crest as well. *Anhanguera* might have had a crest that does not commence at the anterior aspect of the mandible but rather posterior to the anterior aspect and is therefore different (Wellnhofer, 1991b). Recently however, it is suggested that the dentary sagittal crest starts anteriorly as well (see Kellner & Tomida, 2000, figure 66¹⁸). *Pteranodon* does not have a dentary sagittal crest. Furthermore, *Pteranodon* is edentulous, as are Azhdarchidae, Tapejaridae and Nyctosauridae. The teeth of Dsungaripteridae and Pterodaustriidae differ completely from the teeth of the discussed mandible (e.g. Martill *et al.*, 2000; Wellnhofer, 1991a).

The general layouts of the toothed mandible are comparable. A comparison with crested pterosaurs shows that the curvature of the rami is less and the mandible is shorter relative to *Co. spielbergi*. The comparatively long mandible of *Co. robustus* show short rami relative to SMNS 56994. The rami display almost no curving. The powerful teeth of *Co. robustus*, which display a different dentition pattern, clearly distinguish *Coloborhynchus* from the Stuttgart mandible. Furthermore, the mandible of *Coloborhynchus* is anteriorly expanded, in contrast to the straight mandible discussed here. One other species, *Cr. mesembrinus*, has a combination of a dentary sagittal crest, teeth and non-expanding snout as well. The mandible of *Cr. mesembrinus* (BSP 1987 I 46) is

pointed more sharply anteriorly, relative to SMNS 56994, but this is due to the lack of a small part of the left side. Both specimens have the same number of teeth (12) and a comparable dentition pattern. Note that Wellnhofer mentions in his diagnosis erroneously 11 teeth. The curvature of the rami of *Cr. mesembrinus* is slightly less strong relative to *Co. spielbergi* but still stronger relative to SMNS 56994. The main difference between the two mandibles is the size difference. The compared mandible (BSP 1987 I 46) has an estimated (because the retroarticular process is missing) length of 540 mm (Wellnhofer, 1987). The length of the Stuttgart specimen is estimated at 400 mm. This means that the Munich specimen is 35 % larger than the Stuttgart specimen. Although this seems too large a difference to be explained by sexual dimorphism or intraspecific variability, there is too little known at present on these topics to exclude either two possibilities. On the other hand, the lack of identifiable sutures of the Munich specimen suggests a more mature animal than the Stuttgart pterosaur, which might explain the size difference. The difference in ratios¹⁹ seems to support this suggestion but pterosaurs display true allometry (Brower & Veinus, 1981; Wellnhofer, 1970, 1991b). The ratios do not exclude intraspecific variability and are based on individuals only. *Criorhynchus mesembrinus* has a characteristic deep and, towards the symphysis, broad dentary sagittal groove. Because the Stuttgart mandible is not completely freed from its matrix it is proposed, until the remaining matrix is removed and the dorsal aspect is visible, to refer to the mandible as possible (*cf.*) *Cr. mesembrinus*, classified to the Anhangueridae. This systematic interpretation follows Fastnacht (2001) opposed to the classification as *Tr. mesembrinus* in the clade of Anhangueridae by Kellner & Tomida (2000).

3.3.2. Isolated humeri SMNS 55407, 55408, 55409, 55883 (figures 3.3, 3.4; table 3.2)

Humerus SMNS 55407

The right humerus with inventory number SMNS 55407 is incomplete (figure 3.3A, 3.4A; table 3.2). The bone is reconstructed but the transition between the reconstructed parts and bone is hard to distinguish. The reconstruction starts at least 30 mm distal to the deltopectoral crest and extends at least up to 60 mm proximal to the distal aspect. The reconstructions are recognised on the basis of differences of colour and texture. Furthermore, the matrix surrounding the bones might not be the original matrix. The surface is very smooth and there are no signs of preparation. The reverse of the 'nodule' has a far darker yellow colour in contrast with the colour of the matrix of the other bones, and strikes, characteristic for brush strokes, are clearly to recognise. Consequently, there is no certainty whether the proximal and distal parts belong to one bone and therefore no further attention is given to the bone.

Humerus SMNS 55408

Family, genus, species indet.²⁰

The left humerus with inventory number SMNS 55408 is incomplete (figures 3.3B, 3.4B; table 3.2). The bone is still embedded in matrix and only the posterior and dorsal aspects are (partially) visible. The deltopectoral crest is still embedded. A large part of the posterior tuberosity (post.tub.) is missing. The specimen is considered isolated despite the fact that remnants of the ulna and remnants of the scapulocoracoid are still articulated. Isolated from the humerus is a small, straight piece of bone, which cannot be identified due

to its fragmentary state. The head of SMNS 55408 describes a distinct angle compared to the corpus, not unlike SMNS 55883. A further description of the isolated left humerus SMNS 55408 is limited to the measurements. The damaged state of the bones results in the lack of diagnostic features.

Humerus SMNS 55409 (figures 3.3C, 3.4C; table 3.2)

Family Anhangueridae Campos & Kellner, 1985b

Genus *Coloborhynchus* Owen, 1874²¹

Diagnosis *Santanadactylus* according to De Buissonjé (1980: 149): "[...] Humerus with a broad, crescent-shaped proximal articular surface, divided along an oblique line into two areas with slightly different convexity. From the proximal articular surface a gradually broadening deltopectoral radial crest is extending distally along the shaft. A rather low ulnar crest starts at the opposite side of the crescent-shaped proximal surface and extends distally over almost the same length as the radial crest. In the proximal part of its palmar side the humerus is slightly concave lengthwise and deeply concave perpendicular to the shaft. More distally palmar the shaft becomes convex in both directions and becomes nearly circular in cross-section where the distal part of the radial crest meets the shaft. The humerus possesses a wide foramen pneumaticum, two fifth down the ulnar crest on the convex, anconal side. [...]"

Coloborhynchus araripensis (Wellnhofer, 1985)²²

Holotype: BSP 1982 I 89, Bayerische Staatssammlung für Paläontologie und historische Geologie, Munich, Germany. Largely complete skeleton.

Diagnosis *Coloborhynchus araripensis*, according to Wellnhofer (1985: 110): "[...] Oberrand des Processus lateralis des Humerus mit Knick. [...]" (Translation: "Upper edge of the humeral deltopectoral crest with bend.")

Description

The left humerus with inventory number SMNS 55409 (figure 3.3C, 3.4C; table 3.2) is the best preserved humerus in the collection and completely intact. Only superficial damage occurs on the posterior and dorsal aspects. On the other hand, still matrix is attached at the anterior and, to a lesser extent, ventral and dorsal aspects. The humerus is a strong bone with, in anterior and posterior direction expanding, proximal and distal extremities. All condyles and epicondyles are firmly fused with the humerus.

The humeral head is angled relative to the shaft. Seen from proximal, the head is kidney-shaped and divided in a slightly convex dorsal part and a concave ventral part. The transition between the two areas is marked by a kink. The anterior aspect is entirely and the dorsal and ventral aspects partially confined by a characteristic sharp ridge, which is more pronounced anteriorly than dorsally. A distinct but shallow ridge, relative to the aforementioned one, separates the posterior tuberosity from the rest of the head.

Seen from ventral, the ventralmost extension of the strong developed deltopectoral crest extends diagonally distal-proximal and the ventralmost tip is curved in proximal direction. This part of the process is thicker relative to the, in posterior direction bent, ventral edge, which commences from the head and extends towards the ventralmost, curled

tip. The posteroproximal surface of the ventralmost extension of the deltopectoral crest is distinct concave. The ventral aspect of the humerus expands at the opposite side of the deltopectoral crest, *i.e.* the posteroventral corner. This is caused by the posterior tuberosity. The area between the posterior tuberosity and the deltopectoral crest is concave and limited by the slight, but distinct ridge of the recessed ventral border of the proximal aspect. Distally, the area fades towards the posteroproximal surface of the deltopectoral crest. Proximally, the posterior tuberosity extends in posterior direction. A foramen inserts anterodistally in the attachment area between the process and the shaft.

Despite being partly obscured by matrix, it is good to observe that the supracondylar process (sup.pr.) at the distal half, is strongly developed and 3 mm at its highest point. The process extends towards the distal aspect but the sharp ridge changes into a shallow bulging ridge more distally. It forms a separation between the flat area anteriorly and the shallow recess posteriorly. Opposite to the supracondylar process and slightly more posteriorly is another ridge, identified as a muscle scar, which extends towards the ventral condyle (cond.vent.) at the distal aspect. The intercondylar groove (i.cond.gr.) separates the dorsal condyle (cond.dors.) from the ventral one.

Seen from distal, the dorsal condyle is more pronounced and bulbous relative to the ventral condyle and extends farther onto the ventral aspect. A shallow but broad groove separates the dorsal from the ventral one. The ventral condyle is mainly situated at the distal aspect. The large pneumatic foramen is clover shaped.

Seen from dorsal, two broad and shallow grooves flank a raised structure at the distal extremity. The anterior groove is identified as “sulcus anconaeus medialis” (Wellnhofer, 1985: 121), and is, seen from distal, distinct. The opposite, posterior groove extends into the distal aspect, forming a well defined, sharp ridge posterior to the pneumatic foramen (pn.for.) and anterior to the ventral epicondyle. This ridge describes an angle of approximately 90°, with the angle pointed anteroventrally.

Humerus SMNS 55883

Family Ornithocheiridae Seeley, 1870²³
Genus *Santanadactylus* De Buisonjé, 1980
Santanadactylus pricei Wellnhofer, 1985
cf. Santanadactylus pricei

Holotype: BSP 1980 I 122, Bayerische Staatssammlung für Paläontologie und historische Geologie, Munich, Germany. Left front extremities.

Diagnosis *S. pricei* according to Wellnhofer (1985: 132): "Eine Art der Gattung *Santanadactylus*, die kleiner ist als *S. araripensis*²⁴ und *S. brasilensis*. Am Humerus keine Trochlea–Epiphyse, Processus lateralis mit geknicktem Oberrand. [...]". (Translation: "A species of the genus *Santanadactylus* which is smaller than *S. araripensis*²⁵ and *S. brasilensis*. Humerus without epiphysis of trochlea, upper edge of the deltopectoral crest bent.")

Description

The right humerus with the inventory number SMNS 55883, lacks the distal half (figure 3.3D, 3.4D; table 3.2). The humerus is embedded with its posterior aspect, showing only the anterior aspect. The ventral and dorsal aspects are obscured by matrix as well. The

anterior edge of the humeral head is incomplete and the ventralmost edge of the deltopectoral crest is either obscured by matrix or missing.

The proximal end shows a head at a distinct angle with the shaft. The ventral edge of the deltopectoral crest commences at the head and continues straight into distal direction, after which it forms the convex distalmost outcrop of the process. The ventralmost three quarters of the distal edge of the process is at right angles with the shaft, but the remaining quarter, closest to the shaft, bends concavely towards the shaft.

Discussion

The uncertain diagnostic value of the humeri (see below) is, in the present work, further reduced by the incompleteness as well as the largely unprepared state of all but one humerus (SMNS 55409). Consequently, humerus SMNS 55408 cannot be determined on family, genus or species level.

Humerus SMNS 55409 is not Azhdarchid, because the deltopectoral crest of Azhdarchid humeri is substantially larger and the corpus comparatively more robust (Padian & Smith, 1992). The humerus of *Co. spielbergi* has a deltopectoral crest with a straight ventral edge and the ventralmost tip is not as strongly curved proximally. Furthermore, the head lacks the distinct ridge (Veldmeijer, 2003a). The humerus of *Co. piscator* (Kellner & Tomida, 2000) and *An. santanae* (Wellnhofer, 1985, 1991b), compares well with SMNS 55409. In both cases, the ventral edge of the deltopectoral crest curves in posterior direction, the ventral tip of this process is strongly curved, creating a concave posteroproximal surface; the pneumatic foramen is placed at the same position and inserts in a comparable way. The ventral edge, however, is more concave with *Anhanguera*. The comparison of SMNS 55409 with *Santanadactylus* reveals a high degree of resemblance, comparable to the resemblance between the humerus of SMNS 55409 and *Anhanguera*. The head of *Santanadactylus* has a distinct ridge at the proximal surface and since this lacks with *Anhanguera*, SMNS 55409 can be assigned to *Santanadactylus*. This ridge is the most important characteristic of the *Santanadactylus* humerus and forces a determination as *Santanadactylus* (see also De Buisonjé, 1980; Wellnhofer, 1991b).²⁶

The broad (in dorsal–ventral plane) head of *S. brasiliensis*, as described by De Buisonjé (1980), together with the relatively small posterior tuberosity, the drooping ventral tip of the deltopectoral crest if seen from anterior and the relatively short deltopectoral crest differs with SMNS 55409. The main differences with *S. pricei*, published by Wellnhofer (1985, 1991b), are the stronger ventral edge of the deltopectoral crest and the stronger angle of the head relative to the shaft. Furthermore, the general size of *S. pricei* is smaller. The humerus compares therefore best with *Co. araripensis*, especially because of the shape of the head, deltopectoral crest (seen from proximal) and the comparable layout of the various views of the distal extremity. Additional support is the fact that the sulcus anconaeus medialis, seen from distal, is as strongly developed as with SMNS 55409 and the comparable measurements.

Humerus SMNS 55883 has also more points of contact for comparison than SMNS 55408. The deltopectoral crest of Azhdarchid pterosaurs is substantially larger and the shaft comparatively more robust. The general size is larger as well (Padian & Smith, 1992). The deltopectoral crest of the humeri of *Anhanguera*, as presented by Wellnhofer (1991b), has a strong posterior–orientated bending, which apparently lacks with SMNS 55883 but which is also visible in *Co. piscator* (Kellner & Tomida, 2000). The humerus of *Co. spielbergi* has a deltopectoral crest with a straight ventral edge. The humeri of both species are substantially larger as well. According to Wellnhofer (1985), the humerus of *Co.*

araripensis has a comparable deltopectoral process, but a ridge pronounces the head. This cannot be ruled out for the Stuttgart humerus. The ventral edge of the deltopectoral crest of *S. brasiliensis*, described by De Buisonjé (1980) is far straighter and the head is clearly separated from the shaft by a ridge. SMNS 55883 most closely resembles the humerus of *S. pricei*. The measurements of the humeri show less difference in size relative to the humeri of other Brazilian pterosaurs and the shape of the deltopectoral crest is highly comparable. Furthermore, the angle of the head which has no ridge to separate it from the shaft, is comparable. Taking the limited diagnostic value of the above used characters to distinguish humeri into account together with the condition of SMNS 55883, the humerus is tentatively classified as *cf. S. pricei*.

The humerus SMNS 55883, as determined to be *cf. S. pricei*, belongs according to Wellnhofer (1985, 1991b) to the family of Ornithocheiridae, which is in contrast to the designation of *Santanadactylus* to Criorhynchidae by De Buisonjé (1980). Kellner & Tomida (2000) regard all specimens of *S. pricei* except the holotype (BSP 1980 I 122) as 'Pterodactyloidea indet.'. Also the New York specimen (Wellnhofer, 1991b), is referred to as 'Pterodactyloidea indet.'. The comparison of the Stuttgart humerus shows a close relationship with Anhanguerid humeri. However, the clade Anhangueridae as established by Campos & Kellner (1985b) is considered invalid by Unwin (2001), whereas Wellnhofer (1991b) accepts the clade. It is beyond the scope of the present work to evaluate the validity of the different clades in detail on the basis of post cranial elements.²⁷

3.3.3. Isolated ulnae and radii SMNS 55410, 55411, 55413, 82001 (figures 3.5, 3.6; tables 3.3, 3.4)

Ulna SMNS 55410, ulna and radius SMNS 55411

Santanadactylus pricei Wellnhofer, 1985
cf. Santanadactylus pricei

Holotype: BSP 1980 I 122, Bayerische Staatssammlung für Paläontologie und historische Geologie, Munich, Germany. Left front extremities.

Diagnosis *Santanadactylus pricei*, according to Wellnhofer (1985: 132): "[...] Radius nur halb so stark wie die Ulna. [...]". (Translation: "Radius merely half as wide as ulna.")

Description SMNS 55410

The right ulna with the inventory number SMNS 55410 (figures 3.5A, 3.6A; table 3.3) is still embedded in matrix, exposing only the anterior aspect. The bone is badly preserved and substantial parts of the proximal end as well as the distal end are severely damaged or missing. Only a small part remains of the dorsal cotyle. The proximalmost part is missing as well as the area ventral to the dorsal cotyle. An area of about 45 mm of the anterior aspect lacks the outer bone layer.

This ulna is a straight bone with dorsoventrally expanding proximal and distal ends and an elliptical cross-section. The remnants of the severely damaged dorsal cotyle suggest that it is not strongly developed. The shaft is flattened as an imaginary continuation of the dorsal cotyle. The slightly dented area between the proximal view and dorsal cotyle for the reception of the radius, is short, approximately 20 mm, and there is no trace of a pneumatic foramen at the proximalmost border. This might be due to the fact that the proximal part of the ulna lacks.

Description SMNS 55411

The preservation of SMNS 55411 (figures 3.5B, 3.6B; table 3.3) is bad and therefore of no morphological importance. The nodule is broken at two places, both at the distalmost ends of the ulna and radius.

Only the proximal parts of this left ulna is preserved and still largely embedded. A substantial part of the anterior aspect and small parts of the dorsal aspects are visible. The ulnar head is severely damaged and the dorsal cotyle is largely obscured. The radius is not articulated anymore but displaced. The bone is extremely badly preserved. The shaft of the ulna is elliptical in cross-section. The proximal aspect is damaged and the dorsal cotyle is obscured for its larger part but the remaining part suggest that it was stronger developed relative to SMNS 55410. The dent for the reception of the radius is deeper relative to SMNS 55410 and longer as well. Seen from anterior, a circular pneumatic foramen is situated at the proximalmost border. Seen from anterodorsal, the ulna is flattened indicated by a clear ridge.

Ulna SMNS 55413

Family Anhangueridae Campos & Kellner, 1985b²⁸
Genus *Coloborhynchus* Owen, 1874
Coloborhynchus spielbergi Veldmeijer, 2003a
cf. Coloborhynchus spielbergi

Holotype: RGM 401 880, National Museum of Natural History, Leiden, The Netherlands. Nearly complete skeleton.

Diagnosis: The diagnosis of *Coloborhynchus spielbergi* according to Veldmeijer (2003a) does not include the ulna.

Description

The right ulna with inventory number SMNS 55413 (figures 3.5C, 3.6C; table 3.3) is still embedded as well, only exposing the anterior aspect. This ulna is complete and in good condition, despite the crack distal to the proximal end and proximal to the distal end and the crack in the middle of the nodule. The ulnar head, however, is damaged.

The right ulna SMNS 55413 is a straight bone with dorsoventrally expanding proximal and distal ends and an elliptical cross-section. The dorsal cotyle is damaged but from the remnants it is clear that it was strongly developed and stronger relative to the previous discussed ulnae. Seen from anterior, a slightly elongated, circular pneumatic foramen inserts at the proximalmost border of the long (in proximal–distal plane) dent for the reception of the radius. The distal end shows a distally expanding depression, flanked by a low but broad dorsal condyle.

Ulna SMNS 82001

Family, genus, species indet.²⁹

Description

The small fragment of bone with the inventory number SMNS 82001 (figures 3.5D, 3.6D; table 3.3) is still largely embedded and rather damaged, especially the proximal end of which the outer bone layer is lost. The anterior aspect is entirely freed from matrix and the dorsal, ventral and proximal aspects only partially. Two small pieces of bone flaked from the, in this work illustrated, fragment. The bone is identified as a right ulna.

The proximal area shows a small, circular pneumatic foramen of only few millimeters cross-section, ventral to the damaged and obscured proximal aspect. The ulnar head is damaged. Again ventral and proximal to the foramen is a small, but distinct bulb situated, which is separated from the foramen by a depression. The depression for reception of the radius is small and shallow but the damaged state of the bone prohibits a more detailed evaluation. The shaft is slightly elliptical in cross-section and is, as far as can be determined from the incomplete specimen, slightly bent.

Discussion

The fact that the proximal and distal aspects are obscured, limits a classification because the morphology of ulnae and radii are, in general, highly comparable. Furthermore, the lack of detailed published ulnae and radii hinder an extensive comparison, except for *S. pricei*, *Co. araripensis*, *Co. spielbergi* and one example of *Anhanguera*.

The ulna SMNS 55411 is substantially shorter than the ulna of *Co. araripensis* and *An. Santanae*: the ratio is 1:1.5 and 1.4 respectively. The difference in length with *Co. spielbergi* is even larger and is in the ratio of 1:1.6. Tentatively, it can be assumed that the differences in ratio are too large to be explained by intraspecific variety. There are few differences with the ulna of *S. pricei* and SMNS 55410 and 55411, despite a comparable length (table 3.3). The pneumatic foramen at the dorsal cotyle cannot be attested at the Stuttgart ulnae but cannot be precluded as well. The pneumatic foramen at the proximal border of the depression for the reception of the radius seen in SMNS 55411 is also attested with *S. pricei* and cannot be precluded for SMNS 55410.

A comparison of the diameters of the shafts of the ulnae and radii, table 3.4, shows that the diameter of the radius of *S. pricei* measures about 50% of the diameter of the ulna, whereas this is 43% for SMNS 55411. Although the difference is substantial, it is suggested not to assign the ulna and radius to a new taxon, for which no strong evidence can be given. A proposed classification as *cf. S. pricei* for SMNS 55411 on basis of biometrical arguments as well as the presence of a pneumatic foramen at the dent for the reception of the radius, the shape of this dent and shape of the shaft is defensible. The classification '*cf.*' is added to show the awareness of the differences of ratios of the diameter of the ulna and radius of SMNS 55411 relative to *S. pricei*. The resemblance of SMNS 55410 with SMNS 55411 forces to classify this specimen as *cf. S. pricei* as well. SMNS 55413, however, differs from *S. pricei* especially from a biometrical point of view. The length of the ulna of the Munich *S. pricei* (BSP 1980 I 122) and the Stuttgart ulna are in the ratio of 1:1.8 whereas this ratio is 1:2.4 for the New York *S. pricei* (AMNH 22552) and SMNS 55413. This is hardly to explain by intraspecific variation. Seen from anterior, *Co. araripensis* has a pneumatic foramen at the distal end, which lacks with SMNS 55413

and the diameter of the shaft of the Stuttgart ulna is more elliptical contrasting the almost circular cross-section of *Co. araripensis*. The cross-section of the *Anhanguera* ulna is oval in contrast to the elliptical cross-section of SMNS 55413. The ulna of *Co. spielbergi* is more elliptical and compares well with SMNS 55413. The ratio of the length of SMNS 55413 and *Co. spielbergi* are in the ratio of 1:1.04. The general morphological resemblance between the ulna and the compared specimen leaves no doubt on the close relationship between the different specimens. On the basis of the, admittedly meagre, morphological resemblance and the above-mentioned biometrical arguments, the specimen is tentatively referred to as *Co. spielbergi*. The problematic position is visualised by the addition 'cf.'

The ulna SMNS 82001 has no visible diagnostic features due to the incomplete preservation and preparation. Few diagnostic features are recognised at ulnae: traditionally, the diagnosticity of the ulna is combined with the radius in terms of diameters of the shaft (see above). No ratio can be obtained for the ulna and radius, because the radius is not preserved. Other possible diagnostic features, *i.e.* the depression for the reception of the radius and the ulnar head, are severely damaged. On the other hand, the almost circular shaft is seen with ulnae of some pterosaurs, for instance *S. pricei*. Consequently, there is not enough evidence to warrant a more precise classification.

3.3.4. Associated humerus and ulna/radius SMNS 81976

Family, genus, species indet.

Description

A calcareous nodule with the inventory number SMNS 81976 contains a right humerus and the articulated ulna/radius (figures 3.7, 3.8; tables 3.4, 3.5). The humerus is embedded in the matrix with its anterior aspect and the ulna/radius are embedded with their dorsal aspects. The complete humerus is sectioned lengthwise. The proximal halves of the ulna and radius are sectioned lengthwise as well, except for the proximalmost part of approximately 40 mm length. The inner side of the bone shows the typical pterosaurian construction; the shafts of the bones are hollow with thin walls (often less than 1 mm thick) and transverse, with each other interconnecting internal struts that "can be regarded as materialized lines of force" (Wellnhofer, 1991a: 149) providing maximum lightness combined with optimal strength (see also Carter *et al.*, 1992). The ends are composed of spongy bone tissue. It is not known whether the struts are more numerous in the humerus relative to the ulna/radius as observed by Wellnhofer (1985, 1991b) because most of the struts are not preserved.

The humerus and ulna/radius are in contact at a 90° angle approximately. This position is seen with other pterosaurs as well (Wellnhofer, 1985). The ventral edge of the deltopectoral crest has a strong convex course and the humeral head is set at a distinct angle relative to the strikingly slender corpus. The ulna and radius, in articulation with each other and the humerus, are elliptical of cross-section.

Discussion

The length of the humerus is comparable to the humerus of *S. pricei* (BSP 1980 I 43; Wellnhofer, 1985), and the New York specimen of *S. pricei* (the status of *S. pricei* is discussed previously in this chapter).

The shaft of the humerus is very slender relative to its length (ratio 1:10.9), which is,

compared with the ratios established for other pterosaurs, the largest (*cf.* Veldmeijer, 2003a). The bone, however, is sectioned lengthwise but not exactly in the middle. In contrast, the sectioning occurred more anteriorly. The measured diameter, therefore, is smaller than the real diameter. The diameters of radius and ulna are in the ratio of 1:2.3 (table 3.5), which is the same as calculated for SMNS 55411 and differs especially with *S. pricei* (table 3.4). The ratio of the length of the humerus and length of the ulna are about the same in all calculated material (varying from 1:1.4 to 1:1.6).

The one possibly diagnostic (discussed above with 'Isolated humeri') morphological feature, *viz.* the convexity of the (badly preserved) deltopectoral crest, and the biometrical arguments (see also the discussion above with 'Mandible') are not unambiguous enough in this specimen to warrant a classification more precise than on the level of suborder.

3.3.5. Phalanges of wing finger SMNS 55412, 55415 (figures 3.9, 3.10; table 3.6)

Family, genus, species indet.

Description SMNS 55412

The specimen with inventory number SMNS 55412 is a slab and counter slab (figures 3.9A, 3.10A; table 3.6). The phalanx is in good condition despite the breakage at three points and the lack of the distalmost part. Few ostracods are visible in the calcareous matrix.

The ventral and dorsal aspects of this left phalanx are visible. The phalanx is bent into posterior direction. Seen from ventral, the proximal end is expanded posteriorly and inclined anteriorly. The proximal aspect is strongly concave for the reception of the convex distal aspect of the previous wing phalanx. The wing was bent in posterior direction, due to the bending of this phalanx (and of the other phalanges as well), which is a general characteristic of the pterosaur wing. The distal end is missing, but the shaft expands slightly in anteroposterior plane towards this end. The shaft has a flattened, oval cross-section, based on the outside observations. Remarkable of this phalanx is its size (table 3.6), even more so taking the not fully-grown status of the bone (grain and cartilage at the proximal end) into account.

Description SMNS 55415 (figures 3.9B, 3.10B; table 3.6)

The specimen with inventory number SMNS 55415 is a calcareous nodule containing a large, well preserved phalanx (figures 3.9B, 3.10B). The phalanx is complete and displays almost no damage.

The ventral aspect of the left phalanx with inventory number SMNS 55415 is freed from its calcareous matrix. The phalanx is long and slender without bending. The corpus, strongly oval in cross-section at the proximal end and less oval in cross-section at the distal end, based on outside observations, expands in anteroposterior plane towards the proximal end more severely relative to the distal end. Seen from ventral, the proximal aspect has a convex area that overhangs the ventral aspect slightly. Due to the matrix, it remains uncertain whether the remaining part of the proximal aspect is concave or convex. The distal end is slightly recurved, forming a clear ridge that separates the shaft from the distal aspect. The distal end has two small foramina. The rugosities at the proximal end might be, according to Kellner & Tomida (2000: 68): "the insertion surfaces for interphalangeal ligaments."

Discussion

Compared with the few published phalanges (Frey & Martill, 1994; Wellnhofer, 1985, 1991b) SMNS 55412 is regarded as a second phalanx. This is primarily based on the bending. The shape of the proximal articular aspect excludes a determination as first phalanx (*cf.* Kellner & Tomida, 2000; Wellnhofer, 1977, 1985, 1991b) and the bending seems to be too severe for a third phalanx. Furthermore, the proximal aspect is too concave for a third phalanx. The size suggests a large animal since the not fully-grown bone measures 440 mm. Compared with the length of the second phalanx of *S. pricei* (length 325 mm, Wellnhofer, 1985 and 324 mm, Wellnhofer, 1991b) and *Art. conandoylei* (length of 402 mm, Frey & Martill, 1994) the phalanx is large and more in line with the data given of *Co. piscator* (preserved length of 355 mm, with a maximal width of the proximal aspect of 51 mm, Kellner & Tomida, 2000). But again, the remark must be made that there is no insight in the probably large (Dalla Vecchia & Ligabue, 1993) intraspecific variability.

Phalanx SMNS 55415 is not a first phalanx because the proximal aspect of a first phalanx, the extensor tendon process (*cf.* Kellner & Tomida, 2000; Wellnhofer, 1977, 1985, 1991b) serves for the articulation with the metacarpal and differs clearly from the proximal aspects of the following wing phalanges. The straightness of the phalanx and the slight differences between the proximal and distal ends suggests that the phalanx is a third phalanx. If this is true, the size of this animal is large compared with the measurements of the third phalanges of *S. pricei* (a length of 252 mm and a width of the distal end of 13.5 mm, Wellnhofer, 1991b) and *Art. conandoylei* (a length of 313 mm, Frey & Martill, 1994). It is more in line with *Co. piscator* (preserved length of 218 mm and about 17 mm width of distal aspect, Kellner & Tomida, 2000).

The nature of especially the second, third and fourth wing phalanges as well as the lack of detailed published specimens precludes accurate taxonomic designation. The resemblance between the distal end of the present specimen and the distal end published by Della Vecchia & Ligabue (1993), which they interpret as the first phalanx of the wing finger, is apparent despite the slightly more intense curving of the distal aspect, seen from dorsal. However, the incomplete preparation of SMNS 55415 prohibits a firm conclusion; the phalanx published by Dalla Vecchia & Ligabue (*ibidem*) might be a second rather than a first phalanx.

3.3.6. Partial front extremity SMNS 80437 (figures 3.11, 3.12; table 3.7)

Family, genus, species indet.

Description

The specimen with inventory number SMNS 80437 (figures 3.11, 3.12; table 3.7) is a calcareous nodule, containing five fragments of bone (numbered and referred to as 1, 2, 3, 4 and 5). The bones are incomplete and prepared only partially. Bones 1–3 lie parallel to each other and run over bones 4 and 5, which are positioned at an 80° angle approximately, relative to bones 1–3.

The cross-section of the bone numbered '1' is circular to elliptical. The proximal end is not complete and partly obscured by matrix, but the widening of the shaft towards the end (from 7.8 mm to 10.7 mm) as well as the deep articulation socket, which is separated from the shaft by a clear ridge that continues into the shaft as a slight groove, suggests that the bone is the second phalanx of the right fourth wing digit. The close association with

bone '2' provides additional support, because this bone is certainly the first phalanx of the right wing digit. This first phalanx tapers towards the distal end (from 12.4 mm to 6.2 mm). The large pneumatic foramen at the posteroventral aspect is clearly visible. A shallow groove continues as an extension of the pneumatic foramen.

The bone referred to as '3' is a slightly tapering bone with a largest diameter of 10.7 mm. A shallow groove runs longitudinally. The bone is tentatively identified as the fourth phalanx of the wing digit, on the basis of the small size relative to the previously described ones, and its association with the first and second phalanx.

Bone '4' has a flattened circular cross-section. It does not display any morphological features and is indeterminable.

The largest bone beneath the wing digit, numbered '5', can be identified as the right ulna. It lacks the ulnar head entirely and the dorsal cotyle almost completely. The cross-section of the ulna is circular. A pneumatic foramen is situated in the dent for the reception of the radius, close to the edge of the proximal aspect. This depression is not clearly separated from the ulnar head by an elevated concave margin, as seen in SMNS 55413.

Discussion

A discussion on ulnae is presented previously. The ulna of SMNS 80437 differs from the known ulnae by its circular cross-section. The circular cross-section contrasts sharply with the cross-section of the ulna of *Anhanguera* (Wellnhofer, 1985, 1991b), which is oval and the elliptical cross-section of SMNS 55413 and *Co. spielbergi*. The arrangement of the pneumatic foramen, and especially the lacking separation of the radial depression and the ulnar head differs from SMNS 55413 and is more comparable to *Co. spielbergi*. It cannot be ruled out that the mentioned differences are due to the bad preservation and the partial covering by matrix. A classification is therefore not possible.

A discussion on the phalanges is presented previously. The present phalanges have no visible diagnostic features in order to compare it with other material in such way as to being able to classify them. The lack of information results partly from the fragmentary state and partly from the fact that the bones are embedded for the larger part.

3.4. Concluding remarks

The description of the material of the Staatliches Museum für Naturkunde Stuttgart proved to be especially important because the second almost complete mandible of *Cr. mesembrinus* is presented. The additional description of material, post-cranial as well as cranial, of new or existing species helps gaining insight in the diversity of the Santana pterosaurs. Furthermore, the constant adding of data to the fossil record renders comparative anatomy more easy and reliable and more precise diagnoses possible.

The limited diagnostic value of humeri (Kellner & Tomida, 2000; Veldmeijer, 2003a) is partly due to the lack of 'rules' how to regard differences, which was, among others, the reason in the present work for uncertainty with some classifications. On the other hand, a seemingly detailed diagnosis of *S. brasiliensis*, as quoted above, is of no use because most of the features have no diagnostic value (see also Kellner & Tomida, 2000). At present, the general outline and position of the deltopectoral crest can be used for classifying on family level. For instance, the deltopectoral crest of the Nyctosaurid humerus is hatchet-shaped (Bennett, 1993) and the deltopectoral crest of Pterodaustriid humerus is positioned at a completely different angle (Wellnhofer, 1978). The use of slight differences in shape of the deltopectoral crest as a diagnostic feature on species level (*e.g.* Wellnhofer, 1985) neglects

intraspecific variability as well as sexual dimorphism. Furthermore, the convexity of the ventral edge of the deltopectoral crest is seen in species of *Anhanguera* as well as *Santanadactylus* (among others the reason of the problems of Anhangueridae versus Ornithocheiridae). On the other hand, Frey & Martill (1994) mention problems with the classification of distinct different humeri of *Ornithocheirus* and *Santanadactylus* to the same family (Ornithocheiridae). The use of the shape of the humeral head meets comparable problems, although the distinct ridge at the head is an exclusive feature of *Santanadactylus* and is a distinct diagnostic feature on family level (contra the view that this is due to the age of the animal).³⁰

Comparable problems of the ones discussed with humeri occur with all post-cranial (and even cranial) material. It might be useful therefore, to re-evaluate all material and establish diagnoses that also reckons with intraspecific variability and sexual dimorphism.

4. Description of two pterosaur (Pterodactyloidea) mandibles from the Lower Cretaceous Santana Formation, Brazil³¹

4.1. Introduction

The described specimens both originate from the Romualdo Member (Albian) of the Santana Formation (Aptian–Albian), in Chapada do Araripe in the province of Ceará, Brazil.

In this chapter, new material of *Thalassodromeus* is described and compared with other edentulous taxa. The toothed jaw is briefly described; the focus is on the discussion of morphological differences relative to other pterosaurs from Brazil and only a short description is presented. For a broader description of the general layout of these pterosaurs, see Kellner & Tomida (2000), Kellner & Campos (2002), Veldmeijer (2003a), and Wellnhofer (1985, 1991b). Dentition patterns (*i.e.* the graph that visualises the size and position of the teeth) are plotted and discussed only briefly; ample attention is given in chapter 7.

The material is housed in the collection Oberli; casts of SAO 251093 are housed in the Bayerische Staatssammlung für Paläontologie und historische Geologie, Munich, Germany, the Staatliches Museum für Naturkunde, Stuttgart, Germany and Museu Nacional, Rio de Janeiro, Brazil.³²

4.2. Abbreviations

ad.fos.	adductor fossa	pn.for.	pneumatic foramen
ang.	angular	pre.art.	prearticular
ch.t.	foramen chorda tympani	ret.pr.	retroarticular process
d.	dentary	r.	ramus
d.e.	dorsal cutting edge	ri.	ridge
d.sag.cr.	dentary sagittal crest	s.sh.	symphyseal shelf
lat.cot.	lateral cotyle	spl.	splenic
man.gr.	mandibular sagittal groove	sur.	surangular
m.fos.	Meckelian fossa	sym.cav.	symphyseal cavity
med.cot.	medial cotyle	t.b.r.	elevated teeth-bearing rim
pat.	pathology		

4.3. Systematic palaeontology, description and comparison SAO 251093

Order Pterosauria Kaup, 1834
 Suborder Pterodactyloidea Plieninger, 1901
 Family Tapejaridae Kellner, 1989
 Genus *Thalassodromeus* Kellner & Campos, 2002

Type species and specimen: *Thalassodromeus sethi* Kellner & Campos, 2002, large part of skull and mandible, DGM 1476–M, Museu de Ciências da Terra/Departamento Nacional de Produção Mineral, Rio de Janeiro, Brazil.

Diagnosis *Thalassodromeus* according to Kellner & Campos (2002: 389) the same as for the species *T. sethi*. “[...] anterior portion of the premaxillae and dentary with sharp dorsal and ventral edges; [...]”

Species *Thalassodromeus sethi* Kellner & Campos, 2002

Holotype: As for the type specimen.

Etymology note: One of the authors (Kellner pers.com. 2002) explained that the shape of the crest of the pterosaur reminded them of the crown of the ancient Egyptian god Seth. It is however noteworthy that the crown, representing the solar disk with two tall plumes, is typically worn by the god Amon (later Amon–Ra), or manifestations of him, and not by Seth (e.g. Baines & Málek, 1981).

Amended diagnosis: Anterior part, starting from the anterior border of the mandibular groove, bent in dorsal direction.

4.3.1. General

The specimen represents the symphyseal portion of the anterior mandible, but lacks the tip (approximately 10 mm). Rami are missing; the small remaining parts of the right ramus is slightly larger than the left one. The specimen is broken in two parts. The fossil has been completely prepared mechanically except at the tip where some matrix remains to protect the fragile point from breaking. No sutures are discernable.

4.3.2. Description (figures 4.1, 4.2; table 4.1)

The symphysis of the edentulous mandible (figures 4.1, 4.2; table 4.1) is curved dorsally, starting from the anterior border of the symphyseal shelf (s.sh.). The dorsal aspect of the slender terminal point has a sharp cutting edge (d.e.) whereas the ventral aspect is less sharp, resulting in an oval tear–drop cross–section. Posteriorly the dorsal cutting edge terminates at the shelf. The shelf rapidly increases in width posteriorly, diverging with the rami. In dorsal view, two low left and right ridges (ri.) occupy the middle of the shelf, 10 mm ventral to the dorsal edge, with a length of approximately 30 mm. Both are orientated slightly posterodorsally.

The posterior symphysis exposes an anterior cavity (sym.cav.). It appears to extend at least as far as the anterior of the symphyseal shelf. The little part of the rami that is preserved has a slender dorsal edge, which is slightly curved medially. The width of the rami increases posteriorly and ventrally and produces a lingual concavity. In lateral view the rami are convex.

As is common in pterosaurs, the mandible is lightly built with a bone thickness often less than 1.0 mm. A posterior view clearly shows the cross–section of the posterior mandible, including the reinforcement of the hollow bone by means of thin reticulate plates, forming large square–like pneumatized ‘cells’, which gives the bone optimal strength in combination with extreme weight reduction. The dorsal edges of the rami and the symphyseal shelf are more robust. Transverse bony plates here are more compact, resulting in smaller ‘cells’. A clear lateroventral border separates this area from the more lightly constructed central and ventral areas.

Two irregularities are visible at both lateral surfaces. On the left is a small uneven area (pat.), interpreted as pathology. On the right is a comparable irregularity, but longer anteroposteriorly and smaller dorsoventrally. Both protrude slightly; the right one a bit more than the left one. The surrounding surfaces are slightly dented. It is tentatively suggested that these areas may be pathological in origin. Other pathologies are described by Bennett (1989,

2003a), Kellner & Tomida (2000), Mader & Kellner (1999). Reports by Kellner & Tomida (2000) on the left jugal and quadratojugal pathologies in *Co. piscator* resemble the ones observed here.

4.3.3. Comparison and discussion

A detailed comparison of SAO 251093 with other taxa is difficult because only the symphysis is known. Since SAO 251093 lacks teeth and alveoli, comparisons are limited to the edentulous pterosaurs, some of which are yet unknown from Brazil. One toothed exception, *Dsungaripterus* is considered here because the anterior mandible is edentulous (Young, 1964; Martill *et al.*, 2000), curved dorsally and it is laterally compressed. The symphysis in *Dsungaripterus* is marked by a weak ridge that is lacking in SAO 251093. The medial posterior mandibular shelf in *Dsungaripterus* is not present in SAO 251093. Furthermore, anterior teeth erupt in *Dsungaripterus* where no alveoli are present in SAO 251093. Due to the small fragment of SAO 251093, it cannot be determined whether this jaw is part of an edentulous, more advanced *Dsungaripterus* and classification as such is therefore ruled out for the time being.

Pteranodon has a mandibular cavity with a triangular section and thus is not consistent with the flattened circular cross-section in SAO 251093. Furthermore, the symphysis is proportionally larger in *Pteranodon*. The dorsal aspect of the mandible can be straight (*P. longiceps*) or dorsally bent (*P. sternbergi*) (Eaton, 1910; Bennett, 1994, 2001).

In *Nyctosaurus* no dorsal curvature can be seen (Bennett, 2003b; Williston, 1902a, b, 1903). Furthermore, all known nyctosaurs are substantially smaller with a skull length of about 30 cm.

Also the non-Brazilian *Quetzalcoatlus* is an edentulous pterosaur. These azdarchid pterosaurs however are very poorly represented by mandibular remnants. Few mandibles, although not well preserved, serve for comparison (Kellner & Langston, 1996). The elongated symphysis is approximately 60 % of the total length. The cross-section of the dentary is triangular which is not consistent with the oval cross-section in SAO 251093. The dorsal rim of the anterior part of the symphysis in *Quetzalcoatlus* is almost flat. Ventrally, the joined dentaries form a sharp keel that declines posteriorly. A mandibular cavity is present, but its extent is unknown. No statement regarding the cross-section was made by Kellner & Langston (*ibidem*: 230), but they suggest a further investigation into the hypothesis that the cavity “[...] might be linked with the presence of a gular sac [...]”. The transverse section of the rami are laterally convex and medially concave, so no medial decrease in width is observed, as in SAO 251093.

The family Tapejaridae consists of the genera *Tapejara*, *Tupuxuara* and *Thalassodromeus* from Brazil and *Sinopterus* from China. *Tapejara* is an edentulous pterosaur genus, consisting of three species from Brazil, *Tapejara wellnhoferi* Kellner, 1989 (figure 4.3); *Tapejara imperator* Campos & Kellner, 1997 (not illustrated) and the recently described *Tapejara navigans* Frey *et al.*, 2003b (figure 4.4). The mandible in *Ta. wellnhoferi* has a depressed tip, a ventral keel, and a depression shelf bordered by the raised lateral rims of the dorsal margin. Thus it differs from SAO 251093 which lacks a crest, has a dorsal curvature and lacks the depression but has a distinct mandibular shelf. No mandible is known of *Ta. imperator* and *Ta. navigans*, but the depressed rostral tip of the cranium suggests a mandible dorsal contour similar to that of *Ta. wellnhoferi*. *Sinopterus dongi* Wang & Zhou 2002 is similar in gross morphology to *Tapejara* and is therefore dissimilar to SAO 251093.

Tupuxuara is also an edentulous taxon from Brazil but descriptions of complete mandibles have not been published despite the fact that mandibles are known. However, a

nearly complete specimen of *Tu. leonardii* Kellner & Campos, 1994 in the Iwaki Museum of Coal Mining & Fossils, Japan (figure 4.5), and the partial skeleton in the Prefectural Museum of Natural History, Kanagawa, Japan (figure 4.6), include mandibles. In general, the mandible is longer and smaller than in other Tapejarids. In dorsal view the anterior third of the symphyseal shelf is flat, with slightly raised rims, unlike the sharp dorsal cutting edge of SAO 251093. Furthermore, the mandibles in tupuxuarid pterosaurs show no dorsal curve. The mandible in *Tu. leonardii* has a comparable symphyseal shelf but anteriorly the shelf fades into a flat surface. By comparison, the mandibular shelf in SAO 251093 does not flatten into the rim.

The edentulous pterosaur, recently described as *Thalassodromeus sethi* Kellner & Campos, 2002 (not illustrated), was first published in 1990 (Kellner & Campos, 1990). The type specimen includes pieces of the mandible. According to the authors (*ibidem*, 2002: 391): “A strong concavity formed by the palatine and bordered laterally by the maxillae is present under the anterior half of the nasoantorbital fenestrae. Anterior to this concavity, the palate is convex, forming a short ventral keel that turns into a sharp blade anteriorly. The fused dentaries form a perfect counterpart to the palate, with a developed concavity, followed by a short, deep sulcus (that during occlusion encases the palatal keel, forming a strong interlocking mechanism) and an anterior sharp bony blade. Between both blades there is a gap.” Following this preliminary analysis, a complete description is forthcoming in the near future (Kellner, pers.com. 2002).

It is clear that the mandible SAO 251093 can be regarded as *Thalassodromeus*, having a short and deep shelf posterior to the concave, sharp edged blade. However, the rami in *Th. sethi* are straight and diverge slightly posterolaterally. This contrasts with SAO 251093 in which rami diverge stronger posterolaterally and exhibit a slight but distinct bending in lateral direction. The mediodorsal parts of the rami in *Th. sethi* are more concave relative to the rami in the St. Gallen mandible. Here the mediodorsal side of the rami is only slightly concave and slightly extends to the bottom of the shelf. In lateral view the mandible of *Th. sethi* shows a distinct rise, whereas in SAO 251093 its only slightly convex. In ventral view *Thalassodromeus* displays a distinct ventrally bulging area anteriorly. In similar fashion, the anterior tip in SAO 251093 is bent in dorsal direction, starting at the anterior border of the symphyseal shelf. Although the anterior tip in *Th. sethi* is missing, there is no indication of bending at the anterior border of the preserved mandible, contra the reconstruction shown by Kellner & Campos (2002).

So far, only bones were found which show the familiar trabecular system (e.g. in Anhanguerids) or a plate-like construction as encountered in *Tu. leonardii*. But the bone structure described here differs from these; a slightly comparable inner bone structure is mentioned for a *?Pteranodontidae* premaxilla (Wellnhofer & Buffetaut, 1999). Possibly, the internal structure of the lower part of the mandible (*i.e.* the ‘cells’), is comparable to the situation reported for a Romanian giant pterosaurian skull (Buffetaut *et al.*, 2001). The strengthening of the dorsal rims and, to a lesser extent of the symphyseal shelf, compares with the strengthening of the teeth-bearing parts in toothed pterosaurs as reported in *Coloborhynchus* (Veldmeijer, 2003a). This kind of structure might have served to better withstand the forces exerted on these parts of the mandible during feeding. The question rises whether this might be an evolutionary remnant of a primitively dented maxilla.

In conclusion SAO 251093 is a small fragment relative to the type specimen of *Thalassodromeus*, but the general morphological features compare well with this taxon. The two differ in many small details, which are not significant enough to justify the erection of a new species for SAO 251093. The importance of the Swiss specimen lies in the fact that it fills in the grey areas imagined by Kellner & Campos (2002) and thus makes the complete

reconstruction of the skull of *Thalassodromeus* possible and expands the diagnosis of the species.

4.4. Systematic palaeontology, description and comparison mandible SAO 200602

Family Anhangueridae Campos & Kellner, 1985b

Genus *Anhanguera* Campos & Kellner, 1985b

Type species and specimen: *Anhanguera blittersdorffi*, skull, MN 4805–V, Museu Nacional, Rio de Janeiro, Brazil.

Remark to diagnosis: No diagnostic description was provided for the anterior part of the mandible in the original description of the holotype, due to its absence.

Amended diagnosis: Mandible with smooth spoon shaped expanded anterior part, containing the largest teeth. Presence of mandibular sagittal groove, which is flanked by raised rims, extending until the anterior expansion.

Anhanguera sp. indet.

4.4.1. General

The mandible is complete, but broken into three pieces, the two rami and the anterior portion. Remaining matrix protects the teeth from damage but a small area close to the start of the symphysis is prepared. The toothed mandible is long and slender with a ventrally projecting dentary sagittal crest and straight diverging rami. The general anatomical features agree with previous descriptions of *Anhanguera* and *Coloborhynchus* (referred specimen in Kellner & Tomida, 2000; Veldmeijer, 2003a; Wellnhofer, 1985, 1987). Here emphasis is placed on new features. A discussion on the validity of certain characters in other specimens follows.

4.4.2. Description (figures 4.7–4.10; table 4.2)

Dentary (d.)

The dorsal margin of the mandible is largely obscured by matrix, but it can be observed that the anterior part of the mandible is slightly expanded. The teeth-bearing rims are raised. The depressed area between the rims has a sagittal groove (man.gr.), which is flanked by tiny raised ridges. It is uncertain how far the groove extends anteriorly and posteriorly. The dorsal margins of the rami are dentaries (d.) that form the dorsal limit of the adductor fossa (ad.fos.). The left and right dentaries join in a symphysis anterior to the Meckelian fossa (m.fos.). A deep dentary sagittal crest (d.sag.cr.) is present, starting from 45 mm anterior up to dentary joint on the anterior part of the mandible. This crest continuously decreases in width ventrally. Fine features include small (< 1 mm) grooves and a few small (< 1 mm) perforations that insert obliquely, with the grooves leading towards them; a feature highly reminiscent with the observed structures in *Co. spielbergi* (cf. figure 2.3G). The ventral tip of the crest is slightly abraded.

Teeth

The anterior teeth are all complete except for two on the right (numbers 12 and 13), which are broken at the alveoli. The left side has 14 intact teeth, the right side 15. No alveoli could be distinguished at the left ramus. Three teeth of the right ramus are partially embedded and separated from the rest of the ramus (they are not illustrated). In anterior view the first alveolus is oriented anterodorsally. The alveoli two and three are laterodorsally and anteriorly positioned. Alveolus four is placed laterodorsally and slightly anteriorly. The subsequent alveoli, numbers six to ten, are increasingly laterally oriented but less posteriorly.

The largest alveolar cross-section is the third one. The second is only slightly smaller. In general, the teeth are curved in a posteromedial direction, although the curvature decreases posteriorly: teeth one to four are more strongly curved. The teeth cross-section is elliptical with the long axis oriented anteromedially and at right angles to the curvature of the teeth. Right tooth nine has an anterolateral tip facet extending laterally. The polished edges of the facet suggest that the damage is not post-mortem. Right tooth 10 has a similar but much smaller facet.

Retroarticular process (ret.pr.)

The posterior quarter and retroarticular process (ret.pr.) of the diverging rami are twisted medially relative to the anterior portions. The articular (art.) however, is slightly more laterally orientated relative to the surangular. The inner portion of the articulation area (med.cot.), anterior and dorsal to the pneumatic foramen (pn.for.), is separated from the outer portion (lat.cot.) by a diagonal ridge (ri.) that is anteromedially and dorsally orientated. This ridge is more prominent relative to another ridge described for the articular (see below). The articular has a small (50 mm) pneumatic foramen at its anteroventral corner, which is separated from the posterior part by a shallow diagonal ridge that extends anterolaterally. The posterior part is twisted more mediadorsally relative to the medial and lateral cotyles. The posteriormost articular is slightly convex. The ventral aspect of the retroarticular process consists only of the articular. Against the lateral expansion of the surangular, the adductor fossa is provided with a foramen for the transmission of the chorda tympani (ch.t.).

Surangular (sur.)

In dorsal view, the surangular (sur.) overhangs the articulation area dorsally, medially and laterally. The edges of the cotyles (cot.) expand dorsally, laterally and medially. In medial view the surangular forms the dorsal limit of the posterior mandibular opening. The anterior border is not differentiated. Ventrally, the bone does not extend more than a few millimeters.

Angular (ang.)

Ventrally the angular (ang.) extends posteriorly to the articular. In medial view the bone is slender and extends far anteriorly, forming the ventral border of the mandibular ramus. Possibly, the angular extends even further, but the exact course cannot be determined. In lateral view, the angular can be traced to the posterior part of the rami, displaying a small strip of bone of few mm in height. Though not traceable along the entire length of the ramus, the anterior part reveals a small strip of the angular immediately posterior to the symphysis.

Prearticular (pre.art.)

The prearticular (pre.art.) forms the ventral border of the adductor fossa. It is bordered ventrally by the angular, anterodorsally by the splenial (spl.) and posteriorly by the articular. Consequently, it closes the medial aspect of the retroarticular process.

Splenial (spl.)

In medial view the splenial (spl.) covers the majority of each ramus. It forms the posterior border of the Meckelian fossa and extends towards the adductor fossa, forming its anteroventral border. Ventrally, the splenial is bordered by the angular and posteroventrally by the prearticular. The dorsal border is limited by the dentary.

Hyoid apparatus

Small rod-like bones, separated from the mandible *in situ*, are identified as ceratobranchial I of the hyoid apparatus. The anteriormost ends of the long and slender bones diverge slightly laterally. Consequently, the anterior aspects are not in contact with each other. Anteriorly, the rods are blunt and slightly bulbous.

4.4.3. Comparison and discussion

A comparison of SAO 200602 is limited to the toothed taxa from Brazil. Other materials were too fragmentary or poorly described for a worthwhile comparison. Comparison follows publication date.

The validity of the *Anhangueridae* is controversial (Unwin, 2001; but see chapter 7). The Cambridge Greensands material is, in general, severely fragmented and often diagnosed on ambiguous characters, so comparative studies would be extremely limited and, in most cases, not worthwhile. The validity of *Criorhynchus* is controversial as well (Fastnacht, 2001; Kellner & Tomida, 2000; Unwin, 2001), nevertheless the most recent diagnosis of *Criorhynchus* (Fastnacht, 2001), is used here. At present *Coloborhynchus*, with *Co. clavirostis* Owen, 1874 from the Cambridge Greensands as type specimen, is generally accepted.

The mandible of *B. araripensis* has no dentary sagittal crest (see also Sayão & Kellner, 2000; Veldmeijer, 2003b) and is provided with a sagittal groove, starting at the anteriormost tip, which has anteriolaterally side-grooves.

Cearadactylus atrox lacks a sagittal crest (however, the presence cannot be ruled out entirely as explained by Kellner & Tomida, 2000), on the condition that the classification of *Ce.? ligabuei* is accepted and following Dalla Vecchia's interpretation that the different parts belong to the same individual (see Kellner & Tomida, 2000). Furthermore, the dentary is sloping, containing the largest teeth. Recently, Unwin (2002) concluded in his review of *Cearadactylus* that *Ce. atrox* is a valid species and assigned *Ce.? ligabuei* tentatively to *Anhanguera*.

The main problem in comparing the present mandible with *An. blittersdorffi* is the fact that the holotype lacks a mandible. The mandible in the referred specimen (Kellner & Tomida, 2000), is substantially smaller in all respects and lacks the retroarticular process. The dorsal aspect however is comparable. The mandible includes a posteriorly recessed and anteriorly narrow medial portion with raised teeth-bearing rims posterior to the spoon-shaped anterior. Furthermore, a sagittal groove is also found in *An. blittersdorffi* in the indented area.

Comparison with *Co. araripensis* is limited to the rami, which are highly comparable. The foramina of that splenial are not observed in SAO 200602. Furthermore, there is no indication of a mandibular groove but this might be due to the incompleteness of this specimen.

The holotype of *An. santanae* lacks a complete retroarticular process (figure 4.9, 4.10). The anterior portion of the holotype is not preserved, thus the presence of a crest is uncertain, but Wellnhofer (1991b) and Kellner & Tomida (2000) assume its presence (but see Veldmeijer, 2003a). The lack of the anterior mandible in the holotype and in AMNH 22555 (Wellnhofer, 1991b) makes it impossible to determine the dentition pattern in these specimens. The inclination of the retroarticular process and the configuration of the posterior part of the symphysis in SAO 200602 is similar to *An. santanae*.

The present mandible differs from the holotype of *Co. robustus* in that the anterior expansion in *Coloborhynchus* is distinctly more robust and the symphysis is noticeably longer. Fastnacht (2001) notes the enlarged second and third pairs of alveoli relative to the others in another specimen of *Co. robustus* (SMNK 2302 PAL), matching SAO 200602 (see below). The groove originates between the ninth and tenth alveolus, despite the illustration by Fastnacht (*ibidem*) which does not show this. A similar situation is also seen in the referred specimen of *An. blittersdorffi*. The groove in the referred specimen of *An. blittersdorffi* originates at the eighth alveolus, thus not as far anteriorly, and continues posteriorly in ever increasing distinctness and width. The groove originates against the symphysis, and becomes clearly visible at the twelfth alveolus in the holotype of *Co. robustus*; the posterior extent of the groove cannot be observed in SMNK 2302 PAL because it is not preserved.

The mandible in *Cr. mesembrinus* has no anterior expansion (see also Veldmeijer, 2002). The teeth show no distinct variation in size, as seen in *Coloborhynchus* or *Anhanguera*, and the dorsal aspect lacks a sagittal groove as described in the present work. Instead, *Cr. mesembrinus* has a deep and posteriorly widening groove. The retroarticular process is more sharply inclined medially relative to SAO 200602.

Kellner (1996b) notes that in Anhanguerids the fifth and sixth pair of alveoli are smaller relative to the third and seventh pair, as in SAO 200602 and *Co. robustus* (BSP 1987 I 47). Fastnacht (2001) notes that in *Coloborhynchus* the second and third pairs of alveoli are the largest, but in the referred specimen of *Co. araripensis* (SAO 16494) the third and fourth alveoli are the biggest. In *Co. spielbergi* the ninth alveolus is larger than the second one. In *Co. piscator* the second and third alveoli are the biggest (Veldmeijer, 2003a) and again the ninth is larger than the second. Consequently, separating the dental pattern as done by Fastnacht (2001) and Unwin (2001) from the rest may be premature. At the moment too little is known of the diagnostic status of dentition and this character should be considered with great caution.³³

Comparison with the mandible of *Co. piscator* (Kellner & Tomida, 2000) is limited because the mandible is not fully prepared. The difference in size, however, is great. Although not fully co-ossified, the mandible of this juvenile pterosaur is 533 mm (*ibidem*), thus substantially larger relative to the present specimen.

The rami of the Leiden specimen of *Co. spielbergi* are more strongly bent relative to the present one and the symphysis is longer, although less so than the specimen described by Veldmeijer (2003a). Furthermore, the Leiden mandible has no clearly discernible groove. The mandible is 50% larger than SAO 200602. This difference is probably not ontogenetic because all these specimens are adults. The second and third pairs of alveoli are the largest in the Leiden specimen. The mandible cannot be classified in the new genus *Ludodactylus* Frey *et al.*, 2003a because this genus lacks a mandibular crest and no expansion is reported.

Comparison of the ceratobranchials is limited. Taking into account the fact that comparison is made with Brazilian pterosaurs only, the only other examples of ceratobranchials reported are those in *Co. araripensis* and *Cr. mesembrinus* (not published) but the ceratobranchials in both of them are less complete than in SAO 200602. The anterior extremity of the ceratobranchials is similarly expanded and the measurements are similar as well.

In summary, the configuration of SAO 200602 in dorsal view (medial portion recessed relative to the teeth-bearing rims), is also observed in *Brasileodactylus*, *Coloborhynchus*, *Criorhynchus* and *Anhanguera*. The sagittal groove, however, only occurs in *An. santanae* and *An. blittersdorffi* and thus is an important character separating these otherwise similar taxa. The well preserved *Coloborhynchus* specimens have either a groove extending towards the anterior aspect (i.e. *Co. robustus*) or else a weakly developed groove (i.e. *Co. spielbergi*). The groove in *Criorhynchus* shows a different morphology. The sagittal groove in *Brasileodactylus* extends to the anteriormost tip, lacks the associated ridges and has small anteriolaterally extending side-grooves. Consequently, the mandible can be classified to *Anhanguera*. The differences between the present mandible and the compared *Coloborhynchus* mandibles are larger than the differences between the present mandible and the compared *Anhanguera* mandibles, but still minor. The relatively small anterior expansion, the grooves with raised rims and the relatively short symphysis, clearly distinguish the present specimen from the *Coloborhynchus* jaws.

The absence of mandibles in *An. blittersdorffi* (holotype) and *An. santanae*, is sufficient reason to avoid a specific classification. The reconstructed length of the holotype of *An. santanae* as well as the width at the symphysis is comparable to SAO 200602 (in contrast to the slightly shorter and smaller jaw of *An. blittersdorffi*), but this alone is not a strong argument for a classification at species level. The problems distinguishing the various toothed taxa from Brazil are clear (see also Veldmeijer & Signore, 2004); the systematics are often based on one specimen only, despite the fact that material is housed in various collections all over the world. The additional description of this seemingly unimportant material can nevertheless add important details to the discussion, as has been demonstrated in this paper.

5. Preliminary description of a skull and wing of a Brazilian Cretaceous (Santana Formation; Aptian–Albian) pterosaur (Pterodactyloidea) in the collection of the AMNH³⁴

5.1. Introduction

The collection of the American Museum of Natural History, New York, includes numerous remains of pterodactyloid pterosaurs. Apart from the pterosaur fossils that originate from North America (mainly *Pteranodon*), there are some specimens from Brazil. Herein, I discuss a Brazilian pterosaur, AMNH 24444, that was donated to the museum by Dr. Herbert Axelrod.

The present chapter focuses, after a short general morphological description, on the discussion of morphological differences relative to other pterosaurs from Brazil. Measurements are included to complete the presented text; they are not used for comparison because of the preliminary character of this paper. There is no detailed description; comparable general layouts of the pterosaur skeleton are described extensively elsewhere (especially Kellner & Tomida, 2000; Veldmeijer, 2003a; Wellnhofer, 1985, 1991b). The dentition pattern (*i.e.* the graph that visualises the size and position of the teeth) is discussed only in passing.³⁵

5.2. Abbreviations

den.	dentary	nas.	nasal
dig. 1–3	digit 1–3	nas.fen.	nasoantorbital fenestra
dist.car.	distal carpal	or.	orbit
e.t.p.	extensor tendon process	par.	parietal
first ph.	first phalanx wing finger	pr.fr.	prefrontal
fourth met.	fourth metacarpal	pr.max.	premaxilla
fr.	frontal	prox.car.	proximal carpal
fr.cr.	frontoparietal crest	ra.	radius
j.	jugal	s.n.art.	supraneural plate articulation
l.t.f.	lower temporal fenestra	scap.cor.	scapulocoracoid
max.	maxilla	second ph.	second phalanx wing finger
met.	metacarpal	sq.	squamosal
		ul.	ulna

5.3. Preservation

The specimen consists of one concretion (figures 5.1, 5.2), broken into 5 fragments, in which the skull, mandible and partial left wing (consisting of the left scapulocoracoid (scap.cor.), ulna (ul.) and radius (ra.), proximal and distal carpals (prox.carp., dist.carp.), third (met.) and fourth metacarpals (fourth met.), first phalanx of the wing finger (first ph.) and the proximal part of the second phalanx (second ph.), and traces of the first three fingers, dig.1–3) are still embedded. It is assumed that the fragments belong to one individual. In general, the preservation of the bones is good, despite the fractures mentioned before. One small bone is isolated, although it is uncertain whether it came from this concretion or not and will not be discussed further.

The skull is broken at approximately the anterior one third of its total length. The right lateral side is exposed together with the dorsal aspect of the back of the skull. The left lateral

aspect of the back of the skull and the dorsal aspect anterior to the orbit are still partly embedded, as well as the posterior and posteroventral aspects. The orbit and nasoantorbital fenestra of the exposed right aspect are completely filled with matrix. The first six teeth are partially preserved. A small area of the skull, anterior to the nasoantorbital fenestra and extending slightly anterior to the crack that divides the skull in two parts, lacks the outermost bone layer.

The mandible is displaced relative to the skull and its right lateroventral aspect is exposed. The anterior part of the snout is slightly worn; the distal half of the first wing phalanx obscures the anteriormost tip. The retroarticular processes are not complete, although this feature is admittedly rarely preserved in pterosaur fossils (*cf.* Veldmeijer, 2002³⁶). At a few places, the outer bone layer is missing.

Only the entire anterior aspect and small areas of the medial aspect of the left scapulocoracoid are exposed. The bone lacks the proximalmost part of the coracoid; the biceps tubercle is also incomplete. The sternal articulation is severely damaged.

The ulna and radius are embedded in close association with the scapulocoracoid. The bones are broken at approximately two thirds of the length from a proximal point of view and display their dorsal surfaces. The bones lack some parts of the outer bone layer, and the proximal articular surfaces are not completely intact and exposed. The radius is slightly displaced relative to the ulna, but both bones are still in articulation with the carpus.

The dorsal aspect of the articulated carpus is exposed. The carpalia are in good condition, although slightly worn.

The fourth metacarpal is broken at slightly over half of its length, but is still in articulation with the ulna and first phalanx of the wing finger. The exposed dorsal aspect is well preserved, but, as with the carpus, slightly worn. The much smaller third metacarpal is preserved as well, but slightly displaced relative to the fourth metacarpal.

The first three fingers are little more than traces in the matrix. The first phalanx of the wing finger is broken approximately halfway, where it lacks a small piece. This results in a preserved length which is probably close to its original length. Traces of the extensor tendon process are visible. In the middle, the outer bone layer lacks partially. The first phalanx is positioned in front of the skull and mandible, and its dorsal aspect is exposed. Only the proximal part of the second phalanx of the wing finger is preserved, still articulated with the first phalanx.

5.4. Systematic palaeontology and description

Family ?Anhangueridae Campos & Kellner, 1985b³⁷

Genus *Brasileodactylus* Kellner, 1984

Type species and specimen: *Brasileodactylus araripensis* Kellner, 1984, anterior part mandible, MN 4804–V, Museu Nacional, Rio de Janeiro, Brazil.

Diagnosis: *Brasileodactylus* as diagnosed by Kellner, 1984 (580): “Pterosaurier mit Unterkiefer gebildet aus einer länglichen am Ende abgerundeten Symphyse, leicht nach oben gebogen, triangulärem Querschnitt, Schmälerung ab dem proximalen Teil, wobei eine Verbreiterung an dem distalen Bereich ab der dritten Alveole existiert, die eine flache Oberfläche bildet. Vorhandensein einer medialen Furche an der Dorsalseite der Symphyse, sehr ausgeprägt ab dem Beginn des Unterkiefers (distaler Teil), die sich in proximaler Richtung verbreitet. Alveolen mit eliptischer und rundlicher Form, Zahnabstände vergrößern

sich in proximaler Richtung. Bezahnung bis an die Unterkieferspitze, Zähne schmal und spitz, nach vorne stehend.” For an English translation see Kellner & Tomida (2000: 102).

Remarks: Kellner & Tomida (2000: 103) evaluated *Brasileodactylus* and came to the conclusion that the following apomorphies defined the genus; “rostral end expand from the third alveoli, forming a flat surface [...] medial groove on the dorsal part of the symphysis, starting on the rostral tip and widening caudally.” They regarded the degree of expansion as an apomorph. Kellner (1984) regarded *Brasileodactylus* as an Ornithocheirid.

Brasileodactylus sp. indet.

5.4.1. Cranial skeleton (figures 5.1–5.9 ; table 5.1, 5.2, 5.4)

Skull

The elongated skull (figures 5.1–5.7; tables 5.1, 5.2) clearly shows the sutures between various bones. The posterior slightly concave and anterior slightly convex premaxilla (pr.max.) forms the dorsal edge of the anterior part of the skull until the orbit (or.). However, anteriorly, the course cannot be established exactly because the suture disappears in the vicinity of the fourth tooth. Possibly, the suture of the premaxilla and maxilla (max.) ends between tooth 4 and 5, resulting in four premaxillary teeth. An additional support comes from the fact that the following, thus maxillary, teeth are substantially smaller. There are no traces of crests and the anterior aspect is pointed rather than blunt (figures 5.6, 5.7). It is not certain whether the jaws expand anteriorly. The premaxillae extend far posterior and end in a point between the eye sockets. Here it is wedged between the nasals (nas.) and prefrontals (pr.fr.) and end between the frontals (fr.; figures 5.4, 5.5). A sharply defined suture as seen between the premaxilla, nasal and frontal cannot be observed between prefrontal and frontal but instead, a slightly dented, rather vague line marks the separation. Seen from posterior view, approximately 10 mm posterior to the premaxilla, a well developed frontoparietal crest (fr.cr.) begins. Unfortunately, the exact extension of this crest cannot be determined because the posterior and dorsal limits are incomplete. The maxillar process of the jugal (j.) extends into a point anteriorly. The anteriormost extension is unclear, but it extends farther anteriorly relative to the nasopreorbital fenestra (nas.fen.).

The first six of at least 26 teeth (not all visible from a lateral aspect), are somewhat unclear due to damage. The first tooth, positioned at the anterior margin and orientated, according to the direction of the alveolus, anteroventrally, is missing. The second and third teeth are large and thin relative to the following teeth and orientated anteroventrally. The exact curvature cannot be established because of the unprepared state of the fossil, but the teeth show at least a curvature in posterior direction. The following teeth are smaller and subsequently decrease in size posteriorly. These teeth are maxillary teeth. They are orientated ventrally. The most posterior teeth are slightly curved posteromedially.

Mandible

The dorsal aspect of the mandible (figures 5.1–5.3, 5.8, 5.9; table 5.2) is largely obscured by matrix (figure 5.2). Consequently, only the first six teeth are visible; the anterior aspect is obscured as well (figures 5.8, 5.9) and it is therefore not certain whether the first visible tooth is the second or third one. The visible teeth are placed in the slender, non–

crested, anterior part of the dentary. Only a full preparation can reveal whether the anterior part of the mandible is expanded or not.

The ventral aspect of the mandible extends straight from posterior to anterior, but runs dorsally from the seventh visible tooth. From this point it extends dorsally to form a pointed snout. The degree of co-ossification of the mandible is high relative to the skull.

Only six teeth can be seen, orientated anterodorsally and curved in a posterior direction. It cannot be seen whether or not they are curved medially as well, as is mostly seen in comparable pterosaurs. The teeth are placed dorsally and only slightly laterally.

5.4.2. Post-cranial skeleton (figures 5.1, 5.2, 5.6–5.13 ; table 5.3)

The largely unprepared state of the ulna, radius, metacarpus and carpus (figures 5.10, 5.11) does not allow detailed morphological description. Furthermore, the general layout of these bones is directly comparable to previously published material and the diagnostic value is limited, especially if the extremities of the bones are obscured.

The scapula and coracoid are co-ossified into a scapulocoracoid (figures 5.12, 5.13) on which the suture is indicated by a swollen line. The scapulocoracoid is commonly encountered in Cretaceous pterosaurs and has a limited diagnostic value at species level.

The metacarpal of the wing finger (figures 5.6, 5.7, 5.10, 5.11) is by far the strongest of the metacarpus and is elliptical in cross-section, although far less so relative to the first phalanx.

The most remarkable feature of the first phalanx of the wing finger is the elliptical rather than triangular, cross-section of the shaft. The extensor tendon process (e.t.p.) is comparatively high, as far as can be observed at this process (it is badly preserved and only a trace is visible).

5.5. Comparison and discussion

The classification of the specimen is seriously hindered by the incomplete preparation. The classification proposed here is based on the cranial parts only, because of the limited value of post-cranial bones (worsened by the incomplete preparation) and has to be regarded as preliminary.

The presence of teeth in AMNH 24444 rules out the classification as member of the edentulous family Tapejaridae. Comparison with *Araripesaurus*, *Santanadactylus* and *Arthurdactylus* is hindered by the lack of cranial material in these genera.

Comparable taxa from Brazil are *Criorhynchus*, *Coloborhynchus*, *Brasileodactylus*, *Anhanguera* and *Cearadactylus*. Table 5.4 lists the features visible in the New York fossil; various important features are not listed because these cannot be observed in AMNH 24444. These features are the presence or absence of a dentary sagittal groove and its morphology; the divergence of the rami and the morphology of the retroarticular process. Other supposedly diagnostic features are left out; the depression at the anterior aspect in *Coloborhynchus* (Fastnacht, 2001) is not diagnostic (Veldmeijer, *et al.*, in review) and not only the second pair of alveoli project anteroventrally, although these are often the most distinct, but also the first and third pairs.

The absence of premaxillary and dentary sagittal crests excludes an assignment to *Anhanguera*, *Coloborhynchus* or *Criorhynchus*. Further differences between AMNH 24444 and *Anhanguera* are seen in the anterior expansion (absent(?) in the former, but present in the latter) and the dentition pattern (flat and erratic, respectively; table 5.4, but see also chapter 7³⁸). *Anhanguera* and AMNH 24444 have in common the dorsoventrally compressed anterior

end, the anterior positioned first pair of teeth which are not distinct dorsally placed relative to the following teeth and the weak frontoparietal crest.³⁹

Besides the lack of the premaxillary and dentary crests, AMNH 24444 differs from *Coloborhynchus* in that the jaws of the latter are distinctly expanded anteriorly, the anterior aspect of the skull is blunt with the first pair of teeth distinct more dorsal than the rest and the dentition patterns are far more erratic.

Differences with *Criorhynchus* (table 5.4) are the slightly upwards–bent snout with the blunt anterior aspect without projecting teeth (in the holotype; BSP 1987 I 46 has teeth at the anterior aspect), the less erratic dentition pattern (compared to *Anhanguera* and *Coloborhynchus*), which is nevertheless more erratic relative to AMNH 24444 and the strong developed frontoparietal crest in *Criorhynchus*. On the other hand, neither of the two *Criorhynchus* species has expanded jaws and the first pair of teeth is not situated distinctly dorsal relative to the remaining teeth (in *Criorhynchus* only, BSP 1987 I 46).

Comparison with *Brasileodactylus* reveals a high degree of resemblance (table 5.4). However, it is not certain to what extent the skull is expanded anteriorly, because the only known specimen including a part of the skull is not entirely prepared (Sayão & Kellner, 2000). The presence of a frontoparietal crest cannot be ascertained either due to the preservation of only the anterior part of the skull. The slight anterior expansion of the mandible in *Brasileodactylus* seems to exclude the classification of AMNH 24444 to this genus, but as stated above, a slight expansion cannot be entirely ruled out.

The presence of a crest (table 5.4) cannot be excluded in *Ce. atrox*, as explained by Kellner & Tomida, 2000). *Cearadactylus? ligabuei* has no crest, but the status of this specimen is disputed (Kellner & Tomida, 2000). Differences between AMNH 24444 and *Cearadactylus* are the bending of the snout, as seen in *Ce.? ligabuei* (but not in the type specimen, *Ce. atrox*). The dentition pattern is not known in *Cearadactylus* and none of the specimens is preserved completely enough to show a possible frontoparietal crest. There is a slight anterior expansion (but for the meaning of this see above). Another difference between *Ce. atrox* and AMNH 24444 is seen in the shape of the rostrum, which results in a gap between upper and lower jaws when closed (Leonardi & Borgomanero, 1985). However, Kellner & Tomida (2000) pointed out that this can only be observed after complete preparation and they suggested that the gap is far less pronounced as originally proposed. Comparable features are the straight upper jaw (except for *Ce.? ligabuei*, in which the jaw is slightly bent), the dorsoventrally compressed jaws (again, not entirely excluded for *Ce. atrox*) and the presence of an anterior pair of teeth that are positioned at the same level as the following ones.

On the basis of the above comparisons it is suggested that AMNH 24444 is closest to *Brasileodactylus* and should be classified herein. Until preparation is completed it remains uncertain whether the mandible has the characteristic dentary sagittal groove with side–grooves that extends to the anterior aspect and if the teeth are situated at the anterior aspect of the mandible.

6. Description of pterosaurian (Pterodactyloidea) remains from the Lower Cretaceous of Brazil in various German collections⁴⁰

6.1. Introduction

The Staatliches Museum für Naturkunde in Stuttgart possesses various specimens of pterosaurs, Rhamphorhynchoids as well as Pterodactyloids, from Germany. Besides these 'native' pterosaur fossils, the collection incorporates pterosaur remains from the Santana Formation, Brazil. The bulk of the material has been previously described (Veldmeijer, 2002); the remaining elements, a small, almost complete mandible and attached vertebrae with the registration number SMNS 55414, are presented in this chapter.

The State Collection Palaeontology and Geology (Bayerische Staatssammlung für Paläontologie und Geologie) in Munich houses one of the largest pterosaur collections in the world. The collection includes Rhamphorhynchoids as well as Pterodactyloids from Germany. Furthermore, the collection incorporates pterosaur remains from the Santana Formation, Brazil. The bulk of the material is previously described (Wellnhofer, 1985, 1987), except for a partial skeleton (BSP 1991 I 27) presented here.

The mandible from the Stuttgarter museum is the most complete mandible of the genus *Brasileodactylus* so far. The material from the Munich collection is especially important because of the non-crested skull. The aim of the present work is to present a description and classification of the material, which is the most complete hitherto known of *Brasileodactylus*. The comparison is limited to the toothed taxa from Brazil with the exception of type specimens and holotypes from other areas (*viz.* Cambridge Greensands, England).

6.2. Abbreviations

cond.	condyle	n.c.	neural canal
co.	cotyle	n.s.	neural spine
d.sag.gr.	dentary sagittal groove	pal.sag.r.	palatal sagittal ridge
del.cr.	deltpectoral crest	po.z.	postzygapophyses
ex.p.	exapophyses	post.tub.	posterior tuberosity
pn. for.	pneumatic foramen	pr.z.	prezygapophyses
h.	head	r.t.	replacement tooth
hyp.	hypapophysis	s.gr.	side-grooves
d.	indented	t.p.	transverse processes
		tub.	tuberculum

6.3. The *Brasileodactylus* mandible SMNS 55414

6.3.1. Preservation

The specimen is a nearly complete lower jaw, lacking the retroarticular processes. The specimen is still embedded with its left lateral aspect. The matrix obscures the alveoli at this side. It is not clear whether the left ramus is still embedded in the matrix; it might be broken. The right ramus is partially obscured, especially at its medial aspect. The condition of the preserved mandibular part is good and only parts of the dorsal aspect are slightly damaged, resulting in an unclear dentary sagittal groove at some places. All teeth are broken at the alveoli, but remnants are visible in some of the alveoli (sixth to ninth). Remnants of the first pair of teeth are still visible in the matrix.

Attached to the matrix are three vertebrae, which are, judged from the elongated centra, cervicals of the midseries. The vertebrae are still largely embedded; one however is prepared for a large part but the postexpophyses are not preserved. It is assumed that the vertebrae and mandible belongs to the same individual. Due to the incompleteness and unprepared state, no further attention is given to the vertebrae. Bennett (1994) remarked that the vertebrae are like those of *Ornithocheirus*, as presented by Owen (1861⁴¹). However, the conclusion based on this is premature because the largely embedded state of the vertebrae in SMNS 55414 prohibits a detailed comparison.

6.3.2. Systematic palaeontology and description (figures 6.1, 6.2 ; tables 6.1, 6.2)

Family ?Anhangueridae Campos & Kellner, 1985b⁴²

Genus *Brasileodactylus* Kellner, 1984

Type species and specimen: *Brasileodactylus araripensis*, anterior part of mandible, MN 4804–V, Museu Nacional, Rio de Janeiro, Brazil.

Diagnosis: *Brasileodactylus* as diagnosed by Kellner, 1984 (580): "Pterosauriër mit Unterkiefer gebildet aus einer länglichen am Ende abgerundeten Symphyse, leicht nach oben gebogen, triangulärem Querschnitt, Schmälerung ab dem proximalen Teil, wobei eine Verbreiterung an dem distalen Bereich ab der dritten Alveole existiert, die eine flache Oberfläche bildet. Vorhandensein einer medialen Furche an der Dorsalseite der Symphyse, sehr ausgeprägt ab dem Beginn des Unterkiefers (distaler Teil), die sich in proximaler Richtung verbreitet. Alveolen mit elliptischer [sic] und rundlicher Form, Zahnabstände vergrößern sich in proximaler Richtung. Bezahnung bis an die Unterkieferspitze, Zähne schmal und spitz, nach vorne stehend." English translation see Kellner & Tomida (2000: 102).

Emended diagnosis: Combination of first pair of alveoli positioned at the anterior aspect; the second pair of alveoli positioned anterolaterally and the third pair of alveoli laterally. The dentary sagittal groove has small anterolaterally extending side-grooves.

Discussion of diagnosis: Kellner & Tomida (2000: 103) evaluated *Brasileodactylus* and came to the conclusion that the "4) rostral end expand from the third alveoli, forming a flat surface. 5) medial groove on the dorsal part of the symphysis, starting on the rostral tip and widening caudally." have to be regarded as apomorphies of *Brasileodactylus*. They regard the degree of expansion as apomorph (*ibidem*). Kellner (1984) regard *Brasileodactylus* as *Ornithocheirid*. The rostral end starts to expand between the third and fourth alveoli, while between the fourth and fifth alveoli in *Anhanguera* and *Coloborhynchus*. However, the expansion in SMNS 55414 starts between the fourth and fifth alveolus as well. The expansion in *Brasileodactylus* is small but distinct, contrasting the robust expansion in *Coloborhynchus*, and equals the situation in *Anhanguera*. The configuration of the alveoli in the anterior part of the jaw, roughly the spoon-shaped expansion, is not seen in other pterosaurs. The first three pairs of alveoli are at the anterior, anterolateral and lateral aspect respectively (these are positioned anterodorsally and laterodorsally in *Anhanguera* and *Coloborhynchus*; the second and third pairs being orientated anterodorsally). The small side-grooves of the dentary sagittal groove are only seen in *Brasileodactylus* and are regarded as apomorph.

Brasileodactylus araripensis Kellner, 1984
Brasileodactylus araripensis

Holotype: Anterior part of mandible, MN 4804–V, Museu Nacional, Rio de Janeiro, Brazil.

Diagnosis: as for genus.

Description

SMNS 55414 agrees with the former descriptions of *Brasileodactylus* (Kellner, 1984; Sayão & Kellner, 2000). The long and slender lower jaw (figures 6.1, 6.2; tables 6.1, 6.2) is anteriorly slightly expanded and dorsally flattened, which results in a flat spoon-shaped part. This expansion starts between the fourth and fifth alveolus. The jaw has its smallest width immediately posterior to the expansion but widens continuously posteriorly, including the rami. No sutures are observed.

Seen from a dorsal perspective, a dentary sagittal groove (d.sag.gr.), starting at the anterior aspect, continuously increases in width posteriorly and deepens as well. The sloping sides slightly bulge at the dorsal surface. At few points, the groove has small side-grooves (s.gr.), which are orientated anterolaterally. These side-grooves are not limited to the sloping faces of the groove, as in the holotype. Instead, some extend over it.

The first pair of alveoli is positioned at the anterior aspect whereas the second is positioned anterolaterally. The third and fourth alveoli are situated at the lateral aspect (the fourth slightly more laterodorsally) and the subsequent alveoli are positioned increasingly laterodorsally. The alveoli until the tenth point slightly anterodorsally rather than straight dorsally. The specific position of the first three pairs (respectively anterior, anterolateral, lateral) is not seen in any other pterosaur and can be regarded as apomorph for *Brasileodactylus*. The alveoli are slightly elliptical but almost circular in cross-section (with the long axis in an anteroposterior direction). From a laterodorsal position, the area between the alveoli and the diverging dentary sagittal groove at the dorsal aspect, is indented (d.). A replacement tooth can be seen at the posterior aspect of the first tooth right (r.t.).

6.3.3. Comparison and discussion

The presence of teeth excludes the classification as Tapejarid. For the same reason, the specimen cannot be referred to the edentulous Azhdarchids.

Comparison with the remaining, toothed, taxa from Brazil is limited to those that include cranial material. The various *Anhanguera* and *Coloborhynchus* species as well as *Criorhynchus* can be excluded from classificatory comparison because these genera all have premaxillary dentary crests; a feature which is not present in SMNS 55414. The remaining taxa are *B. araripensis* (including a *B. cf. araripensis* and *B. sp. indet.*), *Ce. atrox* and *Ce.? ligabuei*. The presence of a crest cannot be excluded in *Ce. atrox* (see Kellner & Tomida, 2000). *Cearadactylus? ligabuei* has no crest, but doubts have been raised whether the parts of which the specimen consists, actually belong to one individual (*ibidem*, but see Unwin, 2002); comparison should be viewed in this light. Therefore, it is difficult to use this specimen in comparative anatomy. Differences between SMNS 55414 and *Cearadactylus* are the dorsal bending of the snout, as seen in *Ce.? ligabuei* (but not in *Ce. atrox*). The dentition pattern is not known in *Cearadactylus*. There is a slight anterior expansion of the anterior part of the mandible. Another difference between *Ce. atrox* and SMNS 55414 is seen in the morphology of the anterior part of the mandible, which shows a gap between upper and lower jaws when

closed in *Ce. atrox*. It is however pointed out by Kellner & Tomida (2000) that this can only be observed after complete preparation and they suggest that the gap is far less pronounced as originally proposed.

Comparable features are the dorsoventrally compressed jaws (again not entirely excluded for *Ce. atrox*). The number of teeth in the mandible of *Cearadactylus* is larger (28 in *Ce. atrox* and at least 22 in *Ce.? ligabuei* based on the number of teeth in the skull). The skull in *Ce.? ligabuei* has a premaxillary sagittal ridge, which, as is assumed, corresponds with a dentary sagittal groove. If this is so, the groove did not start at the anteriormost aspect but rather more posteriorly, as seen in *Co. robustus* (SMNK 2302 PAL; Fastnacht, 2001).

Various fossils are known that are referred to as *Brasileodactylus*. However, comparison is limited to the holotype (Kellner, 1984) and *B. cf. araripensis* (Sayão & Kellner, 2000). Comparison with *Brasileodactylus* sp. indet., (Veldmeijer, 2003b), is limited because this fossil is still largely embedded, obscuring the dorsal and anterior aspects (which contain most of the diagnostic features). Comparison with *Brasileodactylus* reveals a high degree of resemblance. SMNS 55414 and the two mentioned specimens, have in common the slight anterior expansion of the dorsoventrally compressed anterior part, the lack of a dentary sagittal crest and the presence of a posterior widening dentary sagittal groove, which starts at the anteriormost aspect. Also visible in the holotype as well as the Stuttgarter mandible are the dentary side-grooves; a feature not seen in other pterosaurs. Furthermore, the holotype and the specimen described in the present work have the anterior aspect with the three pairs of alveoli in common. Both the holotype and SMNS 55414 show the indented areas between the alveoli and dentary sagittal groove (a feature also seen in *Co. robustus* SMNK 2302 PAL). This is not visible in the *cf.*-specimen, which is due to the severe compaction of this fossil. The expansion of the anterior part of the mandible in SMNS 55414 however, is more pronounced and the jaw is comparatively more slender than the holotype (not clearly visible in the *cf.*-specimen). Based on the small piece, the holotype seems to widen less strongly relative to SMNS 55414.

Differences with *L. sibbicki* are the fact that the lower jaw in this new species seems not expanded (but this cannot be ruled out entirely) and dorsoventrally compressed. The first three alveoli are positioned anterodorsally rather than anterolaterally and laterally. Apparently, *L. sibbicki* lacks the small side-grooves of the mandibular sagittal groove.

From the comparison it can be concluded that SMNS 55414 must be classified as *Brasileodactylus*. The only known species, *B. araripensis* consist of the anteriormost part and the differences with the described mandible are small (basically only the degree of posterior width and pronounced anterior expansion). This however, does not warrant the establishment of a new species; the posteriorly increasing width in the Stuttgarter mandible seems to be stronger but cannot be properly compared with the incomplete holotype. Furthermore, it is assumed that the overall larger size of the holotype is to be regarded as variation within the species.

6.4. The partial skeleton of *Brasileodactylus* in the Munich collection

6.4.1. Preservation

The fossil (BSP 1991 I 27) is a partial skeleton and consists of the anterior part of the maxilla (lacking the anteriormost part), the proximal parts of both humeri (from the deltopectoral crest onwards), both complete scapulae, both complete coracoids, the distal part of the first wing finger phalanx, the proximal part of the second phalanx of the wing finger, the sixth to ninth almost complete cervical vertebrae, the first to tenth complete dorsal

vertebrae (9 and 10 broken and incomplete respectively), four pieces of rib, the left pubis, the dorsal piece of right ischium (including anteroventral part of acetabulum) and the anterodorsal piece of the left ischium and seven small fragments of vertebrae.

The anterior end of the maxilla is worn, showing rounded edges. This suggests that this end was sticking out of the matrix and eroded by water. This kind of wear is also seen in material from the Cambridge Greensands. Of the vertebrae, the sixth and seventh cervical vertebrae are not complete. Parts of the left postzygapophysis, exapophyses and the neural spine lack in the sixth cervical. The surface of the left lateral side lacks the outer bone layer, displaying a rough surface. The seventh cervical is even less complete, lacking a large part of the posterior condyle and exapophysis, the right prezygapophysis and the neural spine. The postzygapophysis at the right side is slightly damaged. The eighth cervical is complete but ventrally, the rim of the anterior cotyles is a little damaged. Most of the dorsals are slightly damaged; often pieces of the neural spines and the tips of the transverse processes lack. Only three ribs are partially preserved; the right one of the first dorsal vertebra is almost complete. Of the humeri, only the proximal parts, including the attachment of the deltopectoral crest, a feature which is often seen with humeri (*e.g.* De Buissonjé, 1980; Wellnhofer, 1991b), have survived. The left one is almost intact, save some minor damage at the head; the right one is damaged at the inner side of the deltopectoral crest and at the posterior tuberosity.

6.4.2. Systematic palaeontology, description and comparison (figures 6.3–6.11; tables 6.3–6.11)

Brasileodactylus sp. indet.

Maxilla (figures 6.3, 6.4 ; table 6.3, 6.4)

The crestless maxilla, lacking the anteriormost tip, is slender, and broadens in posterior direction. The preserved anterior end of the rostrum shows the beginning of an anterior expansion, the dimensions of which cannot be established. Seen from ventral view, small foramina (for.) insert especially towards the expansion; from lateral view, the expansion starts immediately anterior to a narrowed area, containing three alveoli regarded as the fifth to seventh alveolus on the basis of the comparison with complete specimens. The preserved alveolus at the posterior beginning of the expansion of the left side is substantially bigger relative to the three alveoli in the retracted area and is bigger relative to the other alveoli as well. The three alveoli in the retracted area are amongst the smallest preserved. The alveoli are increasingly wider spaced in posterior direction. Some alveoli have erupting teeth preserved (the fifth and eleventh alveolus right and the sixth and tenth left). Only one fully erupted tooth is visible (tenth right). It points ventrally and faces slightly anteromedially. The cross-section is elliptical, with the inner (lingual) aspect flattened. Seen from ventral view, at the posterior beginning of the retractions, anteroposterior ridges start that separate the teeth-bearing sides from the palate. Slightly posterior to this beginning emerges a small but distinct palatal sagittal ridge (pal.sag.r.), which widens slightly and becomes less well defined posteriorly. In posterior direction, the dorsal border extends continuously dorsally. The cross-section is triangular.

Comparison: *Criorhynchus* is one of the many taxa from the Cambridge Greensands that fuels long lasting discussions and many reviews. More recently, Fastnacht (2001) regards *Criorhynchus* a valid taxon, whereas Unwin (2001) does not and refers to Fastnacht's type specimen as *Ornithocheirus*, regarding it type specimen of Ornithocheiridae.⁴³ Veldmeijer (2003a) refers to the Brazilian specimen as "*Cr.*" *mesembrinus*. In doing so, he

acknowledged the dichotomy but realised that only a detailed evaluation can shed light on this very complicated issue before accepting or refuting one of the conclusions. In the present work however, *Criorhynchus* is regarded a valid taxon (as a result of accepting *O. compressirostris* (Owen, 1851) as type specimen of Ornithocheiridae). The specimen recovered from the Cambridge Greensands is a small anterior piece of the rostrum of only few cm long and can not be compared with BSP 1991 I 27 because this has no anterior parts preserved. Comparison is therefore concentrated on the Munich skull and mandible (BSP 1987 I 46) recovered from the Araripe basin. The presence of a premaxillary sagittal crest, which starts at the blunt anterior aspect, contrasts with the non-crested jaw of BSP 1991 I 27. In *Cr. mesembrinus*, the palatinal sagittal ridge is much stronger (even extending ventrally beyond the teeth-bearing ridges) and extends far anteriorly. The teeth in *Cr. mesembrinus* do not show a strong variation in size as seen in the Munich material but the alveoli can not be regarded completely isometric as suggested by Fastnacht (2001). The skull has no retracted ventral margins with smaller teeth.

Various skulls from the Araripe basin have been described and classified as species of *Coloborhynchus*. The type specimen however, originates from England. In general, *Coloborhynchus* differs from BSP 1991 I 27 in the fact that *Coloborhynchus* has a premaxillary sagittal crest that starts at the anterior rostral margin. Other characteristics, such as the blunt anterior margin with teeth, cannot be compared due to the incompleteness of the material described here.

Comparison with *Co. clavirostris* is limited, because of the fact that the specimen is the anteriormost part of the skull, which is not preserved here. *Co. clavirostris* has a premaxillary sagittal crest and a prominent palatinal sagittal ridge, which extends much further anteriorly (almost until the anterior aspect). BSP 1991 I 27 has no crest and although the palatinal ridge is distinct, it is more delicate and does not extend as far anteriorly. The senior author studied a referred skull of *Co. araripensis* (see Kellner & Tomida, 2000). The skull in having a flat rostrum with the first two teeth projecting, clearly shows features characteristic for *Coloborhynchus*. The holotype of *Co. araripensis* (Wellnhofer, 1985) did not have the anterior part preserved that could be compared with the fossil described here. Except for the presence of the crest, the two specimens show a palatinal ridge that extends in the same way and *Co. araripensis* also shows the retracted margin, containing three alveoli (5–7). Comparison with the holotype of *Co. robustus* is not possible due to the fact that this is only a lower jaw. The Karlsruhe specimen however (SMNK 2302 PAL), consist of the anterior parts of the mandible as well as the cranium (Fastnacht, 2001). *Coloborhynchus robustus* differs, besides the crest, because it has a robust expanded anterior part and the jaw is not dorsoventrally flattened. A palatinal sagittal ridge might have been present, but would not extend far anteriorly. On the other hand, the ventral margin of the premaxilla is slightly retracted in which alveoli 5–7 are situated and this compares well with BSP 1991 I 27. *Coloborhynchus piscator* (Kellner & Tomida, 2000) differs besides the presence of a premaxillary sagittal crest, because of a relatively slight expanded anterior part, the much bigger size and the lack of a retracted ventral premaxillary margin. *Coloborhynchus spielbergi* has a large premaxillary sagittal crest, a medium expanded anterior part and a slightly upwards bent snout. The ill-defined palatinal sagittal ridge extends until well onto the expanded part.

Cearadactylus atrox is not prepared three dimensionally, thus important features might still be obscured. Furthermore, as mentioned previously, the fossil is in bad shape, which resulted in the rejection of few characters (Kellner & Tomida, 2000). *Cearadactylus? ligabuei* shows some comparable characters, but the specimen has a dubious reputation (see above). Nevertheless, the premaxilla has no crest and in this it compares well with the Munich

specimen. Both fossils show a retraction in which smaller alveoli are positioned; on the other hand, the overall size of *Ce.? ligabuei* is bigger and the dentition of *Cearadactylus* and the specimen described clearly differ, the former being much bigger in general.

Anhanguera has also a premaxillary sagittal crest and differs therefore from the presented material. In *Anhanguera* the crest does not start at the anteriormost margin but more posteriorly. The snout anterior to the crest is dorsoventrally compressed. *Anhanguera blittersdorffi* differs, besides the presence of a crest, in the fact that it has no retracted margin. Comparison with *An. santanae* is limited, because the holotype (BSP 1982 I 90) lacks the anterior portion. Still the beginning of a crest is visible. The second specimen of *An. santanae* (AMNH 22555⁴⁴) clearly shows the palatinal sagittal ridge, extending almost until the anterior aspect; the premaxilla has no retracted area.

Brasileodactylus is one of the first described pterosaurs from the region, based on cranial material. *Brasileodactylus* is one of the two specimens known from the basin (together with *Cearadactylus*) lacking a premaxillary sagittal crest. The type specimen of *Brasileodactylus* and holotype of *B. araripensis* consists of the anterior part of the mandible. Comparison with the Munich material is therefore not possible. The specimen described by Sayão & Kellner (2000), originating from the Crato Member, consists of the anterior parts of the rostrum and mandible. The rostrum does not have a crest and no retraction of the ventral margin of the premaxilla. Sayão & Kellner (*ibidem*: 4) mention that: "Despite the fact that MN 4797-V was submitted to lateral compression during the fossilization process, it can be observed that the most anterior portion is expanded." The ventral aspect of the skull is obscured. However, because the lower jaw has a groove, which extends until the anterior aspect⁴⁵ it can only be tentatively assumed that the specimen has a corresponding sagittal ridge at the palate but absolute certainty cannot be obtained. The largely unprepared state of *Brasileodactylus* sp. indet. (AMNH 24444; Veldmeijer, 2003b) did not allow a detailed comparison. However, the specimen lacks a premaxillary sagittal crest and the anteriormost tip of the rostrum is dorsoventrally flattened and in this it compares well with the Munich material. The retraction of the ventral margin cannot be observed because this area is damaged at the exposed right side.

Comparison with the recently described *L. sibbicki* shows that none of the specimens posses a premaxillary crest. On the other hand, the teeth seems to be bigger relative to BSP 1991 I 27 but no measurements are given of the dentition (and the fossil in general!). The jaws are likely not expanded. Seen from lateral, the dorsal line of the maxilla in *Ludodactylus* is slightly concave, contrasting with the Munich mandible which has a straight edge that slopes towards the front continuously. Further comparison is hindered by the fact that *Ludodactylus* is compressed and not fully prepared, obscuring the ventral aspect.

Cervical vertebrae (figure 6.5; table 6.5)

The general anatomical features compare well with previously described cervicals vertebrae (Kellner & Tomida, 2000; Veldmeijer, 2003a; Wellnhofer, 1985, 1991b). The sixth and seventh cervicals are somewhat similar to each other. They are strongly procoelous, with large neural spines. Large pneumatic foramina can be found at the lateral sides of the centra. The eighth and ninth cervicals are more similar to the dorsals; their centra are shorter and their neural spines are blunter and higher. Besides, they posses large attachment areas for ribs.

Sixth cervical vertebra (figure 6.5; table 6.5)

The sixth cervical has a long, elongated centrum, which is, seen from ventral, strongly restricted in width in the middle. The centrum is slightly concave

Anteroventrally, a strongly developed hypapophysis (hyp.) is present, which fades continuously in posterior direction and disappears at approximately one third of the length of the centrum. The strongly concave cotyle (co.) has the characteristic triangular-like shape with a slightly indented middle part surrounded by a pronounced upper edge. The lateral edges continue at the ventral surface of the centrum where they end in small, elongated concave surfaces, orientated anterolaterally, likely for the attachment of the tuberculum (tub.) of a small cervical rib. The cotyle is laterally and slightly dorsally flanked by the prezygapophyses (pr.z.), displaying large anterodorsally and medially orientated articular surfaces, which are oval in shape. Posterior to the surfaces, a distinct protrusion points anteroventrally with a slight anterior orientation. Dorsally of the neural canal (n.c.) are two irregular shaped pneumatic foramina.

Seen from lateral, the centrum has two large foramina on each side. These foramina are separated from each other by a bony bar.

The edges of the ventral surface run into the exapophyses (ex.p.), which extend dorsally and posteriorly. The flat posteroventral surfaces are incomplete, although only small parts are lacking. Although damaged, the size seems relatively large compared to known examples. Between these exapophyses and ventral to the condyle (cond.) is a vague beanshaped dent for the reception of the hypapophysis of the subsequent cervical. It is situated at the transition of the centrum and the ventral surface of the condyle. The condyle is oval and smoothly rounded in ventrodorsal plane; it is also rounded at the lateral sides, though less so. The condyle is dorsolaterally flanked by the postzygapophyses (po.z.). The relatively large and flat ventral surfaces of these processes face posteroventrally and bear some ridges; cartilaginous tissue connected the processes with the subsequent vertebrae. The slightly oval neural canal lies deep between the postzygapophyses and is laterally flanked by foramina.

Comparison: Differences between the sixth cervical in BSP 1991 I 27 and *An. santanae* are slight. The maximal width is larger in the Munich specimen. Seen from ventral, the hypapophysis is stronger and the centrum is more concave in BSP 1991 I 27. The postzygapophyses are larger. Seen from anterior, two pneumatic foramen are seen dorsal to the neural canal whereas there is only one, albeit larger, in *An. Santanae*.

The sixth cervical in *Co. piscator* is substantially larger in all respects, but Kellner & Tomida (2000) give no morphological description of the cervical. According to the authors (Kellner & Tomida, 2000: 33) “[...] the lateral side {of the seventh cervical} shows that the lateral pneumatic foramen is divided by a bony bar, as in the seventh cervical of AMNH 22555 [...] and can be used to identify cervical 7, at least in *Anhanguera* [...]” However, also the sixth cervical of the Munich specimen displays such a bar, albeit tiny. The bar in the seventh cervical of the Munich specimen is, as seen in *Co. piscator* and *An. santanae*, much more robust.

Seventh cervical vertebra (figure 6.4; table 6.5)

The description of the seventh cervical vertebra presents the differences with the sixth cervical. The centrum is shorter and the exapophyses are extending less ventrally. The posterior aspect is smaller; the neural canal is more circular and the ventral portion of the arch is deeper. The postzygapophyses are situated higher and extend less laterally. The large neural canal is also apparent at the anterior aspect. The surfaces of the prezygapophyses are slightly

narrower; the protrusion posterior to the surfaces is more distinct. Seen from lateral, the two foramen are of different sizes; the dorsal one is far bigger relative to the ventral one and they are separated by a distinct and stout bony bar.

Comparison: As with the previous cervical, differences between the presented cervical and *An. santanae* are slight. The size difference is, again, negligible. The centrum, seen from ventral, is more concave in the Munich material and the hypapophysis is stronger. The protrusions posterior to the articular surfaces of the prezygapophyses seem to be stronger developed in BSP 1991 I 27, but due to the incompleteness of the cervical of *An. santanae*, this statement is to be regarded with caution. Seen from lateral, the foramina in the Munich cervical are smaller.

The seventh cervical in *Co. piscator* is incomplete, which is the reason for the lack of measurements. However, based on own observations, it can be concluded that the width over the postzygapophyses is larger in *Co. piscator*. The overall measurements of the seventh cervical in *Co. spielbergi* is slightly larger. Seen from ventral, the centrum in the Munich material is more concave and the hypapophysis is stronger developed. Seen from lateral, the prezygapophyses extend more abrupt laterally from the centrum in the Leiden specimen of *Co. spielbergi*; the anterior part however, containing the articular surfaces, turns stronger medially. The articular surfaces are orientated less dorsally and face stronger anteriorly. The cervical of *Co. spielbergi* does not show signs of the protrusion posterior to the articular surfaces of the prezygapophyses; also the small, elongated concave surfaces at the centrum which supposedly served for the reception of the tuberculum of the rib is not present. On the other hand, the left side of the Leiden cervical vaguely shows a line at the same position as the concave ventral border of the prezygapophysis in BSP 1991 I 27, between the protrusion for the reception of the tuberculum and the anterior articular surface of the prezygapophysis. The pneumatic foramina are smaller in *Co. spielbergi*.

Eighth cervical vertebra (figure 6.5; table 6.5)

The following cervicals are completely different from the previous ones, despite the fact that they possess broad oval cotyles and condyles as well as large zygapophyses. The flat centrum is shorter than it is wide.

The cotyle is oval rather than triangular in shape and lacks a hypapophysis. The dorsal rim of the cotyle is pronounced. The articular surfaces for the cervical rib are distinctly larger. Seen in anterior view, the cotyle is laterodorsally flanked by mediodorsally oriented prezygapophyses. The prezygapophyses have slightly convex and oval surfaces. The ventral portion of the neural arch is deep and extends dorsally from the centrum. Clear ridges extend from the prezygapophyses mediodorsally towards the neural spine. Seen from lateral view, two small foramina insert in the centrum; the dorsal one is slightly larger than the ventral one.

The condyle is less convex and, although clearly oval, it is less obvious relative to the previous cervicals. The exapophyses are wide but short. The dorsal border of the condyle is dented. The neural canal is circular and relatively large. The neural spine (n.s.) is higher, extends far more posteriorly and large prominent postzygapophyses are positioned high on the spine flanking the ventral portion of the neural arch laterodorsally. The large flat surfaces of these postzygapophyses are oval. They face lateroventrally and laterodorsal to them short processes are situated. At the posterior edge of the transverse process there is a foramen, lateral to the neural canal. Seen from ventral view, small foramina insert approximately halfway the centrum and the attachment area for the capitulum of the rib. The transverse process ends in an articular surface for the reception of the capitulum of the rib. The articular

surface of the reception of the tuberculum of the cervical rib is placed at the lateroventral edge of the cotyle.

Comparison: Again, the size difference between the eighth cervical in BSP 1991 I 27 and that of *An. santanae* is negligible. Seen from ventral view, the ridge that separates the condyle from the ventral aspect in *An. santanae* is not present in BSP 1991 I 27. Instead, the condyle extends slightly onto the ventral surface; the exapophyses extend stronger in lateroventral direction. The dent, anterior to the ridge, is distinct in *An. santanae* but is lacking in the Munich material. Seen from anterior, the cotyle in BSP 1991 I 27 has a dent in the dorsal rim; this is not visible in *An. santanae*. The cotyle in the latter however, is slightly larger in dorsoventral plane.

The eighth cervical in *Co. piscator* is substantially larger in all respects. The centrum is not fused, contrasting with the fused state of the Munich cervical, despite the fact that both animals were not yet fully-grown when they died. The eighth cervical in *Co. spielbergi* is longer but especially wider over the prezygapophyses. The proximal parts of the ribs are still attached to the cervical; the sutures are clearly visible. Seen from ventral view, the exapophyses are less pronounced relative to BSP 1991 I 27. From anterior, the prezygapophyses have a higher position in *Co. spielbergi* and the neural arch is less deep. The pneumatic foramina at the posterior aspect of the lateroventrally descending prezygapophyses are not seen in *Co. spielbergi*. The dorsal rim of the cotyle is substantially more pronounced in BSP 1991 I 27 but *Co. spielbergi* has a dent in the dorsal rim as well (contrary to *An. santanae*).

Ninth cervical vertebra (figure 6.5; table 6.5)

This ninth cervical differs considerably from the former; again the description focuses on the differences between the two. The cotyle is oval but the middle is more strongly dented and the lateral sides are pointed. A small rectangular process is situated at the ventral rim; if this process is to be regarded as a hypapophysis, it differs considerably from the ones seen at the midcervicals in the fact that the latter ones are far stronger and pointed. The process is laterally flanked by small protrusions, which are the attachment areas for ribs. The ventral portion of the neural arch is slightly sunken and there are no ridges that extend from the prezygapophyses mediodorsally towards the neural spine. The prezygapophyses face almost entirely medially and the surfaces are completely smooth. They are positioned higher up in respect to the eighth cervical. Ventral to them are two small foramina.

The transverse processes (t.p.) appear lightly constructed; indeed, much more so than in the eighth cervical. They face posterolaterally instead of lateroventrally and anteriorly as seen in the eighth cervical. The processes are stout and robust. Seen in lateral view, the foramina in the centrum are distinctly smaller.

Seen in ventral view, the centrum is again short compared to the midcervicals, but it is almost as wide as long and slightly concave. The condyle is only weakly convex and the exapophyses are vague bulges in the laterodorsal corners. The dorsal border is indented; the indentation is smaller but sharply defined. The large neural canal is rounded triangular. The neural spine is higher but less wide in anterior–posterior plane. The postzygapophyses are considerably smaller and lack the laterodorsal processes.

Comparison: The ninth cervical in *S. brasiliensis* (this notarium, as noted previously, is included in the genus on the basis of its size) is fused with the first dorsal of the notarium, but Wellnhofer *et al.* (1983) does not regard it as part of the notarium. The cervical is incomplete which hinders a detailed comparison with the material described in the present work. The size is comparable to the Munich specimen.

The ninth cervical in *An. santanae* (AMNH 22555) is not entirely fused with the following vertebra but the exact state of fusion is difficult to determine due to the fact that it has not been prepared entirely. The size is comparable (contra Wellnhofer, 1991b) to BSP 1991 I 27 but the prezygapophyses in the Munich cervical are more distinct, protruding slightly more in anterior direction and separating more clearly from the transverse process. From anterior view, the pneumatic foramina on each side of the neural canal and ventral to the prezygapophyses are larger in *An. santanae*; there is one foramen on each side (contra Kellner & Tomida, 2000). In BSP 1991 I 27, the left side has two small foramina whereas the right side has only one.

Coloborhynchus piscator has a larger ninth cervical, which is not fused to other cervicals or dorsals. The suture between the neural arch and centrum is still visible, contrasting with the condition in the Munich specimen. Furthermore, Kellner & Tomida (2000) mention the presence of two small foramina at the anterior aspect, on each side of the neural canal. As mentioned above, BSP 1991 I 27 has only two foramina on the left side. The ninth cervical in *Co. spielbergi*, which is of comparable size to BSP 1991 I 27, is firmly co-ossified with the notarial dorsals. Veldmeijer (2003a) regards the cervical as part of the notarium. Unfortunately, the vertebra is damaged, which limits the extent of a detailed comparison. The foramina on each side of the neural canal consist of one big and few small ones. The small remnants of the transverse processes in *Co. spielbergi* suggest a less ventral and posterior orientation, although no certainty can be obtained. The neural spine is less stout in the Munich cervicals.

In general, the cervical vertebrae of BSP 1991 I 27 does not account for an identification at species level: vertebrae morphology seems conserved throughout pterosaur species. It is noted however, that not all vertebrae were completely fused.

Dorsal vertebrae (figure 6.6; table 6.6)

The general anatomical features compare well with previously described dorsal vertebrae (Veldmeijer, 2003a; Wellnhofer, 1985, 1991b). The dorsals display strong similar morphology, although they got increasingly smaller. The first dorsals (and the last cervical) however, are often fused into a notarium (*cf.* chapter 2, figures 2.11, 2.12). All dorsals display the demarcation between the neural arch and the centrum, but the sutures become clearer with each subsequent posterior dorsal. The neural arch and the centrum of the ninth and tenth dorsal are not fused. Individual attention is given to the first six dorsals.

The description of this first dorsal vertebra concentrates on the differences with the ninth cervical. This vertebra, the first true dorsal, compares with the last cervical but in general the vertebra is smaller. The cotyle is shallow and only the mediodorsal rims are protruding. There is no hypapophysis and the lateral protrusions are only faint traces. Seen from anterior, the ventral portion of the neural arch, having an almost circular neural canal, is slightly sunken. The orientation of the prezygapophyses is comparable with those in the ninth cervical but they are considerably smaller. Large foramina are situated lateroventral to the prezygapophyses. The transverse processes extend posterolaterally. These processes in the ninth cervical are oriented in the same direction but slightly more posteriorly. Foramina are situated at the anterolateral sides of the neural spine (which is thinner than in the ninth cervical) and mediodorsally to the prezygapophyses. The centrum has a more elongated appearance; it is longer than wide. The condyle is almost smooth and there are no exapophyses. Seen from posterior view, the ventral portion of the neural arch is deeply sunken with a strongly protruding posterior side of the neural spine. The postexapophyses are

situated close together and the surfaces are facing less laterally; instead they face posterolaterally and slightly posteroventrally.

The fused second and third dorsal vertebrae are comparable to the first dorsal, despite being of overall smaller dimensions. In general, the vertebrae are even more lightly built, with more and larger foramina. The cotyle of the second dorsal lack the lateral protrusions entirely and the neural canal is slightly elongated and circular. The prezygapophyses are lower on the transverse processes and the surfaces are turned slightly outwards, *viz.* anteriorly. The transverse processes are thinner and less wide. The neural spine of the second dorsal equals the spine of the first in morphology although it is slightly less high. The neural spine of the third however, becomes thicker posteriorly, starting from halfway the anterior–posterior width, and its height decrease. The centrum of the second and third dorsals are more strongly concave relative to the first.

The fourth dorsal differs from the previous ones in the fact that the dorsal is more stout. There are foramina in the same places (flanking the neural canal at the anterior aspect laterally, ventral and posteroventral to the transverse processes and flanking the neural canal at the posterior aspect laterally) but they are less numerous and smaller in size. The transverse processes are flat, broad and relatively short. Seen from lateral, the anterior corner has distinct articular surfaces for the capitulum of the rib. The thick neural spine is much more robust and contains the oval vaguely saddle-shaped scapula articulation surfaces. The centrum is even more concave.

The fifth dorsal is less robust than the fourth and is more comparable to the second and third dorsals. The neural spine is of limited height and smaller. The transverse processes are still short, broad and flat but less so than seen in the fourth dorsal; their orientation is completely lateral, although they are slightly tilted in anterodorsal direction. The thin bony flange between the process and the cotyle, as seen so prominent in the second dorsal, is almost absent, resulting in a ‘freestanding’ transverse process. The foramina are larger in respect to those in the fourth dorsal and of comparable size as those of the second, including the large foramina dorsal to the prezygapophyses. The prezygapophyses are small and the surfaces are slightly anterodorsally directed. The postzygapophyses are more prominent and lack foramina at the transverse processes, lateroventral to the postzygapophyses, in contrast to the situation in the third and fourth ones.

The sixth to tenth dorsal continuously decrease in overall size. The cotyles and condyles are strongly concave and convex, respectively. The neural spines are thinner and the transverse processes smaller (anterior–posterior). There are no articular surfaces for ribs anymore. The prezygapophyses are oriented mediodorsally.

Comparison: Comparison with the dorsals in *An. santanae* is limited due to the damaged state of the material but the remnants suggest a high degree of resemblance, morphologically as well as biometrically. The specimens of *Anhanguera* that includes these parts of the post-cranial skeleton (besides AMNH 22555 also BSP 1982 I 91), never show the dorsals fused into a notarium. This is also the case with BSP 1991 I 27, although two vertebrae already started to fuse. Posteriorly, from the seventh dorsal onwards, the dorsals in *Anhanguera* tend to decrease in size more rapidly relative to BSP 1991 I 27 (on the basis of the length of the neural spine; the only measurement given for AMNH 22555 by Wellnhofer, 1991b). Wellnhofer (1991b) counted 13 dorsals in AMNH 22555; the number in BSP 1991 I 27 is ten, but the unfused remnants of at least two more vertebrae is among the material. The largely unprepared and damaged state of *An. santanae* (BSP 1982 I 91) limits the comparison as well, but suggests a high degree of similarity.

On the comparison with the notarium in *S. brasilensis* see the comparison with the ninth cervical, the first vertebra of the notarium. We can note that morphologically, the material is

highly comparable but the notarial dorsals are larger (on the basis of the measurements of the centra) than the same dorsals in the Munich material; the free dorsals (numbers six to nine) are slightly larger as well, but the difference is less pronounced. These dorsals in *S. brasiliensis* however, do not decrease in size as is visible in the material described in this work.

The dorsals in *Co. spielbergi* differ especially in their overall larger size, besides the fact the *Co. spielbergi* has a true notarium. The only dorsals preserved in *Co. piscator* are the first five, which are comparable in length and morphology to *Co. spielbergi*, but, in contrast to it, show largely unfused centra. They are larger than the dorsals in BSP 1991 I 27.

The attachment area for the scapula is positioned at the fourth dorsal in all discussed *Anhanguera* and *Coloborhynchus* specimens, as is the case in BSP 1991 I 27. This differs strongly from the situation in *Art. conandolei*, in which the notarium consists of three fused spines (nothing can be said on the centra), two serving as attachment area for the scapula. Although Frey & Martill (1994: 395) admit that “[...] nothing can be said about the vertebrae anterior to the preserved part of the notarium. The fact that these vertebrae are missing indicates that there was probably no fusion at all” they nevertheless use the fusion of these three in their diagnosis of *Arthurdactylus*. The unfused state of notaria is generally regarded as an ontogenetic rather than a morphological character.

Ribs (figure 6.7, 6.9; table 6.7)

Three (pieces of) ribs are part of the remains. One of these is the proximal two thirds of the rib of the ninth cervical. In articulation with the cervical, the rib extends posterolaterally. The shaft of the double headed rib extends lateroventrally and is distinctly curved. The shaft is thin: 4.5 mm. The tuberculum is small and situated close to the shaft; the tubercular articulation is oval and flat. The triangular capitulum is more pronounced and extends from the shaft of the rib; the shaft has a flat ventral surface that transforms into the small ventral aspect of the shaft of the rib proper. The capitular articulation is strongly convex. The surrounding bone of both processes are rugose, which likely is, as suggested by Bennett (2001), an indication of the fusion of the rib to the vertebra. A pneumatic foramen is situated between the capitulum and tuberculum at the posterior surface.

One set of ribs is preserved, which is to be regarded as notarial rib, though the first dorsal was not fused into a notarium. The ribs are of comparable size to the previously described cervical rib and the curvature is comparable as well. The shaft extends lateroventrally and is also bent in posterior direction. The capitular shaft extends stronger ventrally and the big capitular articulation is convex and oval. The tuberculum (tub.), positioned at the shaft, is bigger with a flat and almost circular articulation. Also with these notarial ribs, rings of rugose bone are situated along the margins of the articulations, suggesting the fusion of the ribs and the notarial dorsal.

Comparison: Comparison with the partly prepared ribs in *An. santanae* reveal a high degree of similarity. This is also true for the fragments of ribs in *Co. spielbergi*. The ribs in *Co. piscator* are slightly larger but are morphologically highly comparable.

Scapula and coracoid (figure 6.8; table 6.8)

The general morphology of the bones of the shoulder girdle agrees with that described for other pterosaurs from the Araripe Basin (Kellner & Tomida, 2000; Veldmeijer, 2003a; Wellnhofer, 1991b). The scapula is the shortest of the two and a stout bone. Both scapulae are complete, although one is damaged medially. The shaft is restricted and the proximal articular

surface expanded. A deep pit is visible on the proximal articular surface. The articular surfaces with the coracoid are strongly expanded as well. The coracoid is far less stout but longer. The articular surfaces, with the sternum as well as with the scapula, are small.

Comparison: As already stated, the scapulae and coracoids share the same general morphology as the described species of *Coloborhynchus* and *Anhanguera*. However, the shoulder bones are firmly fused in *Co. spielbergi*, contrasting with the unfused state in the Munich specimen as well as in the other *Coloborhynchus* and *Anhanguera* species. The bones in *Co. spielbergi* and *Co. piscator* have slightly larger overall dimensions; the bones in *Anhanguera* are of comparable size. Shoulder bones, fused into a scapulocoracoid, have been described for *S. brasiliensis*. Comparison is hindered by the fact that this specimen is largely incomplete.

Humerus (figure 6.9; table 6.9)

Humeri of Brazilian pterosaurs are relatively common in the fossil record and general morphology of the here presented humeri agree with former descriptions (especially Kellner & Tomida, 2000; Veldmeijer, 2002, 2003a; Wellnhofer, 1985, 1991b). In general, they are comparatively short, but robust, are expanded at their proximal and distal ends and have a prominent deltopectoral crest.

The head (h.) is elongated anteroposteriorly. The articulation surface is kidney-shaped without a ridge. The depression of the head lies ventrally and continues slightly at the ventral surface, where it is limited by a small ridge, which probably served as an insertion for joint-stabilising ligaments. Seen from ventral view, the area distal to this ridge and posteromedial to the deltopectoral crest is depressed.

The posterior tuberosity (post.tub.) extends from the shaft towards the head. It is a large expansion, relative to the head, but substantially smaller relative to the deltopectoral crest. Seen from dorsal, a pneumatic foramen inserts in the tuberosity proximally.

The deltopectoral crest (del.cr.) extends laterally, starting as a thin proximal flange and continuing with a curve inwards (*i.e.* in posterior direction) towards the ventral end of the crest. The margin of the flange has a distinct convex bend at the place where the flange changes its inward direction into more outward (*i.e.* in anterior direction) bending. The lateral end is greatly thickened and curves anterolaterally towards the shaft. The concave inner surface has prominent scars for muscle attachment.

Comparison: The humerus of *An. santanae* compares morphologically as well as biometrically well with the Munich material, although the ventral rim of the deltopectoral crest has a less strong convex bend in *Anhanguera* relative to BSP 1991 I 27. The ventralmost tip of the crest curves stronger inwards in *Anhanguera*.

The humerus of *S. brasiliensis* differ especially in the fact that the head is more bulbous dorsoventrally. The humeral head in *Santanadactylus* is more strongly directed in dorsal direction. This latter feature can be seen in the humerus of *S. pricei* as well; however, the strong convex bend of the rim of the deltopectoral crest, not seen in the other species of *Santanadactylus*, is clearly visible here but the flange does not has a strong inwards (*i.e.* posterior) direction. This humerus is also much smaller.

The humerus of *Co. araripensis* differ also especially in the fact that the head is more bulbous dorsoventrally. A clear ridge is positioned at the anterodorsal edges of the head, lacking in the Munich material. The humerus described here share the same morphology as *Co. piscator* but the latter is larger in overall dimensions. Comparison with the humerus of *Co. spielbergi* is limited due to the fact that the humerus in the latter is relatively damaged, especially the deltopectoral crest. However, the remaining part of the crest seems to incline

inwards (*i.e.* posteriorly) far less and the convex bend of the rim of the crest is faint. A vague ridge is noticed at the humeral head, though this can hardly be the same ridge as described in *Santanadactylus*, since its position and shape is quite different. Nevertheless, a comparable ridge has not been described in BSP 1991 I 27.

Wing finger phalanges (figure 6.10; table 6.10)

Only small parts of the hyperelongated phalanges of the right wing finger are among the remains; the distal end of the first phalanx and the proximal end of the second phalanx of the wing finger are preserved. Both bones show rugose areas near the articular surfaces.

In dorsal view, the first phalanx is flat, but seen from ventral it is convex. The cross-section of the distal part of the first phalanx is rounded triangular; the bone is slightly thicker at the edges (3.5 mm vs 1.3 mm) (*cf.* Frey & Rieß, 1981). In distal direction, the shaft increases in all directions towards the articular surface. The articular surface is expanded towards the proximal and the surface is strong convex.

The oval articular surface of the second phalanx is concave and expanded posteriorly; it corresponds perfectly with the convex surface of the first phalanx. The bone is distinctly smaller. The phalanx is slightly bent in ventral direction. Seen from ventral, the shaft exhibits a longitudinal groove, resulting in an irregular triangular cross-section.

Comparison: Only few wing finger phalanges have been published, of which only some are complete (Wellnhofer, 1985, 1991b); various others are incomplete (Frey & Martill, 1994; Kellner & Tomida, 2000) or incompletely prepared. The comparison of the distal articular area of the first phalanx reveals great similarity with the known specimens. The complete second phalanx of the wing finger in *Co. piscator* has not been illustrated, but on the basis of own observations by the senior author, it can be concluded that the two phalanges share the same morphology. The second phalanges in *S. pricei* differ in the fact that these do not exhibit the longitudinal groove, seen in the Munich material and in *Co. piscator*. It is interesting to note that this configuration of the second phalanx is considered by Martill & Frey (1999) as a character diagnostic for the pterodactyloid family Azhdarchidae.

Pelvic girdle (figure 6.11; table 6.11)

Three parts are preserved of the pelvic girdle. The left pubis, a laterally compressed bone and relatively long, is preserved. The morphology compares well with previous described specimens (Kellner & Tomida, 2000; Veldmeijer, 2003a; Wellnhofer, 1988). The dorsal part is strong and massive and closes the acetabulum posteroventrally; the ventral plate is gradually more compressed ventrally and has a twisted appearance.

The other part is the dorsalmost part of the left ischium; the part makes up the anteroventral part of the acetabulum. It is broken at the rim. The anterodorsal corner of the right ischium is the third part. Also this bone compares well with previous descriptions.

6.5. Final remarks

As explained previously, the material housed in the Stuttgart and Munich collections is only compared with toothed taxa from Brazil and, if necessary, with taxa from the Cambridge Greensands, England. The morphology of the lower jaw separates it from all known mandibles, except *Brasileodactylus*. The Munich specimen, lacking a mandible, has been assigned to *Brasileodactylus* because of the lack of a premaxillary crest (only seen in *Cearadactylus* and *Ludodactylus*) but the dentition is clearly distinct from *Cearadactylus*. It

has not been assigned *Ludodactylus* due to the stronger teeth in this new genus as well as the non-expanding configuration of the jaws.

Various authors have suggested *Brasileodactylus* to be synonymous with *Anhanguera* (Unwin, 2001) or *Coloborhynchus* (Frey *et al.*, 2003a). As remarked by Veldmeijer & Signore (2004) “The explanation of the supposed difference as the result of ontogeny, sexual dimorphism or variation cannot be proven, mainly due to the scanty fossil record (most of the species are represented by only one (published) specimen, often consisting only of parts of the skull); the fossils should therefore be treated as a different species unless proven (and not just suggested) otherwise.”. On the other hand, as pointed out elsewhere (Kellner & Tomida, 2000; Veldmeijer *et al.*, 2005b; Veldmeijer & Signore, 2004), *Brasileodactylus* is a valid taxon, exhibiting unique configuration of dentition and morphology of the dorsal aspect of the lower jaw, as explained in the emended diagnosis.

The situation on family level of the Brazilian pterosaurs (family in the traditional sense) is complex. The Ornithocheiridae are primarily composed of taxa from the Cambridge Greensands; the Anhangueridae mainly from taxa from the Araripe Basin. The two taxonomic units have been synonymised by various authors (*e.g.* Unwin, 2001) but this is based on the difference in view of the assignment of the type species for Ornithocheiridae with authors who regard them separated (Kellner, 1990; for an overview see Kellner & Tomida, 2000).⁴⁶ It is beyond the scope of the present work to untangle this complicated issue but we regard Anhangueridae as valid and different from Ornithocheiridae, in this agreeing with the designation of *Ornithocheirus compressirostris* as type species of Ornithocheiridae (see Kellner & Tomida, 2000).

7. Updating the toothed taxa

Ever since the first pterosaur was discovered, this extraordinary group of vertebrates has been the subject of much debate and discussion. This is partly due to the fact that the pterosaur skeleton is extremely fragile and as a consequence, there are only relatively few fossils and even fewer well preserved, complete ones (especially those that have been adequately prepared). The present work has presented new material which has increased the knowledge on the morphology and taxonomy of these extinct animals. However, so far, one feature (the dentition pattern) has consequently been referred to ‘study in progress’. Here, these patterns are presented, together with a short summary of all distinct cranial features of the various taxa. This discussion offers suggestions for classification.

7.1. *Brasileodactylus* (Pterosauria, Pterodactyloidea, ?Anhangueridae); an update⁴⁷

7.1.1. Introduction

The aim of this chapter is to present an update of the toothed pterodactyloid taxon *Brasileodactylus* on the basis of the skull, the most distinctive element in the pterosaur skeleton. As done throughout this work, only comparable taxa from Brazil will be taken into account and only those of which cranial material is known. Therefore *Art. conandoylei*, *Ara. castilhoi*, *Ara. dehmi*, *S. brasiliensis*, *S. pricei* and “*S.*” *spixi* are left out.

Dentition is sometimes used for systematic purposes. Unwin (2001) used the relative size of teeth, but the material he uses is extremely fragmented and no reliable picture of the entire dentition can be obtained.⁴⁸ Often, the measurements are not included (exceptions are Fastnacht, 2001; Lee, 1994; Veldmeijer, 2003a; Veldmeijer *et al.*, submitted). Therefore, measurements of dentition are included and discussed.

7.1.2. The known specimens⁴⁹

Systematic palaeontology

Order Pterosauria Kaup, 1834
Suborder Pterodactyloidea Plieninger, 1901
Family ?Anhangueridae Campos & Kellner, 1985b
Genus *Brasileodactylus* Kellner, 1984

Type species and specimen: *Brasileodactylus araripensis*, anterior part of mandible, MN 4804–V, Museu Nacional, Rio de Janeiro, Brazil (figure 7.1).

Diagnosis *Brasileodactylus* as diagnosed by Kellner (1984: 580): ”Pterosauriër mit Unterkiefer gebildet aus einer länglichen am Ende abgerundeten Symphyse, leicht nach oben gebogen, triangulärem Querschnitt, Schmälerung ab dem proximalen Teil, wobei eine Verbreiterung an dem distalen Bereich ab der dritten Alveole existiert, die eine flache Oberfläche bildet. Vorhandensein einer medialen Furche an der Dorsalseite der Symphyse, sehr ausgeprägt ab dem Beginn des Unterkiefers (distaler Teil), die sich in proximaler Richtung verbreitet. Alveolen mit elliptischer und rundlicher Form, Zahnabstände vergrößern sich in proximaler Richtung. Bezahnung bis an die Unterkieferspitze, Zähne schmal und spitz, nach vorne stehend.” English translation see Kellner & Tomida (2000: 102).

Emended diagnosis: Combination of first pair of alveoli positioned at the anterior view; the second pair of alveoli positioned anterolateral and the third pair of alveoli lateral. The dentary sagittal groove has small anterolaterally extending sub-grooves.

Discussion of diagnosis: Kellner & Tomida (2000: 103) evaluated *Brasileodactylus* and came to the conclusion that “4) rostral end expand from the third alveoli, forming a flat surface. 5) medial groove on the dorsal part of the symphysis, starting on the rostral tip and widening caudally.” have to be regarded as apomorphies of *Brasileodactylus*.” They regard the *degree* of expansion as apomorphic (*ibidem*: 103). Kellner (1984) regards *Brasileodactylus* as an Ornithocheirid.⁵⁰ The rostral end of *Brasileodactylus* starts to expand between the third and fourth alveoli, which is between the fourth and fifth alveoli in *Anhanguera* and *Coloborhynchus*. However, the expansion in SMNS 55414 starts between the fourth and fifth alveolus as well. The rostral expansion in *Brasileodactylus* is small but distinct, very similar to the situation in *Anhanguera*, and not consistent with the robust expansion in *Coloborhynchus*. The first three pairs of alveoli are at the anterior, anterolateral and lateral aspect respectively (these are positioned anterodorsally and laterodorsally in *Anhanguera* and *Coloborhynchus*; both second and third pairs are orientated anterodorsally). The remaining alveoli are placed strongly laterodorsally, relative to for example comparable alveoli in *Coloborhynchus*.

In general, the alveoli of the holotype are small (figures 7.2, 7.8). The first one is the smallest, after which the size increases. The third alveolus is the largest one found in the distal expansion; the following alveoli decrease in size continuously but the size increases again steadily from the sixth alveolus onwards. This results in the ninth alveolus being as large as the third one (remarkable is Kellner’s statement on the teeth, as they are not preserved in the specimen).

The small side-grooves of the dentary sagittal groove are only seen in *Brasileodactylus* (holotype and SMNS 55414) and are regarded as apomorphic. Furthermore, the symphysis is extremely elongated relative to other Brazilian pterosaurs like *Anhanguera*, *Criorhynchus* and *Coloborhynchus*.

Although the absence of features is not to be used in diagnoses the absence of crests is important in the studied taxa. Most pterosaurs from this area have crests, premaxillary as well as dentary (recently, a new pterosaur has been published (Frey *et al.*, 2003a) without premaxillary and dentary sagittal crests but with a parietooccipital crest, discussed in more detail below). So far, *Cearadactylus* and *Brasileodactylus* are the only genera without the premaxillary and dentary sagittal crests.

The Crato specimen (MN 4797–V; figures 7.2, 7.3, 7.8)

Various fossils have been assigned to *Brasileodactylus*. The fossil in figure 7.3, originating from the Crato Formation of the Araripe plateau (in the collection of the Museu Nacional, Rio de Janeiro; MN 4797–V), has been assigned to the genus by Sayão & Kellner (2000) as *Brasileodactylus* sp. indet. mainly on the basis of the absence of crests and the presence of a mandibular groove. However, a mandibular groove starting at the tip of the dentary can be found in other pterosaurs as well (*e.g. Co. robustus*) but the type specimen of *Brasileodactylus* as well as the mandible in the Stuttgarter collection (see below) clearly shows small anterolateral running side-grooves. Due to the fact that the fossil is severely deformed by compression, it cannot be determined whether these peculiar side-grooves are present or not. Furthermore, it is difficult to determine the exact position of the alveoli, due to the deformation, although at least the right second and third alveoli seem to be in a

laterodorsal position rather than anterolateral and lateral respectively. According to the authors, the most anterior portion is expanded, containing the largest teeth, although it is not stated which ones exactly. However, the graph shows that the second to fourth alveoli are the biggest together with alveolus seven (see below).

The measurements are comparable to the type specimen of *Brasileodactylus* and holotype of *B. araripensis* (MN 4804–V), although slight differences can be noticed (e.g. the first and sixth alveolus). A major difference is seen in the measurements of the eighth, tenth and eleventh alveolus, which decrease in size relative to the previous alveoli (figure 7.2). This contrasts with the holotype (MN 4804–V), which shows an increase in alveolar diameter, relative to the preceding ones.

The dentition of the skull of MN 4797–V (figure 7.2) shows a comparable pattern as seen for the mandible but with two distinct differences. The third alveolus is clearly the biggest; the differences in measurement of this and the other alveoli are distinct bigger than seen for the mandible. Furthermore, the eleventh mandibular alveolus is the smallest, but in the skull, the smallest alveoli are the fifth and sixth; the size of the eleventh alveolus equals that of the tenth and is of comparable size to the fifth and sixth.

The New York specimen (AMNH 24444; figures 7.2, 7.4, 7.8)

The fossil in the collection of the American Museum of Natural History (AMNH 24444), preliminary described by Veldmeijer (2003b) as *Brasileodactylus* sp. indet., has been assigned to this genus for several characters, among which the most important ones are the lack of premaxillary and dentary sagittal crests and the teeth. However, the published table (*ibidem*: 11) should be revised in due course because more details can be added due to a complete preparation of the fossil. The complete preparation of this specimen, which at this moment is being undertaken in The Netherlands, is important because characteristic features, such as the exact position of the first three alveoli, a possible expansion of the jaws and the side-grooves, are obscured by matrix. Recently, a new genus and species has been published, which originates from the Crato member (figure 7.5), *L. sibbicki* (in the collection of the Staatliches Museum für Naturkunde Karlsruhe, Germany) that looks remarkably similar to *Brasileodactylus* sp. indet. (toothed, crestless dentary and premaxilla) but seems to differ in the presence of a parieto-occipital crest, seemingly lacking in the AMNH 24444 specimen. However, the dorsal view of the cranium (Veldmeijer, 2003b: figures 3 and 4) shows a possible start of a parieto-occipital crest (referred to as frontoparietal crest in Veldmeijer, 2003b). The crest might have been broken off so that the exact shape and extent cannot be determined. A detailed study of *L. sibbicki*, currently in progress, will have to shed light on the attachment of the crest to the skull. Only after the full preparation of AMNH 24444 a detailed comparison can be done and conclusions can be drawn.

The first alveolus of the mandible is comparable to the size of this alveolus in the other discussed specimens (figure 7.2), but the second, third and fourth alveoli are substantially smaller. The curve shows a deep dent at the second third, and fourth alveoli; the fifth alveolus is bigger and equals the size of the first. The position of the alveoli could not be established due to the unprepared state; the mandible faces lateroventrally, limiting necessary visibility to describe alveolar position as well as reliable measurements.

The right side of the skull is exposed, allowing the measurement of 26 alveoli. The graph (figure 7.2) shows that the alveoli are small with bigger measurements for the second, third, fourth, ninth and sixteenth alveoli. These are substantially bigger than the corresponding alveoli in the mandible; most others in the mandible are smaller, except for the eleventh alveolus. Although the ninth and sixteenth alveoli are bigger relative to the previous

and following ones, they still are smaller relative to the second, third and fourth alveoli. The curve shows that the biggest alveoli of the skull are positioned opposite to the smallest alveoli of the mandible; a pattern that, if confirmed after preparation, is not seen in the other discussed specimen that includes cranial alveoli (MN 4797–V). Differences with the alveolar pattern in the skull of MN 4797–V are clear. MN 4797–V has a distinct larger third alveolus where AMNH 24444 has a larger ninth alveolus, lacking in MN 4797–V.

The Stuttgarter mandible (SMNS 55414; figures 7.2, 7.6, 7.8)

This small, partly prepared but largely complete mandible in the Staatliches Museum für Naturkunde, Stuttgart (SMNS 55414; figure 7.6), has been assigned to *Brasileodactylus* as well (Veldmeijer *et al.*, submitted), as it shows diagnostic features for this genus. The extremely elongated mandible clearly shows the dorsoventrally compressed anterior part with the expansion, the particular position of the first three alveoli and the mandibular sagittal groove with side-grooves. This specimen differs from *B. araripensis* in the smaller size and in the fact that the distal expansion is longer and smoother, although the authors do not think that the differences justify the erection of a new species.

SMNS 55414 shows a small first alveolus (the smallest of all known specimens) and a large second alveolus (the biggest of all known specimens); this is in contrast with MN 4804–V which has the third alveolus as its biggest (figure 7.2). The following alveoli (up to the seventh) follow the pattern and approximate size as seen in the holotype of *B. araripensis*; the eighth, ninth and tenth alveolus show the opposite pattern and are slightly smaller.

The Munich specimen (BSP 1991 I 27; figures 7.2, 7.7, 7.8)

The material housed in the Bayerische Staatssammlung für Paläontologie und historische Geologie, Munich, Germany is tentatively classified as *Brasileodactylus* by Veldmeijer *et al.* (submitted). This material consists largely of post-cranial material and includes only a small portion of the crestless maxilla; a direct comparison between this specimen and the type specimen is not possible because the Munich material does not include the mandible. Nevertheless, in assigning the specimen to *Brasileodactylus* on the basis of the comparable dentition (which is clearly distinct from the dentition in *Cearadactylus*) and the crestless maxilla (only occurring in this taxon as well as *Cearadactylus*), the first fully prepared post-cranial material of this taxon was presented, thus avoiding the establishment of another taxon.

The first visible alveolus on the left side was identified as the fourth one. If however, the measurements of this specimen are compared with those of MN 4797–V (figure 7.2) the following observations can be made. The graph is comparable for the first four measurements of BSP 1991 I 27. After that, the differences are slightly bigger. This questions the conclusions by Veldmeijer *et al.* (submitted), whether the fourth alveolus is the fourth and not the third because if so, the curves would be more or less equal in pattern. We also have to take into account that the graph of the Munich maxilla is based on average measurements of both sides, in contrast to MN 4797–V which is only based on the right side. Differences with AMNH 24444 are basically the same as described for MN 4797–V.

7.1.3. Diastemae (figure 7.8)

The graph of the diastemae of the mandibles (figure 7.8) shows a remarkable uniform picture, *i.e.* a strong increase in size posteriorly, despite some small fluctuations. As with the alveoli, the graph of AMNH 24444 differs.

The diastemae of the skull are shown in figure 7.8. The pattern of the diastemae of the cranium in MN 4797–V is remarkably similar, despite small differences, to the curves of the mandible. Again, a difference can be noted for the graph of AMNH 24444. Here, a steady increase in diastemae size can be seen until the diastema 7–8. The following diastemae decrease in size at least until diastema 9–10 after which the diastemae increase in size (it remains uncertain whether this starts with diastema 10–11 or with the following). Another strong decrease in size occurs with diastemae 14–15 and 15–16 after which again a strong increase in size occurs. A last sharp decrease can be seen with diastemae 19–20 and 20–21, after which for the last time an increase in size can be noted, but far less relative to the more anterior ones.

This means that, when the fluctuations are included, the size of diastemae increases first posteriorly, but decreases from diastema 10–11 or 11–12. Full preparation of the specimens, allowing the measurement of the left side, is needed in order to confirm this deviating pattern. The pattern of diastemae in BSP 1991 I 27 is, despite small fluctuations, in line with the pattern seen in MN 4797–V, except for the decrease in size, which starts later relative to the others (with diastema 11–12 instead of 10–11 for MN 4797–V), but differ markedly with AMNH 24444. These differences are more or less the same as explained with the comparison of the New York specimen with the Crato specimen.

7.2. *Coloborhynchus* from the Lower Cretaceous Santana Formation, Brazil (Pterosauria, Pterodactyloidea, Anhangueridae); an update

7.2.1. Introduction

Despite the fierce debates on Brazilian pterosaurs, some characteristics of the pterosaur skeleton (and especially of the skull) have either been overlooked, given only slight attention, or dismissed as insignificant. Here these data of the taxon *Coloborhynchus* are presented together with an update of this toothed pterodactyloid taxon. The following discussion is limited to the skull, the most diagnostic element of the pterosaur skeleton.⁵¹

7.2.2. The known specimens

Systematic palaeontology

Order Pterosauria Kaup, 1834
 Suborder Pterodactyloidea Plieninger, 1901
 Family Anhangueridae Campos & Kellner, 1985b
 Genus *Coloborhynchus* Owen, 1874

Type species and specimen: *Coloborhynchus clavirostris*, anteriormost part of the cranium, BMNH 1822, British Museum of Natural History, London, Great Britain (figure 7.9).

The holotype consists of a severely worn anteriormost part of the cranium, which has been the cause of much debate and various synonymies. As a consequence, the history of

Coloborhynchus is complex and related to the history of *Criorhynchus* (see e.g. Hooley, 1914; Wellnhofer, 1978). *Coloborhynchus*'s most characteristic feature is that the two front teeth protrude from the blunt anterior aspect on a more dorsal level relative to the subsequent teeth on the lateral margins (see for overviews and recent participations in the discussion Fastnacht, 2001; Lee, 1994 and Veldmeijer, 2003a). The premaxillary sagittal crest, commencing from the anterior view, is broken and reconstruction of the shape of the crest remains dubious, further hindered by the severely eroded state. The palate has a strongly developed ridge, which widens posteriorly.

Diagnosis by Fastnacht (2001: 24), modified after Lee (1994: 756): "Median depression on the anterior margin of the upper jaw. Flattened anterior margin of the premaxilla triangular. Pair of teeth projecting anteriorly from the blunt anterior margin of the upper jaw at a significant elevation above the palate relative to subsequent teeth. Medial crest on the upper jaw rises from the tip of the snout. Upper jaw laterally expanded in a spoon-shape in dorsal view from the second to the fourth pair of alveoli. Lower jaw with medial crest rising from its anterior end. Lower jaw laterally expanded in a spoon-shape from the first to the third pair of alveoli. Second and third pair of alveoli of the upper and lower jaw enlarged relative to other alveoli." Diagnosis of species according to Lee (1994) is the same as for the genus.

Discussion of diagnosis: A true diagnosis of the genus was never given by Owen; he only gave a description with special attention to the position of the first pair of teeth. The most recent diagnosis was given by Fastnacht (2001: 24), modified after Lee (1994: 756), cited above. Several problems with this modified diagnosis can be noted. As explained below, the median depression on the anterior margin of the upper jaw cannot be used as diagnostic feature on species level. Another feature, not included in Fastnacht's diagnosis and only with certainty seen in the Karlsruhe specimen, is the mandibular groove, extending all the way to the anterior margin of the mandible. Mandibular grooves are seen in various other taxa as well but the true value lies in the different morphology: the groove in *Brasileodactylus* has small side-grooves (Veldmeijer *et al.*, submitted), in *Criorhynchus* the groove is deep and wide (Wellnhofer, 1987) and in *Anhanguera* the groove is flanked with slightly raised edges (Veldmeijer *et al.*, 2005a). Furthermore, the shape and size of the premaxillary sagittal crest shows an enormous variety and is therefore not to be regarded as diagnostic (Veldmeijer, 2003a) as supposed by Kellner & Tomida (2000). The anteroventral projection of the second pair of teeth of the cranium is not unique to *Coloborhynchus* but seen in almost all other toothed taxon from the Araripe Basin. It is important to note that the expansion of the jaws in *Coloborhynchus* is robust ('squarish'), contrasting the smooth (spoonshaped) expansion in the other crested taxon *Anhanguera* and the more emphasised expansion in the non-crested *Brasileodactylus*. The jaws in the crested *Criorhynchus* are not expanded. The teeth are, in general, bigger and less numerous than in *Anhanguera* and in size much more comparable to *Criorhynchus*.

In the type specimen, no teeth are preserved, although remnants of the teeth are still visible in some alveoli. Note that some of the alveoli are damaged and thereupon smoothed by most likely water erosion. The first pair of alveoli are positioned at the anterior aspect, distinct dorsal to the teeth-bearing border of the cranium; these point forward. The position of the second pair of alveoli is strongly lateral and slightly ventral; they point slightly anterior. The positions of the third pair of alveoli is lateroventrally as well, but far more lateral than ventral. The subsequent alveoli (at the start of the expansion), numbers four, five and six are lateroventrally orientated but with increasing emphasis ventrally. All alveoli are directed

slightly anteriorly. The rest of the dentition, based on the few complete skulls, are increasingly ventrally orientated but the last ones (in *Co. piscator*) again have an increasing lateral orientation.

In the mandible, the first pair of alveoli (based on the Munich mandible of *Co. robustus*), is positioned at the border of the anterior and dorsal aspect, although for the largest part at the anterior aspect. They stand slightly lateral relative to a true anterior position. The orientation of the alveoli are anterodorsal but the anterior orientation is far less relative to the dorsal orientation. The orientation of the second to third pairs of alveoli is laterodorsal. These are the alveoli, which are positioned at the expansion. The fourth, although also at the expansion, is positioned more dorsal relative to the previous ones. The smaller alveoli five and six are positioned laterodorsally but more dorsally relative to the previous alveoli; these are positioned in the laterally indented area posterior to the expansion. All of these alveoli point anterodorsally, but the more posterior ones point less strongly anterodorsally. The subsequent pairs, 7–15, are positioned laterodorsally, but more dorsal than lateral. The last three alveoli have a straight dorsal position.

The front teeth are hook shaped and posteriorly bent. The following two teeth are hook shaped as well and posterolaterally curved; the remaining teeth are only slightly bent and more or less straight. The teeth are rounded lingually and flattened labially (for a detailed description see especially Wellnhofer & Buffetaut, 1999). Thus the front of the beak forms a perfect grasping device with large, interlocking teeth, whereas the teeth more towards the back serve, with their orientation and more upright position, to hold and transport the prey towards the throat.

The graph of the measurements of the alveoli (figure 7.10) shows that the second and third pairs of alveoli are the biggest. The first pair of alveoli, projecting from the anterior aspect, are substantially smaller and of comparable size to the fourth pair of alveoli. The fifth and sixth pairs of alveoli are smallest. The graph of the diastemae (figure 7.18) shows a clear depression, with the smallest measurement for the diastemae between alveolus 4 and 5.

Coloborhynchus araripensis (BSP 1981 I 89, MN 4735–V; SAO 16494; figures 7.10, 7.11, 7.12, 7.17)

Initially, the Munich specimen (BSP 1982 I 89), consisting of the middle part of the cranium (figure 7.11) and various post-cranial elements, was described as *Santanadactylus* (Wellnhofer, 1985). Kellner (1990) reclassified it as *An. araripensis*, using another, unpublished and only partially prepared cranium in Museu Nacional (MN 4735–V; Kellner & Tomida, 2000). But the referred specimen and a hitherto unpublished specimen housed in the Collection Oberli, St. Gallen, Switzerland (SAO 16494; figure 7.12) suggest a reclassification as *Coloborhynchus* because the anterior aspect in the referred specimen is blunt and the first pair of alveoli is situated distinct more dorsal relative to the subsequent alveoli: a distinct feature of *Coloborhynchus*. *Brasileodactylus* lacks a crest, whereas the premaxillary crest in *Anhanguera* terminates well before the anterior margin. And this in turn contrasts with *Coloborhynchus*, because in this taxon the crest terminates at the anterior margin. Kellner & Tomida (2000) conclude that it is justified to classify *An. araripensis* as separate species, rather than include them in the already known species, because the holotype as well as the referred specimen have a small process at the pterygoid. Because the St. Gallen specimen has exactly such a process too, the fossil is re-classified as *Co. araripensis*.

The presence of a depression on the anterior aspect, mentioned in the diagnosis of the genus *Coloborhynchus*, is not attested in *Co. araripensis* (SAO 16494; the holotype has no anterior part preserved and the anterior part in the referred specimen is damaged too much).

This feature is not generic for *Coloborhynchus*, but might be specific for certain species or just a feature of fossilisation rather than a morphological feature.

The pattern of alveolar size in the cranium SAO 16494 shows the familiar erratic pattern (figure 7.10) but in general the size is smaller relative to all other *Coloborhynchus* specimens. Furthermore, there is not one really big alveolus, as seen with the other specimens and other *Coloborhynchus* species; instead, the second, third and fourth pairs are about equal in size and comparable in size with number 8. Still there is a strong decrease in size with alveolus 5 and 6. After the eighth alveolus, size decrease continuously posteriorly.

The graph of MN 4735–V (figure 7.10) shows a comparable pattern but with one distinct difference: alveolus 2, 3 and 4 are substantially bigger than the rest and are more in line with the other *Coloborhynchus* graphs (in fact, it is SAO which differs from the others in this respect).

Coloborhynchus robustus (BSP 1987 I 47, SMNK 2302–PAL; figures 7.10, 7.13, 7.14, 7.17)

The holotype, BSP 1987 I 47, housed in the Bayerische Staatssammlung für Paläontologie und historische Geologie, Munich, Germany, is an isolated mandible (figure 7.13), which was described by Wellnhofer (1987). Wellnhofer classified it to the new erected genus *Tropeognathus* as *Tropeognathus robustus*, differentiating it from the other species of *Tropeognathus*, *Tr. mesembrinus* (currently known as *Cr. mesembrinus*). Kellner & Campos (1988) however, classified the mandible to *Anhanguera* because they observed the features mentioned by Wellnhofer (1987) present in *Anhanguera* as well (see also Kellner & Tomida, 2000). Veldmeijer (1998, 2002) however, regarded the specimen as a species of *Coloborhynchus*, supported by Fastnacht (2001), who came to the same conclusion on the basis of the study of the anterior part of the cranium and mandible of another specimen of *Co. robustus* in the collection of the Staatliches Museum für Naturkunde, Karlsruhe (SMNK 2302 PAL; figure 7.14). The Munich mandible is characterised by a steep and relatively short crest and long narrow symphysis. The anteriormost part is expanded with a flat anterior view. A mandibular sagittal groove, narrow and of equal width (approximately 3 mm), is present but fades in the anterior direction.

Fastnacht (2001) argued the specimens (thus both the Munich mandible and the Karlsruhe front parts of cranium and mandible) being different from the other species of *Coloborhynchus* (the type specimen and the American *Co. wadleighi*, Lee, 1994). The jaws have all characteristics of *Coloborhynchus*, such as the blunt roughly triangular anterior view with the teeth sticking out (the median depression has been discussed above) as well as the robustly expanded anterior part. The premaxillary sagittal crest has a concave anterior edge. The mandible has a small dentary sagittal crest with a distinct, well defined, mandibular sagittal groove (much clearer than in the holotype). Note that this groove has no counterpart on the cranium.

In the Munich mandible, there is a large gap between tooth four and six on the right side, whereas on the left side this gap is filled with alveolus five. This feature has been observed in various other specimens as well (among which the Karlsruhe specimen of *Co. robustus*). There are indications that the extra tooth is pathological and thus that the normal situation at the transit of expansion and symphysis is the occurrence of an extra large diastema. There is, save the fifth and sixth pair of alveoli and some individual small increases in size, a continuous decrease in size in posterior direction (figure 7.10). The second and third pairs are the biggest alveoli and the fifth pair is the smallest. The seventh and eighth pair of alveoli are larger again, which results in a peak in the graph. The subsequent alveoli decrease in size gradually, with the exception of the twelfth pair.

In the Karlsruhe specimen of *Co. robustus*, the pattern made by the alveoli does not take into account the replacement teeth (replacement teeth are visible posterior to the first functional tooth right, posteromedial to the second right, the third left and the fourth tooth right). The second and third pairs of alveoli of the cranium are the biggest (figure 7.10). These are followed by a smaller pair, which are followed by the two smallest pairs of alveoli (five and six). Four larger alveoli occur after these latter two, which are of comparable size to the first pair of alveoli. The eighth pair is slightly larger relative to the other three of these four last pairs. The pattern of the mandibular alveoli is highly comparable with one notable exception. Alveolus 6 has one of the largest diameters, whereas alveolus 6 in the cranium is the smallest of all.

Coloborhynchus piscator (NSM–PV 19892; figures 7.10, 7.15, 7.17)

The most complete and best preserved fossil of a toothed pterosaur from Brazil is the specimen in the National Museum, Tokyo (NSM–PV 19892; figure 7.15), which initially has been described as *An. piscator* (Kellner & Tomida, 2000). However, various features, such as the blunt anterior aspect, the robust expanded jaws and crests have led many scholars to classify it as *Coloborhynchus*, because of the similarities as *Co. robustus*. However, Veldmeijer (2003a) argued, without going into further detail, that the specimen should be regarded as *Co. piscator*. He came to this conclusion because of the far larger size relative to the other known specimens, even though the Tokyo fossil is certainly a juvenile animal.

The dentition in *Co. piscator* is complete and well preserved. However, observation is hindered by the fact that the skull has not been prepared completely: the matrix between the jaws remain. As can be seen in figure 7.10, the pattern is largely comparable to *Co. robustus* but with few differences. The biggest alveolus is by far the third one. In none of the other specimens is the difference in size so obvious. Furthermore, the smallest alveoli are 5 and 6, after which the size increase, with a peak at alveolus 9 and 10; later than seen in the other *Coloborhynchus* fossils (mostly the peak is at number 8) except *Co. spielbergi* (see below). Other less severe peaks in size occur at number 21 and the last ones; but these alveoli are enlarged and contain two teeth.

Coloborhynchus spielbergi (RGM 401 880; figure 7.10, 7.16, 7.17)

The description of the nearly complete skeleton housed in the Nationaal Natuurhistorisch Museum, Leiden, The Netherlands resulted in the fourth known species of *Coloborhynchus* and the first one with post–cranial material (RGM 401 880; figure 7.16). Characteristic of course, as with all *Coloborhynchus* species, is the large crest on the anterior part of the cranium and mandible, the two front teeth projecting from the anterior view (here identified with CT scans, because the anterior view is damaged) and the expanded anterior parts of the cranium and mandible. There are some clear differences with the other species, the most important ones being that the anterior expansion of the jaw is less robust and far more spoon–shaped (in this more comparable to the morphology in *Anhanguera*), the rami bend strongly medial and the palatal sagittal ridge and corresponding mandibular groove are faint and do not extend onto the anterior aspect of the mandible.

The alveolar pattern of the cranium (figure 7.10) shows the large second, third and fourth pairs, followed by the far smaller fifth and sixth pairs. The seventh, eighth and ninth pairs again are large, but slightly smaller relative to the first series large alveoli. The alveoli after the ninth pair are of equal size but small relative to the series 3–5 and 7–9. On the other hand, these equal the size of pairs 5 and 6. The pattern compares well with *Co. robustus* and

less with *Co. piscator*. The alveoli of the mandible shows a slightly comparable pattern but, as also seen in *Co. robustus*, the drop in alveolar size occurs earlier (with numbers 4 and 5). The increase thereafter is also earlier, namely with alveolus 8 (number 9 of the skull is biggest).

7.2.3. Diastemae (figure 7.17)

The diastemae (7.17) show a uniform picture, *i.e.* a strong increase in size posteriorly until about halfway the tooth row and a decrease in size in diastemae from that point onwards. There are few exceptions, noted below.

The mandible of *Co. robustus* SMNK 2302 PAL shows a large diastema 4–5 and after a low value for 5–6, which is comparable to the value of diastema 5–6 in the other specimens, the size of diastemae increases far more rapidly than seen in the others. This rapid increase is also seen for the skull but only with diastema 8–9; previous it is in line with the other graphs.

The value for diastemae 11–12 and 12–13 in the cranium of *Co. spielbergi* are slightly bigger relative to the others; the value for diastema 15–16 is 45 and thus by far the biggest encountered and is probably a result of restoration (Veldmeijer, 2003a).

7.3. *Anhanguera* from the Lower Cretaceous Santana Formation, Brazil (Pterosauria, Pterodactyloidea, Anhangueridae); an update

7.3.1. Introduction⁵²

The present subchapter is the third update, resulting from the description of new material as well as the detailed analysis of the cranial skeleton of known Brazilian pterodactyloid pterosaurs (Araripe Basin, Lower Cretaceous Santana Formation). The previous updates evaluated the taxa *Brasileodactylus* and *Coloborhynchus*. Besides a summary and a short description of the various fossils, this subchapter also presents new data.

7.3.2. The known specimens

Systematic palaeontology

Order Pterosauria Kaup, 1834
 Suborder Pterodactyloidea Plieninger, 1901
 Family Anhangueridae Campos & Kellner, 1985b
 Genus *Anhanguera* Campos & Kellner, 1985b

Type species and specimen: *Anhanguera blittersdorffi*, cranium, MN 4805–V, Museu Nacional, Rio de Janeiro, Brazil (figure 7.18).

Diagnosis *Anhangueridae*, *Anhanguera* and *Anhanguera blittersdorffi* as presented by Campos & Kellner (1985b: 459): “Pterosaurs with a large sagittal crest on the anterior part of the skull, situated on the premaxillas, which ends almost at the beginning of the external naris; presence of a small parietal sagittal crest on the posterior part of the skull; dentition from distal part of the skull on to the middle region of the naris preorbital opening, corresponding to the beginning of the internal naris; presence of an enlargement of the distal part of the skull, where the premaxillar teeth, the biggest teeth of all, are found.”

Discussion of diagnosis. Kellner & Tomida (2000) reviewed and refined the diagnosis, stating that (*ibidem*: 114) “The presence of a premaxillary sagittal crest confined to the anterior part of the skull and not reaching above the nasoantorbital fenestra [...] and a small parietal crest [...] can be regarded as synapomorphies of the Anhangueridae [...]”. If this is to be followed, the closely related taxon *Brasileodactylus* should be excluded because it lacks the premaxillary and dentary sagittal crests, but *Coloborhynchus* and *Criorhynchus* should be included. Kellner (2003) discussed the taxon as well and presents features of post-cranial material, based partially on *Co. piscator*, which he regards as *An. piscator* (but see Veldmeijer, 2003a).

The position of the first alveolus is unclear due to the remaining matrix surrounding the right tooth and the damaged state of the left side. The right tooth point anteroventrally. The subsequent alveoli (2–13) are located ventrally; the remaining ones (14–26) lateroventrally (but the alveoli 14–16 slightly less lateral relative to the last eight). The orientation of the first is unclear for the reason explained but the following three point slightly anteriorly. The remaining alveoli are orientated distinctly ventrally. The cross-section of the first alveolus is unclear but the rest are elliptical with slight variation in the degree of being elliptical. The long axis of the alveoli are orientated anteromedial–posterolateral. The curvature of the first tooth is posteromedial.

In their description Campos & Kellner (1985b) mention that the size of the alveoli in the posterior part becomes smaller. Although this is true, the size difference is remarkably small (figure 7.19: the difference between the smallest alveolus (number 26) and the largest (number 4 because number 10 is unreliable) is 4.7. The remark that the biggest teeth are to be found in the enlargement is true, but the difference between these and the seventh until ninth alveoli can be neglected (differences of half a mm or less). It is clear from the graph however, that the alveoli posterior to the enlargement (numbers 5 and 6) are substantially smaller.

Another specimen of *An. blittersdorffi*, presented by Kellner & Tomida (2000: n. 40 Pz–DBAV–UERJ), includes the mandible as well. This beautifully preserved skull shows a largely complete dentition, with reliable measurements of both sides of the cranium as well as mandible, in contrast to the situation with the cranium of the holotype in which no teeth (except the first and tenth tooth right) has been preserved and the preservation is far worse resulting in unreliable measurements of only one side. The dentition is very well preserved. Most of the teeth (1–9, 11–12 of the skull and 1–4, 6–14 of the mandible) are completely or partially preserved.

The first pair of alveoli of the cranium are positioned anteroventrally and the subsequent six alveoli (2–7) lateroventrally (but increasingly ventrally). The alveoli 8–14 are positioned ventrally; the last seven (15–21), again, lateroventrally. The orientation of the first is anteroventral as well as the following ones (2–7), although increasingly less anteriorly. After the seventh, all alveoli point ventrally. The cross-section of the first pair of alveoli is circular whereas this is rounded elliptical for the next three (2–4). The cross-section of the next alveoli are elliptical. The long axis of the alveoli are orientated anteromedially–posterolaterally from tooth number five onwards. Though this orientation is observed at the enlargement as well, it is less distinct. The curvature posteromedial in varying degree.

Figure 7.19 shows that there is a steady increase in size for the first three alveoli. The third alveolus reaches the highest value of the dentition. The next two (4 and 5) are of comparable size to the second whereas the sixth alveolus approximately equals the size of the first. The next series starts with the seventh, which is of the size of 4 and 5. After this, the cross-section decreases in size continuously until number 18. This alveolus is slightly larger as are the last three, although these are smaller relative to number 18. This small increase

might be due to the fact that all sizes are based on the average of both sides, except for the last four. These are not preserved at the right side.

In general, the alveoli of the mandible tend to be slightly smaller relative to those of the cranium. Differences between the dentition of the cranium and mandible are especially seen with the third, fifth, seventh and eighth alveoli which are all smaller relative to these of the cranium. In the mandible, the first pair of alveoli are positioned laterodorsally as well as all the others. Numbers 2–4 however are more laterally positioned relative to the first one. The alveoli 5–7 are continuously stronger dorsally positioned. After the seventh alveoli they are all in laterodorsal position. The orientation of the first pair of alveoli is laterodorsal as well. The alveoli 2–9 are slightly pointing anteriorly and the last alveoli (10–21) are orientated dorsally. The cross-section is elliptical with the long axis orientated anteriomedially–posterolaterally. The curvature of all preserved teeth is posteromedial.

Though the general layout of the dentition pattern is comparable to the skull, there are some differences. The first four alveoli are of approximately the same size (numbers 1 and 2 are bigger than 3 and 4). Alveolus 5 is smaller and 6 and 7 increase in size. Alveolus 8 is of comparable size to alveolus 2; they are the biggest alveoli. After this, there is a steady decrease in size posteriorly.

Anhanguera santanae (figures 7.19, 7.20, 7.22)

The skull in *An. santanae* (BSP 1982 I 90; figure 7.20) shows the posterior start of a crest. Because the anterior extension is not known, the crest cannot be used as diagnostic feature and the generic classification, as either *Anhanguera* or *Coloborhynchus*, is uncertain. Comparison of this specimen with *An. santanae* (AMNH 22555, Wellnhofer, 1991b) shows some striking differences (Veldmeijer, 2003a). The quadrate in AMNH 22555 is more robust, the lower temporal fenestra smaller, the nasal longer and wider, and the prefrontal extends less posteriorly. The straight posteroventral back of the skull in *An. santanae* (BSP 1982 I 90) inclines more sharply, through which it has a taller appearance. Note also that AMNH 22555 almost lacks anteriorly expanded jaws. The only other Anhanguerid with straight jaws is *Criorhynchus*.

The anterior aspect of the cranium of *An. santanae* (AMNH 22555) is equipped with the first pair of alveoli, which still bears the roots of the teeth. The position as well as the orientation of this pair of alveoli is anteriorly (and very slightly laterally). The alveoli are positioned more dorsally relative to the subsequent alveoli. The second pair of alveoli are positioned anteroventrally and slightly lateral, but less anteriorly relative to the first pair. The next alveoli up to the tenth are positioned lateroventrally. They are orientated continuously less anteroventrally and the last five are orientated ventrally only.

Only few teeth have been preserved and all of these partially. The remnants of the teeth all suggest a posteromedial curvature. The first two pair of teeth have a circular cross-section; the other teeth are elliptical, although the teeth in the anterior part, up to and including the seventh, are slightly more circular. The long axis is positioned anteroposteriorly.

The alveolar pattern (figure 7.19) shows that the smallest pair of alveoli is the first pair (but note that the anterior aspect is damaged and therefore the measurement might be too small). A remarkable drop in size occurs with the fifth alveolar pair. The largest size is measured for the eighth pair after which a gradual decrease in alveolar size is noticeable. The eleventh is small, relative to the previous and subsequent (pairs of) alveoli.

Anhanguera sp. indet. (figure 7.19, 7.21, 7.22)

This mandible (SAO 200602) is among the best preserved, but has not been prepared entirely (figure 7.21). According to Veldmeijer *et al.* (2005a) “The left side has 14 intact teeth. The right has 15. No alveoli could be distinguished at the left ramus. Three teeth of the right ramus are partially embedded and separated from the rest of the ramus (they are not illustrated). In anterior view the first alveolus is oriented anterodorsally. The alveoli two and three are laterodorsally and anteriorly positioned. Alveolus four is placed laterodorsally and slightly anteriorly. The subsequent alveoli, numbers six to ten, are increasingly laterally oriented but less posteriorly.”

So, in terms of position and orientation, this mandible is very similar to the mandible of *An. blittersdorffi* (n. 40 Pz–DBAV–UERJ). The largest alveolar cross-section is the third one (figure 7.19). The second is only slightly smaller. In general, the teeth are curved in a medial and posterior direction, although the curvature decreases posteriorly. Teeth one to four are more strongly curved. The teeth are elliptical in cross-section, with the long axis oriented anteromedially and at right angles to the curvature of the teeth.

7.3.3. Diastemae (figure 7.22)

The pattern seen for the diastemae in the holotype of *An. blittersdorffi* (MN 4805–V) shows a small increase for the diastemae up to 9–10. Then a rapid increase in size occurs (10–11 and 11–12), followed by slightly less large diastemae (12–13 and 13–14) after which the size increase again (14–15). Then, the sizes decrease rapidly (15–15 and 16–17) after which they keep decreasing but less rapidly. Only with the last diastemae does the size become comparable to the first, pre-peak area (2–3 and 9–10). The pattern of the cranial dentition in the referred specimen (n. 40 Pz–DBAV–UERJ) shows a relatively flat line up to the 7–8 after which a steady increase in size occurs and having its peak at 12–13. The gradual decrease in size is followed by a more rapid one for the last three. This however, is also likely to be due to the fact that these are not based on the average values of the measurements of both sides. The pattern of the mandibular diastemae is comparable to that of the cranium: it shows a relatively flat, but slightly more erratic line than the skull up to the 7–8 diastema after which a steady increase in size occurs and having its peak at 14–15 (slightly more posterior than in the skull). After the peak, the values only slightly decrease in size.

The pattern of diastemae size in *Anhanguera* sp. indet. differs in that it shows almost identical measurements until diastema 6–7. After this, there is an increase and decrease in size, resulting in a fluent curve, unique for this jaw.

In the New York specimen of *An. santanae*, the diastemae pattern shows a continuous increase in size. The drop in size of the diastema 10–11 is remarkable and seems odd.

7.4. *Criorhynchus* from the Lower Cretaceous Santana Formation, Brazil (Pterosauria, Pterodactyloidea, Anhangueridae); an update

7.4.1 Introduction⁵³

Topic of this last update is the crested taxon *Criorhynchus*. As with all discussed pterosaurs, the fossils from Brazil and England are intimately linked to each other, despite the fragmentary state of the Cambridge material.

7.4.2. The known specimens

Systematic palaeontology

Order Pterosauria Kaup, 1834
Suborder Pterodactyloidea Plieninger, 1901
Family Anhangueridae Campos & Kellner, 1985b
Genus *Criorhynchus* (Owen, 1861)

Type species and specimen: *Criorhynchus simus*, anteriormost part of the cranium, B54.428, Sedgwick Museum, Cambridge, England, Great Britain (figure 7.23).

Diagnosis by Fastnacht (2001) of the genus “Convex-shaped, medial crest on the upper jaw, rising from the tip of the snout. First pair of teeth on the upper jaw smaller than subsequent teeth. Teeth on the upper jaw orientated vertically. Longitudinal ridge on palate. Lower jaw with mandibular crest on the symphysis. Upper and lower jaw not expanded anteriorly. Facies rostralis anterior and depressis medianus anterior triangular-shaped with tip pointing dorsally, wider than high.”

Discussion of diagnosis. The diagnosis of Fastnacht (2001) is based on his study of the cranium and mandible from Brazil in the Munich collection; Fastnacht came to his conclusion due to the study and re-diagnosis of the *Co. robustus* fossil in the Karlsruhe collection. The type specimen, *Cr. simus*, is only a very small fragment which lead Fastnacht (2001: 35) to conclude that “a clear distinction of *Cr. mesembrinus* and *Cr. simus* is not possible, until more complete material of *Cr. simus* is found.” Nevertheless, the front of the cranium is remarkably similar to *Cr. mesembrinus*. The premaxillary sagittal crest as described also occurs in *Coloborhynchus*. *Anhanguera* has a crest too but in this taxon it starts well posterior to the anterior aspect of the cranium. Not all teeth are placed truly vertical as more posteriorly they are rather placed lateroventrally (see below). A mandibular crest is seen in *Coloborhynchus* and *Anhanguera* as well. In *Coloborhynchus* the shape of the depression on the anterior aspect is of only limited diagnostic value. The big difference between *Criorhynchus* and the closely related *Anhanguera* and *Coloborhynchus* lies in the fact the teeth in *Criorhynchus* are more or less isometric in diameter (see below), the jaws are not expanded anteriorly, the presence of a robust mandibular groove and corresponding palatal ridge and a very robust parietal crest (remarkably not mentioned in the diagnosis cited).

Holotype of *Criorhynchus mesembrinus* (Wellnhofer, 1987) (figure 7.24, 7.25, 7.27)

Initially, Wellnhofer (1987) classified BSP 1987 I 46 (figure 7.24) as new genus and species *Tropeognathus mesembrinus* within the Ornithocheiridae, but here, the evaluation of Fastnacht is followed (see above), in this opposing the vision of Kellner & Tomida (2000) who regard *Tropeognathus mesembrinus* valid.

The first pair of alveoli are of comparable size of alveoli 11 and 14 (figure 7.25). In general, the fluctuations in size of the alveoli are small. The last four alveoli at the right side of the cranium of *Cr. mesembrinus* (the left ones are not preserved), are substantially smaller relative to the third up to and including the ninth pair of alveoli. The first pair of alveoli of the cranium are placed at the anterior aspect, slightly dorsally relative to the second pair of alveoli. They are placed anteroventrally, although the anterior orientation is only slight. The second and third pairs of alveoli are ventrally orientated and the subsequent teeth have a

increasing tendency towards a more lateral position. This laterally orientated position is even more noticeable at the last four alveoli. None of the teeth 14 teeth (right side) of the cranium are completely preserved.

The 13 teeth (left side) of the mandible are much more complete relative to the teeth of the cranium. The first pair of alveoli (and teeth) are orientated anterolaterally, as is the second pair, and the teeth point dorsally. The second pair however, are less strongly anteriorly orientated, but more strongly laterally, relative to the first pair of teeth. The following alveoli are positioned laterodorsally. As with the cranial alveoli, there are not large differences in size, although there is a steady decrease in diameter in posterior direction. This differs from the cranial situation, as this graph first shows a small increase and only the seventh alveolus, a decrease in size can be seen.

The curvature of the mandibular teeth is posteromedial. The teeth are flattened; the anteroposterior diameter is larger relative lateral diameter. The shape of the diameter of the first pair of teeth cannot be determined.

Cf. Criorhynchus mesembrinus SMNS 55414 (figure 7.25, 7.26, 7.27)

The specimen (figure 7.26), housed in the Staatliches Museum für Naturkunde, Stuttgart, Germany, shows a large dentary sagittal crest and has large teeth. It has been argued by (Veldmeijer, 2002) that the mandible must be assigned to *Cr. mesembrinus*, but with reservations because of the fact that the bone is not completely prepared and thus no certainty could be obtained of the characteristically wide and deep mandibular sagittal groove.

The curve of the alveoli (figure 7.25) shows that the first seven pairs are of the same size although the fifth and sixth are slightly larger. This difference is negligible. The eighth alveolar pair is substantially smaller, followed by the ninth pair which is of comparable size to the first four pairs. The last three pairs of the twelve pairs of alveoli are small and of comparable size to the eighth pair.

The alveoli of the ninth up to and including the twelfth pair of teeth are elliptical and positioned with their long axis anteroposteriorly. The alveoli are positioned at the dorsal aspect of the rami. In contrast, the alveoli of the first eight pair of teeth, which are also elliptical of shape, are placed slightly anteromedial–posterolateral except for the first pair of alveoli, which is placed anterodorsally.

The first pair of teeth is curved posteromedially and point anterodorsally. The second pair of teeth is curved posteromedially as well and the teeth point also anterodorsally, although less anteriorly relative to the first pair of teeth. The following teeth, at least up to the eighth pair, display a comparable curving but less severely so. They point dorsally rather than anterodorsally. The following teeth are not preserved, except for the tenth tooth on the left. This tooth is substantially smaller and does not display curving.

7.4.3 Diastemae (figure 7.27)

The diastemae pattern in the cranium of BSP 1987 I 64 is rather erratic, with a significant increase in size for the diastemae between alveolus 7–8 and 8–9, after which the increase changes into a decrease in size between alveolus 10–11. The pattern of the diastemae in the mandible is erratic as well. The sharp decrease in size of diastema 9–10 is possibly caused by the fact that it is uncertain whether the alveolus marked as 10 is an alveolus or not; if not, the pattern would be more in line with the expected pattern, because the size of the diastema between tooth 9 and 11 is approximately 32. This however, does not explain the difference in size of the subsequent diastemae. The size of the diastemae in the Stuttgarter

mandible increase sharply from the beginning onwards. However, the diastemae between alveoli 10–11 and 11–12 decrease in size rather sharply, although not as sharp as seen with the holotype.

7.5. Discussion

As shown, in many cases teeth are not preserved and the alveolar diameter serves as an indicator of tooth size. However, it is not necessary that a positive relationship between alveolar size and tooth size exists; a large diameter of the alveolus could mean a long, perhaps fanglike tooth, but a short bulblike tooth would have been possible as well. On the other hand, the taxa discussed here all have comparable dentition inferred from the few (remnants) of teeth and the assumption that the bigger the alveolus, the longer the tooth, is reasonable. The second problem is that measurements of the teeth/alveoli and diastemae almost never have been published prohibiting scientific evaluation.

Various authors have suggested *Brasileodactylus* being synonymous with *Anhanguera* (Unwin, 2001 although in a later paper, Unwin (2002) still refers to it as *B. araripensis*) or even *Coloborhynchus* (Frey *et al.*, 2003a). As remarked by Veldmeijer & Signore (2004) “The explanation of the supposed difference as the result of ontogeny, sexual dimorphism or variation cannot be proven, mainly due to the scanty fossil record (most of the species are represented by only one (published) specimen, often consisting only of (parts of) the skull); the fossils should therefore be treated as different species unless proven (and not suggested) otherwise.”, hence the designation as *Brasileodactylus*. *Brasileodactylus* is here regarded as a valid taxon, on the basis of lack of a premaxillary sagittal crest and a dentary sagittal crest and the presence of the unique configuration of dentition and morphology of the dorsal aspect of the lower jaw, as pointed out above. The hitherto most complete cranial dentition cannot be assigned to *Brasileodactylus* with full confidence yet (Veldmeijer, 2003b) but the graphs of the dentition of the upper and lower jaw in MN 4797–V shows a more erratic pattern of the skull, with larger differences in diameter of alveoli. Furthermore, it can be suggested that if AMNH 24444 can be classified as *Brasileodactylus* as suggested in the preliminary description and if it can be established that AMNH 24444 and *L. sibbicki* are the same (which seems to be so on the basis of the preliminary observations on the half prepared holotype in 1998), *L. sibbicki* should be re-named as *Brasileodactylus* (either *B. araripensis* or *B. sibbicki*). The generally larger alveoli in the skull of AMNH 24444 relative to MN 4797–V might be explained by the fact that AMNH 24444 is ontogenetically younger relative to MN 4797–V. This however, cannot be the explanation for the large difference in size between AMNH 24444 and BSP 1991 I 27, as the latter is regarded as not fully-grown as well.

Coloborhynchus clearly differs from *Brasileodactylus* in the fact that the expansion of the jaws is more robust, the presence of premaxillary and dentary sagittal crests and the blunt front of the cranium with teeth sticking out. Furthermore, the morphology of the dentary groove differs. The dentition patterns support the difference between *Brasileodactylus* and *Coloborhynchus*. The latter show a more erratic pattern, especially in the anterior portion, with larger alveoli. Unfortunately, as most of the *Brasileodactylus* fossils are partial, predominantly anterior portions of the rostrum, little can be said on the last part of the dentition and comparison with *Coloborhynchus* is therefore impossible. The graphs also provide further support for the classification of *Co. piscator* as a valid taxon (see Veldmeijer, 2003a): it is the only species of *Coloborhynchus* with as many as 25 alveoli on one side.

Although *Anhanguera* has a crest as well, it terminates well before the anterior view of the cranium; the expansion of the jaws is far less robust and the morphology of the mandibular groove differs. In general the dentition (the diameter of the alveoli) is much

smaller with far smaller size differences within the dentition than *Coloborhynchus*. The graph of the diastemae size shows a greater increase and decrease with *Coloborhynchus*. On the other hand, the dentition is much more comparable to *Brasileodactylus*, but the morphological differences between the two taxa, discussed above, are apparent.

The morphology of the dentary groove in *Criorhynchus* differs from the other taxa. Furthermore, *Criorhynchus* has a strongly developed parietal crest and the jaws are not expanded. The dentition shows less fluctuation in size as seen with *Coloborhynchus* and, to a lesser extent, *Brasileodactylus* and *Anhanguera*. Finally, *Criorhynchus* has less teeth than all other discussed taxa.

8. Final remarks

8.1. Ornithocheiridae versus Anhangueridae

The situation on family level is complex (see Veldmeijer *et al.*, submitted), but the acceptance of the crestless, laterally compressed jaws that strongly decrease in width in anterior direction resulting in a sharp pointed beak (figure 8.1) of *O. compressirostris* as the type species for Ornithocheiridae forces to exclude *Brasileodactylus* from Ornithocheiridae, as proposed by Unwin (2001) because the morphology contrast distinctly from the expanded and dorsoventrally compressed jaws of *Brasileodactylus* and indeed from all other known taxa from Brazil (*Coloborhynchus*, *Anhanguera*, *Criorhynchus*, *Cearadactylus*, *Ludodactylus*). The acceptance of the mentioned type species contradicts with Unwin's vision and diagnosis through which he classified *Brasileodactylus* to Ornithocheiridae. It is interesting to note that Unwin assigned the specimen, in the present work referred to as *Cr. simus*, as type species of Ornithocheiridae. The diagnosis is, according to Unwin (2001: 204)⁵⁴: "The first three teeth are relatively large, forming a terminal rosette, and show a marked increase in size posteriorly. The fourth tooth pair is much reduced in size and smaller than the first pair of teeth. Proceeding posteriorly, there is a steady decrease in tooth size up to, typically, the ninth pair, which are of similar basal dimensions to the largest teeth in the terminal rosette. Further posteriorly, tooth size decline again. Consequently, in dorsal view, the rostrum has an expanded anterior tip [...]. The expansion of the anterior end of the rostrum is most marked in large species and adult individuals, but may be practically absent in small species and juveniles." Without going into detail too much, as a detailed discussion of his vision is clearly beyond the scope of this work, few remarks need to be made in light of the systematic palaeontology used here. First, as shown in figure 7.23, the type specimen is a small piece, in which only four alveoli are preserved, mostly badly damaged. So, the description of dentition given by Unwin apparently has been based on other material (not on the type specimen), but he does not mention it: the description fits the dentition of Anhangueridae surprisingly well. *Criorhynchus*, on the basis of the Munich specimen of *Cr. mesembrinus*, does not have expanded jaws (in this clearly differs from *Anhanguera*, *Coloborhynchus* and *Brasileodactylus*), no rosette with teeth and does not have a ninth tooth larger than the other ones (this is almost never encountered, see dentition graphs). The non-expanding jaws is a feature that, among others, separates *Criorhynchus* from the others and is seen in other toothed pterosaurs as well, such as *O. compressirostris*. In other words, if a character is used in the diagnosis, as Unwin does, specimens not exhibiting this feature should not be classified to this group. Furthermore, explaining differences by means of ontogeny is extremely difficult as there is no way in the scanty pterosaur fossil record to know in most cases what a juvenile and what an adult is (or better 'not fully-grown' and 'fully-grown'). At present, too little is known to be sure on the ontogenetic status (see also Veldmeijer & Signore, 2004).

8.2. The *Brasileodactylus*-problem

The present work has no intention to give a full pterosaur phylogeny, but rather wants to pinpoint some flaws in the analysis of pterosaurian remains thus far. If we accept the diagnosis for Anhangueridae as presented and discussed in 7.3., *Brasileodactylus* cannot be assigned to it due to the lack of crests. But clear is that *Brasileodactylus* shares many features with *Coloborhynchus* and *Anhanguera* (anterior expansion of the jaws, dentition pattern, mandibular groove (even though the morphology varies in the various taxa) and post-cranial

characteristics as well), making classification close to Anhangueridae obvious. The type specimen of Ornithocheiridae is crestless as well, but the overall morphology of the jaw differs far more (*cf.* figure 8.1) from *Brasileodactylus*. None of the existing models create a satisfying solution (Kellner, 2003; Unwin, 2003). The creation of a new family including the crestless taxa (thus *Brasileodactylus*, *Cearadactylus* and also *Ludodactylus*) which are closely related to the Anhanguerids (closer than to the non-crested Ornithocheirids) seems to be an option. The alternative would be a subfamily, together with the Anhanguerids, within a larger group, based on dental characters. However, as shown above, this would lead to exclusion of *Criorhynchus*, even though the non-dental morphology clearly shows a close relationship. Until more complete material of especially *Brasileodactylus* has been published, it seems irresponsible to erect such a group; therefore, reference to classification is marked with ‘?’.

9. Acknowledgements

This work would not have been possible without the help and continuous support of John de Vos (Nationaal Natuurhistorisch Museum, Leiden/Teylers Museum, Haarlem, The Netherlands) who not only gave me the opportunity to study the pterosaurs in the collection of Naturalis and Teylers Museum, but always remained understanding and patient when faced with another delay and Erno Endenburg, who not only helped with collecting data and making photographs in various visits to collections all over the world, but also helped processing the data into graphs and tables and photographs into publishable pictures. Special thanks also to Jelle Reumer, my promoter.

The following persons are acknowledged for kindly allowing access to the collections under their care or for helping with visiting it (in alphabetical order): T. Bürgin, C. Collins, F. Dalla Vecchia (unfortunately, all his efforts in trying to establish contact with the Centro Studi e Ricerche Ligabue, Venice, Italy, in order to study the Brazilian material remained unsuccessful), M. Dorling, E. Frey, J. Gamble, A. Keefer, A.W.A. Kellner, G. Mauricio, H. Mayr, A.C. Milner, S. Nabana, M.A. Norell, U. & S. Oberli, Y. Okazaki, M. Oshima, I. Rutzky, Y. Takakuwa, Y. Tomida, J. de Vos, P. Wellnhofer, R. Wild.

I thank Dr. S. Boor and Prof. Dr. P. Stoeter (Department of Neuroradiology, University of Mainz, Germany) for making the CT-scans and M. Fastnacht is thanked for his help.

Many people have been involved one way or the other: B.L. Beatty, W. Brinkmann, E. Bucci, J.E.M.F. Bos, D.A. Campos, S.K. Donovan, R. Harling, A.M. Hense, A. 't Hooft, M. van Kuik, M. van Kuik-Woudstra, C. Mehling, H.J.M. Meijer, R. Muller, D. Peters, M. Signore, C.P. Strang, D.M. Unwin, J. van Veen, L. Veldmeijer, R. van Walsem, R. van Zelst.

AMNH 24444 was shipped to The Netherlands and is currently being prepared due to the courtesy of the American Museum of Natural History, New York, USA (Mark Norell and Carl Mehling) and has kindly made possible by the Natuurmuseum Rotterdam, The Netherlands. This institute as well as the National Museum of Natural History (Naturalis), Leiden are thanked for their all-round support.

The study of various collections (Germany, Rio de Janeiro and New York) have been made possible due to the financial support to by the Jan Joost ter Pelkwijkfonds, Stichting Molengraaff Fonds, Mej. A.M Buitendijkfonds and Mr. & Mrs. Endenburg. The Nationaal Natuurhistorisch Museum, Leiden, is thanked for financing the costs involved in scanning the skull in Mainz, Germany. The study of the material in various collections in Japan was made possibly by the Netherlands Organization for Scientific Research (NWO). Due to the grant of the Egypt Exploration Society for studying archaeological material in Cambridge, I was able to study some of the type specimens from the Cambridge Greensands.

Finally, Hanneke and Erno...thank you for all your help and support in organising my promotion: without your help it would have been impossible in such a short time!

10. Cited literature

- Baines, J. & J. Málek, J. 1981 [1980].** Atlas van het oude Egypte. – Amsterdam/Brussel, Elsevier.
- Bennett, S.C. 1989.** Pathologies of the large pterodactyloid pterosaurs *Ornithocheirus* and *Pteranodon*. – Journal of Vertebrate Paleontology 9: 13A
- Bennett, S.C. 1990.** A pterodactyloid pterosaur pelvis from the Santana formation of Brazil. Implications for terrestrial locomotion. – Journal of Vertebrate Paleontology 10: 80–85.
- Bennett, S.C. 1992.** Sexual dimorphism of *Pteranodon* and other pterosaurs, with comments on cranial crests. – Journal of Vertebrate Paleontology 12: 422–434.
- Bennett, S.C. 1993.** The ontogeny of *Pteranodon* and other pterosaurs. – Paleobiology 19: 92–106.
- Bennett, S.C. 1994.** Taxonomy and systematics of the Late Cretaceous pterosaur *Pteranodon* (Pterosauria, Pterodactyloidea). – Lawrence, The University of Kansas (Occasional Papers of the Natural History Museum 169).
- Bennett, S.C. 2001.** The osteology and functional morphology of the Late Cretaceous pterosaur *Pteranodon*. – Palaeontographica A 260: 1–153.
- Bennett, S.C. 2003a.** A survey of pathologies of large pterodactyloid pterosaurs. – Palaeontology 46: 185–198.
- Bennett, S.C. 2003b.** New crested specimens of the Late Cretaceous pterosaur *Nyctosaurus*. – Paläontologische Zeitschrift 77: 61–75.
- Beurlen, K. 1971.** As condições ecológicas e faciológicas da Formação Santana na Chapada do Araripe (Nordeste do Brasil). – Anais Academia Brasileira de Ciências 43: 411–415.
- Brower, J.C. & J. Veinus. 1981.** Allometry in pterosaurs. – The University of Kansas Paleontological Contributions 105: 1–32.
- Buffetaut, E., D. Grigorescu & Z. Csiki. 2001.** Giant pterosaurs from the Upper Cretaceous of Transylvania (western Romania). – Strata 1: 26–28.
- Buissonjé, de, P.H. 1980.** *Santanadactylus brasilensis* nov. gen. nov. sp., a long-necked, large pterosaur from the Aptian of Brazil, Part I & II. – Koninklijke Akademie der Wetenschappen, Proceedings B 83: 145–172.
- Buissonjé, de, P.H. 1993.** Provisional evaluation of a large, rather flat concretion from the Santana-Formation, Chapada do Araripe, Brazil, containing the complete skull and the lower jaw, as well as more than twenty post-cranial skeletal remains of a large pterosaur: *Tropeognathus cf. robustus* (Wellnhofer 1987), examined on Thursday 2eighth January 1993 at the National Museum of Natural History in Leiden. – Internal Report National Museum of Natural History, Leiden: 1–11 (see appendix).
- Campos, D.A. & A.W.A. Kellner. 1985a.** Um novo exemplar de *Ananguera blittersdorffi* (Reptilia, Pterosauria) da formação Santana, Cretáceo Inferior do nordeste do Brasil. – 9º Congresso Brasileiro de Paleontologia (resumos): 13.
- Campos, D.A. & A.W.A. Kellner. 1985b.** Panorama of the flying reptiles study in Brazil and South America. – Anais Academia Brasileira de Ciências 57: 453–466.
- Campos, D.A. & A.W.A. Kellner. 1997.** Short note on the first occurrence of Tapejaridae in the Crato Member (Aptian), Santana Formation, Araripe Basin, northeast Brazil. – Anais Academia Brasileira de Ciências 69: 83–87.
- Campos, D.A., G. Ligabue & T. Taquet. 1984.** Wing membrane and wing supporting fibres of a flying reptile from the Lower Cretaceous of the Chapada do Araripe Aptian, Ceará State, Brazil. In: **Reif, W.E. & F. Westphal. Eds. 1984.** Third Symposium on Mesozoic Terrestrial Ecosystems. – Tübingen, Attempto Verlag: 37–40.

- Carter, D.R., M.C.H. van der Meulen & K. Padian. 1992.** Historical and functional factors in the construction of pterosaur bones. A preliminary analysis. – *Journal of Vertebrate Paleontology* 12: 21A.
- Dalla Vecchia, F.M. 1993.** *Cearadactylus? ligabuei* nov.sp., a new early Cretaceous (Aptian) pterosaur from Chapada do Araripe (northeastern Brazil). – *Bollettino della Società Paleontologica Italiana* 31: 401–409.
- Dalla Vecchia, F.M. & G. Ligabue. 1993.** On the presence of a giant pterosaur in the Lower Cretaceous (Aptian) of Chapada do Araripe (northeastern Brazil). – *Bollettino della Società Paleontologica Italiana* 32: 131–136.
- Eaton, G.F. 1903.** The characters of Pteranodon. – *American Journal of Science* XVI: 82–86.
- Eaton, G.F. 1910.** Osteology of Pteranodon. – New Haven, Yale University (Memoirs of the Connecticut Academy of Arts and Sciences 2).
- Fastnacht, M. 2001.** First record of *Coloborhynchus* (Pterosauria) from the Santana Formation (Lower Cretaceous) of the Chapada do Araripe of Brazil. – *Paläontologisches Zeitschrift* 75: 23–36.
- Frey, E. & D.M. Martill. 1994.** A new pterosaur from the Crato Formation (Lower Cretaceous, Aptian) of Brazil. – *Neues Jahrbuch für Geologie und Paläontologie, Abhandlungen* 206: 379–412.
- Frey, E. & D.M. Martill. 1998.** Late ontogenetic fusion of the processus tendinosus extensoris in Cretaceous pterosaurs from Brazil. – *Neues Jahrbuch für Geologie und Paläontologie, Mitteilungen* 10: 587–549.
- Frey, E. & Rieß. 1981.** A new reconstruction of the pterosaur wing. – *Neues Jahrbuch für Geologie und Paläontologie, Abhandlungen* 161, 1: 1–27.
- Frey, E. & H. Tischlinger. 2000.** Weichteil-anatomie der Flugsaurierfüße und Bau der Scheitelkämme: Neue Pterosaurierfunde aus den Solnhofener Schichten (Bayern) und der Crato-Formation (Brasilien). – *Archaeopteryx* 18: 1–16.
- Frey, E., D.M. Martill & M.–C. Buchy. 2003a.** A new crested ornithocheirid from the Lower Cretaceous of northeastern Brazil and the unusual death of an unusual pterosaur. In: **Buffetaut, E. & J.–M. Mazin. Eds. 2003.** Evolution and palaeobiology of pterosaurs. – London Geological Society (Special publications): 55–63.
- Frey, E., D.M. Martill & M.–C. Buchy. 2003b.** A new species of tapejarid pterosaur with soft-tissue head crest. In: **Buffetaut, E. & J.–M. Mazin. Eds. 2003.** Evolution and palaeobiology of pterosaurs. – London Geological Society (Special publications): 65–72.
- Frey, E., H. Tischlinger, M.–C. Buchy & D.M. Martill. 2003c.** New specimens of Pterosauria (Reptilia) with soft parts with implications for pterosaurian anatomy and locomotion. In: **Buffetaut, E. & J.–M. Mazin. Eds. 2003.** Evolution and palaeobiology of pterosaurs. – London Geological Society (Special publications): 233–266.
- Hooley, R.W. 1914.** On the ornithosaurian genus *Ornithocheirus* with a review of the specimens from the Cambridge Greensand in the Sedgwick Museum, Cambridge. – *Annals and Magazine of Natural History* 8: 529–557.
- Kaup, J. 1834.** Versuch einer Eintheilung der Säugethiere in 6 Stämme und der Amphibien in 6 Ordnungen. – *Isis*: 315.
- Kellner, A.W.A. 1984.** Occorrência de uma mandíbula de Pterosauria (*Brasileodactylus araripensis*, nov. gen., nov. sp.) na Formação Santana, Cretáceo da Chapada do Araripe, Ceará–Brasil. – *33º Anais Congresso Brasileiro de Geologia* 2: 578–590.
- Kellner, A.W.A. 1989.** A new edentate pterosaur of the Lower Cretaceous from the Araripe Basin, northeast Brazil – *Anais Academia Brasileira de Ciências* 61: 439–446.

- Kellner, A.W.A. 1990.** Os répteis voadores do Cretáceo Brasileiro. – Anuário do Instituto de Geociências, CCMN, UFRJ 1989: 86–106.
- Kellner, A.W.A. 1994a.** Pterosaur soft tissue from Brazil. To be or not to be a wing, that is the question. – *Journal of Vertebrate Paleontology* 14: 31A–32A.
- Kellner, AWA. 1994b.** Remarks on pterosaur taphonomy and paleoecology. – *Acta Geologica Leopoldensia* 39, 1: 175–189.
- Kellner, AWA., 1995a.** Description of a juvenile specimen of *Tapejara* (Pterodactyloidea, Tapejaridae) from Brazil. – *Journal of Vertebrate Paleontology* 15: 38A–39A.
- Kellner, A.W.A. 1995b.** The relationship of the Tapejaridae (Pterodactyloidea) with comments on pterosaur phylogeny. In: **Sun, A. & Y. Wang. Eds. 1995.** Sixth Symposium on Mesozoic Terrestrial Ecosystems and Biota, short papers. – Beijing, China Ocean Press: 73–77.
- Kellner, A.W.A. 1996a.** Description of the braincase of two Early Cretaceous pterosaurs (Pterodactyloidea) from Brazil. – *American Museum Novitates* 3175:1–34.
- Kellner, AWA. 1996b.** Description of new material of Tapejaridae and Anhangueridae (Pterosauria, Pterodactyloidea) and discussion of pterosaur phylogeny. – Ann Arbor, University Microfilms International.
- Kellner, A.W.A. 1996c.** Reinterpretation of a remarkably well preserved pterosaur soft tissue from the Early Cretaceous of Brazil. – *Journal of Vertebrate Paleontology* 16: 718–722.
- Kellner, A.W.A. 2003.** Pterosaur phylogeny and comments on the evolutionary history of the group. In: **Buffetaut, E. & J.-M. Mazin. Eds. 2003.** Evolution and palaeobiology of pterosaurs. – London Geological Society (Special publications): 105–137.
- Kellner, AWA. & D.A. Campos. 1989.** Sobre um novo pterossauo com crista sagital da Bacia do Araripe, Cretáceo Inferior do Nordeste do Brasil. – *Anais Academia Brasileira de Ciências* 60 (1988): 459–469.
- Kellner, A.W.A. & D.A. Campos. 1990.** Preliminary description of an unusual pterosaur skull of the Lower Cretaceous from the Araripe Basin. – *Atas I Simposio sobre a Bacia do Araripe e Bacias Interiores do Nordeste, Crato*: 401–405.
- Kellner, AWA. & D.A. Campos. 1994.** A new species of *Tupuxuara* (Pterosauria, Tapejaridae) from the Early Cretaceous of Brazil. – *Anais Academia Brasileira de Ciências* 66: 467–473.
- Kellner, A.W.A. & Campos, D.A. 2002.** The function of the cranial crest and jaws of a unique pterosaur from the Early Cretaceous of Brazil. – *Science* 297: 389–392.
- Kellner, AWA. & Y. Hasegawa. 1993.** Postcranial skeleton *Tupuxuara* (Pterosauria, Pterodactyloidea, Tapejaridae) from the Lower Cretaceous of Brazil. – *Journal of Vertebrate Paleontology* 13: 44A.
- Kellner, A.W.A. & W. Langston Jr. 1996.** Cranial remains of *Quetzalcoatlus* (Pterosauria, Azhdarchidae) from Late Cretaceous sediments of Big Bend National Park, Texas. – *Journal of Vertebrate Paleontology* 16: 222–231.
- Kellner, AWA. & Y. Tomida. 1996.** New information on *Anhanguera* and the systematic position of the Anhangueridae (Pterosauria, Pterodactyloidea). – *Journal of Vertebrate Paleontology* 16: 45A.
- Kellner, AWA. & Y. Tomida. 2000.** Description of a new species of Anhangueridae (Pterodactyloidea) with comments on the pterosaurfauna from the Santana Formation (Aptian–Albian), northeastern Brazil. – Tokyo, National Science Museum (National Science Museum Monographs 17).
- Lee, Y-N. 1994.** The Early Cretaceous pterodactyloid pterosaur *Coloborhynchus* from North America. – *Palaeontology*, 37: 755–763.

- Leonardi, G. & G. Borgomanero. 1985.** *Cearadactylus atrox* nov. gen., nov. sp.: novo pterosauria (Pterodactyloidea) da Chapada do Araripe, Ceara, Brasil. – DNPM, Coletânea de Trabalhos Paleontológicos. Série Geologia 27: 75–80.
- Leonardi, G. & G. Borgomanero. 1987.** The skeleton of a pair of wings of a pterosaur (Pterodactyloidea, ?Ornithocheiridae, *cfr. Santanadactylus*) from the Santana Formation of the Araripe Plateau, Ceara, Brasil. – Anais Congresso Brasileiro de Paleontologia, Rio de Janeiro 1: 123–129.
- Lü Junchang & Ji Qiang. 2005.** A new Ornithocheirid from the Early Cretaceous of Liaoning Province, China. – Acta Geologica Sinica 79, 2: 157–163.
- Mader, B.J. & A.W.A. Kellner. 1999.** A new anhanguerid pterosaur from the Cretaceous of Morocco. – Boletim do Museu Nacional. Série Geologia 45: 1–11.
- Maisey, J.G. Ed. 1991.** Santana fossils. An illustrated atlas. – New Jersey, T.F.H. Publications.
- Martill, D.M. Ed. 1993.** Fossils of the Santana and Crato Formations, Brazil. – Oxford, Blackwell Publishing (Palaeontology Field Guides to Fossils 5).
- Martill, D.M. & E. Frey. 1998.** A new pterosaur Lagerstätte in N.E. Brazil (Crato Formation, Aptian, Lower Cretaceous). Preliminary observations. – Oryctos 1: 79–85.
- Martill, D.M. & E. Frey. 1999.** A possible azhdarchid pterosaur from the Crato Formation (Early Cretaceous) of northeast Brazil. – Geologie & Mijnbouw 78: 315–318.
- Martill, D.M. & D.M. Unwin. 1989.** Exceptionally preserved pterosaur wing membrane from the Cretaceous of Brazil. – Nature 340: 138–140.
- Martill, D.M., E. Frey, G. Chong Diaz & C.M. Bell. 2000.** Reinterpretation of a Chilean pterosaur and the occurrence of Dsungaripteridae in South America. – Geological Magazine 137: 19–25.
- Owen, R. 1851.** Monograph on the fossil Reptilia of the Cretaceous Formations. – Palaeontographical Society Monograph 5: 1–118.
- Owen, R. 1861.** Supplement (III) to the monograph on the fossil Reptilia of the Cretaceous Formations. – Palaeontographical Society Monograph 12: 1–19.
- Owen, R. 1874.** Monograph of fossil Reptilia of the Mesozoic formations. 1. Pterosauria. – Palaeontographical Society Monograph 27: 1–14.
- Padian, K. & M. Smith. 1992.** New light on Late Cretaceous pterosaur material from Montana. – Journal of Vertebrate Paleontology 12: 87–92.
- Plieninger, R. 1901.** Beiträge zur Kenntnis der Flugsaurier. – Palaeontographica A 48: 65–90.
- Pons, D., P.Y. Berthou & D.A. Campos. 1990.** Quelques observations sur la palynologie de l'Aptien Supérieur et de l'Albien du bassin d'Araripe (N.E. du Brésil). – Atas do 1. Simposio sobre a Bacia do Araripe e bacias interiores do Nordeste, Crato: 241–252.
- Price, L.I. 1971.** A Presença de Pterosauria no Cretáceo Inferior da Chapada do Araripe, Brasil. – Anais Academia Brasileira de Ciências 43 (suppl.): 452–461.
- Sayão, J.M. & A.W.A. Kellner. 2000.** Description of a pterosaur rostrum from the Crato Member, Santana Formation (Aptian–Albian) northeastern Brazil. – Boletim do Museu Nacional. Série Geologia 54:1–8.
- Seeley, H.G. 1870.** The Ornithosauria. An elementary study of the bones of Pterodactyles. – Cambridge, Cambridge University Press.
- Unwin D.M. 2001.** An overview of the pterosaur assemblage from the Cambridge Greensand (Cretaceous) of eastern England. – Mitteilungen Museum für Naturkunde Berlin, Geowissenschaftliche Reihe 4: 189–221.

- Unwin, D.M. 2002.** On the systematic relationships of *Cearadactylus atrox*, an enigmatic Early Cretaceous pterosaur from the Santana Formation of Brazil. *Mitteilungen Museum für Naturkunde Berlin, Geowissenschaftliche Reihe* 5: 239–263.
- Unwin, D.M. 2003.** On the phylogeny and evolutionary history of pterosaurs. In: **Buffetaut, E. & J.-M. Mazin. Eds. 2003.** Evolution and palaeobiology of pterosaurs. – London Geological Society (Special publications): 139–190.
- Urlichs, M., R. Wild & B. Ziegler. 1994.** Der Posidonien-Schiefer und seine Fossilien. – Stuttgart, Staatliches Museum für Naturkunde Stuttgart/Gesellschaft zur Förderung des Naturkundemuseums in Stuttgart, e. V. (Stuttgarter Beiträge zur Naturkunde C 36).
- Veldmeijer, A.J. 1998.** The Leiden specimen of *Coloborhynchus* (Pterosauria). In: **Jagt, J.W.M, P.H. Lambers, E.W.A. Mulder & A.S. Schulp. Eds. 1998.** Third European Workshop on Vertebrate Palaeontology, Maastricht, 6–9 May 1998, Programme and Abstracts, Field guide. – Maastricht, Natuurhistorisch Museum Maastricht: 69.
- Veldmeijer, A.J. 2002.** Pterosaurs from the Lower Cretaceous of Brazil in the Stuttgart Collection. – *Stuttgarter Beiträge zur Naturkunde B* 327: 1–27. (This work, chapter 3).
- Veldmeijer, A.J. 2003a.** Description of *Coloborhynchus spielbergi* sp. nov. (Pterodactyloidea) from the Albian (Lower Cretaceous) of Brazil. – *Scripta Geologica* 125: 35–139. (This work, chapter 2).
- Veldmeijer, A.J. 2003b.** Preliminary description of a skull and wing of a Brazilian Cretaceous (Santana Formation; Aptian–Albian) pterosaur (Pterodactyloidea) in the collection of the AMNH. – *PalArch*, series vertebrate palaeontology 0, 0: 1–14. (This work, chapter 5).
- Veldmeijer, A.J. & A.M. Hense. 2004.** Supplement to: Pterosaurs from the Lower Cretaceous of Brazil in the Stuttgart collection, in: *Stuttgarter Beiträge zur Naturkunde, Serie B (Geologie und Paläontologie)* 2002, 327: 1–27. – *PalArch*, series vertebrate palaeontology 1, 3: 14–21.
- Veldmeijer, A.J. & Signore, M. 2004.** Book review of: **Buffetaut, E. & J.-M. Mazin. Eds. 2003.** Evolution and palaeobiology of pterosaurs. (London, Geological Society Special publications 217). – *PalArch*, book reviews.
- Veldmeijer, A.J., M. Signore & H.J.M. Meijer. 2005a.** Description of two pterosaur (Pterodactyloidea) mandibles from the Lower Cretaceous Santana Formation, Brazil. – *Deinsea* 11. (This work, chapter 4).
- Veldmeijer, A.J., M. Signore & H.J.M. Meijer. 2005b.** *Brasileodactylus* (Pterosauria, Pterodactyloidea, Anhangueridae); an update. – *Cranium* 22, 1: 45–56. (This work, chapter 7, section 7.1.).
- Veldmeijer, A.J., Signore, M. & H.J.M. Meijer. Submitted.** Description of pterosaurian (Pterodactyloidea) remains from the Lower Cretaceous of Brazil in various German collections. – *PalArch*, series vertebrate palaeontology. (This work, chapter 6).
- Veldmeijer, A.J., Signore, M. & H.J.M. Meijer. In review.** *Coloborhynchus* from the Lower Cretaceous Santana Formation, Brazil (Pterosauria, Pterodactyloidea, Anhangueridae); an update. (This work, chapter 7, section 7.2.).
- Wang Xiaolin & Lü Junchang. 2001.** Discovery of a pterodactylid pterosaur from the Yixian Formation of western Liaoning, China. – *Chinese Science Bulletin* 46, 13: 1112–1117.
- Wang Xiaolin & Zhou Zhonghe. 2002.** A new pterosaur (Pterodactyloidea, Tapejaridae) from the Early Cretaceous Jiufotang Formation of western Liaoning, China and its implications for biostratigraphy. – *Chinese Science Bulletin* 47, 20: 1521 (in Chinese; English version: *Chinese Science Bulletin* 48, 1: 16–23).

- Wellnhofer, P. 1970.** Die Pterodactyloidea (Pterosauria) der Oberjura–Plattenkalke Süddeutschlands. – Munich, Verlag der Bayerischen Akademie der Wissenschaften (Bayerischen Akademie der Wissenschaften, Mathematisch–Naturwissenschaftliche Klasse, Abhandlungen, Neue Folge 141).
- Wellnhofer, P. 1977.** *Araripedactylus dehmi* nov. gen., nov. sp., ein neuer Flugsaurier aus der Unterkreide von Brasilien. – Mitteilungen der Bayerische Staatsammlung für Paläontologie und historische Geologie 17: 157–167.
- Wellnhofer, P. 1978.** Handbuch der Paläoherpetologie. Teil 19. Pterosauria. – Stuttgart/New York, Gustav Fischer Verlag.
- Wellnhofer, P. 1985.** Neue Pterosaurier aus der Santana–Formation (Apt.) der Chapada do Araripe, Brasilien. – *Palaeontographica A* 187: 105–182.
- Wellnhofer, P. 1987.** New crested pterosaurs from the Lower Cretaceous of Brazil. – Mitteilungen der Bayerische Staatsammlung für Paläontologie und historische Geologie 27: 175–186.
- Wellnhofer, P. 1988.** Terrestrial locomotion in pterosaurs. – *Historical Biology* 1: 3–16.
- Wellnhofer, P. 1991a.** The illustrated encyclopedia of pterosaurs. – New York, Crescent Books.
- Wellnhofer, P. 1991b.** Weitere Pterosaurierfunde aus der Santana–Formation (Apt) der Chapada do Araripe, Brasilien. – *Palaeontographica A* 215: 43–101.
- Wellnhofer, P. & E. Buffetaut. 1999.** Pterosaur remains from the Cretaceous of Morocco. *Paläontologische Zeitschrift* 73: 133–142.
- Wellnhofer, P. & A.W.A. Kellner. 1991.** The skull of *Tapejara wellnhoferi* Kellner (Reptilia, Pterosauria) from the Lower Cretaceous Santana Formation of the Araripe Basin, northeastern Brazil. – Mitteilungen der Bayerische Staatsammlung für Paläontologie und historische Geologie 31: 89–106.
- Wellnhofer, P., E. Buffetaut & G. Gigase. 1983.** A pterosaurian notarium from the Lower Cretaceous of Brazil. – *Paläontologisches Zeitschrift* 57: 147–157.
- Williston, S.W. 1902a.** On the skull of *Nyctodactylus*, an Upper Cretaceous pterodactyl. – *Journal of Geology* 10: 520–531.
- Williston, S.W. 1902b.** On the skeleton of *Nyctodactylus*, with restoration. *American Journal of Anatomy* 1: 297–305.
- Williston, S.W. 1903.** On the osteology of *Nyctosaurus* (*Nyctodactylus*), with notes on American pterosaurs. – Field Columbian Museum Publication, Geological Series 2: 125–163.
- Young, C.C. 1964.** On a new pterosaurian from Sinkiang, China. – *Vertebrata Palasiatica* 8: 239–255.
- Ziegler, B. 1992.** Guide to the Löwentor Museum. – Stuttgart, Staatliches Museum für Naturkunde Stuttgart/Gesellschaft zur Förderung des Naturkundemuseums in Stuttgart, e. V. (Stuttgarter Beiträge zur Naturkunde C 27).

11. General appendix**11.1. Additional data chapter 7****11.1.1. Measurements dentition**

ALVEOLI																		
number	mandible <i>Brasileodactylus</i> <i>araripensis</i> (MN 4804-V)			mandible <i>Brasileodactylus</i> <i>araripensis</i> (SMNS 55414)			mandible <i>Brasileodactylus</i> <i>cf. araripensis</i> (MN 4797-V)			cranium <i>Brasileodactylus</i> <i>cf. araripensis</i> (MN 4797-V)		mandible <i>Brasileodactylus</i> sp. indet. (AMNH 24444)			cranium <i>Brasileodactylus</i> sp. indet. (AMNH 24444)			
	left	right	average	left	right	average	left	right	average	left	right	average	left	right	average			
1	3.2	3.2	3.2	-	2.6	2.6	4.4	-	4.4	-	4.1	4.1	-	-	-	-	2.5	2.5
2	5.3	4.6	4.95	-	6.6		4.9	-	4.9	-	5.2	5.2	-	-	-	-	4.7	4.7
3	5.8	5.6	5.7	-	5.4	5.4	5.4	5.3	5.35	-	7.1	7.1	-	3.8	3.8	-	4.4	
4	4.9	5.6	5.25	-	5.4	5.4	4.3	5.2	4.75	-	5.6	5.6	-	3.1	3.1	-	4.4	4.4
5	4	4.5	4.25	-	4.2	4.2	-	4.3	4.3		3.9	3.9	-	2.4	2.4	-	2.3	2.3
6	4	4.9	4.45	-	4.4	4.4	-	3.8	3.8	-	3.8	3.8	-	2.6	2.6	-	2.8	2.8
7	5.2		5.3	-	4.4	4.4	-	5.2	5.2	-	5.3	5.3	-	3.5	3.5	-	2.9	2.9
8	5.3	4.9	5.1	-	4.8	4.8	-	4.3	4.3	-	4.9	4.9	-			-	2.7	2.7
9	6	5.4	5.7	-	4.2	4.2	-	-	-	-	5.1	5.1	-	-	-	-	3.8	3.8
10	5.8	5.3	5.55	-	4.8		-	4	4	-	4.1	4.1	-	-	-	-	3.4	3.4
11	-	-	-	-	2.7	2.7	-	2.9	2.9	-	4.2	4.2	-	-	-	-	2.8	
12	-	-	-	-	-	-	-	-	-	-	-	-	-	-	-	-	3	3
13	-	-	-	-	-	-	-	-	-	-	-	-	-	-	-	-	2.5	2.5
14	-	-	-	-	-	-	-	-	-	-	-	-	-	-	-	-	2.1	2.1
15	-	-	-	-	-	-	-	-	-	-	-	-	-	-	-	-	1.3	1.3
16	-	-	-	-	-	-	-	-	-	-	-	-	-	-	-	-	2.5	2.5
17	-	-	-	-	-	-	-	-	-	-	-	-	-	-	-	-	1.2	1.2
18	-	-	-	-	-	-	-	-	-	-	-	-	-	-	-	-	1.4	1.4
19	-	-	-	-	-	-	-	-	-	-	-	-	-	-	-	-	1	
20	-	-	-	-	-	-	-	-	-	-	-	-	-	-	-	-	1.5	1.5
21	-	-	-	-	-	-	-	-	-	-	-	-	-	-	-	-	1.3	1.3
22	-	-	-	-	-	-	-	-	-	-	-	-	-	-	-	-	1.5	1.5
23	-	-	-	-	-	-	-	-	-	-	-	-	-	-	-	-	1.3	1.3
24	-	-	-	-	-	-	-	-	-	-	-	-	-	-	-	-	1.6	1.6
25	-	-	-	-	-	-	-	-	-	-	-	-	-	-	-	-	1.5	1.5
26	-	-	-	-	-	-	-	-	-	-	-	-	-	-	-	-	1.5	1.5
DIASTEMAE																		
number	mandible <i>Brasileodactylus</i> <i>araripensis</i> (MN 4804-V)			mandible <i>Brasileodactylus</i> <i>araripensis</i> (SMNS 55414)			mandible <i>Brasileodactylus</i> <i>cf. araripensis</i> (MN 4797-V)			cranium <i>Brasileodactylus</i> <i>cf. araripensis</i> (MN 4797-V)		mandible <i>Brasileodactylus</i> sp. indet. (AMNH 24444)			cranium <i>Brasileodactylus</i> sp. indet. (AMNH 24444)			
	left	right	average	left	right	average	left	right	average	left	right	average	left	right	average			
1-2	1	1	1	-	1.3	1.3	0	-	0	-	0	0	-	-	-	-	-	-
2-3	2.6	2.2	2.4	-	3.1	3.1	3.9	-	3.9	-	2.4	2.4	-	-	-	-	4.4	4.4
3-4	3.1	3.2	3.15	-	5.7	5.7	4.1	3.4	3.75	-	2.6	2.6	7.2	4.9	7.2	-	3.5	3.5

4-5	4.7	3.7	4.2	-	6	6	-	4.7	4.7	-	4.9	4.9	7.2	6.05	6.625	-	4.6	4.6
5-6	5.7	6.2	5.95	-	5.4	5.4	-	4.3	4.3	-	4.5	4.5	6	5.25	5.625	-	6.0	6.0
6-7	6.7	6.7	6.7	-	7.6	7.6	-	5.7	5.7	-	5.4	5.4	5.4	5.4	5.4	-	4.7	4.7
7-8	8.8	9.4	9.1	-	9	9	-	8.7	8.7	-	6.9	6.9	-	-	-	-	6.8	6.8
8-9	11.5	12	11.75	-	11.2	11.2	-	-	-	-	10.6	10.6	-	-	-	-	10.0	10.0
9-10	11.1	12.4	11.75	-	13.8	13.8	-	-	-	-	15.4	15.4	-	-	-	-	9.3	9.3
10-11	-	-	-	-	15.2	15.2	-	15.2	15.2	-	15.4	15.4	-	-	-	-	7.1	7.1
11-12	-	-	-	-	-	-	-	-	-	-	-	-	-	-	-	-	-	-
12-13	-	-	-	-	-	-	-	-	-	-	-	-	-	-	-	-	11.6	11.6
13-14	-	-	-	-	-	-	-	-	-	-	-	-	-	-	-	-	11.3	11.3
14-15	-	-	-	-	-	-	-	-	-	-	-	-	-	-	-	-	10.4	10.4
15-16	-	-	-	-	-	-	-	-	-	-	-	-	-	-	-	-	4.0	4.0
16-17	-	-	-	-	-	-	-	-	-	-	-	-	-	-	-	-	3.4	3.4
17-18	-	-	-	-	-	-	-	-	-	-	-	-	-	-	-	-	10.0	10.0
18-19	-	-	-	-	-	-	-	-	-	-	-	-	-	-	-	-	11.0	11.0
19-20	-	-	-	-	-	-	-	-	-	-	-	-	-	-	-	-	9.6	9.6
20-21	-	-	-	-	-	-	-	-	-	-	-	-	-	-	-	-	3.2	3.2
21-22	-	-	-	-	-	-	-	-	-	-	-	-	-	-	-	-	5.5	5.5
22-23	-	-	-	-	-	-	-	-	-	-	-	-	-	-	-	-	7.7	7.7
23-24	-	-	-	-	-	-	-	-	-	-	-	-	-	-	-	-	5.7	5.7
24-25	-	-	-	-	-	-	-	-	-	-	-	-	-	-	-	-	6.6	6.6
25-26	-	-	-	-	-	-	-	-	-	-	-	-	-	-	-	-	5.0	5.0

	mandible <i>Criorhynchus mesembrinus</i> (BSP 1987 I 46)			cranium <i>Criorhynchus mesembrinus</i> (BSP 1987 I 46)			mandible <i>cf. Criorhynchus mesembrinus</i> (BSP 1987 I 46)		
number	left	right	average	left	right	average	left	right	average
1	-	7.4	7.4	6.3	4.5	5.4	6.8	6.5	6.65
2	-	8.8	8.8	7.8	5.5	6.65	6.6	6.4	6.5
3	-	7.7	7.7	8.6	7.8	8.2	6.2	6.4	6.3
4	7.2	7	7.1	7.3	8.6	7.95	6.1	6.5	6.3
5	7.6	7.3	7.45	8.1	8	8.05	6.4	7.3	6.85
6	8.2	7.5	7.85	7.4	8.2	7.8	6.8	7.4	7.1
7	6.9	-	6.9	8.8	8.3	8.55	6.4	6.3	6.35
8	5.4	-	5.4	8.1	8.3	8.2	4.9	5.3	4.9
9	5.1	-	5.1	-	7.9	7.9	6	6	6
10	3.5	-	3.5	-	-	-	4.3	5.3	4.8
11	4.2	-	4.2	-	5.5	5.5	4.5	4.4	4.45
12	4.3	-	4.3	-	4.8	4.8	4	4.1	4.05
13	-	-	-	-	4.1	4.1	-	-	-
14	-	-	-	-	5.2	5.2	-	-	-
	mandible <i>Criorhynchus mesembrinus</i> (BSP 1987 I 46)			cranium <i>Criorhynchus mesembrinus</i> (BSP 1987 I 46)			mandible <i>cf. Criorhynchus mesembrinus</i> (BSP 1987 I 46)		
number	left	right	average	left	right	average	left	right	average

1-2	-	4	4	3.4	-	3.4	4.5	3.5	4
2-3	-	12.6	12.6	8.6	-	8.6	6.7	7.4	7.05
3-4	-	10.6	10.6	10.9	6.8	8.85	6.3	6.3	6.3
4-5	10.1	10.6	10.35	9.2	11.6	10.4	8.9	8.9	8.9
5-6	13.9	16.4	15.15	11.9	8.6	10.25	8.1	13.7	10.9
6-7	22.2	-	22.2	19.3	10.6	14.95	15.6	18.1	16.85
7-8	31	-	31	27.7	20.3	24	22.9	18.9	22.9
8-9	34.4	-	34.4	-	29.1	29.1	23.8	23.2	23.8
9-10	12.3	-	12.3	-	36	36	24	25.2	24.6
10-11	15.9	-	15.9	-	29	29	20.2	17.4	17.4
11-12	14.8	-	14.8	-	31.3	31.3	13.2	15.6	15.6
12-13	-	-	-	-	29.6	29.6	-	-	-
13-14	-	-	-	-	33	33	-	-	-

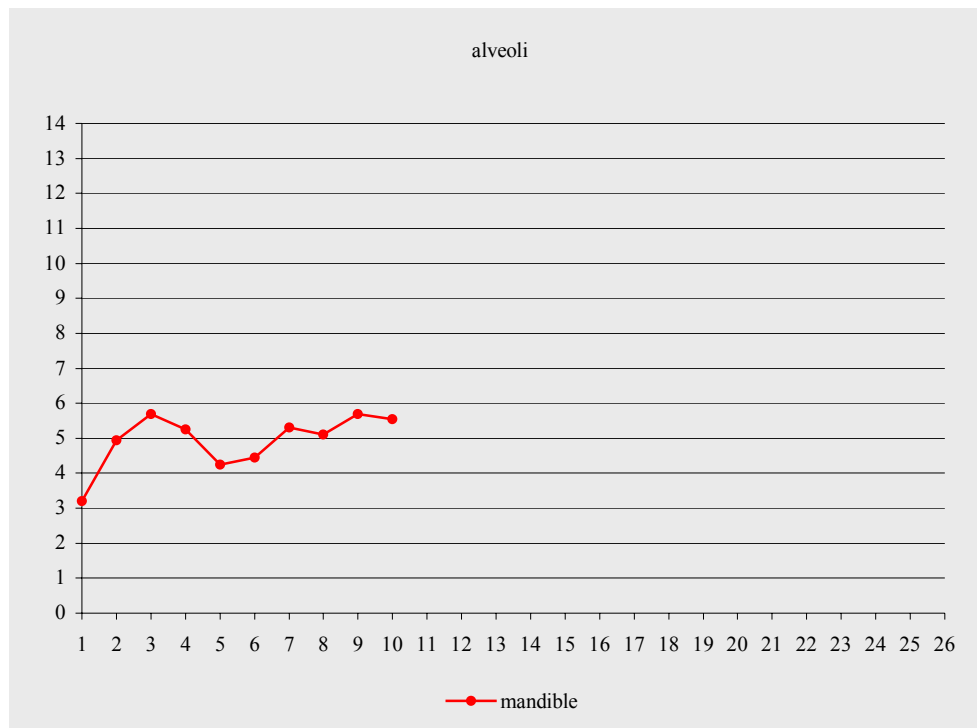
ALVEOLI	cranium <i>Coloborhynchus clavirostris</i> (BMNH 1822)			cranium <i>Coloborhynchus araripensis</i> (SAO 16494)			cranium <i>Coloborhynchus araripensis</i> (MN 4735-V)			mandible <i>Coloborhynchus robustus</i> (BSP 1987 I 47)			mandible <i>Coloborhynchus robustus</i> (SMNK 2302 PAL)			cranium <i>Coloborhynchus robustus</i> (SMNK 2302 PAL)			mandible <i>Coloborhynchus spielbergi</i> (RGM 401 880)			cranium <i>Coloborhynchus spielbergi</i> (RGM 401 880)			mandible <i>Coloborhynchus piscator</i> (NSM-PV 19892)			cranium <i>Coloborhynchus piscator</i> (NSM-PV 19892)		
	number	left	right	average	left	right	average	left	right	average	left	right	average	left	right	average	left	right	average	left	right	average	left	right	average	left	right	average	left	right
1	6.4	6.2	6.3	5.1	4.2	4.65	5.4	5.8	5.6	8.5	7.8	8.2	8.6	10.5	9.55	6.7	8.1	7.4	7.9	7.9	7.9	-	-	-	6.3	-	6.3	5.5	5.7	5.6
2	10.3	9	9.7	8.4	6.8	7.6	10.3	8.6	9.45	10.6	11.3	11	12.5	11.7	12.1	12.3	12.1	12.2	8.5	11	9.75	8.6	9.6	9.1	9.3	-	9.3	9.6	9.8	9.7
3	11.9	12.2	12.1	8.4	7.9	8.15	11.7	10.6	11.15	10.9	9.2	10.1	12.1	11.8	11.95	13.6	12.2	12.9	11.4	11.3	11.35	12.2	11.4	11.8	9.2	-	9.2	13.1	-	13.1
4	8.7	7.2	8	7.8	8.5	8.15	13.2	9.7	11.45	7.3	7.4	7.4	8.4	7.4	8.4	9.4	9.1	9.25	6.1	5.9	6	10	10.1	10.05	8.7	-	8.7	8.2	-	8.2
5	5.4	4.9	5.2	5.4	4.5	4.95	6.9	6.1	6.5	4.5	-	4.5	8.4	6.8	7.6	6	5.9	5.95	6.1	4.9	5.5	6.9	6.5	6.7	5.7	5.2	5.45	5.1	-	5.1
6	5.5	4.6	5.1	5.1	4.9	5	4.8	5.4	5.1	4.8	4.6	4.7	10.8	10.3	10.55	4.9	5.4	5.15	7.1	6.9	7	5.4	-	5.4	5.4	6.1	5.75	4.8	4.8	4.8
7	-	-	-	6.3	7.4	6.85	-	-	-	7	7.2	7.1	10.3	9.9	10.1	8.7	8.8	8.75	9.2	7	8.1	9.2	8.4	8.8	7.7	6.6	7.15	6	5.5	5.75
8	-	-	-	8.4	7.9	8.15	7.3	-	7.3	9.3	8.9	9.1	8.5	6.7	7.6	10.3	9.4	9.85	8.7	-	8.7	9.3	10.7	10	7.4	8.1	7.75	6.2	-	6.2
9	-	-	-	7.2	6.8	7	6.9	6.8	6.85	8.1	6.9	7.5	8.4	-	8.4	8.4	8	8.2	7.3	7.5	7.4	10.8	-	10.8	8	7.5	7.75	8.6	8.4	8.5
10	-	-	-	6.7	6.1	6.4	6.3	6.9	6.6	6.8	5.2	6	-	-	-	9.5	7.4	8.45	7.3	7	7.15	-	6.9	6.9	7.7	7.3	7.5	8.6	8.4	8.5
11	-	-	-	6.4	7.1	6.75	5.1	6.2	5.65	6.8	5.2	6	-	-	-	-	-	-	6.7	6.2	6.45	-	7.3	7.3	7.5	7.7	7.6	7.3	6.5	6.9
12	-	-	-	5.6	6.2	5.9	5.5	5.2	5.35	6.7	7.7	7.2	-	-	-	-	-	-	7.5	5.8	6.65	-	7.8	7.8	7.7	8.1	7.9	6.3	5.8	6.05
13	-	-	-	5.7	-	5.7	-	4.6	4.6	6.4	5.6	6	-	-	-	-	-	-	7.6	5	6.3	-	7.3	7.3	6.6	5.9	6.25	6.1	5.1	5.6
14	-	-	-	4.3	-	4.3	-	-	-	5.8	5.9	5.85	-	-	-	-	-	-	6.8	6.9	6.85	-	7.5	7.5	4.7	6	5.35	7	5.7	6.35
15	-	-	-	5.3	-	5.3	-	-	-	5.4	6.6	6	-	-	-	-	-	-	6.3	6.7	6.5	-	7.6	7.6	5.2	6.1	5.65	8	5.4	6.7
16	-	-	-	4.6	-	4.6	-	-	-	4.9	5.2	5.05	-	-	-	-	-	-	6.4	5.5	5.95	-	5.3	5.3	5.2	5.6	5.4	5.5	-	5.5
17	-	-	-	4	-	4	-	-	-	5.3	5.2	5.25	-	-	-	-	-	-	-	-	-	-	5	5	5.6	6.7	6.15	5.8	7.4	6.6
18	-	-	-	4	-	4	-	-	-	3.9	5.2	-	-	-	-	-	-	-	-	-	-	-	5	5	7.1	7.5	7.3	5.9	6.2	6.05
19	-	-	-	-	-	-	-	-	-	-	-	-	-	-	-	-	-	-	-	-	-	-	5	5	-	-	-	6	6.2	6.1
20	-	-	-	-	-	-	-	-	-	-	-	-	-	-	-	-	-	-	-	-	-	-	-	-	-	-	-	-	8.1	8.1
21	-	-	-	-	-	-	-	-	-	-	-	-	-	-	-	-	-	-	-	-	-	-	-	-	-	-	-	-	5.9	5.9
22	-	-	-	-	-	-	-	-	-	-	-	-	-	-	-	-	-	-	-	-	-	-	-	-	-	-	-	-	5.2	5.2
23	-	-	-	-	-	-	-	-	-	-	-	-	-	-	-	-	-	-	-	-	-	-	-	-	-	-	-	-	5.5	5.5
24	-	-	-	-	-	-	-	-	-	-	-	-	-	-	-	-	-	-	-	-	-	-	-	-	-	-	-	-	7.7	7.7
25	-	-	-	-	-	-	-	-	-	-	-	-	-	-	-	-	-	-	-	-	-	-	-	-	-	-	-	-	9.5	9.5

DIASTEMAE	cranium <i>Coloborhynchus clavirostris</i> (BMNH 1822)			cranium <i>Coloborhynchus araripensis</i> (SAO 16494)			cranium <i>Coloborhynchus araripensis</i> (MN 4735-V)			mandible <i>Coloborhynchus robustus</i> (BSP 1987 I 47)			mandible <i>Coloborhynchus robustus</i> (SMNK 2302 PAL)			cranium <i>Coloborhynchus robustus</i> (SMNK 2302 PAL)			mandible <i>Coloborhynchus spielbergi</i> (RGM 401 880)			cranium <i>Coloborhynchus spielbergi</i> (RGM 401 880)			mandible <i>Coloborhynchus piscator</i> (NSM-PV 19892)			cranium <i>Coloborhynchus piscator</i> (NSM-PV 19892)			
	number	left	right	average	left	right	average	left	right	average	left	right	average	left	right	average	left	right	average	left	right	average	left	right	average	left	right	average	left	right	average
1-2	-	-	-	1.7	2.4	2.05	4.4	7.3	5.85	4.2	4.5	4.35	6.5	6.4	6.45	2.5	3.4	2.95	6	4	5	-	-	-	3.1	3.6	3.35	2.1	3	2.55	
2-3	4.7	6.8	5.8	1.8	3.2	2.5	5.3	5.3	5.3	5.6	7.2	6.4	8.6	7.9	8.25	8.4	8.3	8.35	8	5	6.5	8.1	8	8.05	4.6	-	4.6	3	5	4	
3-4	3.4	4.3	3.9	3.8	3.8	3.8	5.6	4.4	5	3*	2.4*	2.7	6.2	5.3	5.75	7.8	7.4	7.6	4	5	4.5	7.8	8	7.9	4.6	-	4.6	5.4	-	5.4	
4-5	2.3	3.3	2.8	5.2	7.1	6.15	4.5	6.5	5.5	4.3	16.8	10.55	20.3	21.2	20.75	6.8	7.5	7.15	8	6	7	4.2	6	5.1	4.1	5	4.55	6.1	-	6.1	
5-6	3.6	5.7	4.7	6	5.9	5.95	5.7	4.5	5.1	5.8	-	5.8	8.4	10.9	9.65	7.4	6.4	6.9	9	10	9.5	6.2	-	6.2	4.6	6.1	5.35	4.5	7.1	5.8	
6-7	-	-	-	5	7.1	6.05	-	-	-	5.4	6.3	5.85	12.7	16.6	14.65	7.3	7.7	7.5	10	11	10.5	10.9	-	10.9	5.7	7.1	6.4	5.7	6.2	5.95	
7-8	-	-	-	6.9	8.2	7.55	-	-	-	8.5	9.7	9.1	24.5	24	24.25	10.3	10.4	10.35	16	-	16	11	15	13	8.3	10.5	9.4	7.9	10.8	9.35	
8-9	-	-	-	8.6	12.3	10.45	17	-	17	11.4	13	12.2	32	-	32	17.2	19.8	18.5	18	-	18	18	15	18	14.5	16.5	15.5	11.2	15.9	13.55	
9-10	-	-	-	11.9	15.5	13.7	17.5	18	17.75	18.6	21	18.6	-	-	-	26.9	33.9	30.4	16	18	17	20	18	20	18.4	19.8	19.1	13.8	18.2	16	
10-11	-	-	-	14.7	17.4	16.05	26	23.4	24.7	17	21	17	-	-	-	-	-	-	24	20	22	-	15	15	20	18.9	19.45	17.3	21.2	19.25	
11-12	-	-	-	18.4	16.6	17.5	20	-	20	21.8	21.8	21.8	-	-	-	-	-	-	23	23	23	-	25	25	21	18.9	19.95	20.7	18.8	19.75	
12-13	-	-	-	16.1	-	16.1	-	-	-	21.7	20.4	21.05	-	-	-	-	-	-	20	20	20	-	28	28	20.1	17.3	18.7	20.2	18.6	19.4	
13-14	-	-	-	15.3	-	15.3	-	-	-	19.4	19	19.2	-	-	-	-	-	-	19	20	19.5	-	20	20	18.5	16.1	17.3	18.9	17	17.95	
14-15	-	-	-	17	-	17	-	-	-	17.9	18.9	18.4	-	-	-	-	-	-	18	21	19.5	-	17	17	17.9	16.8	17.35	20.2	17.9	19.05	
15-16	-	-	-	14.4	-	14.4	-	-	-	16.4	16.8	16.6	-	-	-	-	-	-	19	22	20.5	-	45	45	14.2	15.5	14.85	14	16.6	15.3	
16-17	-	-	-	13.8	-	13.8	-	-	-	16	16.9	16.45	-	-	-	-	-	-	-	-	-	-	12	12	11.6	10.5	11.05	19.3	11.8	15.55	
17-18	-	-	-	11.2	-	11.2	-	-	-	15	16	-	-	-	-	-	-	-	-	-	-	-	13	13	9.5	15.5	12.5	17.9	10.9	14.4	
18-19	-	-	-	-	-	-	-	-	-	-	-	-	-	-	-	-	-	-	-	-	-	-	-	-	-	-	-	-	5.2	10.6	7.9
19-20	-	-	-	-	-	-	-	-	-	-	-	-	-	-	-	-	-	-	-	-	-	-	-	-	-	-	-	-	7.6	7.6	
20-21	-	-	-	-	-	-	-	-	-	-	-	-	-	-	-	-	-	-	-	-	-	-	-	-	-	-	-	-	6.3	6.3	
21-22	-	-	-	-	-	-	-	-	-	-	-	-	-	-	-	-	-	-	-	-	-	-	-	-	-	-	-	-	4.8	4.8	
22-23	-	-	-	-	-	-	-	-	-	-	-	-	-	-	-	-	-	-	-	-	-	-	-	-	-	-	-	-	1.9	1.9	
23-24	-	-	-	-	-	-	-	-	-	-	-	-	-	-	-	-	-	-	-	-	-	-	-	-	-	-	-	-	1	1	
24-25	-	-	-	-	-	-	-	-	-	-	-	-	-	-	-	-	-	-	-	-	-	-	-	-	-	-	-	-	4.3	4.3	

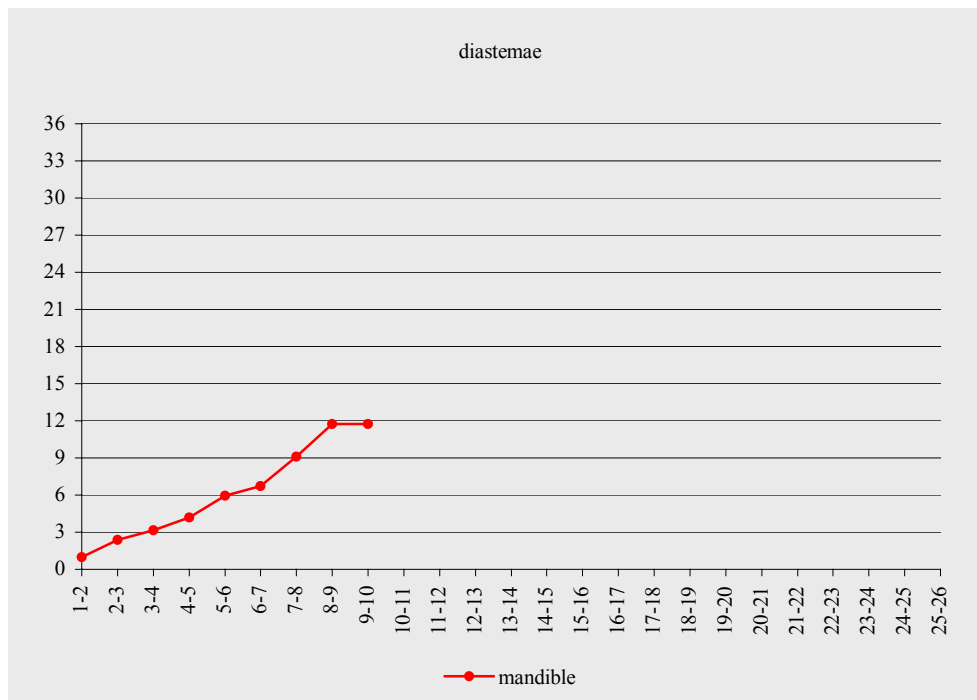
	cranium <i>Anhanguera blittersdorffi</i> (MN 4805-V)			mandible <i>Anhanguera blittersdorffi</i> (n. 40 Pz-DBAV-UERJ)			cranium <i>Anhanguera blittersdorffi</i> (n. 40 Pz-DBAV-UERJ)			cranium <i>Anhanguera santanae</i> (AMNH 22555)		
number	left	right	average	left	right	average	left	right	average	left	right	average
1	-	4.1	4.1	5	5.1	5.05	4.3	4.5	4.4	3.6	4.4	4
2	-	4.5	4.5	5.9	5.3	5.6	5.7	5	5.35	7.1	5.2	6.15
3	-	7.1	7.1	4.6	5	4.8	6.4	7	6.7	6	7.4	6.7
4	-	7.2	7.2	4.5	5.2	4.85	5.3	5.3	5.3	7.3	6.2	6.75
5	-	4.4	4.4	3.7	4.2	3.95	6	5	5.5	5.5	4.8	5.15
6	-	3.9	3.9	3.8	4.6	4.2	4.2	4.1	4.15	6.2	5.9	6.05
7	-	6.6	6.6	3.9	5.1	4.5	5.6	5.7	5.65	7.2	6.3	6.75
8	-	7	7	5.3	5.4	5.35	-	5.8	5.8	8.2	6.9	7.55
9	-	6.8	6.8	4.7	4.7	4.7	5.4	5.5	5.45	5.9	6	5.95
10	-	8.6	8.6	4.1	4.5	4.3	4.6	5.4	5	6.7	4.7	5.7
11	-	6.2	6.2	4	4.3	4.15	4.6	4.8	4.7	4.7	-	4.7
12	-	4.4	4.4	3.5	4.2	3.85	4.6	4.2	4.4	5.7	-	5.7
13	-	5.5	5.5	4	3.8	3.9	3.9	4	3.95	5.5	-	5.5
14	-	5.4	5.4	3	3.5	3.25	3.5	4.6	4.05	-	-	-
15	-	4	4	3.2	3.3	3.25	4.1	3.5	3.8	-	-	-
16	-	5.9	5.9	3.3	3.2	3.25	2.6	3.2	2.9	-	-	-
17	-	4.7	4.7	2.9	3	2.95	2.6	2.8	2.7	-	-	-
18	-	4.1	4.1	2.7	2.7	2.7	3.5	-	3.5	-	-	-
19	-	4.2	4.2	2.5	2.7	2.6	3	-	3	-	-	-
20	-	3.5	3.5	2.4	2.9	2.65	3.3	-	3.3	-	-	-
21	-	3.6	3.6	2.5	-	2.5	3.2	-	3.2	-	-	-
22	-	3.7	3.7	-	-	-	-	-	-	-	-	-
23	-	3.5	3.5	-	-	-	-	-	-	-	-	-
24	-	3.6	3.6	-	-	-	-	-	-	-	-	-
25	-	3.7	3.7	-	-	-	-	-	-	-	-	-
26	-	2.5	2.5	-	-	-	-	-	-	-	-	-
	cranium <i>Anhanguera blittersdorffi</i> (MN 4805-V)			mandible <i>Anhanguera blittersdorffi</i> (n. 40 Pz-DBAV-UERJ)			cranium <i>Anhanguera blittersdorffi</i> (n. 40 Pz-DBAV-UERJ)			cranium <i>Anhanguera santanae</i> (AMNH 22555)		
number	left	right	average	left	right	average	left	right	average	left	right	average
1-2	-	-	-	1.1	2.1	1.6	3.5	1.3	2.4	1.7	3.2	2.45
2-3	-	2.5	2.5	2.8	2.6	2.7	3.9	3.3	3.6	4.2	3.4	3.8
3-4	-	3.3	3.3	1.9	2.7	2.3	2.6	2.8	2.7	4	4.4	4.2
4-5	-	3.7	3.7	4.7	4.6	4.65	2.9	2.6	2.75	5.3	5	5.15
5-6	-	3.2	3.2	3.2	3.2	3.2	3.3	3.3	3.3	6.7	7.1	6.9
6-7	-	5.7	5.7	3.6	2.8	3.6	2.3	2.6	2.45	8	6.9	7.45
7-8	-	4.8	4.8	2	3.3	2	-	2.5	2.5	11.8	8.8	10.3
8-9	-	5.6	5.6	5.7	4.4	5.05	-	3.4	3.4	13.3	15.8	14.55
9-10	-	5.1	5.1	5.6	5.2	5.4	5.2	4.1	4.65	15.4	15.9	15.65
10-11	-	9.1	9.1	6.9	7.8	7.35	5.3	6.2	5.75	12.3	-	12.3
11-12	-	17.8	17.8	8	7.8	7.9	9.2	7.8	8.5	20.3	-	20.3
12-13	-	15.5	15.5	7.9	8.4	8.15	10	9.2	9.6	27.7	-	27.7

13-14	-	14.7	14.7	9.3	8.8	9.05	9.4	9	9.2	-	-	-
14-15	-	18.3	18.3	11.1	9.6	10.35	8.8	8.8	8.8	-	-	-
15-16	-	14.6	14.6	8.2	12	10.1	-	9.1	9.1	-	-	-
16-17	-	10.5	10.5	8.4	8.5	8.45	7	8.3	7.65	-	-	-
17-18	-	10.3	10.3	9.1	8.6	8.85	6.9	8.2	7.55	-	-	-
18-19	-	11.1	11.1	8.8	8.2	8.5	5.2	-	5.2	-	-	-
19-20	-	8.6	8.6	8.2	8.1	8.15	6.2	-	6.2	-	-	-
20-21	-	7.4	7.4	9.9	-	9.9	4	-	4	-	-	-
21-22	-	7.5	7.5	-	-	-	-	-	-	-	-	-
22-23	-	4.8	4.8	-	-	-	-	-	-	-	-	-
23-24	-	6.1	6.1	-	-	-	-	-	-	-	-	-
24-25	-	4.2	4.2	-	-	-	-	-	-	-	-	-
25-26	-	3.4	3.4	-	-	-	-	-	-	-	-	-

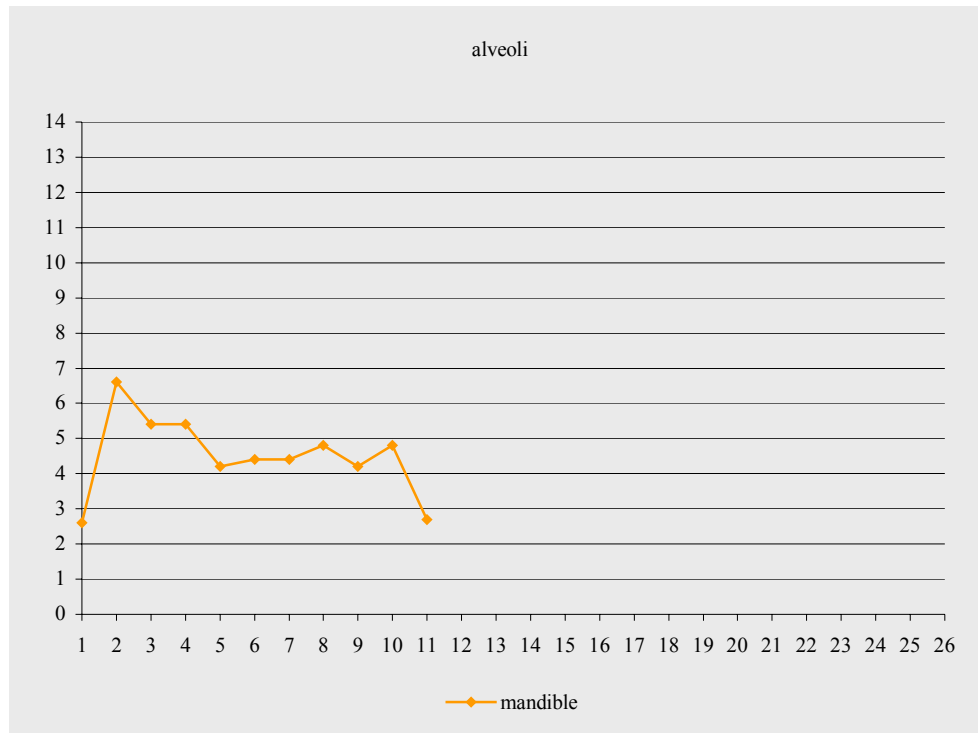
11.1.2. Individual graphs dentition taxon *Brasileodactylus*



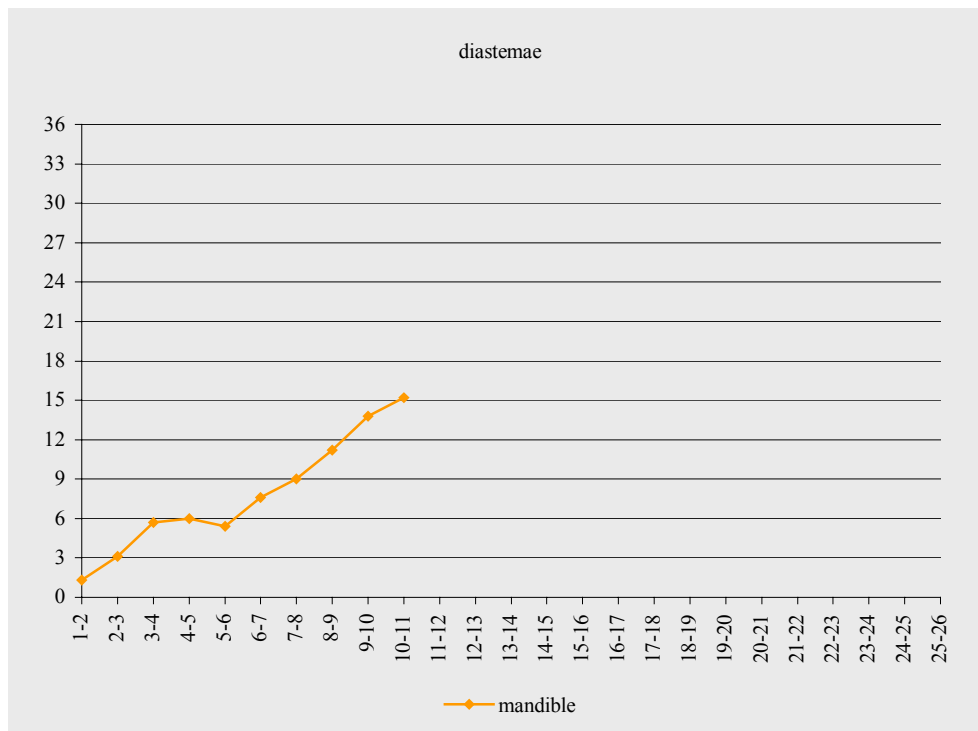
The graph of the alveolar diameter of the holotype of *B. araripensis* (MN 4804-V). Vertical the diameter in mm; horizontal the number of alveolus, starting anteriorly.



The graph of the size of the diastemae of the holotype of *B. araripensis* (MN 4804-V). Vertical the size in mm; horizontal the number of diastemae, starting anteriorly.



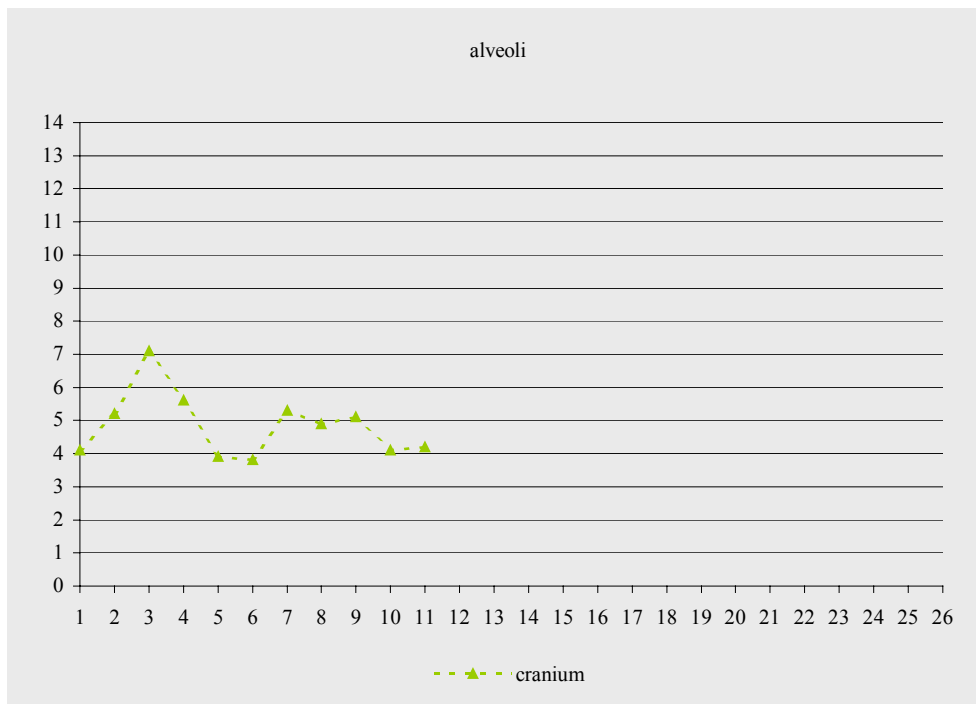
The graph of the alveolar diameter of the mandible of *B. araripensis* (SMNS 55414). Vertical the diameter in mm; horizontal the number of alveolus, starting anteriorly.



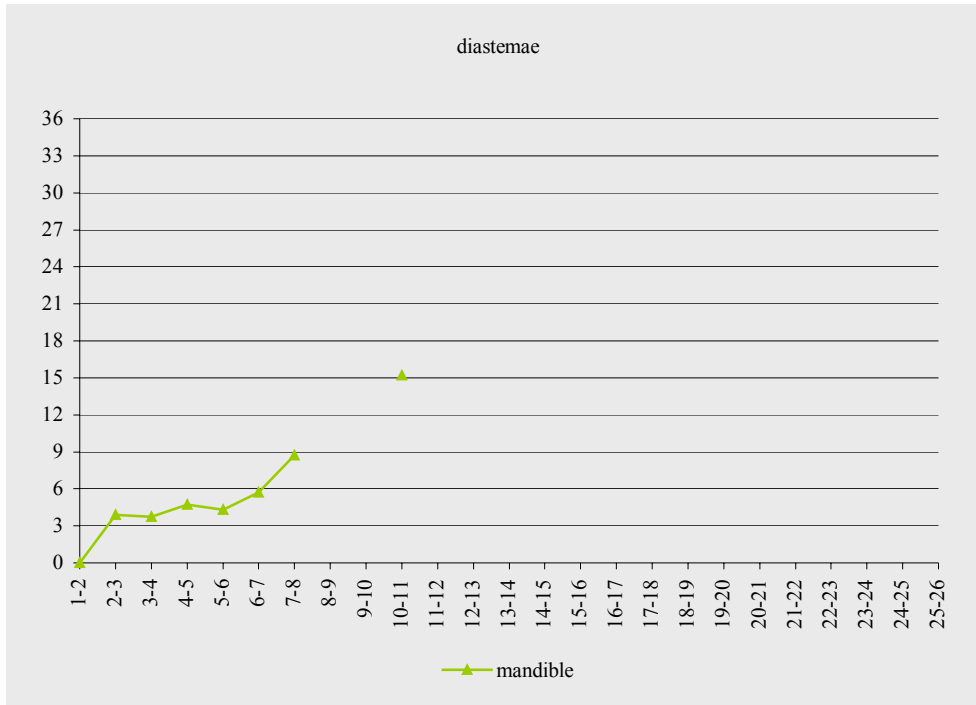
The graph of the size of the diastemae of the mandible of *B. araripensis* (SMNS 55414). Vertical the size in mm; horizontal the number of diastemae, starting anteriorly.



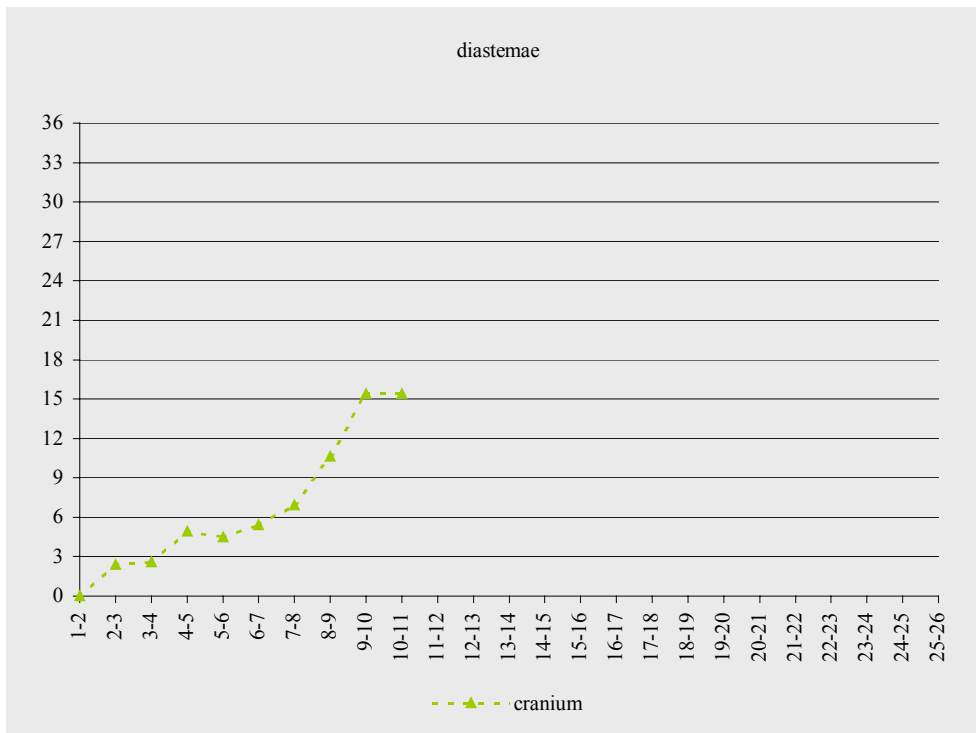
The graph of the alveolar diameter of the mandible of *B. cf. araripensis* (MN 4797-V). Vertical the diameter in mm; horizontal the number of alveolus, starting anteriorly.



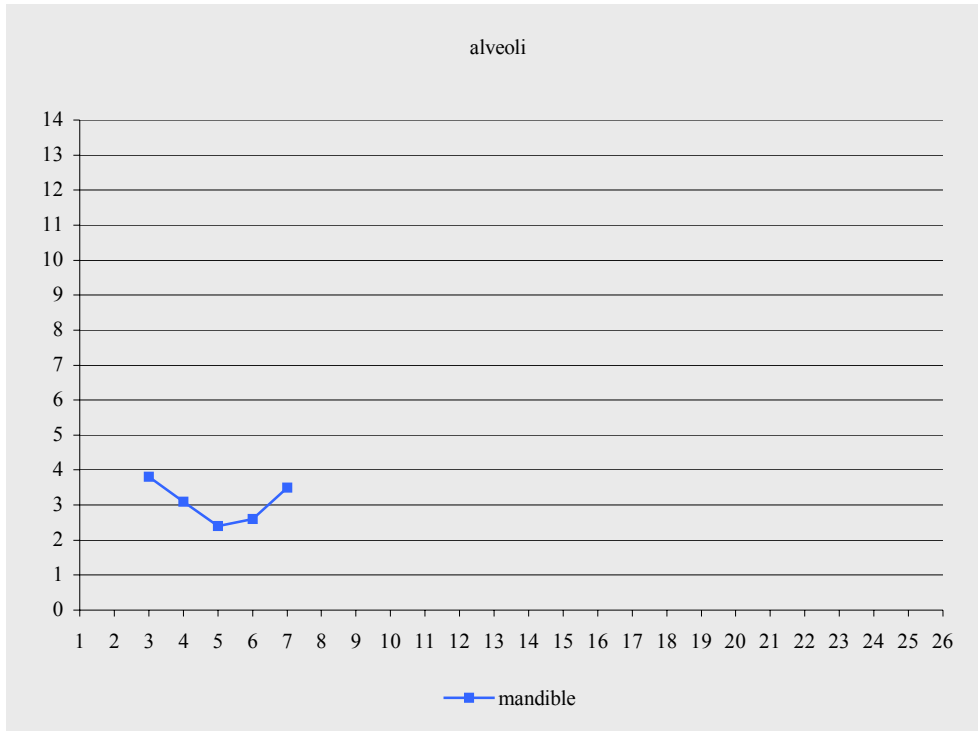
The graph of the alveolar diameter of the cranium of *B. cf. araripensis* (MN 4797-V). Vertical the diameter in mm; horizontal the number of alveolus, starting anteriorly.



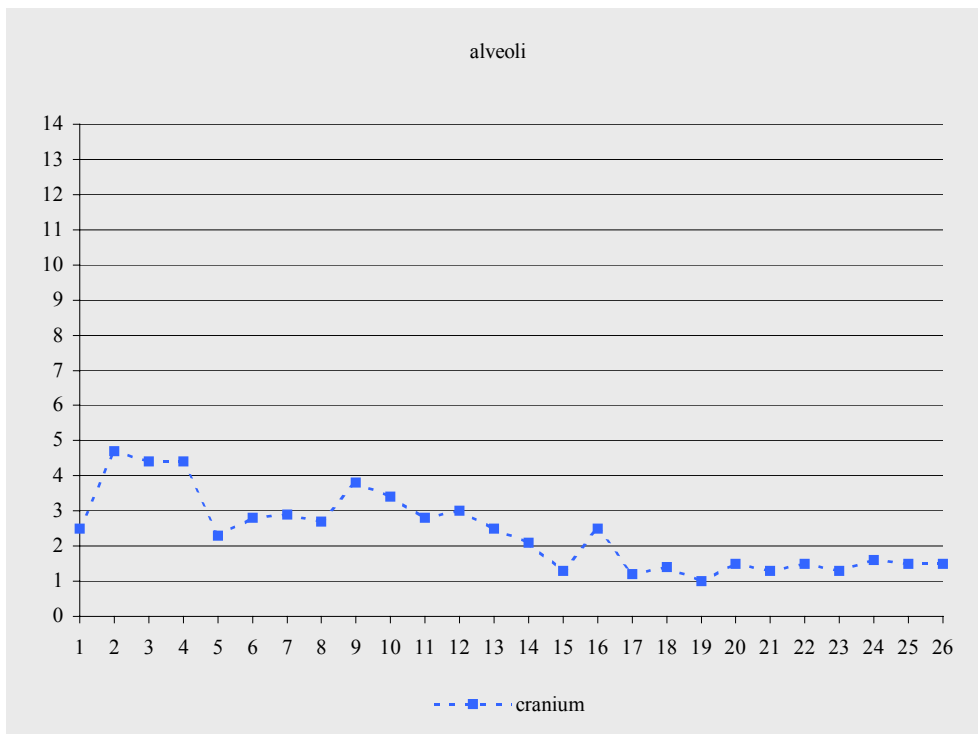
The graph of the size of the diastemae of the mandible of *cf. B. araripensis* (MN 4797-V). Vertical the size in mm; horizontal the number of diastemae, starting anteriorly.



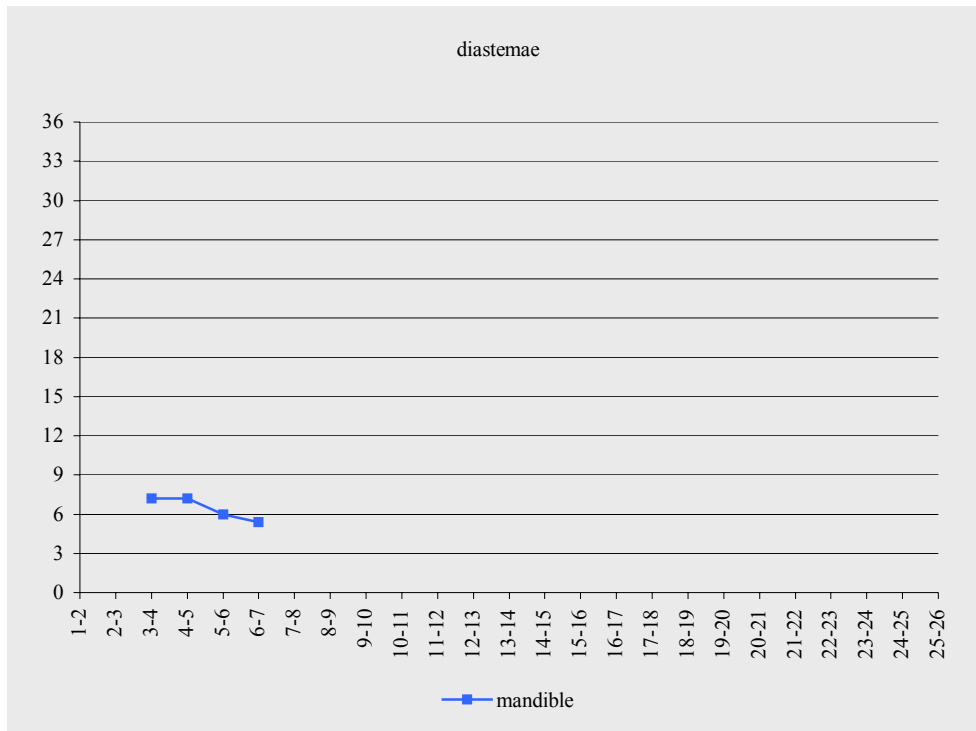
The graph of the size of the diastemae of the cranium of *cf. B. araripensis* (MN 4797-V). Vertical the size in mm; horizontal the number of diastemae, starting anteriorly.



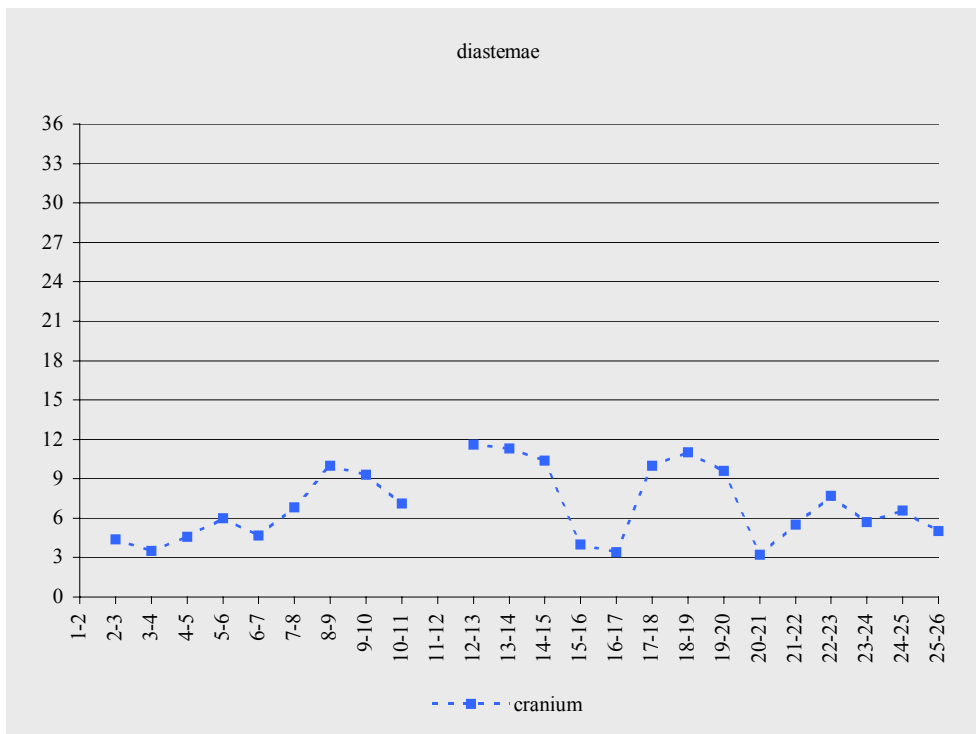
The graph of the alveolar diameter of the mandible of *Brasileodactylus sp. indet.* (AMNH 24444). Vertical the diameter in mm; horizontal the number of alveolus, starting anteriorly.



The graph of the alveolar diameter of the cranium of *Brasileodactylus sp. indet.* (AMNH 24444). Vertical the diameter in mm; horizontal the number of alveolus, starting anteriorly.

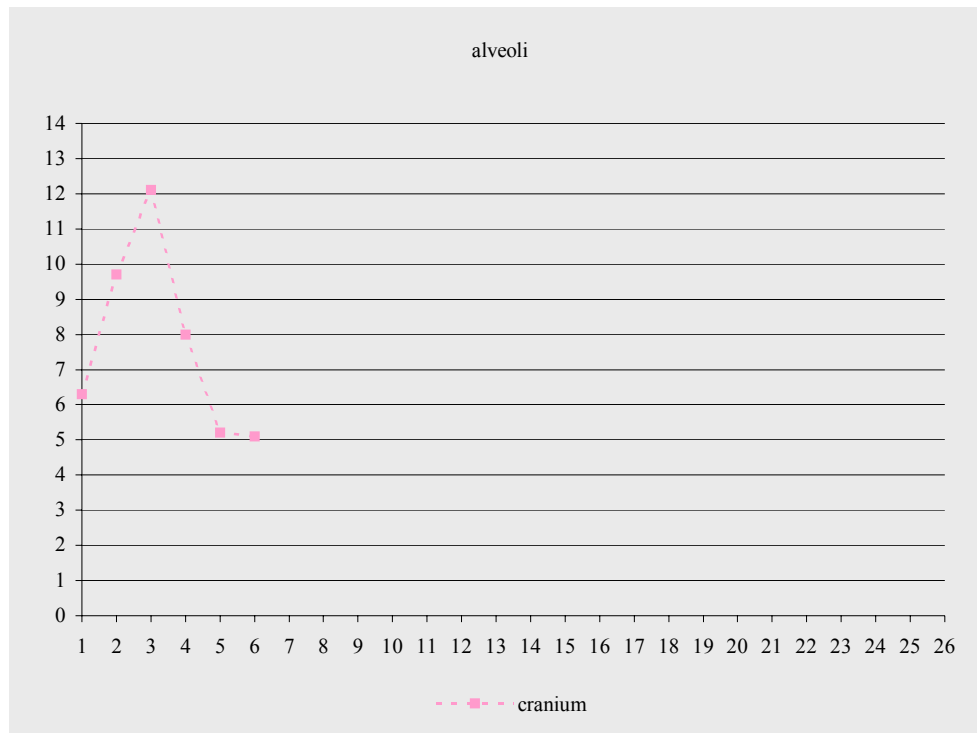


The graph of the size of the diastemae of the mandible of *Brasileodactylus sp. indet.* (AMNH 24444). Vertical the size in mm; horizontal the number of diastemae, starting anteriorly.

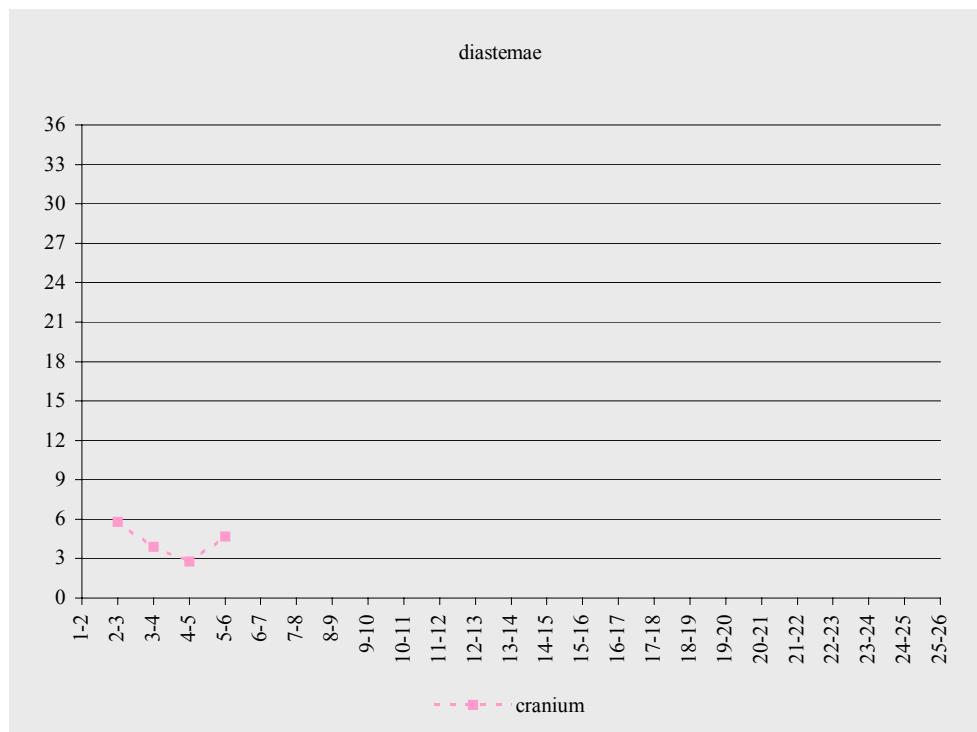


The graph of the size of the diastemae of the cranium of *Brasileodactylus sp. indet.* (AMNH 24444). Vertical the size in mm; horizontal the number of diastemae, starting anteriorly.

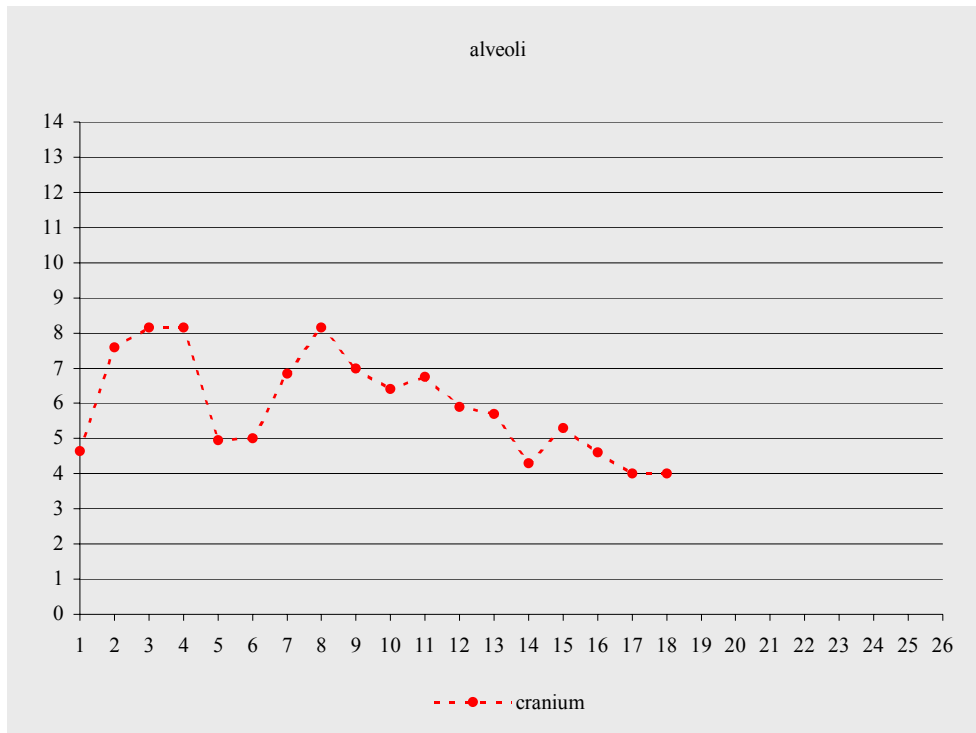
11.1.3. Individual graphs dentition taxon *Coloborhynchus*



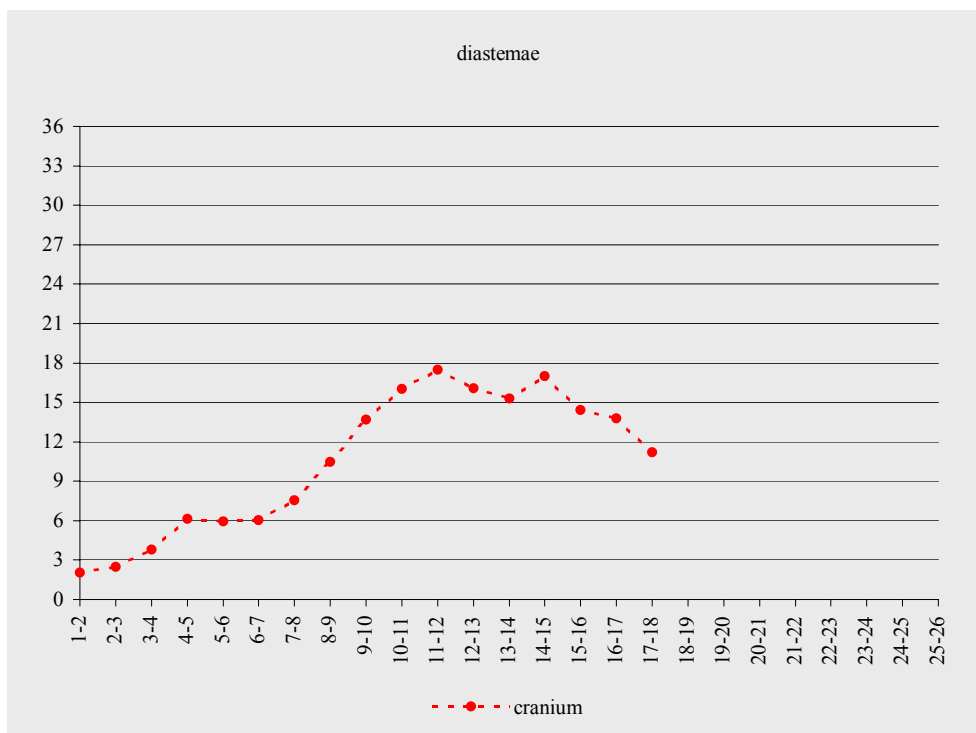
The graph of the alveolar diameter of the cranium of *Co. clavirostris* (BMNH 1822). Vertical the diameter in mm; horizontal the number of alveolus, starting anteriorly.



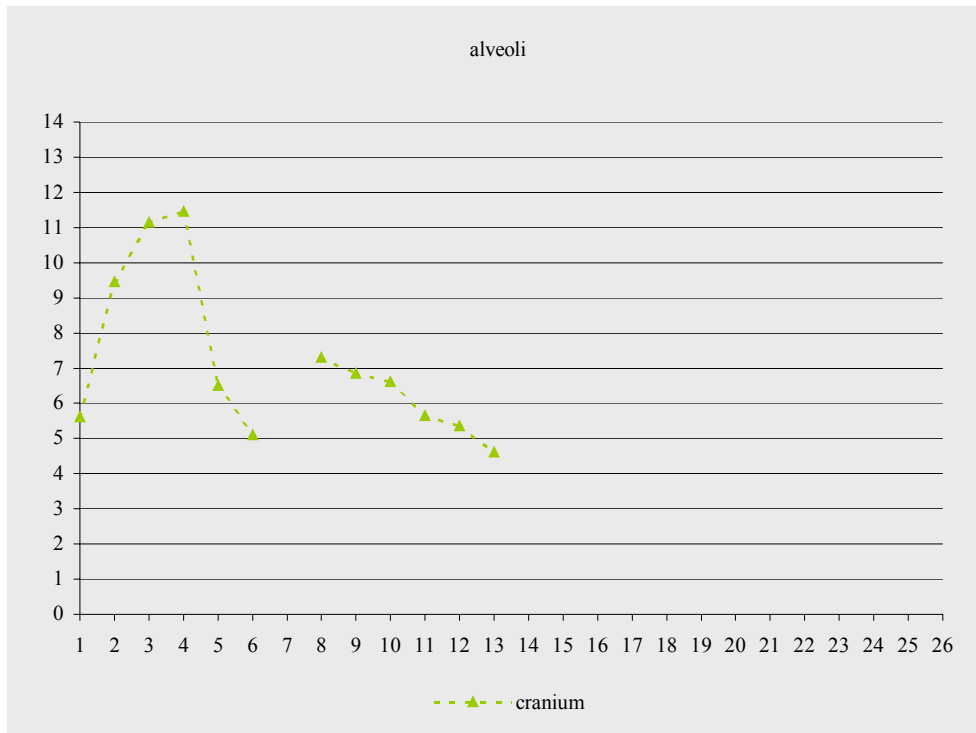
The graph of the size of the diastemae of the cranium of *Co. clavirostris* (BMNH 1822). Vertical the size in mm; horizontal the number of diastemae, starting anteriorly.



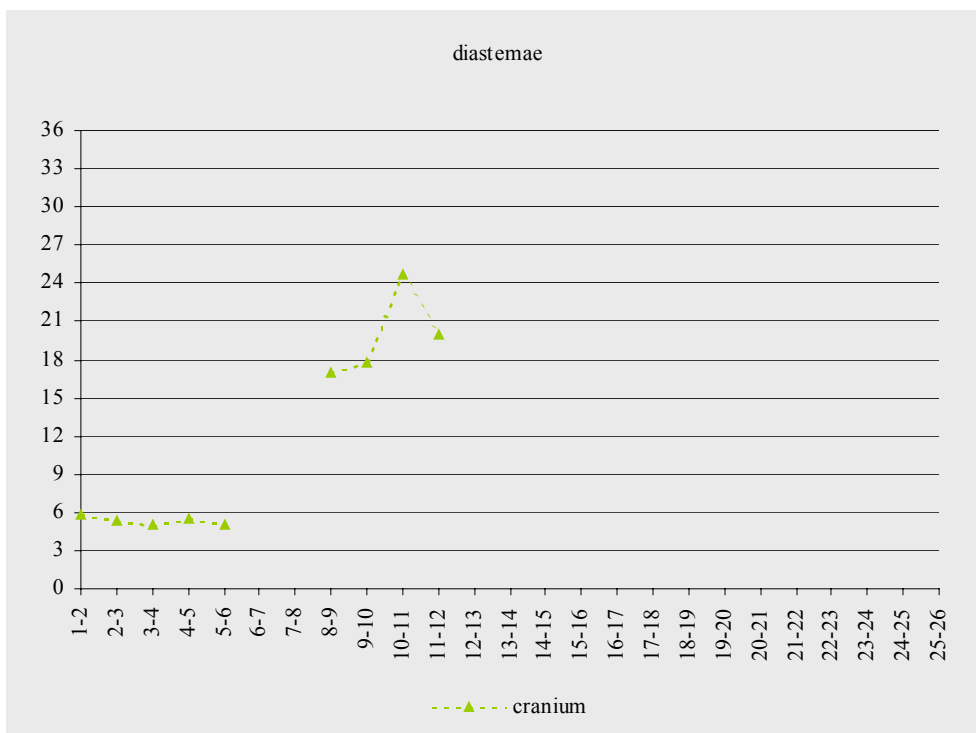
The graph of the alveolar diameter of the cranium of *Co. araripensis* (SAO 16494). Vertical the diameter in mm; horizontal the number of alveolus, starting anteriorly.



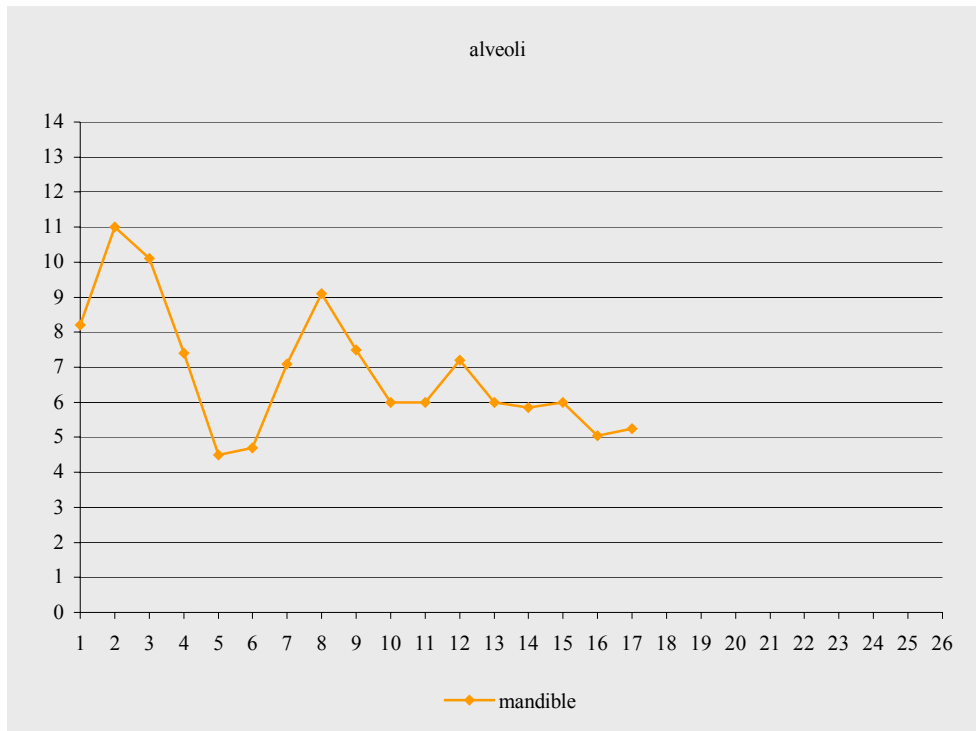
The graph of the size of the diastemae of the cranium of *Co. araripensis* (SAO 16494). Vertical the size in mm; horizontal the number of diastemae, starting anteriorly.



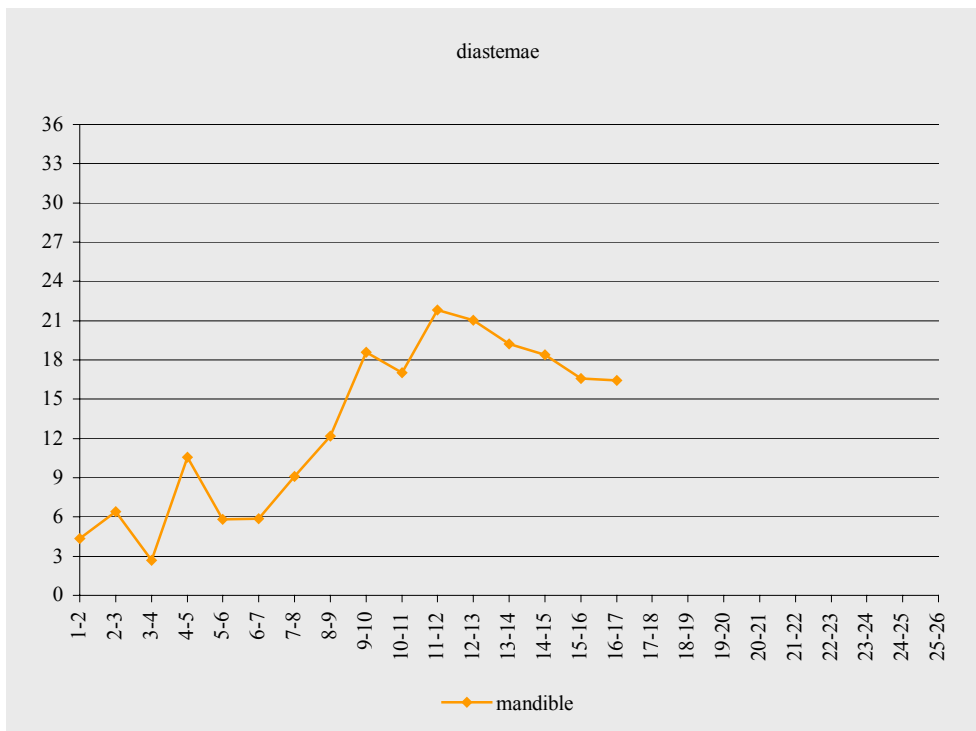
The graph of the alveolar diameter of the cranium of *Co. araripensis* (MN 4735-V). Vertical the diameter in mm; horizontal the number of alveolus, starting anteriorly.



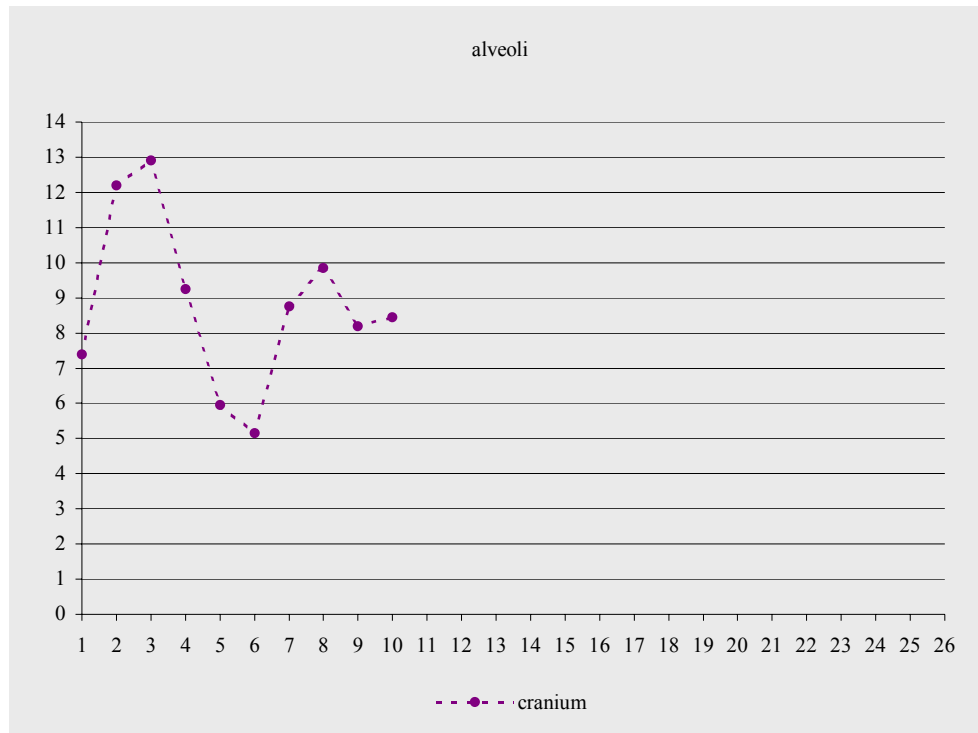
The graph of the size of the diastemae of the cranium of *Co. araripensis* (MN 4735-V). Vertical the size in mm; horizontal the number of diastemae, starting anteriorly.



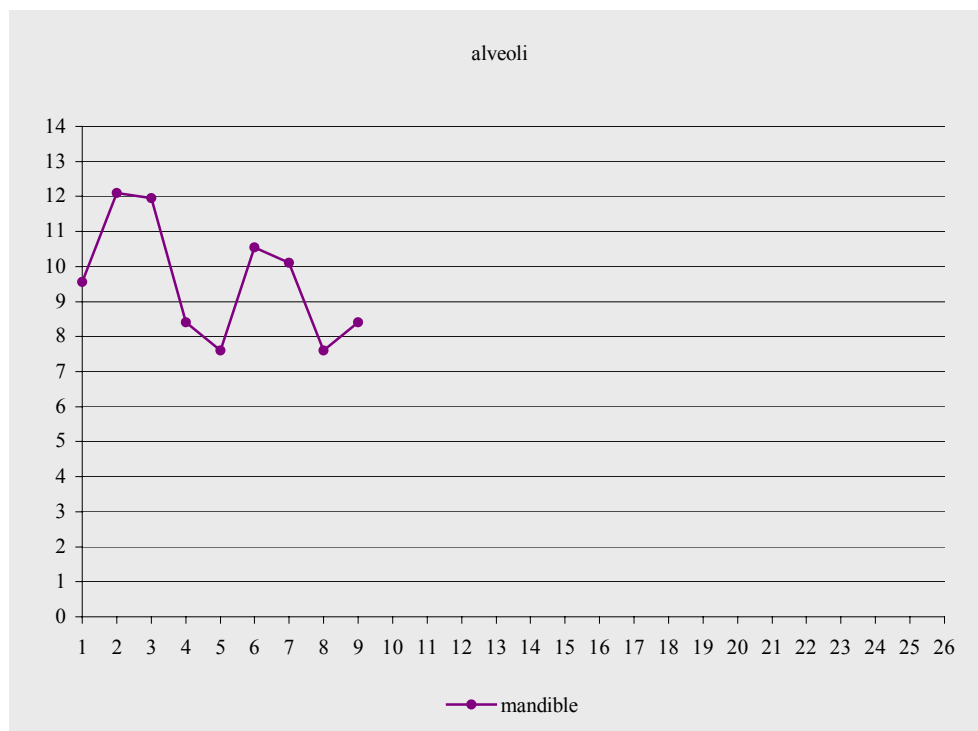
The graph of the alveolar diameter of the mandible of *Co. robustus* (BSP 1987 I 47). Vertical the diameter in mm; horizontal the number of alveolus, starting anteriorly.



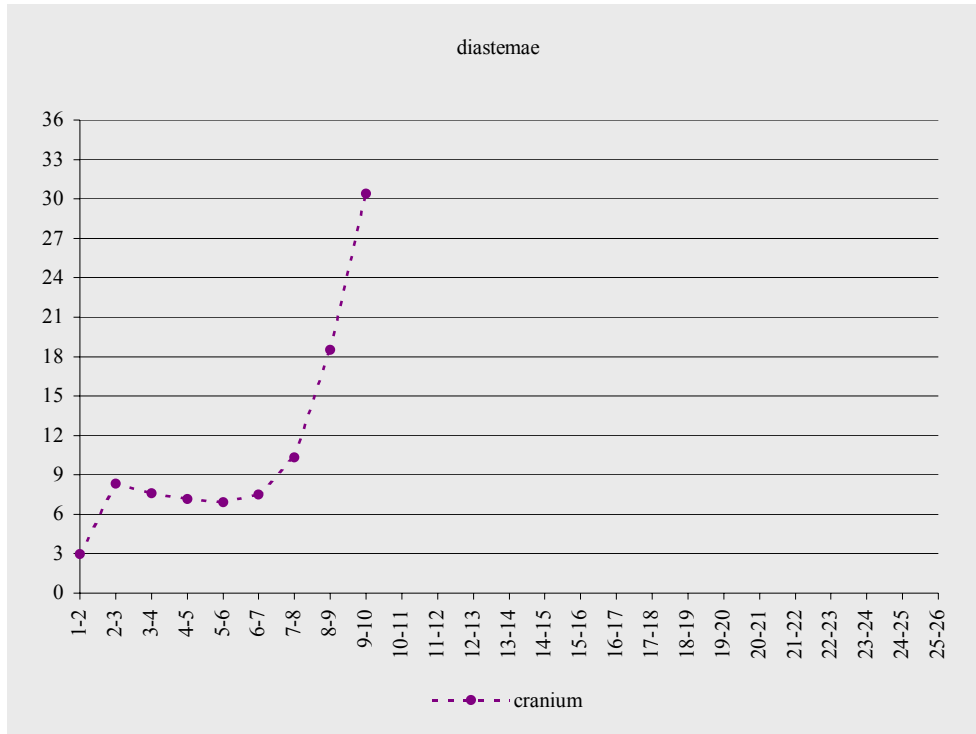
The graph of the size of the diastemae of the mandible of *Co. robustus* (BSP 1987 I 47). Vertical the size in mm; horizontal the number of diastemae, starting anteriorly.



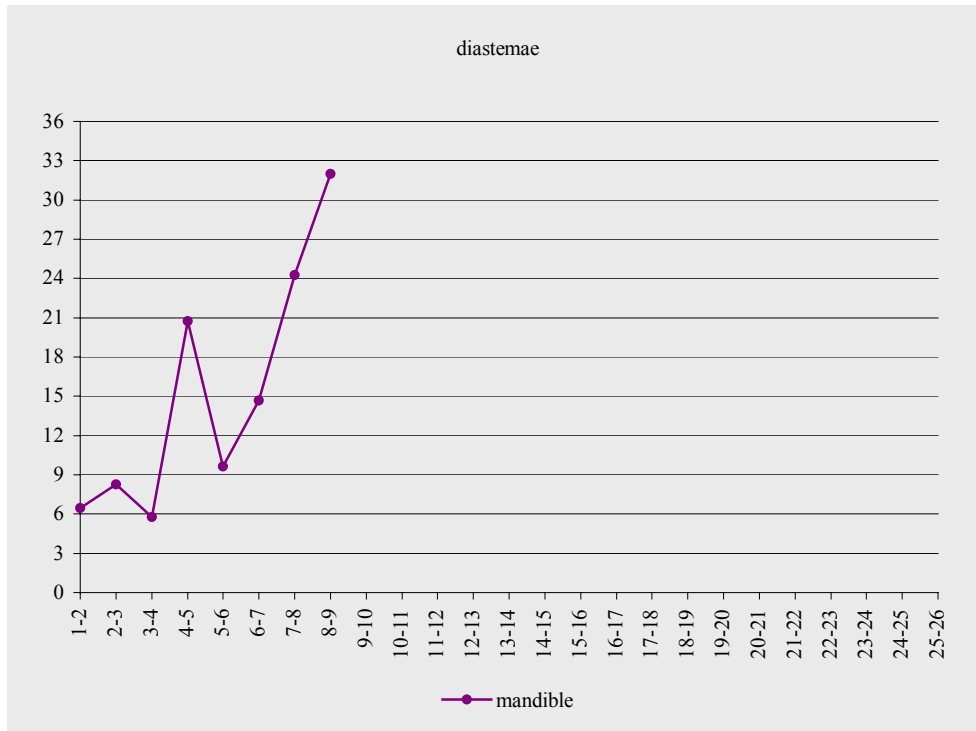
The graph of the alveolar diameter of the cranium of *Co. robustus* (SMNK 2302 PAL). Vertical the diameter in mm; horizontal the number of alveolus, starting anteriorly.



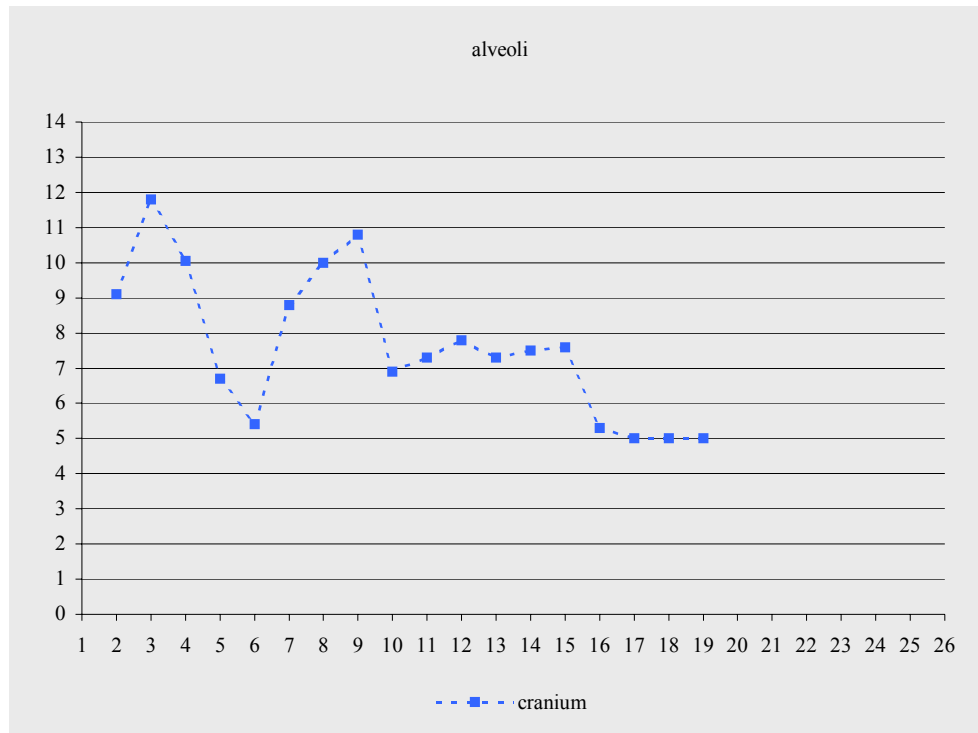
The graph of the alveolar diameter of the mandible of *Co. robustus* (SMNK 2302 PAL). Vertical the diameter in mm; horizontal the number of alveolus, starting anteriorly.



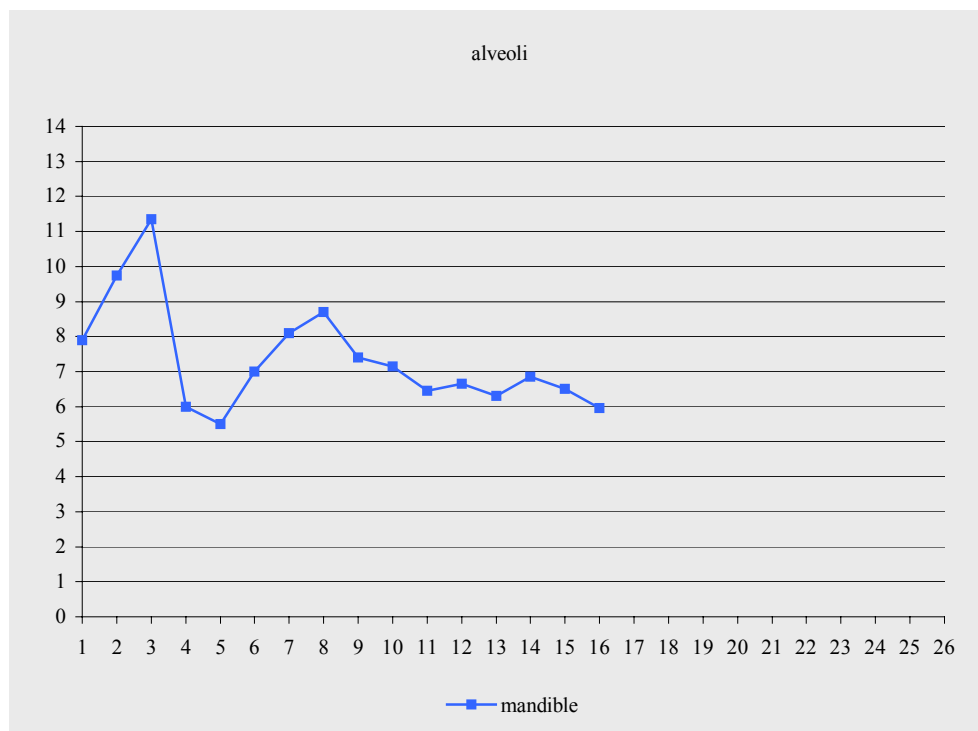
The graph of the size of the diastemae of the cranium of *Co. robustus* (SMNK 2302 PAL). Vertical the size in mm; horizontal the number of diastemae, starting anteriorly.



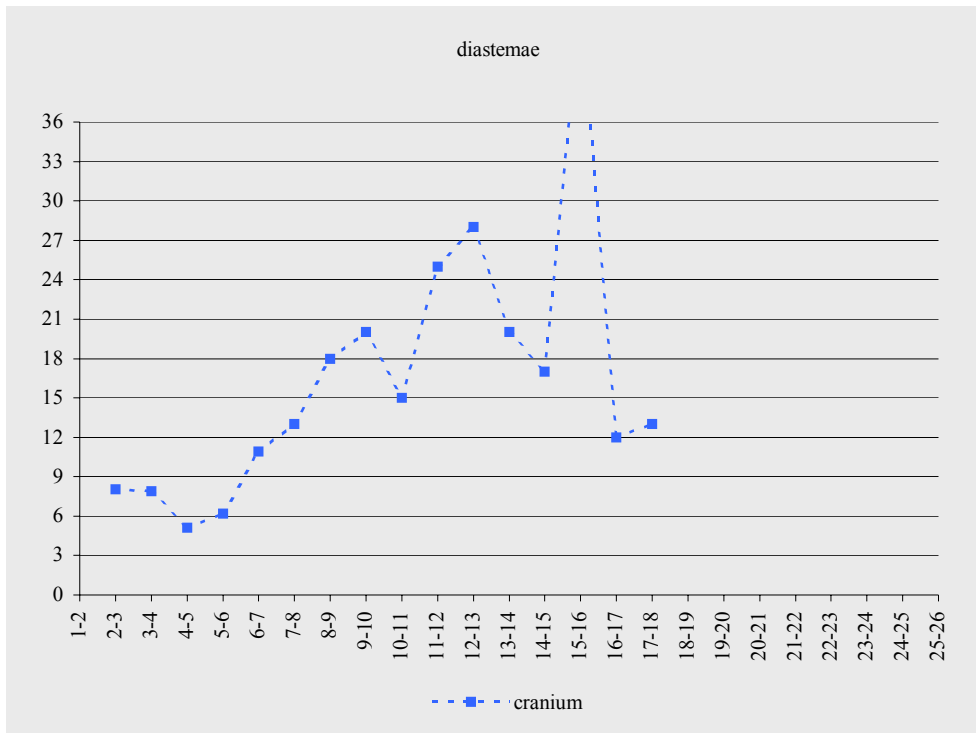
The graph of the size of the diastemae of the mandible of *Co. robustus* (SMNK 2302 PAL). Vertical the size in mm; horizontal the number of diastemae, starting anteriorly.



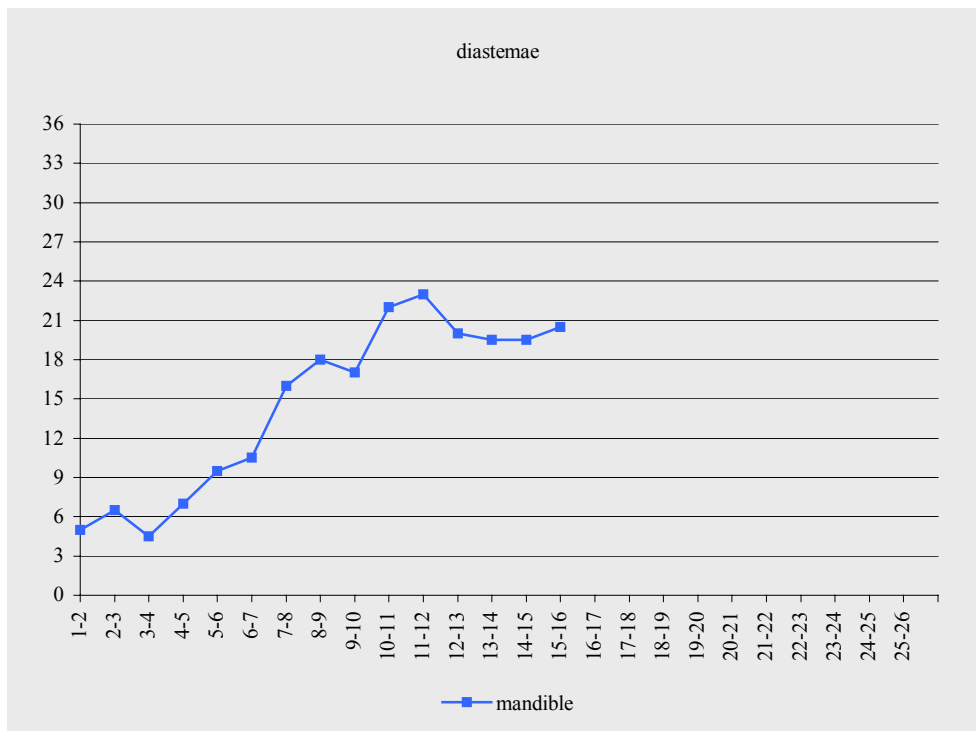
The graph of the alveolar diameter of the cranium of *Co. spielbergi* (RGM 401 880). Vertical the diameter in mm; horizontal the number of alveolus, starting anteriorly.



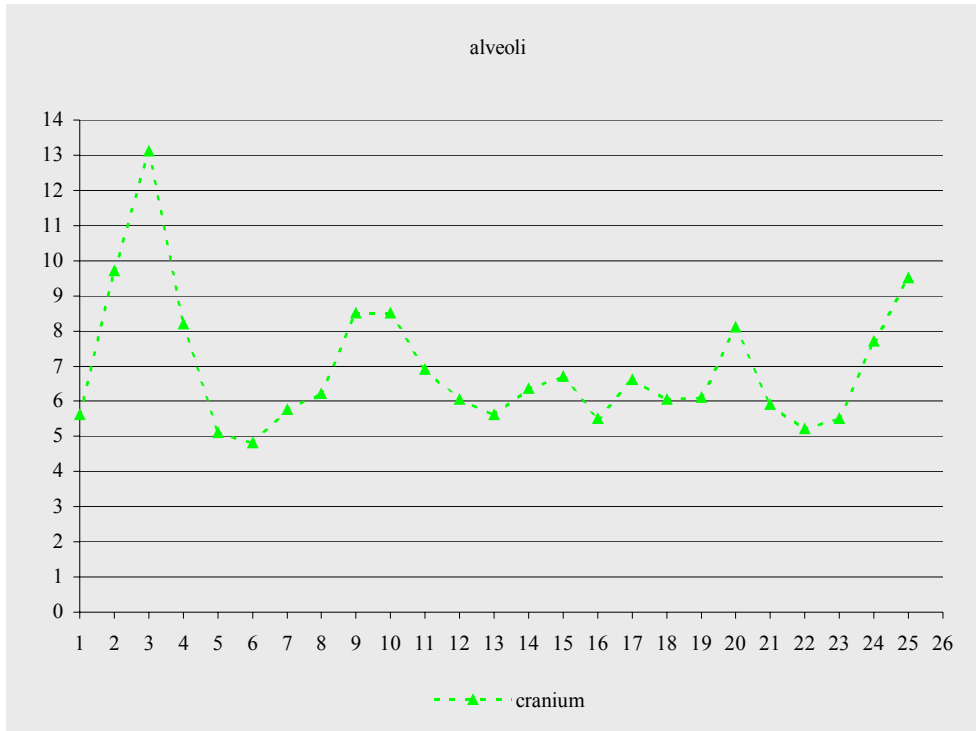
The graph of the alveolar diameter of the mandible of *Co. spielbergi* (RGM 401 880). Vertical the diameter in mm; horizontal the number of alveolus, starting anteriorly.



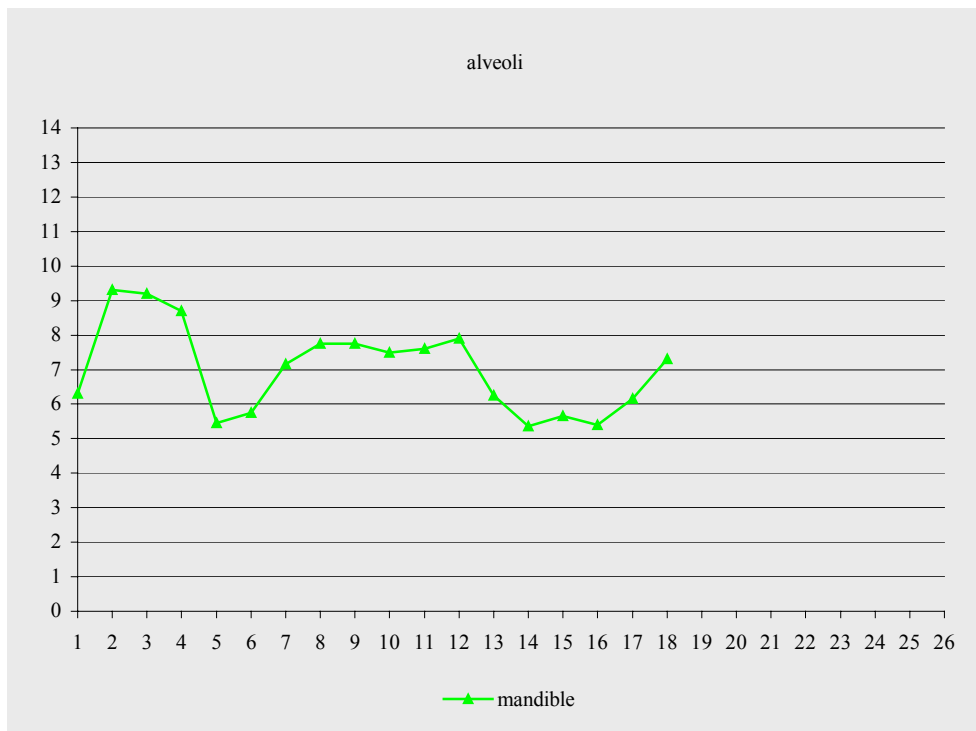
The graph of the size of the diastemae of the cranium of *Co. spielbergi* (RGM 401 880). Vertical the size in mm; horizontal the number of diastemae, starting anteriorly.



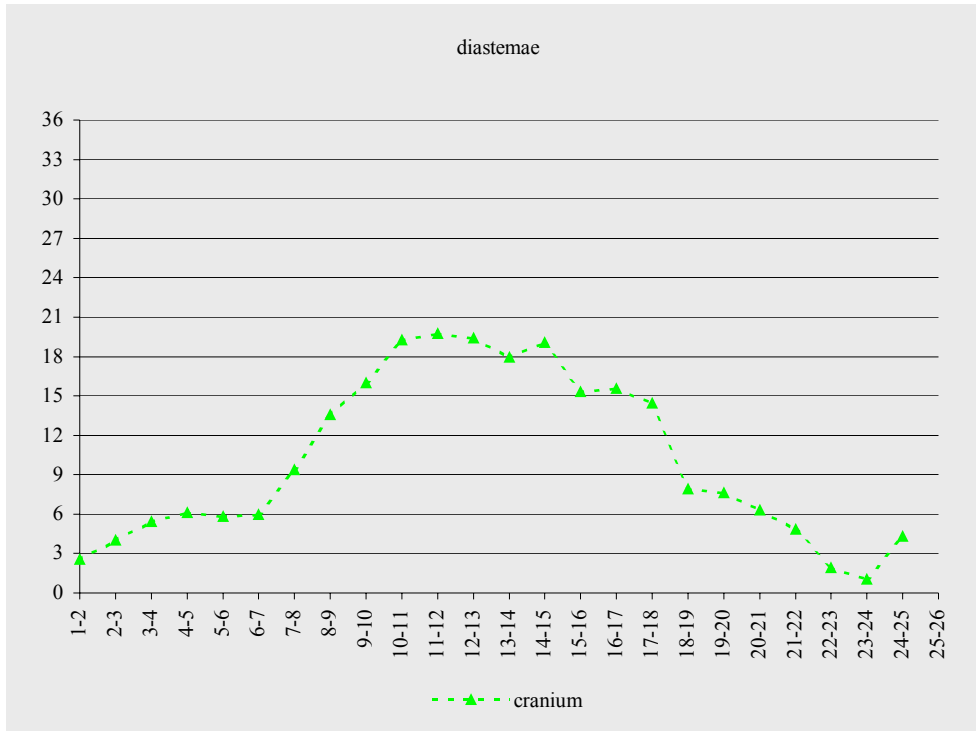
The graph of the size of the diastemae of the mandible of *Co. spielbergi* (RGM 401 880). Vertical the size in mm; horizontal the number of diastemae, starting anteriorly.



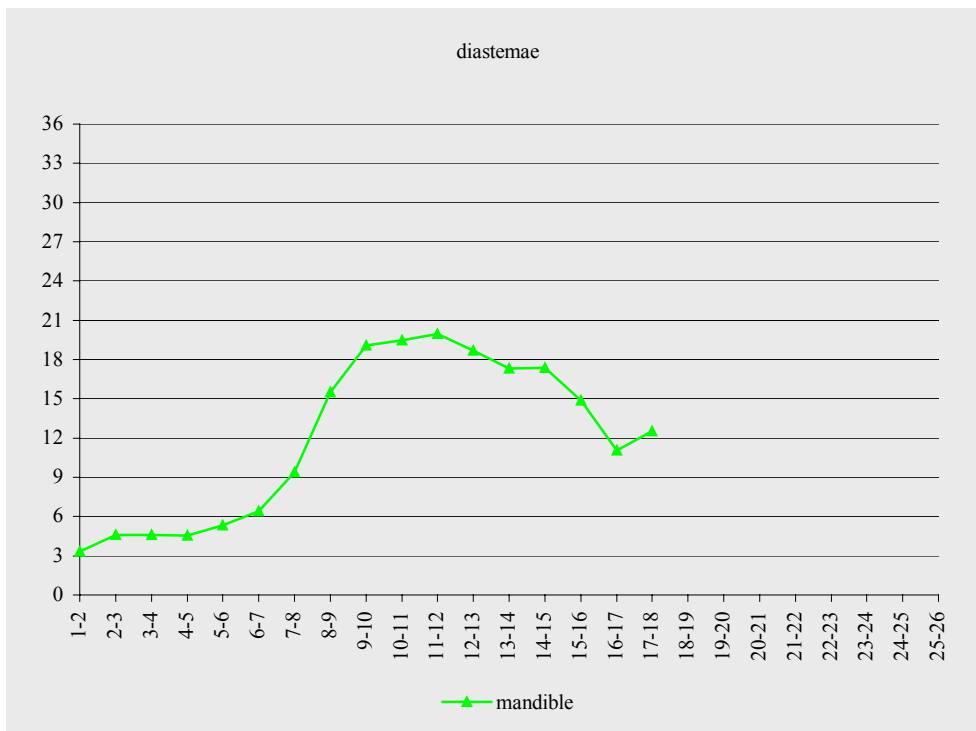
The graph of the alveolar diameter of the cranium of *Co. piscator* (NSM PV-19892). Vertical the diameter in mm; horizontal the number of alveolus, starting anteriorly.



The graph of the alveolar diameter of the mandible of *Co. piscator* (NSM PV-19892). Vertical the diameter in mm; horizontal the number of alveolus, starting anteriorly.

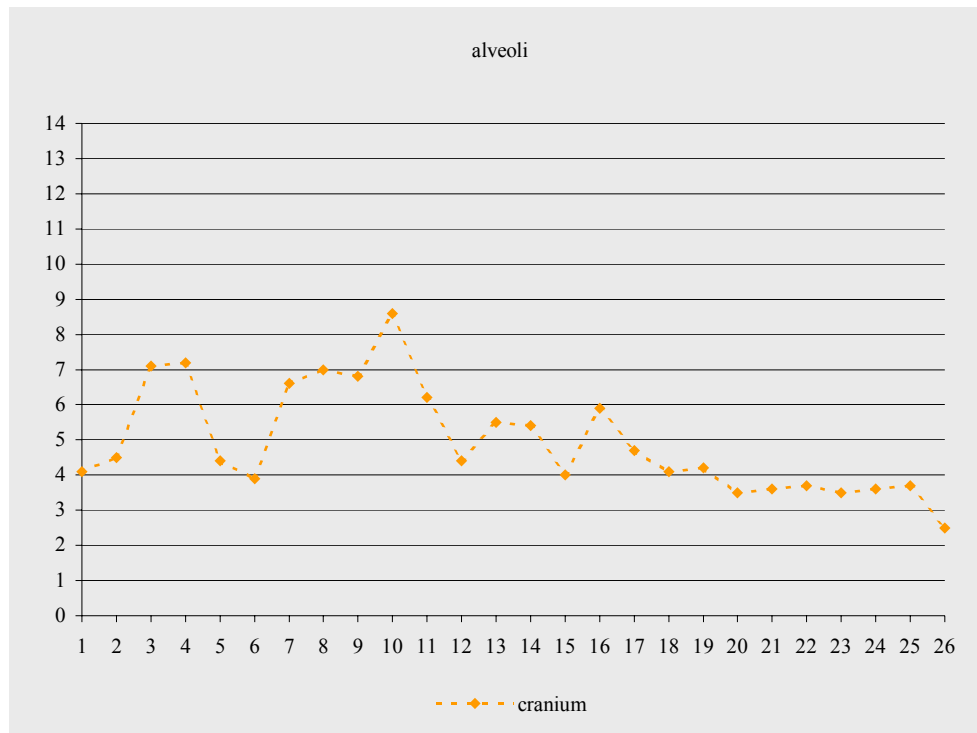


The graph of the size of the diastemae of the cranium of *Co. piscator* (NSM PV-19892). Vertical the size in mm; horizontal the number of diastemae, starting anteriorly.

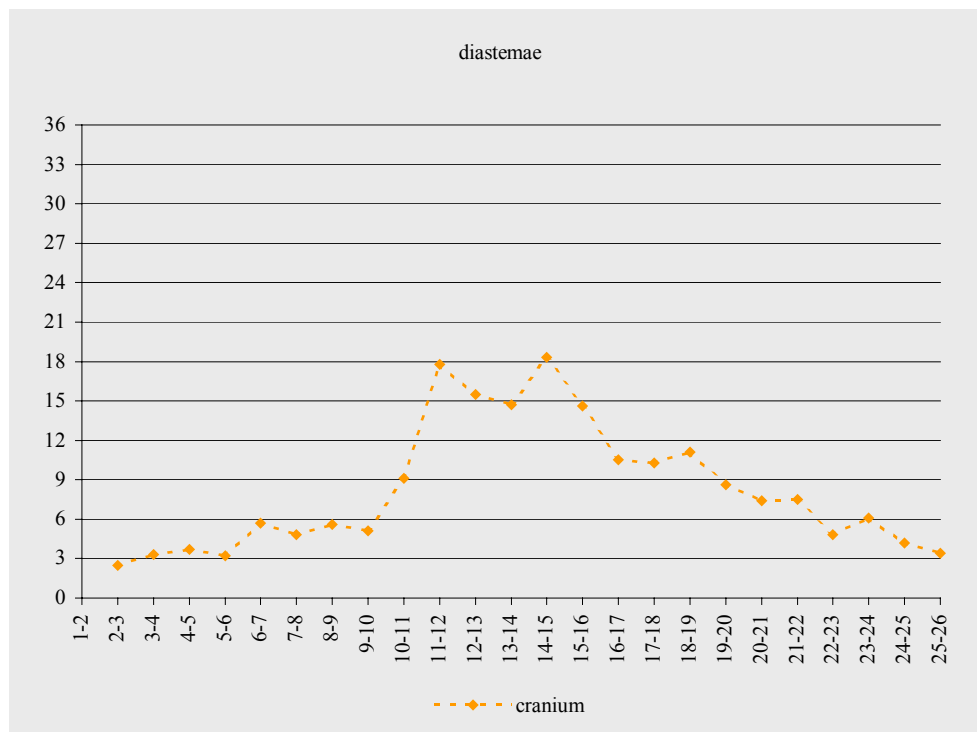


The graph of the size of the diastemae of the mandible of *Co. piscator* (NSM PV-19892). Vertical the size in mm; horizontal the number of diastemae, starting anteriorly.

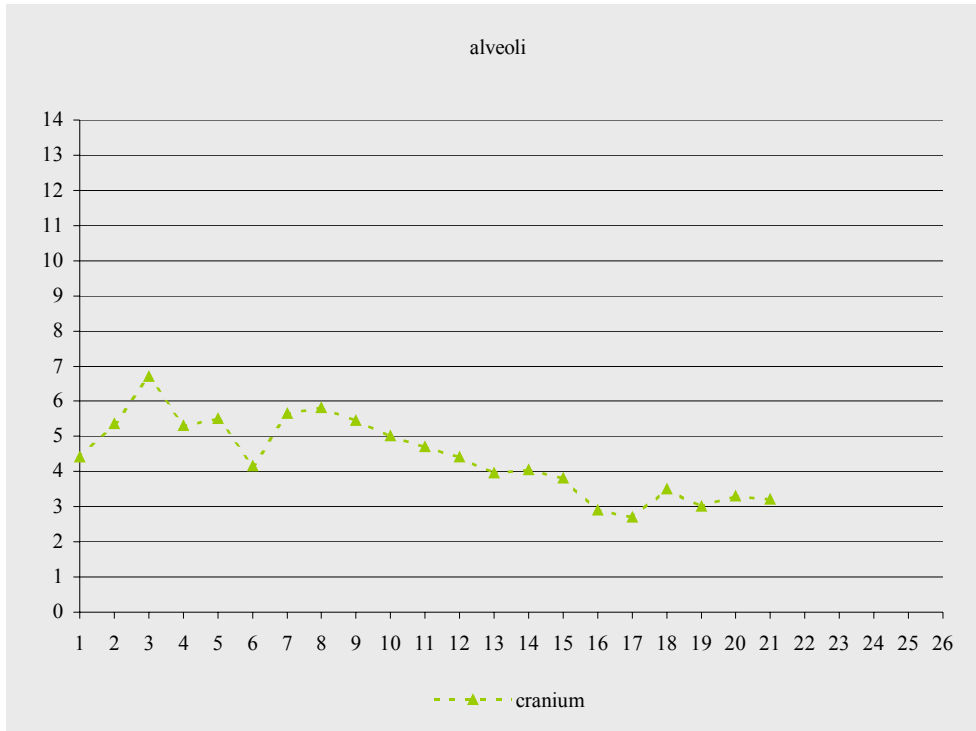
11.1.4. Individual graphs dentition taxon *Anhanguera*



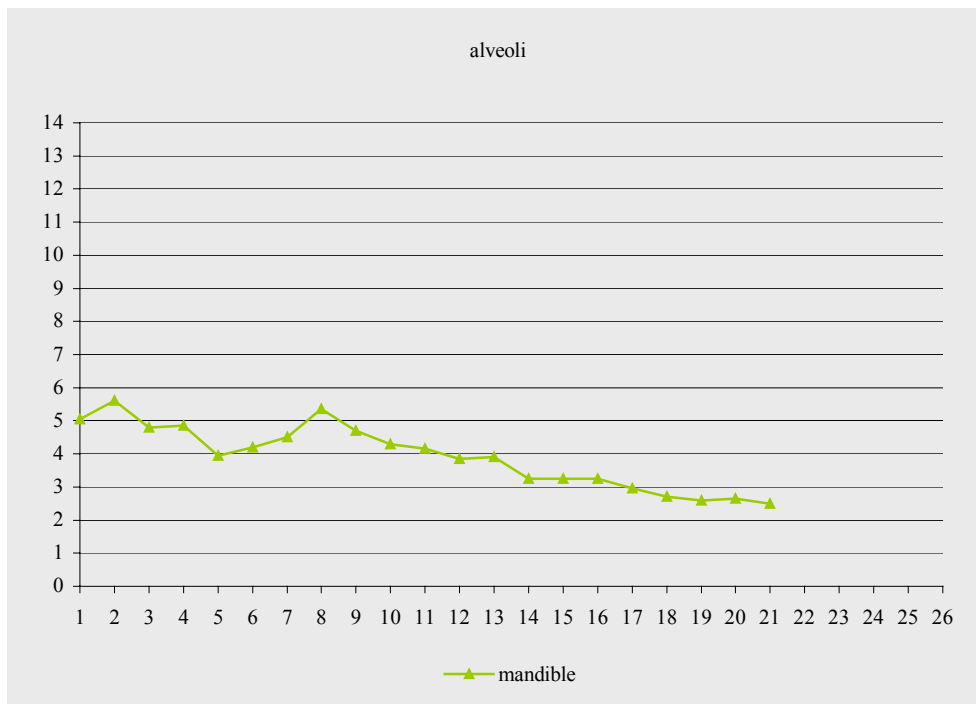
The graph of the alveolar diameter of the cranium of *An. blittersdorffi* (MN 4805-V). Vertical the diameter in mm; horizontal the number of alveolus, starting anteriorly.



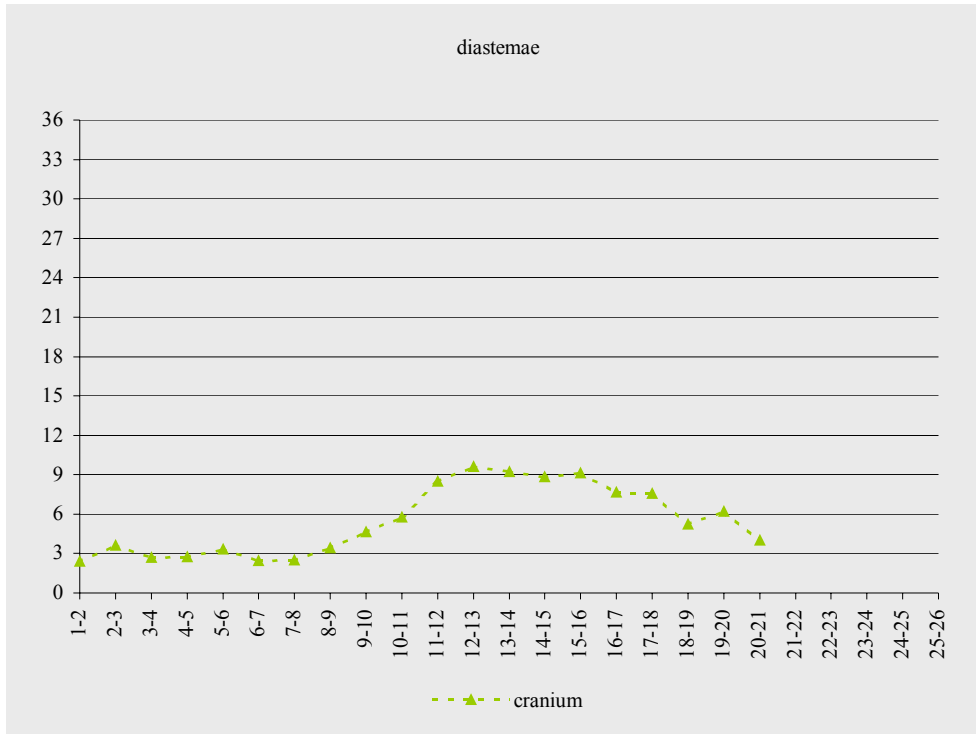
The graph of the size of the diastemae of the cranium of *An. blittersdorffi* (MN 4805-V). Vertical the size in mm; horizontal the number of diastemae, starting anteriorly.



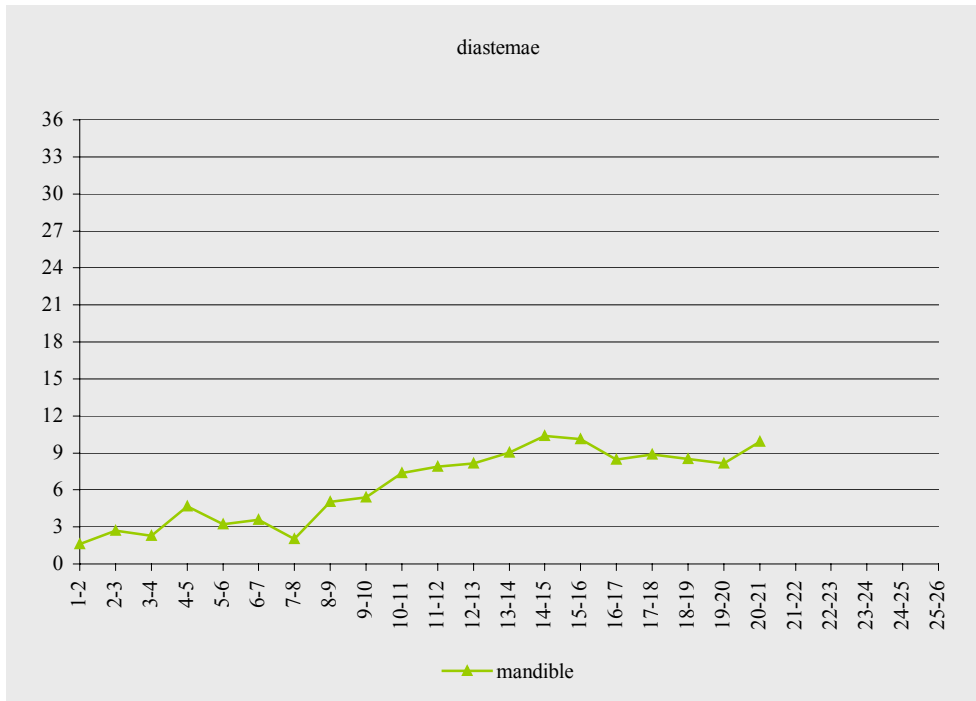
The graph of the alveolar diameter of the cranium of *An. blittersdorffi* (n. 40 Pz-DBAV-UERJ). Vertical the diameter in mm; horizontal the number of alveolus, starting anteriorly.



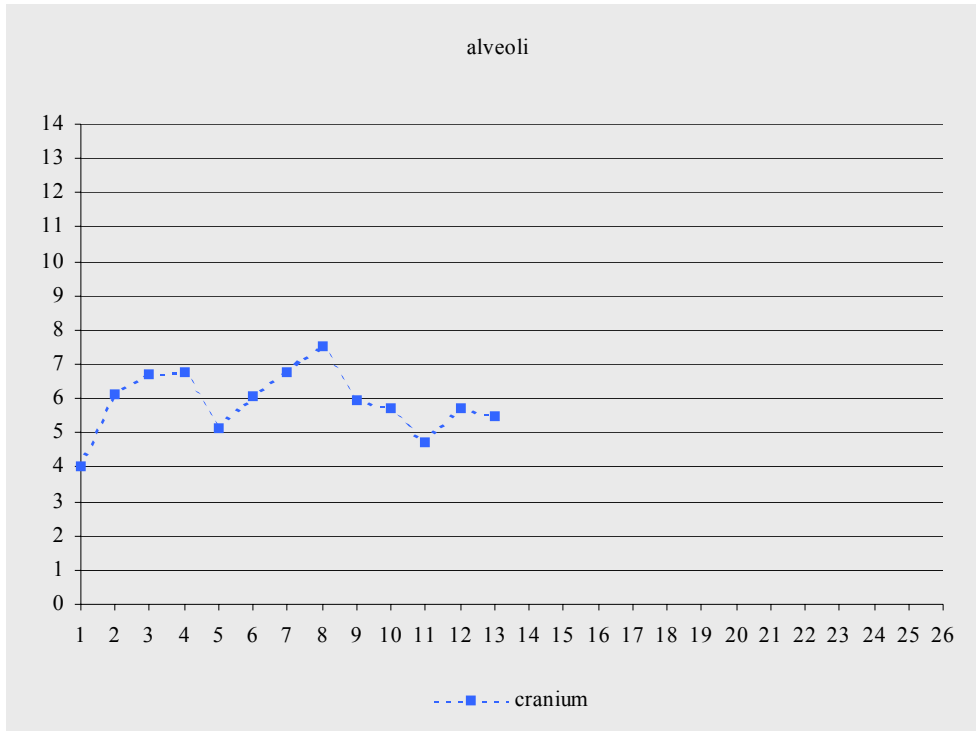
The graph of the alveolar diameter of the mandible of *An. blittersdorffi* (n. 40 Pz-DBAV-UERJ). Vertical the diameter in mm; horizontal the number of alveolus, starting anteriorly.



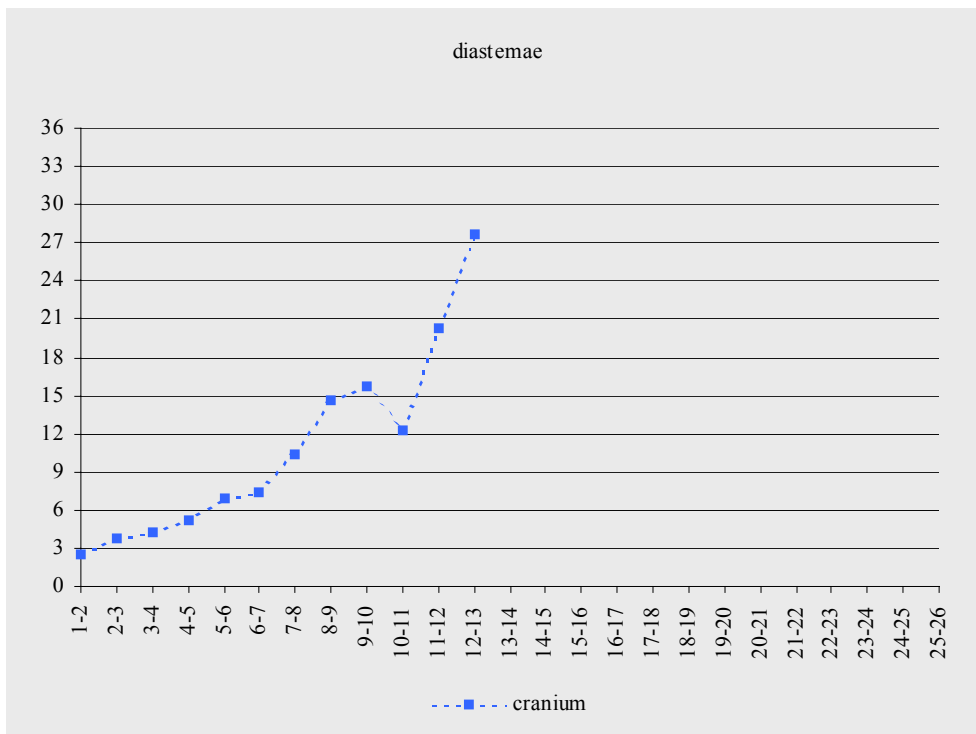
The graph of the size of the diastemae of the cranium of *An. blittersdorffi* (n. 40 Pz-DBAV-UERJ). Vertical the size in mm; horizontal the number of diastemae, starting anteriorly.



The graph of the size of the diastemae of the mandible of *An. blittersdorffi* (n. 40 Pz-DBAV-UERJ). Vertical the size in mm; horizontal the number of diastemae, starting anteriorly.

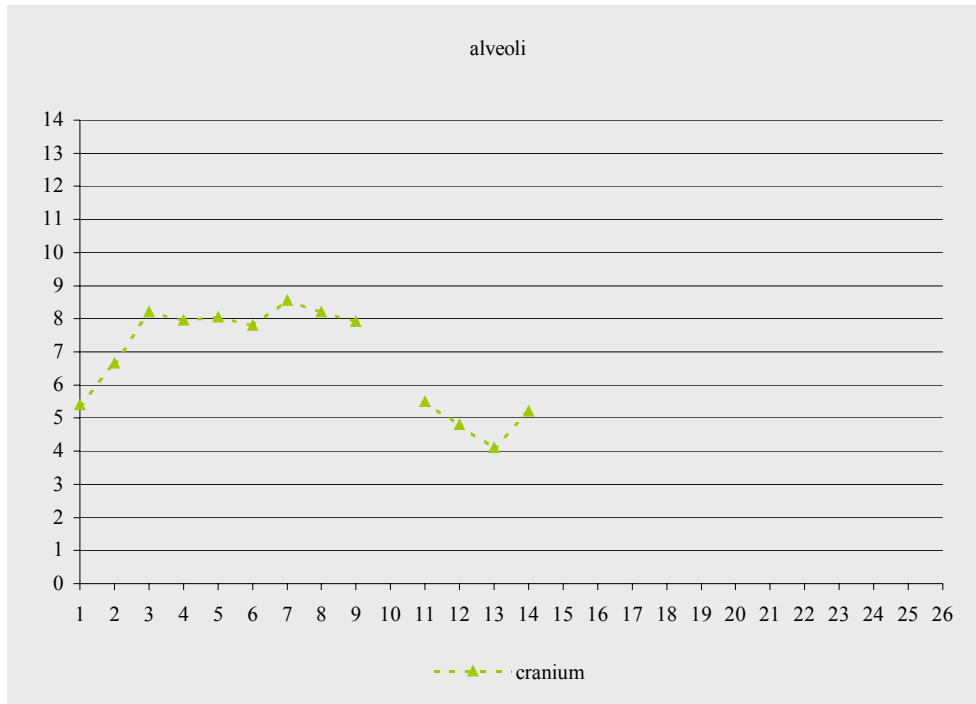


The graph of the alveolar diameter of the cranium of *An. santanae* (AMNH 22555). Vertical the diameter in mm; horizontal the number of alveolus, starting anteriorly.



The graph of the size of the diastemae of the cranium of *An. santanae* (AMNH 22555). Vertical the size in mm; horizontal the number of diastemae, starting anteriorly.

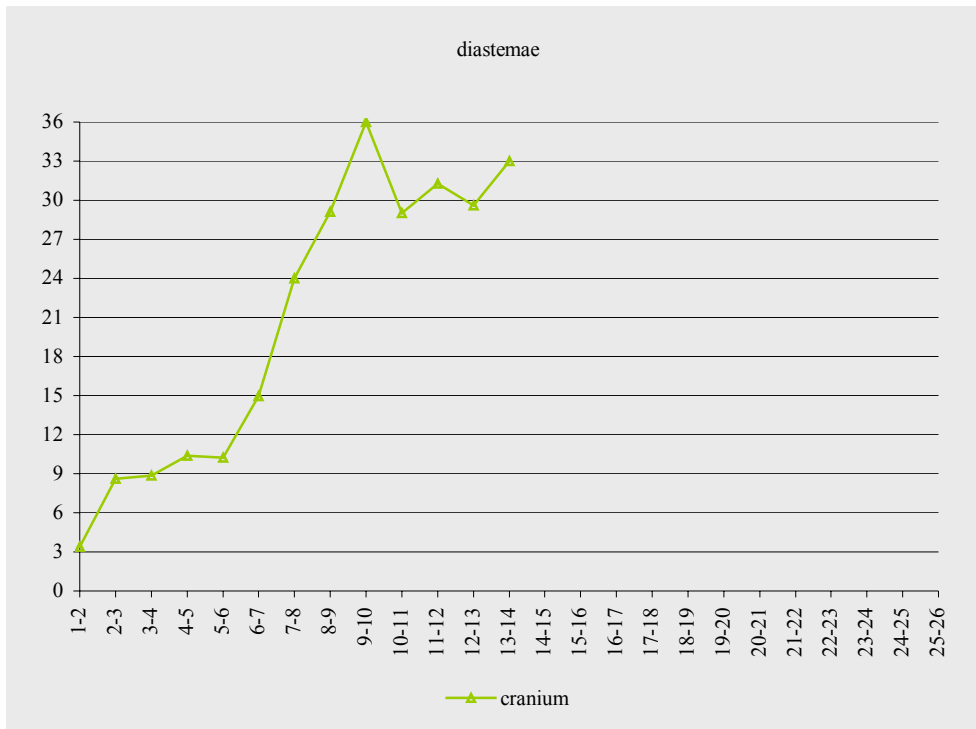
11.1.5. Individual graphs dentition taxon *Criorhynchus*



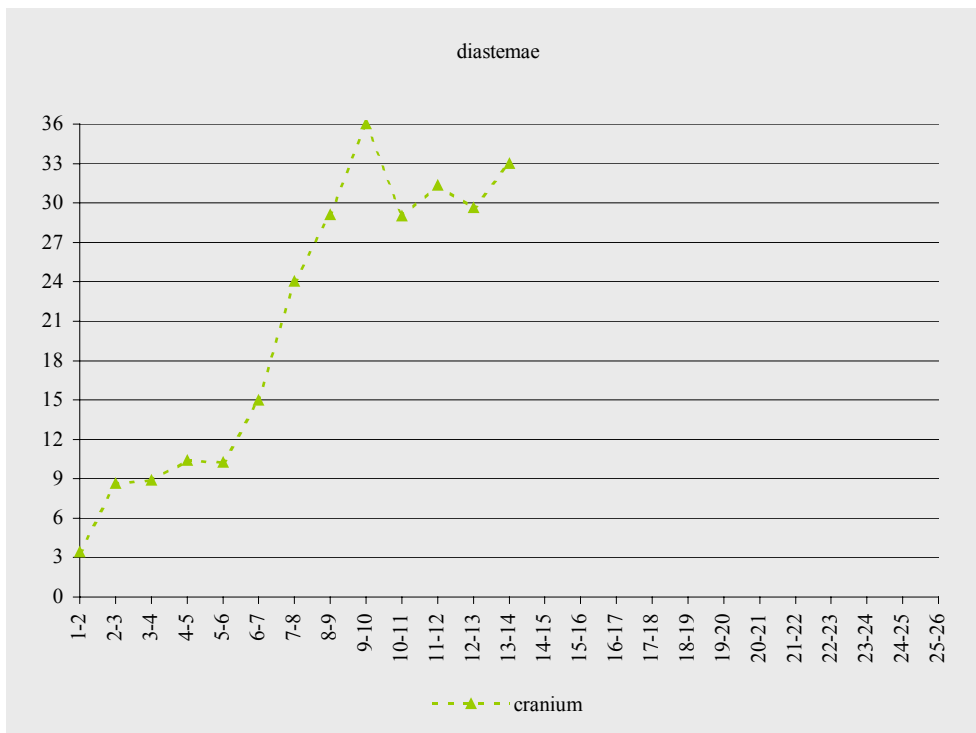
The graph of the alveolar diameter of the cranium of *Cr. mesembrinus* (BSP 1987 I 46). Vertical the diameter in mm; horizontal the number of alveolus, starting anteriorly.



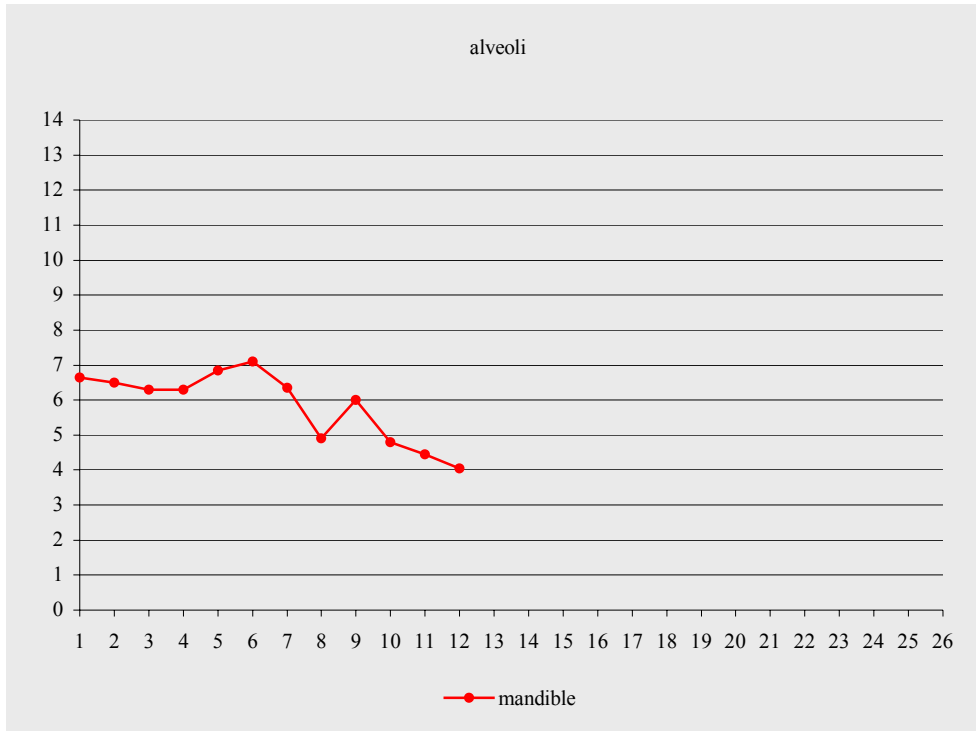
The graph of the alveolar diameter of the mandible of *Cr. mesembrinus* (BSP 1987 I 46). Vertical the diameter in mm; horizontal the number of alveolus, starting anteriorly.



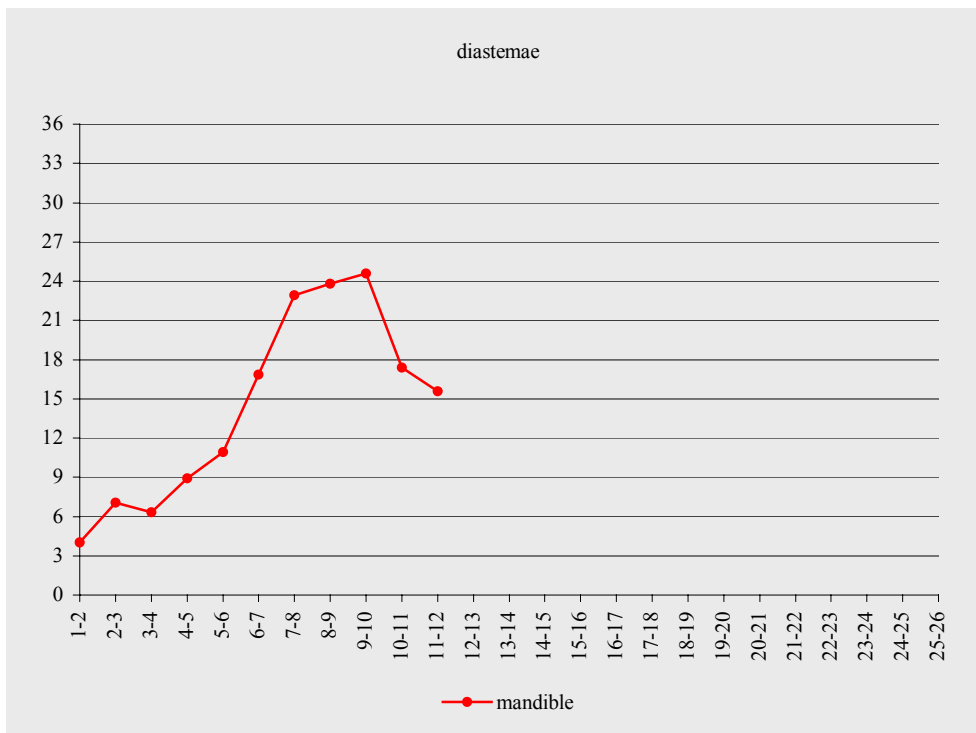
The graph of the size of the diastemae of the cranium of *Cr. mesembrinus* (BSP 1987 I 46). Vertical the size in mm; horizontal the number of diastemae, starting anteriorly.



The graph of the size of the diastemae of the mandible of *Cr. mesembrinus* (BSP 1987 I 46). Vertical the size in mm; horizontal the number of diastemae, starting anteriorly.



The graph of the alveolar diameter of the mandible of *cf. Cr. mesembrinus* (SMNS 56994). Vertical the diameter in mm; horizontal the number of alveolus, starting anteriorly.



The graph of the size of the diastemae of the mandible of *cf. Cr. mesembrinus* (SMNS 56994). Vertical the size in mm; horizontal the number of diastemae, starting anteriorly.

12. Notes

¹ Material from non-marine sediments, from a clear context from Mongolia, currently in Berlin, remained inaccessible.

² Edited version of Veldmeijer (2003a). Note that the introduction of the original version has been partly moved to the introduction in the present work.

³ But see Veldmeijer (2003b).

⁴ See <http://members.lycos.nl/palarch/> for the complete CT-scan.

⁵ This morphology of the dentary sagittal groove is a feature of *Anhanguera* (Veldmeijer *et al.*, 2005a).

⁶ Veldmeijer *et al.* (2005a).

⁷ Veldmeijer *et al.* (submitted).

⁸ See also Veldmeijer *et al.* (2005a).

⁹ See below, but also Veldmeijer *et al.* (in review).

¹⁰ Measurements, taken by the author of the original specimen in Tokyo, confirm this.

¹¹ Veldmeijer *et al.* (in review).

¹² Veldmeijer *et al.* (2005a).

¹³ Veldmeijer *et al.* (in review).

¹⁴ Edited version of Veldmeijer (2002). The introduction of the original version has been partly removed as to avoid repetition. The photographs of the material, have been inserted here; these are colour photographs rather than the black and white ones, published by Veldmeijer & Hense (2004).

¹⁵ Note that this differs from the original (see chapter 7). Veldmeijer (2002: 3) erroneously referred to *Criorhynchus* as Owen, 1874.

¹⁶ The measurements of the dentition are included in chapter 7.

¹⁷ In the present work regarded as *Co. piscator*, see Veldmeijer (2003a).

¹⁸ See also Veldmeijer (2003a), Veldmeijer *et al.* (2005a). The anterior start of the dentary sagittal crest is now generally accepted.

¹⁹ Veldmeijer (2003a).

²⁰ This differs from Veldmeijer (2002).

²¹ This differs from Veldmeijer (2002). Here, SMNS 55409 was classified as Ornithocheirid (see also note 26).

²² Kellner & Tomida (2000: 104) reclassified *S. araripensis* as *An. araripensis*, because "the preserved dorsal portion of the praemaxilla becomes gradually sharper toward the preserved rostral part of the skull, suggesting the presence of a sagittal crest, rostral to the nasoantorbital fenestra". However, Veldmeijer (2003a) regards *S. araripensis* as *Co. araripensis* as explained by Veldmeijer *et al.* (in review). In this chapter the material is referred to as *Co. araripensis*.

²³ This is the conservative view by Wellnhofer (1985). Currently, *S. pricei* is regarded *An. pricei* by Unwin (2003) and should accordingly be classed in Ornithocheiridae. However, the present work does not support this view due disagreement of type specimen (explained in chapter 7) and a tentative classification of *S. pricei* within Anhangueridae is proposed here.

²⁴ *Co. araripensis*.

²⁵ *Co. araripensis*.

²⁶ Because *S. araripensis* has been renamed *Co. araripensis*, this feature is seen in *Coloborhynchus* as well.

²⁷ See chapter 7.

²⁸ This differs from Veldmeijer (2002). See chapter 7.

²⁹ Note that this differs from Veldmeijer (2002).

- ³⁰ Note, as previously mentioned, that the re-classification of *S. araripensis* as *Co. araripensis*, this ridge not an feature is exclusively for *Santanadactylus*.
- ³¹ Edited version of Veldmeijer *et al.* (2005a).
- ³² Although it is not common to publish material from private collections, the decision to do so is based on the fact that the collection is unconditionally accessible. Furthermore, other scientists (*i.e.* Wellnhofer & Kellner, 1991) have used the collection in their studies, which underlines the quality of the collection and its professional management. Finally, none of the fossils are holotypes. Access to the original specimens can be arranged through the owner of the collection (St. Gallen, Switzerland, oberliurs@gmx.ch) or the Natural History Museum at St. Gallen (Nature Museum St. Gallen, Museumstrasse 32, info@naturmuseumsg.ch).
- ³³ See chapter 7.
- ³⁴ Edited version of Veldmeijer (2003b).
- ³⁵ Ample attention to this topic is given in chapter 7.
- ³⁶ Also Veldmeijer *et al.* (submitted).
- ³⁷ This differs from Veldmeijer (2003b); see chapter 7 for the explanation.
- ³⁸ See Veldmeijer *et al.* (2005b).
- ³⁹ This seems premature, as the crest is clearly broken or at least damaged. Full preparation and comparison with *Ludodactylus* needs to shed light on this, but the visible remnant seems to suggest a stronger developed crest relative to *Anhanguera* (also Veldmeijer *et al.*, 2005b).
- ⁴⁰ Edited version of Veldmeijer *et al.* (submitted).
- ⁴¹ The publication in Bennett's bibliography, Owen's supplement no. III to the monograph on the fossil reptilian, has been published in 1861, rather than 1860 as suggested by Bennett.
- ⁴² See chapter 7 for the explanation.
- ⁴³ See chapter 7.
- ⁴⁴ See Veldmeijer (2003a) for a discussion on the classification of this holotype and *An. santanae* in the AMNH collection).
- ⁴⁵ Note that Sayão & Kellner (2000: 2) erroneously mention the presence of a medial ridge on the dorsal aspect of the lower jaw.
- ⁴⁶ See chapter 7.
- ⁴⁷ Edited version of Veldmeijer *et al.* (2005b). Additional data (measurements, individual graphs of the dentition of the various specimens) can be found in 11.1).
- ⁴⁸ This contrast to his own analysis (see also below).
- ⁴⁹ Although this systematic part has been included in chapter 6, it is included here again to better understand the discussion in this chapter. The same has been done for the updates of *Coloborhynchus*, *Anhanguera* and *Criorhynchus*.
- ⁵⁰ This classification however, can be abandoned as the differences between *B. araripensis* and *O. compressirostris* (see below) are obvious (*cf.* figure 7.1 and 7.30).
- ⁵¹ See also the introduction to the *Brasileodactylus* update (7.1.1). Note that an exception is made for type the specimen of *Coloborhynchus*, originating from the Cambridge Greensands, England.
- ⁵² See also the introduction to the *Brasileodactylus* update (7.1.1.).
- ⁵³ See the introduction to the *Brasileodactylus* update (7.1.1.).
- ⁵⁴ Note that Unwin refers to his *unpublished* revision of the Cambridge material.

Samenvatting

De eerste beschrijving van resten van pterosauriërs afkomstig uit de Krijt Formaties in het noordoosten van Brazilië (Chapada do Araripe), in de jaren '70 van de vorige eeuw, luidde het begin in van een toenemende interesse in deze uitgestorven tijdgenoten van de dinosauriërs. Pterosauriërs waren tot dan toe wel bekend uit Duitsland (met name Solnhofen) en de V.S. (voornamelijk *Pteranodon*), maar deze nieuwe vindplaats zou zich al snel ontwikkelen tot de belangrijkste voor deze eerste vliegende vertebraten die de evolutie gekend heeft. De toename van vondsten en publicaties heeft onze kennis uiteraard vergroot, maar in de loop der jaren is de taxonomie er niet helderder op geworden. Verschillende redenen zijn hier voor aan te geven. Eén daarvan is dat belangrijke morfologische kenmerken niet zijn meegenomen in de discussie, terwijl anderen juist wel zijn meegenomen, maar geen taxonomische waarde hebben. Ook spelen aannames soms een rol op grond waarvan sommige pterosauriërs zijn ge-herclassificeerd. De connectie met de pterosauriërs van de Cambridge Greensands in Engeland waarnaar wordt gezocht, is begrijpelijk, maar heeft een negatieve uitwerking gehad als het gaat om de systematiek: de fossielen van de Cambridge Greensands zijn zelf al sinds de eerste vondst halverwege de 19^e eeuw, onderwerp van verhitte discussies en veel verwarring. Aan de andere kant stelt de bestudering van nieuwe fossielen ons in staat om diagnoses te verfijnen en de verwarring die de systematische classificatie omringt, te verhelderen.

In dit werk kom ik tot een herwaardering van vier nauw verwante taxa van pterosauriërs (*Anhanguera*, *Brasileodactylus*, *Coloborhynchus* en *Criorhynchus*) die voorzien zijn van tanden (één tandloze kaak wordt ook besproken), door middel van de bestudering van zowel onbeschreven als reeds gepubliceerd materiaal in de belangrijkste collecties ter wereld, hierbij concentrerend op craniaal materiaal. In hoofdstuk 2 wordt een grotendeels compleet skelet van *Coloborhynchus* beschreven. Het skelet was, toen het in Leiden aankwam, het meest complete exemplaar dat op dat moment bekend was. Op basis van kleine verschillen met de andere soorten is de pterosauriër als nieuwe soort gepubliceerd. In hoofdstuk 3 wordt verschillend post-craniaal materiaal gepresenteerd, waaruit de conclusie getrokken kan worden dat tussen deze taxa, de post-craniale verschillen zo klein zijn dat een gedetailleerde evaluatie nodig is. Belangrijker is echter de beschrijving van de *Criorhynchus* onderkaak, die het afwijkende tandpatroon van dit genus bevestigt. Hoofdstuk 4 presenteert de tandloze onderkaak, maar van groter belang voor dit werk is de beschrijving van één van de meest complete onderkaken van *Anhanguera*. De bestudering hiervan heeft onder andere geleid tot de ontdekking van een belangrijk onderscheidend kenmerk van de morfologie van de onderkaak. Het volgende hoofdstuk (hoofdstuk 5) presenteert een nog grotendeels ongeprepareerde schedel en vleugel uit de collectie van het AMNH, New York, waarvan de beschrijving nog preliminair is en de classificatie als *Brasileodactylus* (hoofdzakelijk gebaseerd op het ontbreken van een kam op de snuit) als voorlopig moet worden gezien (momenteel is het fossiel volledig uitgeprepareerd en wordt het bestudeerd). In hoofdstuk 6 wordt een bijna complete onderkaak van *Brasileodactylus* beschreven; de meest complete, met zekerheid tot dit taxon behorende exemplaar. Daarnaast worden post-craniale elementen en een stuk bovenkaak behorende tot hetzelfde individu gepresenteerd dat wordt ingedeeld, met name op basis van de kamloze bovenkaak, tot *Brasileodactylus*. Dit betekent dat voor het eerst het post-craniale skelet van dit genus beschreven is; zoals verwacht, is het in hoge mate gelijk aan het post-craniale skelet van de andere taxa. Hoofdstuk 7 heeft een samenvattend karakter waarin in het kort alle taxa worden besproken en de conclusies nog eens voorbij komen. Daarnaast worden de afmetingen van de gebitten gepresenteerd. Door de diameters van de alveolen en de afmetingen van de diastemen in grafieken uit te zetten, blijkt dat ieder

taxon een eigen gebitspatroon heeft. In de slotopmerkingen in hoofdstuk 8 wordt dieper ingegaan op de problemen rondom het materiaal van de Cambridge Greensands (*Ornithocheiridae* versus *Anhangueridae*).

Deze studie heeft erin geresulteerd dat verschillende diagnoses zijn verfijnd en dat de vier taxa duidelijk van elkaar onderscheiden kunnen worden: de dieren met een premaxillaire sagittale kam (*Coloborhynchus*, *Criorhynchus* en *Anhanguera*) behoren tot de *Anhangueridae*; de kamloze *Brasileodactylus* kan hier niet in worden ondergebracht, ondanks de nauwe verwantschap. De onvolledigheid van *Brasileodactylus* overblijfselen, echter, staat op dit moment een duidelijk alternatief in de weg. Daarnaast zijn verschillende problemen geconstateerd met de classificatie van materiaal. De diagnose van *Ornithocheiridae*, zoals onlangs in een herwaardering is voorgesteld, is niet gebaseerd op het type exemplaar en het gebruikte exemplaar vertoont niet de beschreven kenmerken. Door de acceptatie van *Ornithocheirus compressirostris* als type exemplaar, is *Ornithocheiridae* teruggebracht tot slechts enkele fossielen, alleen bekend uit Engeland.

Summary

The first description, in the 1970s, of pterosaur remains from the Cretaceous Formations in northeast Brazil (Chapada do Aripe) marks the starting point of renewed interest in these extinct contemporaries of the dinosaurs. Up until then, pterosaurs were known from Germany (mainly Solnhofen) and the U.S. (mainly *Pteranodon*) but this new site would become the most important place for finds of earth's evolution first flying vertebrates in only few years time. The increasing numbers of finds and publications obviously increased our knowledge, but through the years, taxonomy has become less clear as one would expect. Various reasons can be given for this. One is that important morphological features have not been incorporated in the discussion whereas others are, but have questionable taxonomic value. Also, sometimes unstated assumptions play an important role on which pterosaurs have been re-classified. It is understandable that one seeks a connection with the pterosaurs from the Cambridge Greensands in England, but this has had a negative impact on the systematics: the fossils from the Cambridge Greensands themselves have been subject to fierce debates and much confusion ever since their first discovery in the latter half of the 19th century. On the other hand, the study of new material allows us to refine diagnoses and clear up some of the mist surrounding the systematic classification.

The present work presents a reappraisal of four closely related taxa with teeth (*Anhanguera*, *Brasileodactylus*, *Coloborhynchus* en *Criorhynchus*; one edentulous mandible will be discussed as well) by means of the study of unpublished and published material in the major collections all around the world, concentrating on cranial parts. In chapter 2, a largely complete skeleton of *Coloborhynchus* is described. When the skeleton came to Leiden, it was the most complete specimen known. The specimen has been classified as new species on the basis of small differences with the other species. Chapter 3 presents various post-cranial elements, on the basis of which it is concluded that interspecific differences in the post-cranial skeleton are so small that an evaluation is necessary. More important for the present work, however, is the description of the mandible of *Criorhynchus*, which confirms the strong deviating dentition pattern relative to the other taxa. Chapter 4 presents the edentulous jaw, but also the description of one of the most complete mandibles of *Anhanguera*. The study of this specimen resulted among others in the discovery of an important diagnostic morphological feature of the mandible. The next chapter (chapter 5) is a preliminary description of a largely unprepared skull and wing of a fossil in the collection of the AMNH, New York. The specimen is tentatively classified as *Brasileodactylus* mainly because of the

crestless jaws (currently, the fossil is completely prepared and under study). In chapter 6, an almost complete mandible is described, which is the most complete mandible that can be classified to *Brasileodactylus* with certainty. Furthermore, post-cranial material as well as a small piece of maxilla, belonging to the same individual is presented. It is classified as *Brasileodactylus*, again, mainly on the basis of the crestless condition of the maxilla. This is the first description of post-cranial material of this genus; as expected, there is a high degree of conformity with the other taxa. Chapter 7 summarises and shortly discusses all taxa, presents the main conclusions again, and furthermore, presents the measurements of the dentition. When the diameters of the alveoli and measurements of the diastemae are put in graphs, certain dentition patterns characteristic for each taxon can be distinguished. The final remarks in chapter 8 offer a more detailed discussion on the problems with the Cambridge Greensands (Ornithocheiridae versus Anhangueridae).

This study resulted in the refinement of various diagnoses and makes the distinction between the four taxa clearer: animals with a premaxillary and dentary sagittal crest (*Coloborhynchus*, *Criorhynchus* and *Anhanguera*) belong to Anhangueridae; the crestless *Brasileodactylus* however, cannot be classified to Anhangueridae, despite the close relationship due to the incompleteness of its remains. Furthermore, various problems have been observed with the classification of some material. The diagnosis of Ornithocheiridae, as recently proposed in a re-evaluation, is not based on the type specimen and the used specimen does not show the described characters. In accepting *Ornithocheirus compressirostris* as type specimen, Ornithocheiridae has been brought back to few fossils, only known from England.

Curriculum Vitae

Date of birth: 13 April 1969
Place of birth: Vlissingen, The Netherlands
Education: VWO 1990-1991
University of Leiden 1991-2000

During my study I participated in various archaeological expeditions (mainly in Egypt, like Berenike and Qasr Ibrim but in The Netherlands as well, for example Wynaldum) and research groups (Tutankhamun's clothing). After finishing University in 2000, my research, in archaeology as well as palaeontology, intensified, leading among others to the present work.

In 2003 I founded, together with three colleagues, the PalArch Foundation, of which I am the chairman. The goals of the foundation are stimulating scientific research, to improve the interaction between researchers and enhance true scientific discussion. One of the focal points of the foundation is the webbased, peer reviewed scientific journal www.PalArch.nl which consist of three independent sections (among which vertebrate palaeontology), of which I am the managing editor of the section archaeology of Egypt/Egyptology.

Currently, I am working on various projects and participate in various expeditions, among which are the study of pterosaur remains housed in the AMNH, New York (but currently in Natuurmuseum Rotterdam), leatherworks in ancient Egypt (Qasr Ibrim, Amarna, Hierakonpolis, Elephantine), cordage and basketry in ancient Egypt (Qasr Ibrim, Hierakonpolis) and the study of various collections of ancient Egyptian footwear (among others British Museum, Metropolitan Museum, Ägyptisches Museum). For a detailed *curriculum vitae*, including a list of publications, please visit my homepage at <http://members.lycos.nl/palarch/>.

Appendix chapter 1 : Introduction

1.1. Appendix

1.1.1. Figures and plates

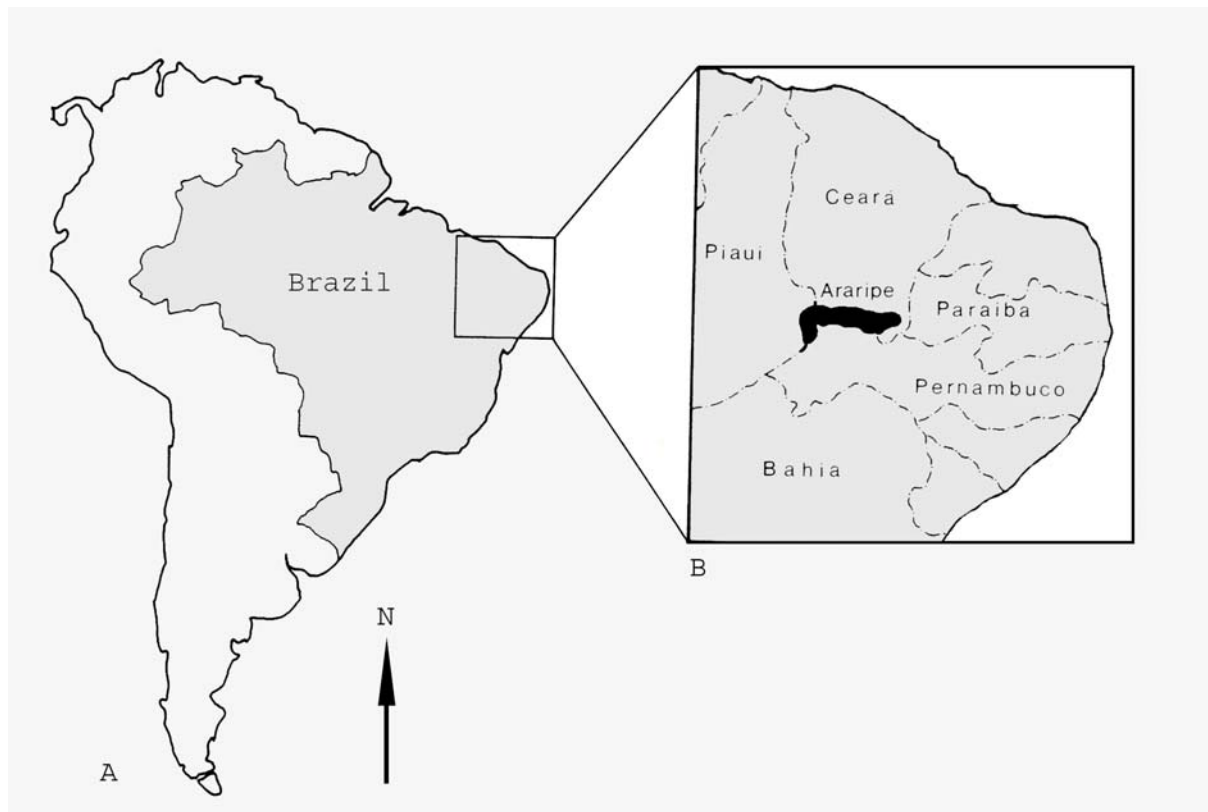


Figure 1.1. Chapada do Araripe, northeastern Brazil, on the boundaries of Piauí, Ceará and Pernambuco (After Wellnhofer, 1985).

Appendix chapter 2: Description of *Coloborhynchus spielbergi* sp. nov. (Pterodactyloidea) from the Albian (Lower Cretaceous) of Brazil

2.7. Appendix

2.7.1. Measurements

Skull	original	15	present	12
Mandible		10		10
Cervical		7		2
Dorsals		10		7
Sacrum		6		6
Ribs		5		2
Wings		20		6
Legs and feet		12		9
Shoulder girdle		7		7
Total		100		69

Table 2.1. Sixty-nine percent of the specimen is complete. The figures in the tables are percentages of the total of the complete skeleton (heading 'original') and the amount of prepared bone (heading 'present') relative to the percentage of that bone of a complete skeleton. (From: De Buissonjé, 1993).

Length skull	712
Maximal & minimal width anterior spoon-shaped expansion (ventrally)	36, 26
Height premaxillary sagittal crest	109
Length premaxillary sagittal crest	300
Width over quadrates	150*
Height of right orbit	97
Height quadrate-occiput	130
Length & height nasoantorbital fenestra	230, 60*
Centrum occipital condyle-posterior skull	60
Diameter occipital condyle (sagittal plane)	11

Table 2.2. *Co. spielbergi* (RGM 401 880), measurements of the skull in mm. *: approximate.

Left side					Right side				
Number	Diameter alveolus	Length of tooth	Size diastema	Measurement	Number	Diameter alveolus	Length of tooth	Size diastema	Measurement
1	–	–	1–2	n/a	1	–	–	1–2	–
2	8.6	–	2–3	8.1	2	9.6	–	2–3	8.0
3	12.2	20.1	3–4	7.8	3	11.4	20.4	3–4	8.0
4	10.0	11.7	4–5	4.2	4	10.1	19.5	4–5	6.0
5	6.9	8.9	5–6	6.2	5	6.5	8.7	5–6	n/a
6	5.4	–	6–7	10.9	6	?	n/a	6–7	n/a
7	9.2	12.6	7–8	11.0	7	8.4	14.2	7–8	15.0
8	9.3	11.2	8–9	18.0	8	10.7	22.2	8–9	15*
9	10.8	11.5	9–10	20*	9	–	–	9–10	18*
10	–	–	–	–	10	6.9	–	10–11	15*
11	–	–	–	–	11	7.3	9.3	11–12	25.0
12	–	–	–	–	12	7.8	9.0	12–13	28.0
13	–	–	–	–	13	7.3	8.1	13–14	20*
14	–	–	–	–	14	7.5	8.2	14–15	17.0
15	–	–	–	–	15	7.6	6.6	15–16	45*
16	–	–	–	–	16	5.3	–	16–17	12.0
17	–	–	–	–	17	5.0	–	17–18	13.0
18	–	–	–	–	18	5.0	–	–	–

Table 2.3. *Co. spielbergi* (RGM 401 880), measurements of alveoli and diastemae of the cranium in mm.

		<i>An. blittersdorffi</i> (MN 4805-V)	<i>Co. araripensis</i> (BSP 1982 I 89)	<i>Cf. Co. araripensis</i> (MN 4735-V)	<i>Co. araripensis</i> (SAO 16494)	<i>An. santanae</i> (BSP 1982 I 90)	<i>An. santanae</i> (AMNH 22555)	<i>Cr. mesembrinus</i> (BSP 1987 I 46)	<i>Co. piscator</i> (NSM-PV 19892)
Measurements	Length	520	600*	680	535	520*	475	640	620
	Width over quadrates	80	98	121	80	98	–	137**	–
	Length premaxillary sagittal crest	200	–	290	220	–	125*	225	201
	Maximal height premaxillary crest	64	–	140	86	–	–	105	63
	Length nasoantorbital fenestra	160	160	170 [#]	148	156	162	220	190
Ratios	Width quadrate–total length skull (RGM 401 880 = 21)	15	16	18	15	19	–	21	–
	Length premaxillary sagittal crest–length skull (<i>Co. spielbergi</i> , RGM 401 880 = 42)	38	–	43	41	–	26	35	32
	Height–length premaxillary sagittal crest (<i>Co. spielbergi</i> , RGM 401 880 = 36)	32	–	48	39	–	–	47	31
	Length nasoantorbital fenestra–total length skull (<i>Co. spielbergi</i> , RGM 401 880 = 32)	31	27	25	28	30	34	34	31

Table 2.4. Measurements and ratios of the skull of compared pterosaurs (in mm). All specimen are studied first hand of original material except for *Co. piscator* (cast in Museu Nacional, Rio de Janeiro, Brazil). *: approximate, from Wellnhofer (1985); **: from Wellnhofer (1987); #: approximate.

Mandible	Length mandible	606
	Length retroarticular process–symphysis	355
	Thickness ramus at last alveolus	10
	Maximal width anterior spoon-shaped expansion (dorsally)	38
	Maximal width at symphysis	56
	Maximal width rami (laterally)	155
	Width over surangular	150
	Minimal width anterior to symphysis (dorsally)	25
	Maximal height of dentary sagittal crest	55
	Height at posteriormost alveolus	55
	Length dentary sagittal crest	245
?Ceratobranchial	Length, as preserved (illustrated fragment)	104
	Length, as preserved (not illustrated fragments)	35,65
	Cross-section (illustrated fragment)	2.5
	Cross-section (not illustrated fragment)	2.5

Table 2.5. *Co. spielbergi* (RGM 401 880), measurements of the mandible and ?ceratobranchial in mm.

Left side					Right side				
Number	Diameter alveolus	Length of tooth	Size diastema	Measurement	Number	Diameter alveolus	Length of tooth	Size diastema	Measurement
1	7.9	–	1–2	6.0	1	7.9	–	1–2	4.0
2	8.5	21.1	2–3	8.0	2	11.0	–	2–3	5.0
3	11.4	33.6	3–4	4.0	3	11.3	23.4	3–4	5.0
4	6.1	–	4–5	8.0	4	5.9	–	4–5	6.0
5	6.1	–	5–6	9.0	5	4.9	–	5–6	10.0
6	7.1	9.0	6–7	10.0	6	6.9	–	6–7	11.0
7	9.2	19.6	7–8	16*	7	7.0	19.8	7–8	–
8	8.7	17.3	8–9	18*	8	?	n/a	8–9	–
9	7.3	16.4	9–10	16.0	9	7.5	12.7	9–10	18.0
10	7.3	9.7	10–11	24.0	10	7.0	11.5	10–11	20.0
11	6.7	11.2	11–12	23.0	11	6.2	–	11–12	23.0
12	7.5	9.1	12–13	20.0	12	5.8	–	12–13	20.0
13	7.6	12.1	13–14	19.0	13	5.0	8.8	13–14	20.0
14	6.8	9.9	14–15	18.0	14	6.9	10.3	14–15	21.0
15	6.3	9.2	–	–	15	6.7	7.9	–	–
15a	n/a	n/a	15–15a	n/a	15a	6.2	–	15–15a	18.1
16	6.4	7.8	15–16	19.0	16	5.5	5.0	15–16	22.0

Table 2.6. *Co. spielbergi* (RGM 401 880), measurements of alveoli and diastemae of the mandible in mm. *: approximate; –: not preserved; n/a: not applicable.

		<i>Cf. An. blittersdorffi</i> (ref.spec. n. 40 Pz-DBAV-UFRJ)	<i>Co. araripensis</i> (BSP 1982 I 89)	<i>An. santanae</i> (BSP 1982 I 90)	<i>Anhanguera</i> sp. (SAO 200602)	<i>Anhanguera</i> sp. (AMNH 22573)	<i>Cr. mesembrinus</i> (BSP 1987 I 46)	<i>Cf. Cr. mesembrinus</i> (SMNS 56994)	<i>Co. robustus</i> (BSP 1987 I 47)	<i>Co. robustus</i> (SMNK 2302 PAL)	<i>Co. piscator</i> (NSM-PV 19892)
Measurements	Length	315	500*	460*	403	435**	540*	385	555	–	533 ^{##}
	Length dentary sagittal crest	100	–	–	115	145**	126	118	145**	170	145
	Depth dentary sagittal crest	–	–	–	40	40	51 [#]	35	76 [#]	62	50
	Width at symphysis	25	43	37	37	38	23 [#]	34	33 [#]	–	35
Ratios	Width at symphysis–length mandible <i>Co. spielbergi</i> , RGM 401 880 = 9.2)	7.9	8.6	8.0	9.2	8.7	4.3	8.8	5.9	–	6.6

Length dentary sagittal crest–length mandible (<i>Co. spielbergi</i> , RGM 401 880 = 40)	32	–	–	29	33	23	31	26	–	27
Depth–length dentary sagittal crest (<i>Co. spielbergi</i> , RGM 401 880 = 22)	–	–	–	35	28	40	30	52	36	34

Table 2.7. Measurements and ratios of the mandible of compared pterosaurs in mm. All specimens are studied first hand except for *Co. piscator* (cast in Museu Nacional, Rio de Janeiro, Brazil). *: approximate, from Wellnhofer (1985); **: approximate; #: from Wellnhofer (1987); ##: from Kellner & Tomida (2000).

	Seventh cervical	Eighth cervical
Length centra (incl. postzygapophysis)	49	27
Height	69	64
Width over postzygapophyses	36	31*
Width over prezygapophyses	52	45
Width over transverse processes	–	60
Maximal thickness neural spine	8.5	9

Table 2.8. *Co. spielbergi* (RGM 401 880), measurements of the cervical vertebrae in mm. *: approximate.

Length (at centra)	135*
Length supraneural plate	144
Length centrum first vertebra (notarial cervical)	23
Length centrum second vertebra (notarial dorsal)	21
Length centrum third vertebra (notarial dorsal)	22
Length centrum fourth vertebra (notarial dorsal)	22
Length centrum fifth vertebra (notarial dorsal)	21
Length centrum sixth vertebra (notarial dorsal)	26*
Width centrum first vertebra (notarial cervical)	19
Width centrum sixth vertebra (notarial dorsal)	14
Width supraneural plate at first vertebra (notarial cervical)	12
Width supraneural plate at fourth vertebra (notarial dorsal: anterior to scapular articulation)	13
Width supraneural plate at fourth vertebra (notarial dorsal: posterior to scapular articulation)	16
Width supraneural plate at sixth vertebra (notarial dorsal)	7
Height anterior aspect	61
Height posterior aspect	48
Length scapular articulation	22
Height scapular articulation	17

Table 2.9. *Co. spielbergi* (RGM 401 880); measurements of the notarium in mm. *: approximate.

	sixth	seventh	eighth	ninth	tenth	eleventh	twelfth
Length centra	23	19	17	18	19	20	19
Height	49	45	45	47	49	43	44
Width over transverse processes	47	49	48	46	41	32	50
Width over postzygapophyses	18	15	18	12*	14	16	15*
Width over prezygapophysis	21	21*	20	19*	19*	19*	19*
Length neural spine	17	17	18	13	19	14*	13
Thickness neural spine (dorsalmost)	3	2.5	3.5	2.5	2.5	4.5*	4*

Table 2.10. *Co. spielbergi* (RGM 401 880), measurements of the dorsals in mm. *: approximate.

Total length	165*
Length supraneural plate	98*
Height pelvis posterodorsal most point ischium~dorsal aspect	56
Width illii (anteriormost)	18
Width illii (posteriorly)	14
Width over illii	106
Width over anterior edges of acetabulae	99
Width over posterior edges of acetabulae	78
Width over postacetabular process (anteriorly)	40
Width over postacetabular process (posteriorly)	23
Width posterior to ischia	32
Width at prepubic articulation	99
Height articulation for the prepubes–postacetabular process	95

Table 2.11. *Co. spielbergi* (RGM 401 880), measurements of the pelvis in mm. *: approximate.

Width mediolateral cervical ribs	10.5–12.0
Length notarial rib (as preserved)	100

Table 2.12. *Co. spielbergi* (RGM 401 880), measurements of the ribs in mm.

Width (measured dorsally)	135
Width (measured ventrally)	180
Length (measured dorsally)	200
Length (measured ventrally)	180
Width cristospine (ventral to coracoid facet)	23
Height cristospine (at coracoid facet)	55
Thickness posterior plate (left anterior margin)	3

Table 2.13. *Co. spielbergi* (RGM 401 880), measurements of the sternum in mm.

Width supraneural plate articulation	35
Width shaft of the scapula	23
Width sternal articulation	27
Width shaft of the coracoid	14
Length (measured laterally)	340
Length scapula	130
Length coracoid	175

Table 2.14. *Co. spielbergi* (RGM 401 880), measurements of the scapulocoracoid in mm.

Length	290
Width proximal end	70
Width distal end	83
Width shaft, anterior aspect (begin of deltopectoral crest)	34
Width shaft, ventral aspect (begin of deltopectoral crest)	37
Width shaft–maximal height deltopectoral crest	69

Table 2.15. *Co. spielbergi* (RGM 401 880), measurements of humerus in mm.

Length	410
Minimal width, anterior aspect	35
Minimal width, ventral aspect	22
Maximal width anterior aspect, proximal end	75
Maximal width ventral aspect proximal end	45

Table 2.16. *Co. spielbergi* (RGM 401 880), measurements of the ulna in mm.

Length	401
Width, anterior aspect	12
Width, ventral aspect	10
Width anterior aspect over biceps tubercle	21
Width proximal end (anterior aspect)	44
Width proximal end (ventral aspect)	18
Width distal end (anterior aspect)	40
Width distal end (ventral aspect)	16

Table 2.17. *Co. spielbergi* (RGM 401 880), measurements of the radius in mm.

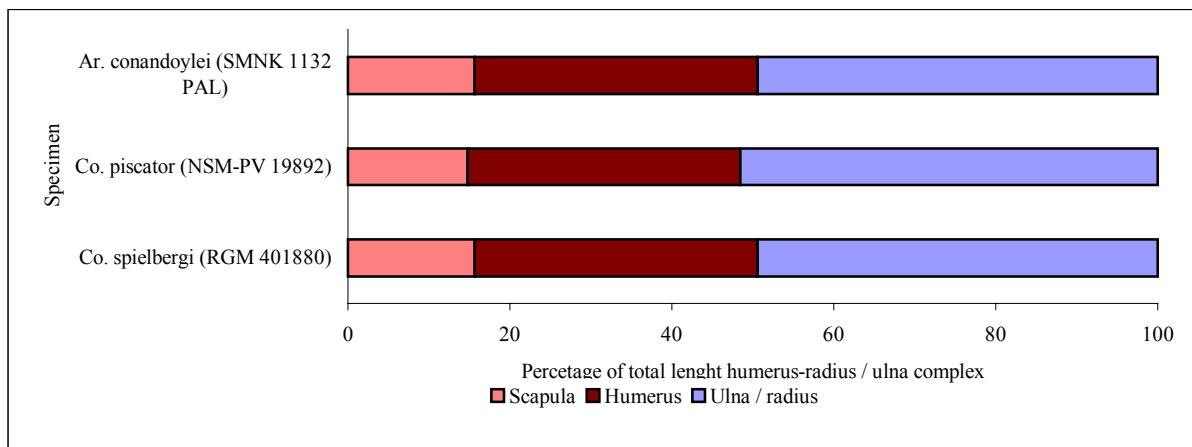
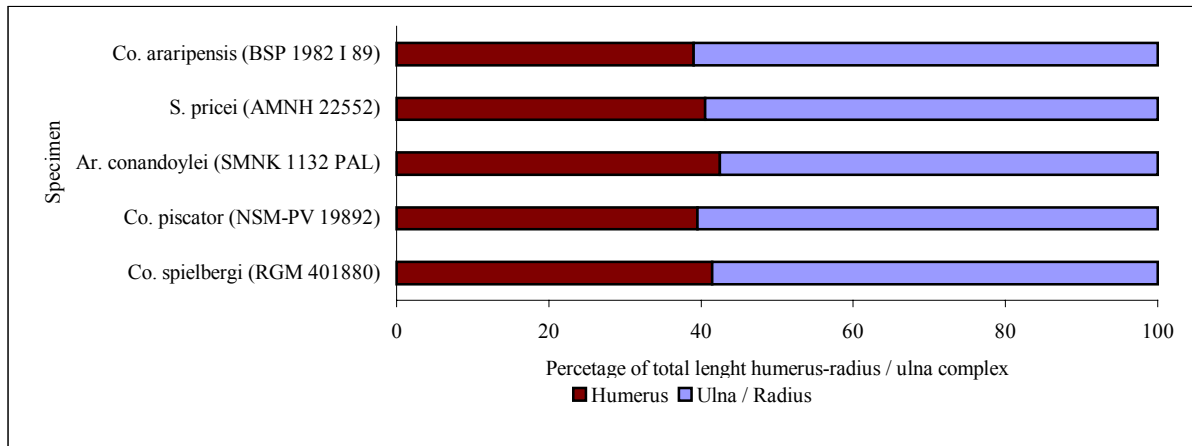


Table 2.18. Ratios of humerus and ulna/radius (above) and ratios of scapula, humerus and ulna/radius (below) of different Brazilian pterosaurs.

Maximal width proximal aspect	50
Minimal width proximal aspect	37
Maximal width dorsal aspect	30
Minimal width dorsal aspect	26
Length (measured anterior–posterior)	73

Table 2.19. *Co. spielbergi* (RGM 401 880), measurements of the proximal syncarpal in mm.

?Metacarpals	Length, longest	100
	Cross-section, longest	4.5
	Cross-section, smallest	3
Phalanx	Length	28
	Width (anteroposterior plane)	2.5
	Width (dorsoventral plane)	3
Unguals	Length	27–28
	Width at tubercle	14–17
	Thickness of tubercle	5–6

Table 2.20. *Co. spielbergi* (RGM 401 880), measurements of the third phalanx of the third digit and unguals in mm.

Length	285
Maximal diameter head, lateromedially	20
Width at greater trochanter	22
Width neck, anterior aspect	12
Width shaft, anterior aspect	15
Width shaft, lateral aspect	17
Width distal end, anterior aspect	35

Table 2.21. *Co. spielbergi* (RGM 401 880), measurements of the femur in mm.

Length	355
Width shaft, lateral aspect	9
Width shaft, anterior aspect	11
Width proximal end, lateral aspect	30
Width proximal end, anterior aspect	23
Width distal end, lateral aspect	14
Width distal end, anterior aspect	15

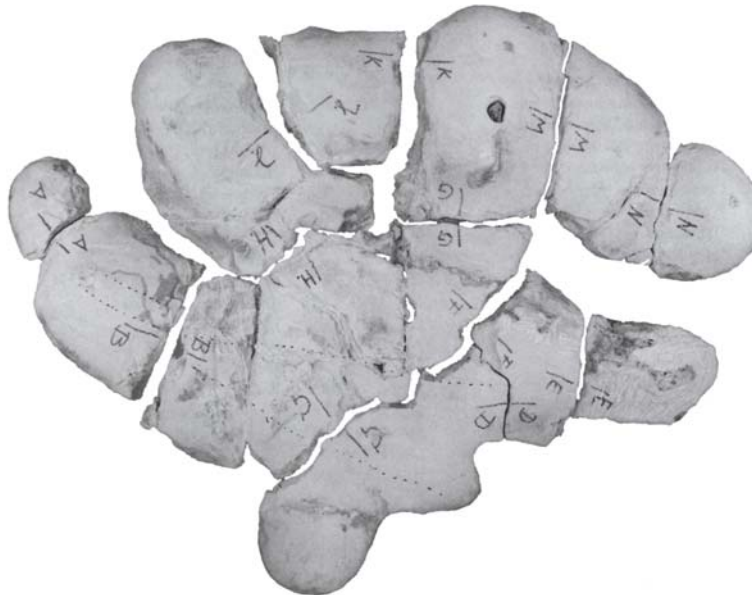
Table 2.22. *Co. spielbergi* (RGM 401 880), measurements of the tibia in mm.

* <i>Coloborhynchus clavirostris</i>	BMNH 1822	Owen, 1874
* <i>Santanadactylus brasiliensis</i>	UvA M 4894	De Buissonjé, 1980
<i>Santanadactylus brasiliensis</i>	V-201	Wellnhofer <i>et al.</i> , 1983
* <i>Brasileodactylus araripensis</i>	MN 4804-V	Kellner, 1984
* <i>Santanadactylus araripensis</i> =		(Wellnhofer, 1985)
<i>Anhanguera araripensis</i> =	BSP 1982 I 89	(Kellner, 1990)
<i>Coloborhynchus araripensis</i>		Veldmeijer <i>et al.</i> , in review
* <i>Santanadactylus pricei</i>	BSP 1980 I 122	Wellnhofer, 1985
* <i>Santanadactylus pricei</i>	BSP 1980 I 43	Wellnhofer, 1985
* <i>Santanadactylus pricei</i>	BSP 1980 I 120	Wellnhofer, 1985
* " <i>Santanadactylus</i> " <i>spixi</i>	BSP 1980 I 121	Wellnhofer, 1985
* <i>Araripesaurus santanae</i> =		(Wellnhofer, 1985)
<i>Anhanguera santanae</i>	BSP 1982 I 90	Kellner, 1990
* <i>Araripesaurus</i> sp. indet. =		(Wellnhofer, 1985)
<i>Anhanguera santanae</i>	BSP 1982 I 91	Wellnhofer, 1991b
* <i>Araripesaurus</i> sp. indet. =		(Wellnhofer, 1985)
? <i>Anhanguera</i> sp. indet.	BSP 1982 I 93 [□]	Wellnhofer, 1991b
<i>Cearadactylus atrox</i>	CB-PV-F-093	Leonardi & Borgomanero, 1985
* <i>Anhanguera blittersdorffi</i>	MN 4805-V	Campos & Kellner, 1985b ^{□□}
* <i>Tropeognathus mesembrinus</i> =		(Wellnhofer, 1987)
<i>Criorhynchus mesembrinus</i>	BSP 1987 I 46	Fastnacht, 2001
* <i>Tropeognathus robustus</i> =		(Wellnhofer, 1987)
<i>Anhanguera robustus</i> =	BSP 1987 I 47	(Kellner & Campos, 1989)
<i>Coloborhynchus robustus</i>		Veldmeijer, 1998
* <i>pterodactylid</i>	AMNH 22569	Bennett, 1990

* <i>Anhanguera blittersdorffi</i> (ref. spec.)	n. 40 Pz-DBAV-UERJ	Campos & Kellner, 1985a
* <i>Santanadactylus pricei</i>	BSP 1987 I 1	Wellnhofer, 1991b
* <i>Santanadactylus araripensis</i> =	BSP 1987 I 66	(Wellnhofer, 1991b)
<i>Coloborhynchus araripensis</i>	BSP 1987 I 65	Veldmeijer <i>et al.</i> , in review
* <i>Santanadactylus brasiliensis</i>	AMNH 22555	Wellnhofer, 1991b
* <i>Anhanguera</i> sp. indet. =	AMNH 22552 ^Δ	(Wellnhofer, 1988)
<i>Anhanguera santanae</i>	CCSRL 12692/12713	Wellnhofer, 1991b
* <i>Santanadactylus pricei</i>	SMNK 1132 PAL	Wellnhofer, 1991b
<i>Cearadactylus? ligabuei</i>	LINHM 016	Dalla Vecchia, 1993
<i>Arthurdactylus conandoylei</i>	NMS-PV 19892	Frey & Martill, 1994
<i>Siroccopteryx moroccensis</i>	MN 4735-V	Mader & Kellner, 1999
* <i>Anhanguera piscator</i> =	MN 4797-V	(Kellner & Tomida, 2000)
<i>Coloborhynchus piscator</i>	SMNK 2302 PAL	present work
* <i>Anhanguera araripensis</i> (ref. spec.)	SMNS 56994	(Kellner & Tomida, 2000)
<i>Coloborhynchus araripensis</i>	SAO 16494	Veldmeijer <i>et al.</i> , in review.
* <i>Brasileodactylus</i> cf. <i>araripensis</i>	SAO 200602	Saydo & Kellner, 2000
* <i>Coloborhynchus robustus</i>	AMNH 22573	Fastnacht, 2001
* Cf. <i>Criorhynchus mesembrinus</i>		Veldmeijer, 2002
* <i>Coloborhynchus araripensis</i>		Veldmeijer <i>et al.</i> , in review
<i>Anhanguera</i> sp. indet.		
<i>Anhanguera</i> sp. indet.		

Table 2.23. Compared material in sequence of publication. Specimens marked with * are studied first hand. □: Wellnhofer (1991b) refers erroneously to this specimen as BSP 1982 192; □: the specimen was first mentioned by Campos (1983); ^Δ: note that Kellner & Tomida (2000) erroneously refer to this specimen as AMNH 22555; ^{ΔΔ}: note that Kellner & Tomida (2000) mistakenly refer to this specimen as SMNK 1133 PAL.

2.7.2. Figures and plates



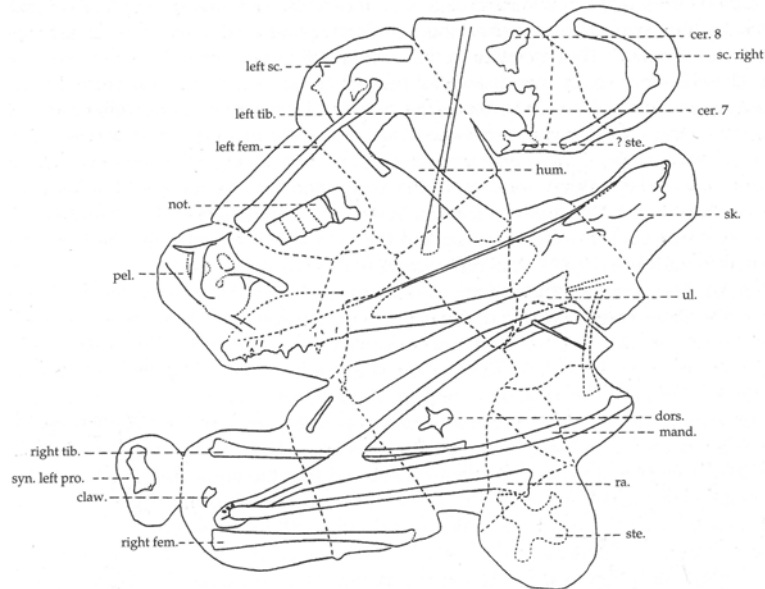


Figure 2.1 (top). *Co. spielbergi* sp. nov. (RGM 401 880), the skeleton embedded in nodules. The sides of a nodule that connected to another nodule were marked by characters in red ink. Photographer unknown. Figure 2.2 (bottom). Drawing of the skeleton as embedded in the nodules. Not to scale. (Redrawn after working-drawing De Buissonjé).

A



B



C



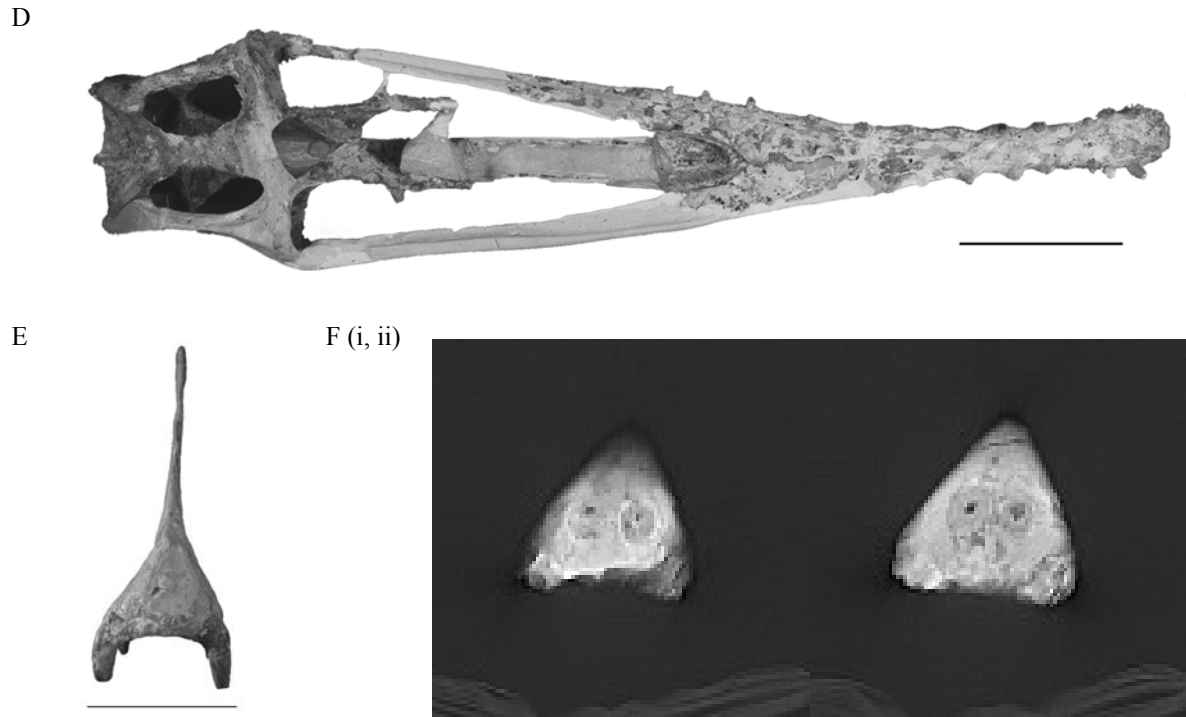


Figure 2.3. *Co. spielbergi* sp. nov. (RGM 401 880), the skull in various aspects. A: left lateral; B: right lateral; C: dorsal; D: ventral; E: anterior (scale bar = 50 mm); F(i, ii): CT-scans of anterior aspect (scan by S. Boor and P. Stoeter, Department of Neuroradiology of the University of Mainz, Germany). Scale bar = 100 mm (unless mentioned otherwise). All other photographs by A. 't Hooft. Courtesy RGM, Leiden (except F).

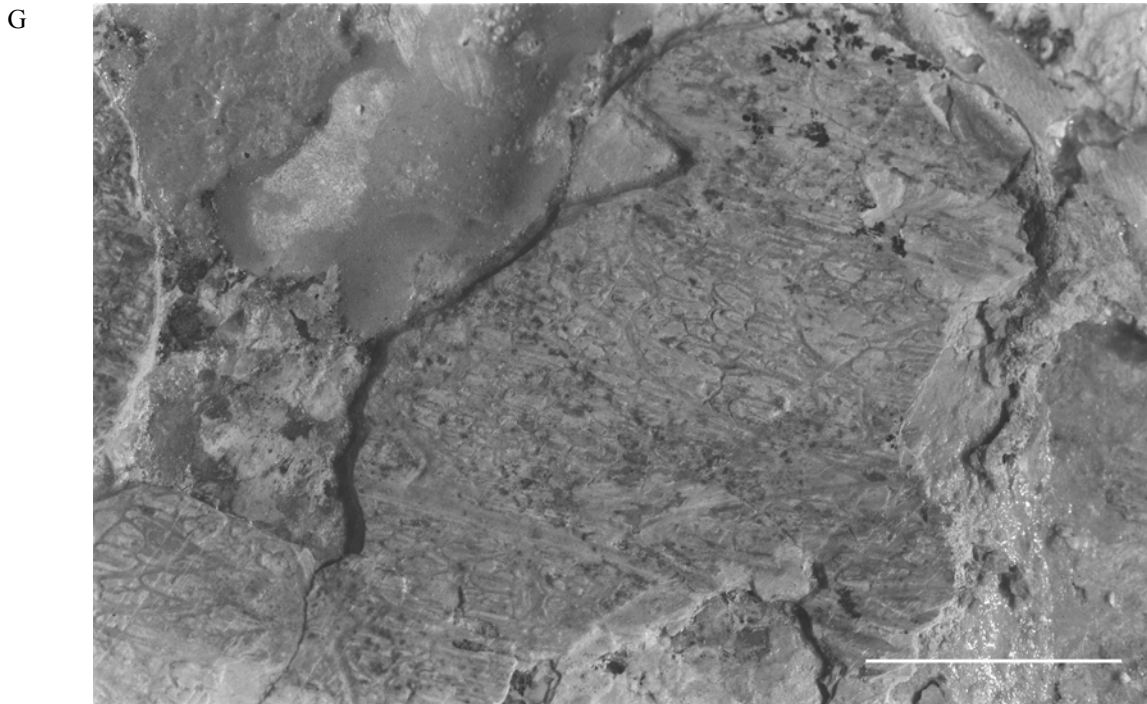


Figure 2.3. *Co. spielbergi* sp. nov. (RGM 401 880). G: network of grooves at the premaxillary crest (scale bar = 10 mm). Scale bar 10 mm. All other photographs by A. 't Hooft. Courtesy RGM, Leiden.

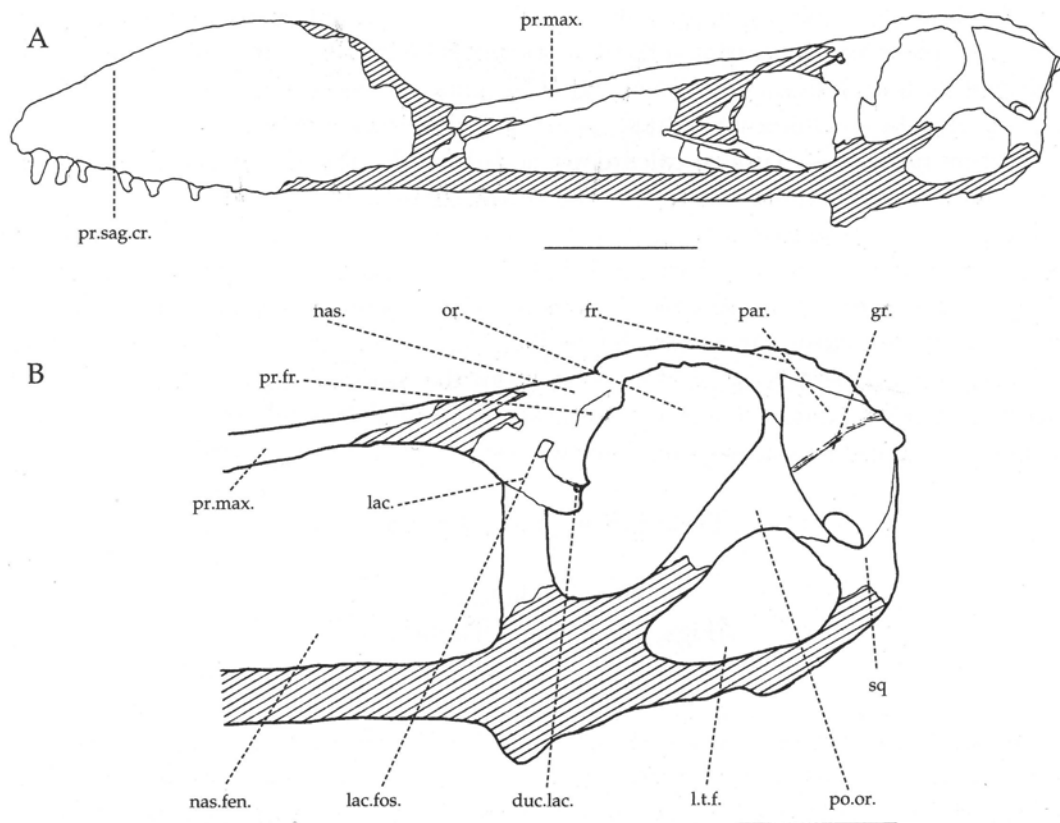


Figure 2.4. *Co. spielbergi* sp. nov. (RGM 401 880), the skull in various aspects (with details separately). A: skull, left lateral (scale bar = 100 mm); B: back of skull, left lateral (scale bar = 50 mm) Drawings by the author.

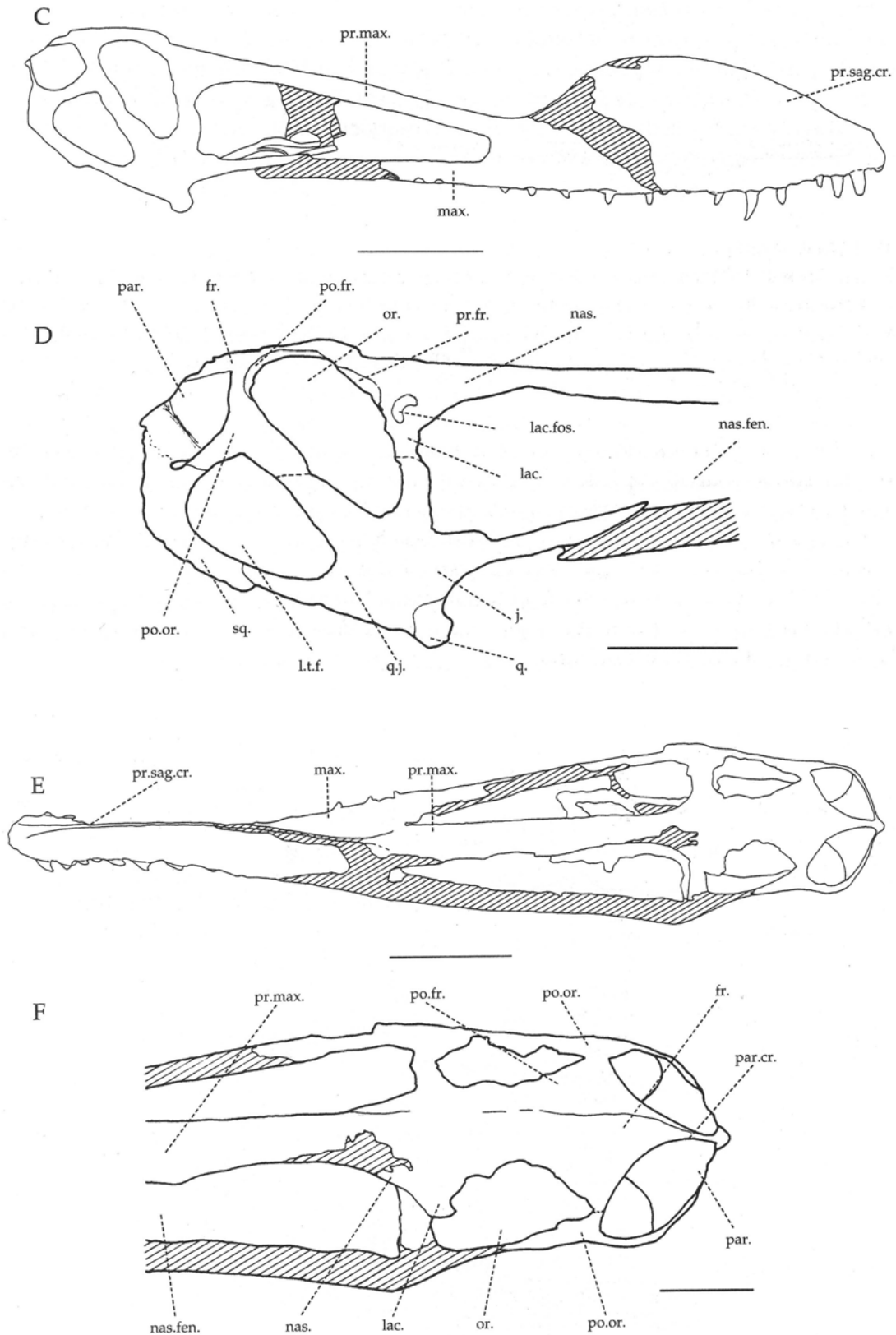


Figure 2.4. *Co. spielbergi* sp. no. (RGM 401 880), the skull in various aspects (with details separately). C: skull, right lateral (scale bar = 100 mm); D: back of skull, right lateral (scale bar = 50 mm); E: skull, dorsal (scale bar = 100 mm); F: back of skull, dorsal (scale bar = 50 mm). Drawings by the author.

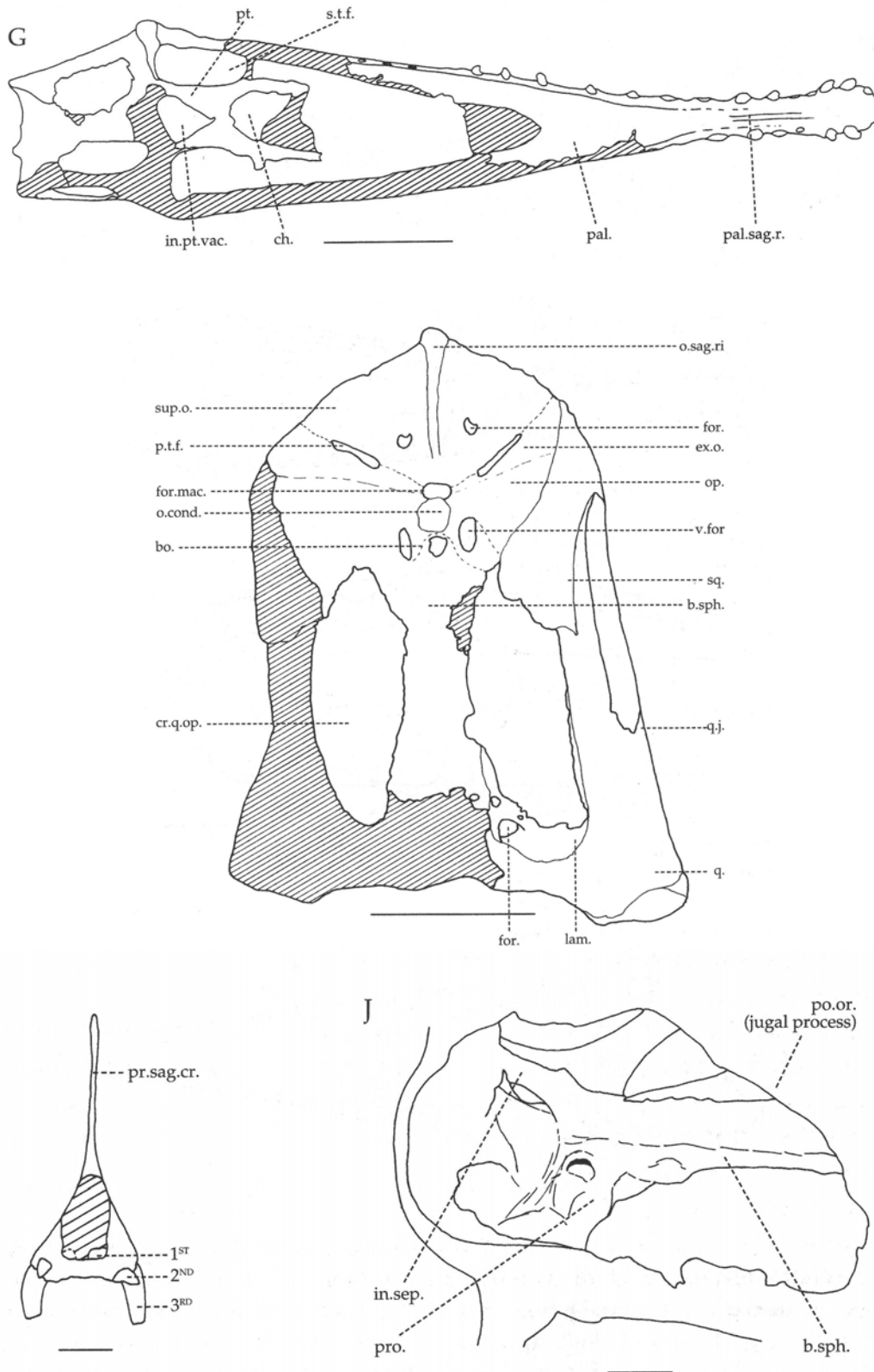


Figure 2.4. *Co. spielbergi* sp. no. (RGM 401 880), the skull in various aspects (with details separately). G: skull, ventral (scale bar = 100 mm); H: base of skull (scale bar = 50 mm); I: skull, anterior (scale bar = 20 mm); J: inner temporal and otic region, oblique anterolateral view (scale bar = 20 mm). Drawings by the author.

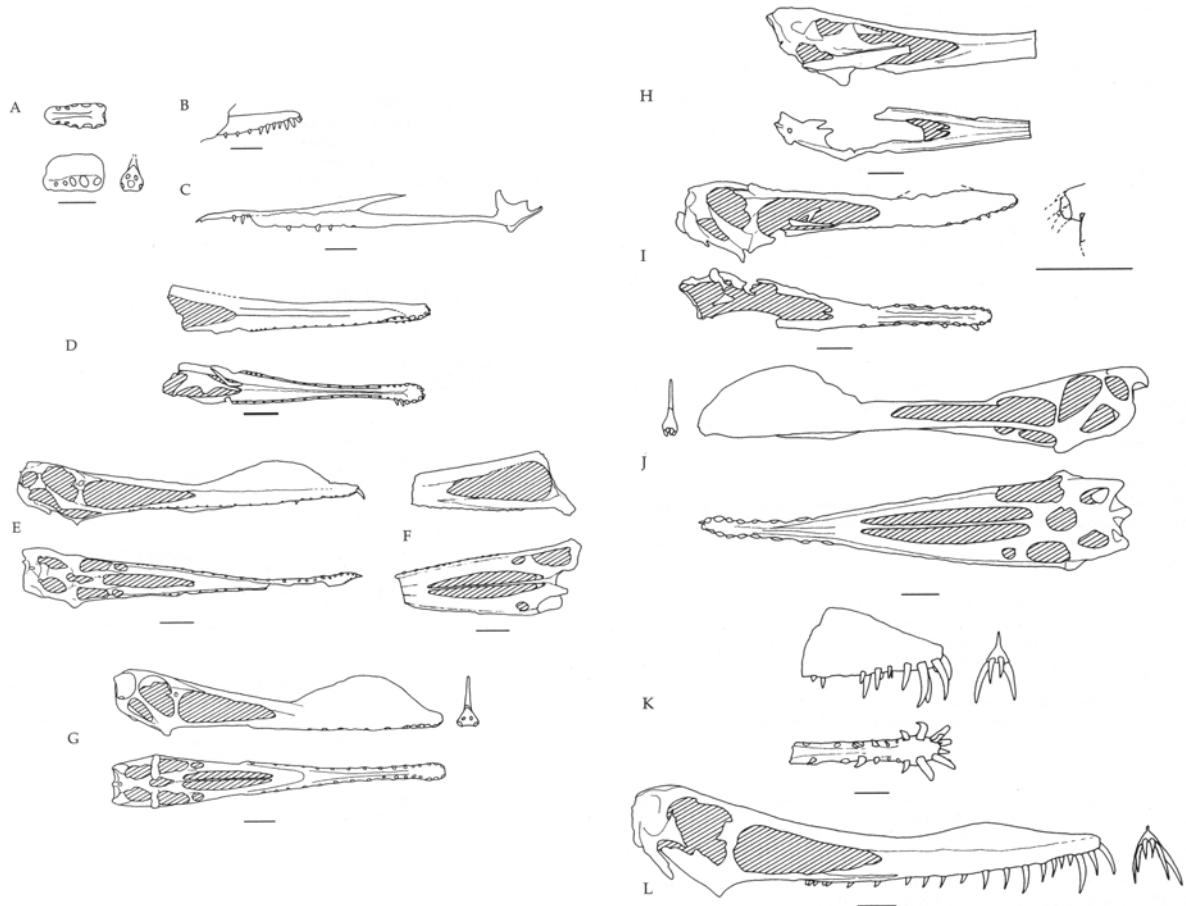


Figure 2.5. Skulls of compared pterosaurs in various aspects. A: *Co. clavirostris* (BMNH 1822/ BMNH 39409); B: *B. cf. araripensis* (MN 4797-V); C: *Ce. atrox* (after Leonardi & Borgomanero, 1985: 77); D: *Ce.? ligabuei* (after Dalla Vecchia, 1993: 404); E: *An. blittersdorffi* (MN 4805-V); F: *Co. araripensis* (BSP 1982 I 89); G: *Co. araripensis* (SAO 16494); H: *An. santanae* (BSP 1982 I 90); I: *An. santanae* (AMNH 22555: reconstruction after Wellnhofer, 1991b: 48); J: *Cr. mesembrinus* (BSP 1987 I 46); K: *Co. robustus* (SMNK 2302 PAL); L: *Co. piscator* (reconstructed, after Kellner & Tomida, 2000: 10, 23). Scale bar = 50 mm (note the different scale of the reconstruction in figure 2.5I). Drawings by E. Endenburg and the author.

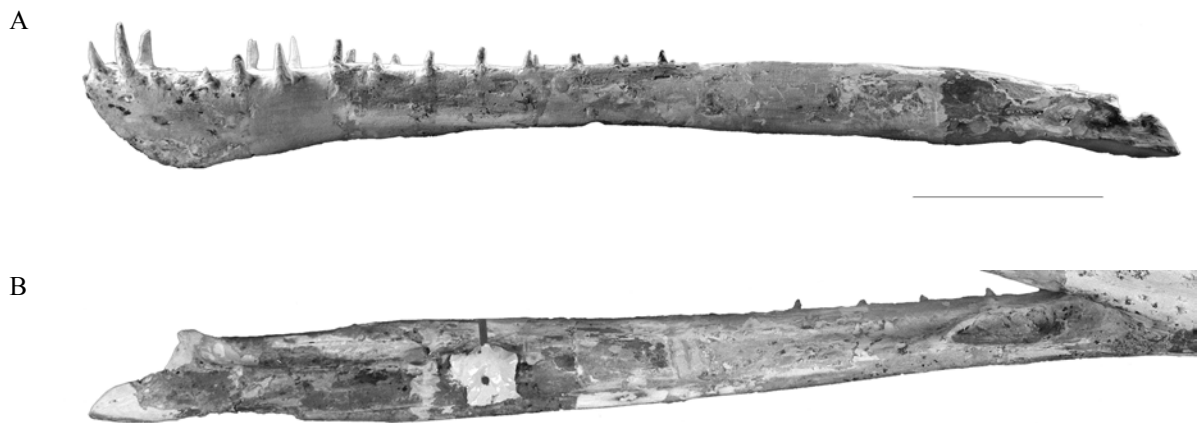


Figure 2.6. *Co. spielbergi* sp. nov. (RGM 401 880), the mandible in various aspects. A: left lateral; B: left ramus, media. Scale bar = 100 mm (unless stated otherwise). Photographs by A. 't Hoofst. Courtesy RGM, Leiden.

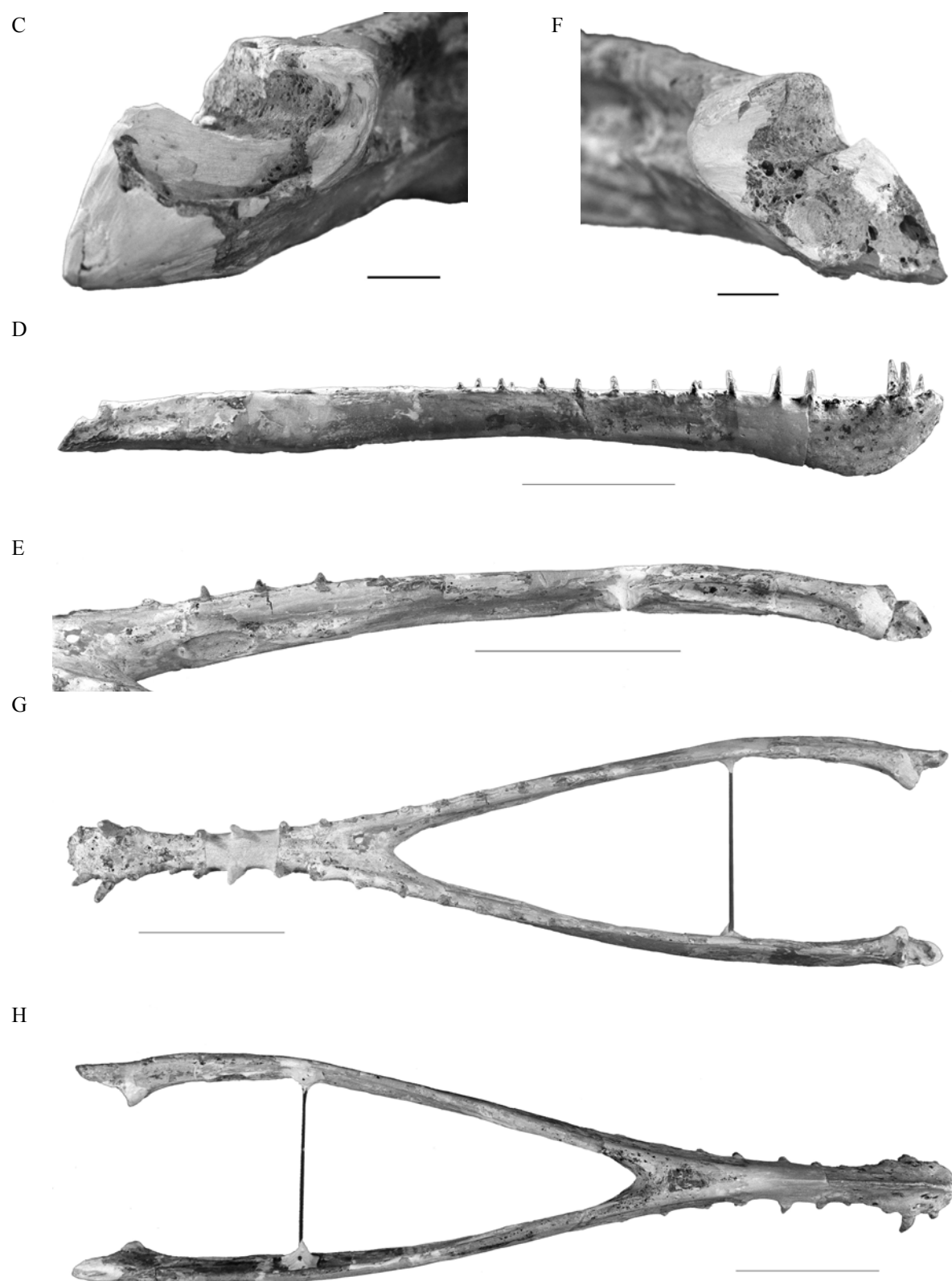


Figure 2.6. *Co. spielbergi* sp. nov. (RGM 401 880), the mandible in various aspects. C: left posterior articular area (scale bar = 10 mm); D: right lateral; E: right ramus, medial; F: right posterior articular area (scale bar = 10 mm); G: dorsal; H: ventral; I: anterior (scale bar = 10 mm). Scale bar = 100 mm (unless stated otherwise). Photographs by A. 't Hooft. Courtesy RGM, Leiden.

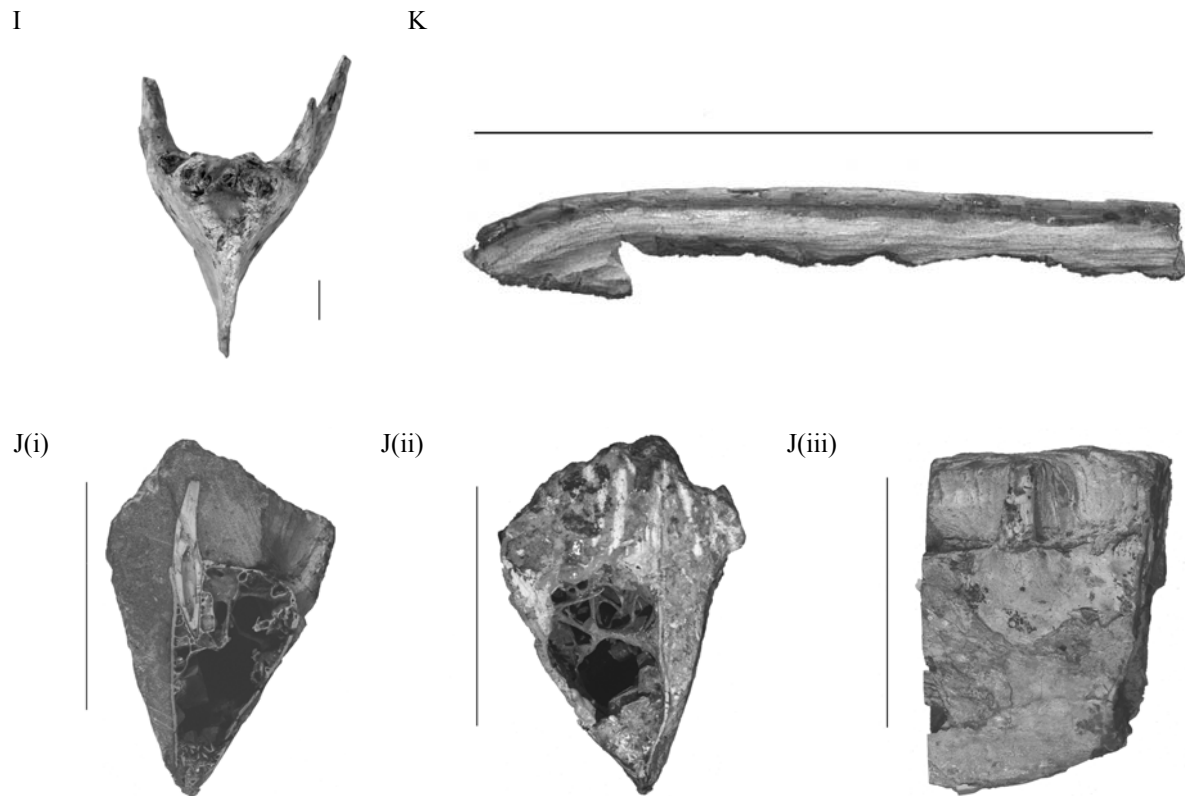


Figure 2.6. *Co. spielbergi* sp. nov. (RGM 401 880), the mandible in various aspects. I: anterior (scale bar = 10 mm); J: cross-section of the mandible in anterior (i), posterior (ii), and left lateral (iii) aspects (scale bar = 50 mm); K: largest part of ?ceratobranchial. Scale bar = 100 mm (unless stated otherwise). Photographs by A. 't Hooft. Courtesy RGM, Leiden.

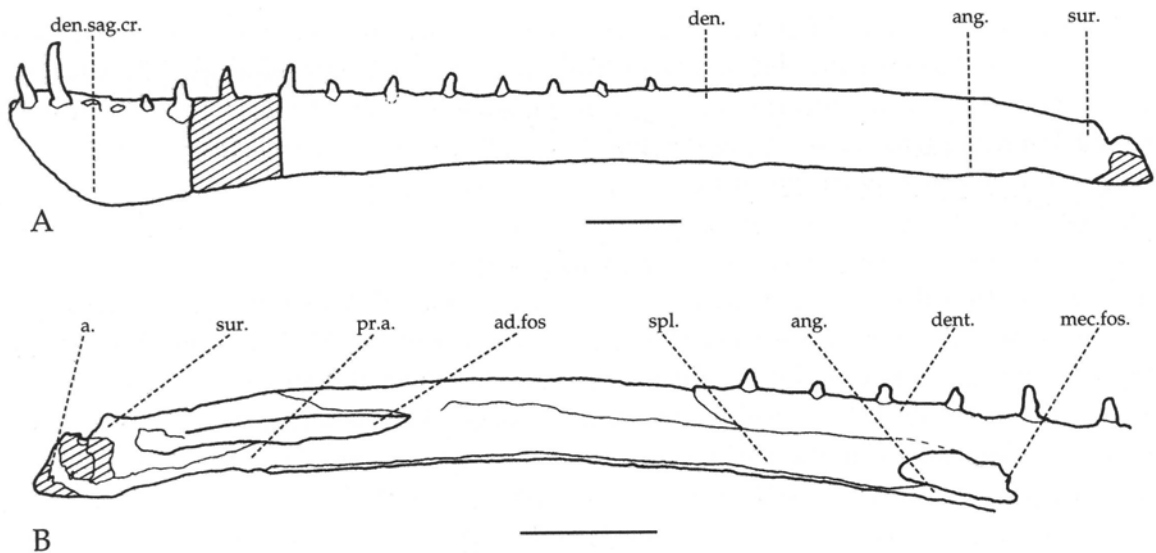


Figure 2.7. *Co. spielbergi* sp. nov. (RGM 401880), the mandible in various aspects (with details separately). A: mandible, left lateral; B: left ramus, medial. Scale bar = 50 mm (unless mentioned otherwise). Drawings by the author.

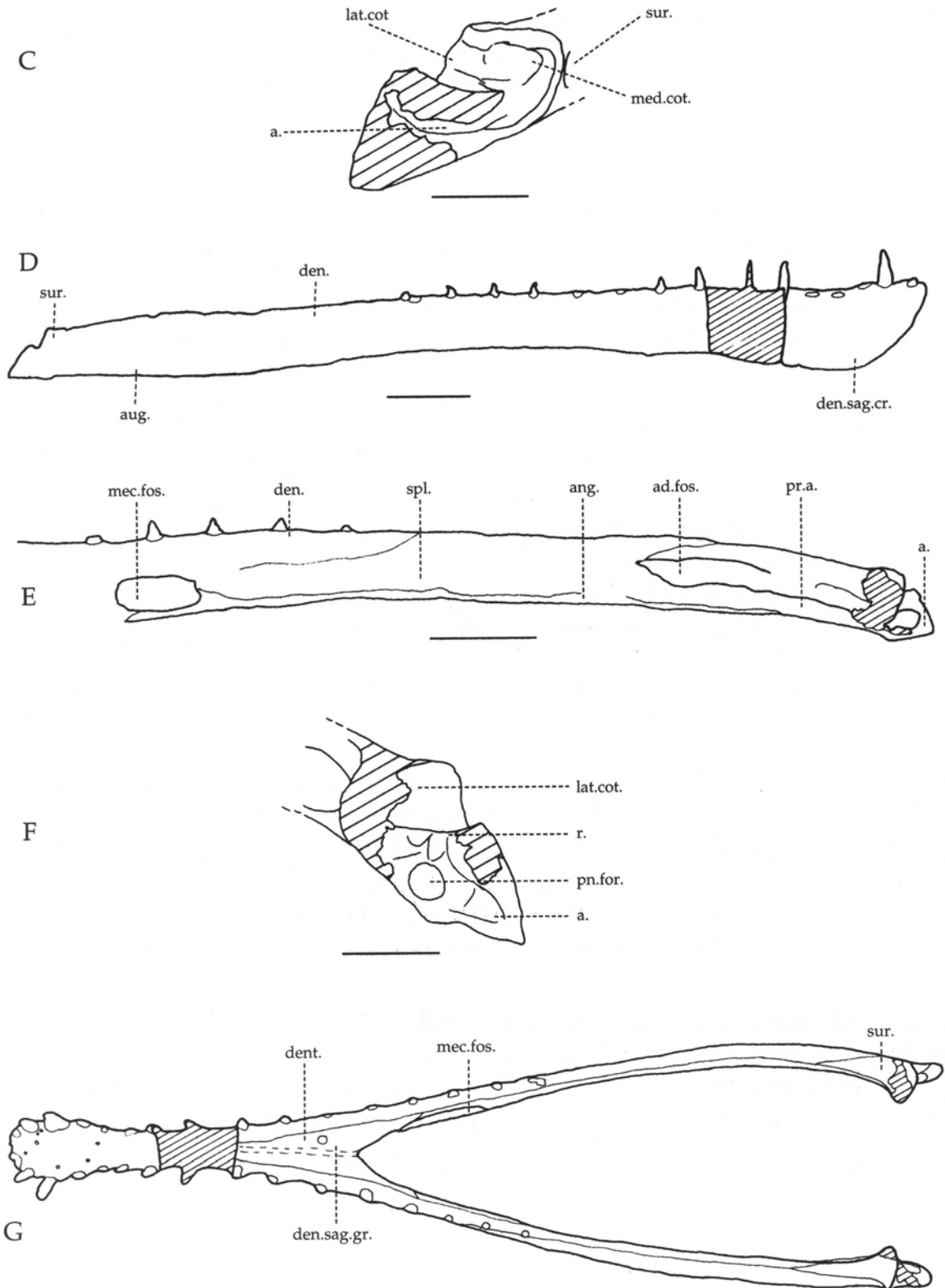


Figure 2.7. *Co. spielbergi* sp. nov. (RGM 401880), the mandible in various aspects (with details separately). C: left retroarticular process, posteromedial view (scale bar = 20 mm); D: mandible, right lateral; E: right ramus, medial; F: right retroarticular process, posteromedial view (scale bar = 20 mm); G: mandible, dorsal. Scale bar = 50 mm (unless mentioned otherwise). Drawings by the author.

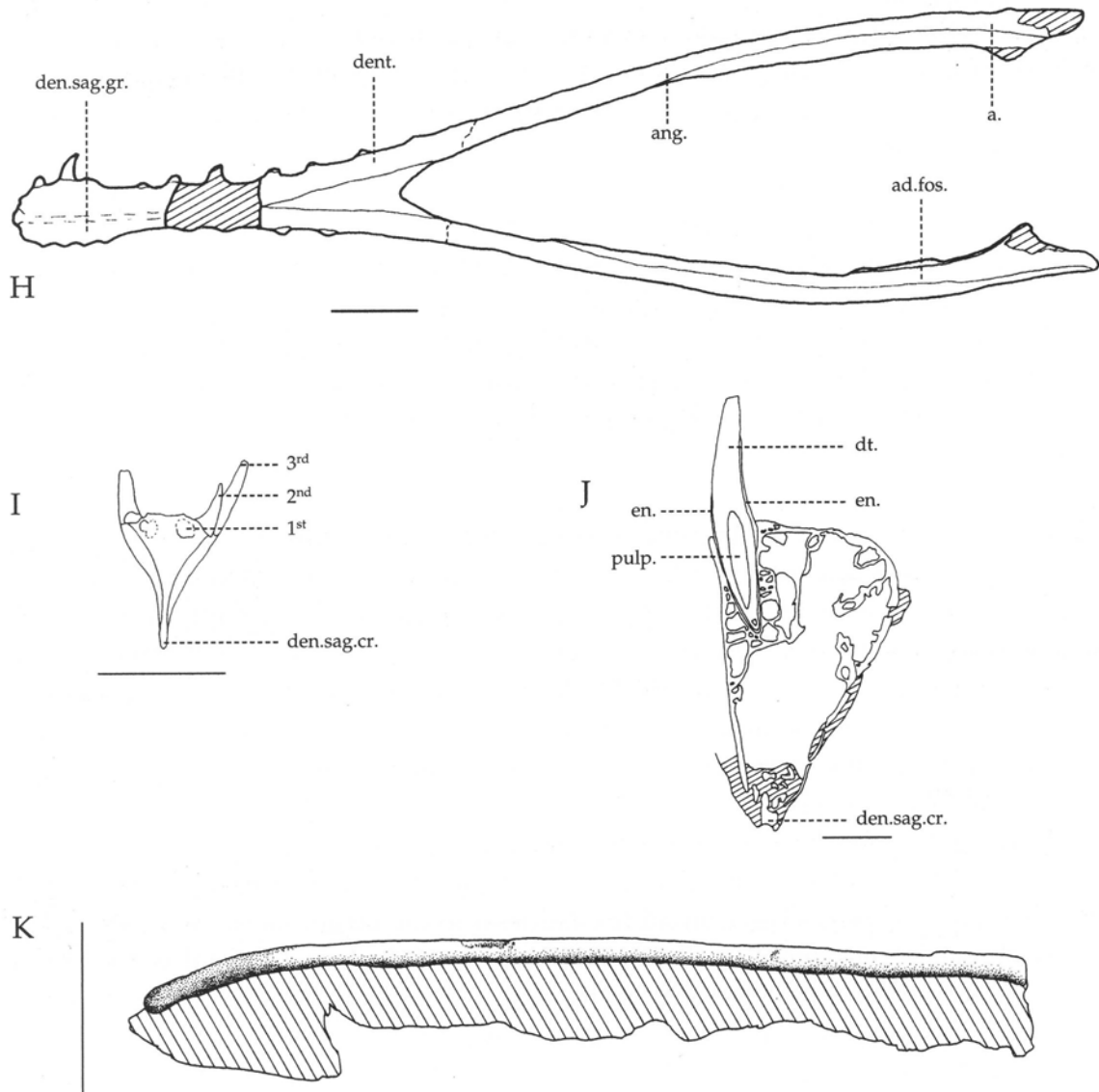


Figure 2.7. *Co. spielbergi* sp. nov. (RGM 401880), the mandible in various aspects (with details separately). H: mandible, ventral; I: mandible, anterior; J: cross section of the mandible (anterior aspect with longitudinal section of tooth seven, right side: scale bar = 10 mm); K: piece of ?ceratobranchial (scale bar = 20 mm). Scale bar = 50 mm (unless mentioned otherwise). Drawings by the author.

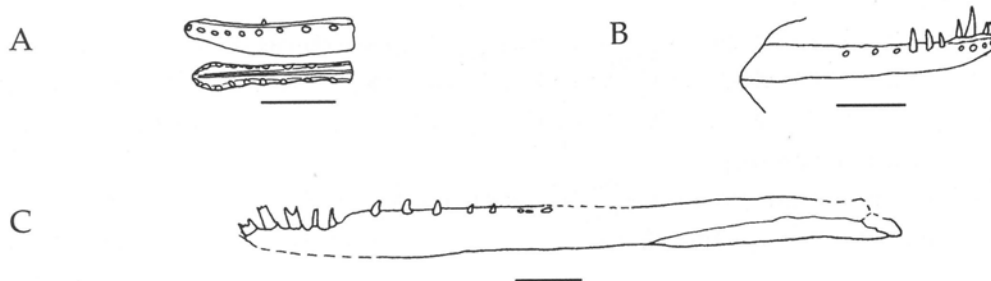


Figure 2.8. Mandibles of compared pterosaurs in various aspects. A: *B. araripensis* (MN 4804-V: after Kellner & Tomida, 2000: 103); B: *B. cf. araripensis* (MN 4797-V); C: *Ce. Atrox*. Scale bar = 50 mm. Drawings by E. Endenburg and the author.

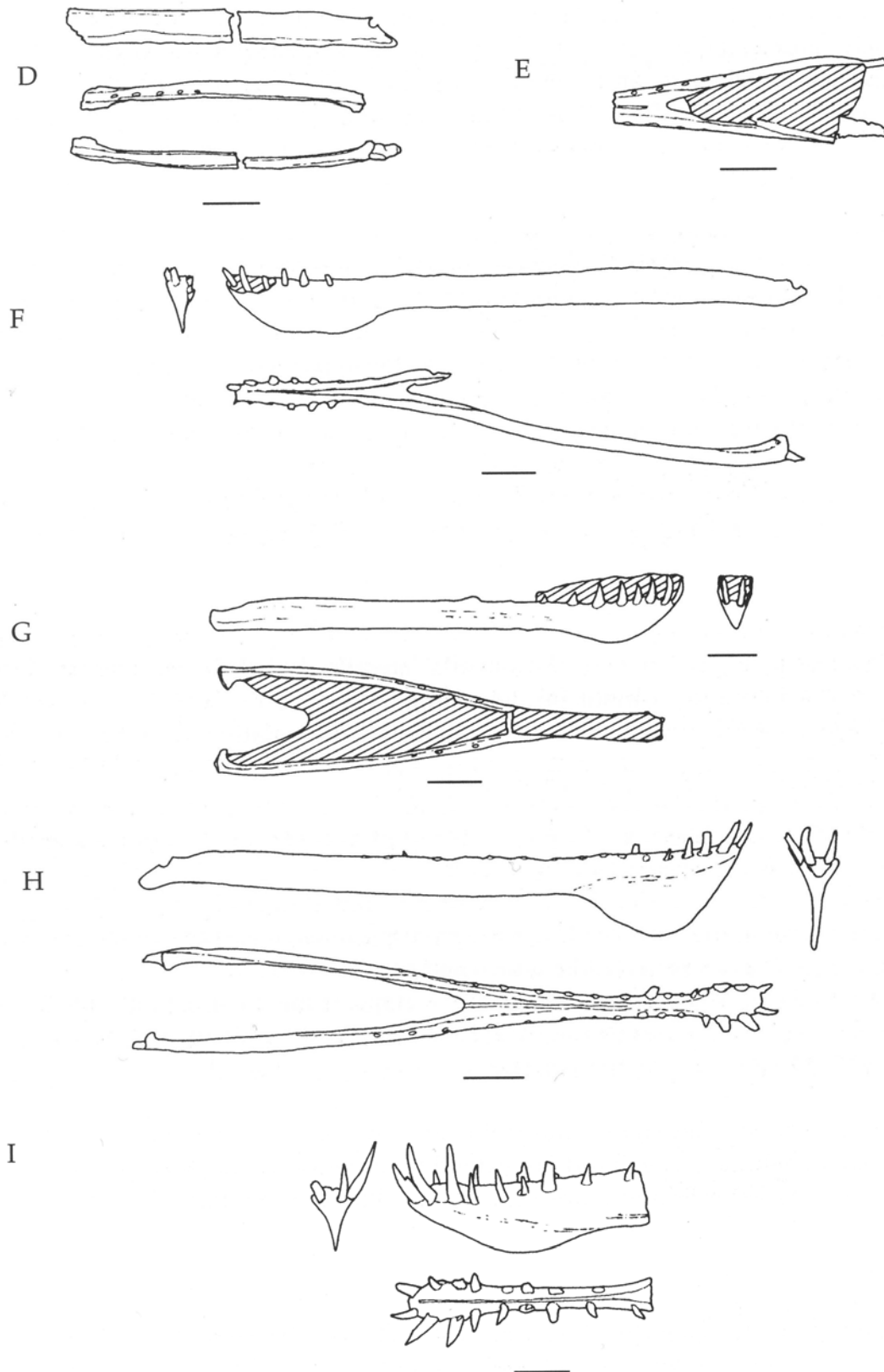


Figure 2.8. Mandibles of compared pterosaurs in various aspects. D: *Co. araripensis* (BSP 1982 I 89); E: *An. santanae* (BSP 1982 I 90); F: *Cr. mesembrinus* (BSP 1987 I 46); G: cf. *Cr. mesembrinus* (SMNS 56994); H: *Co. robustus* (BSP 1987 147); I: *Co. robustus* (SMNK 2302 PAL). Scale bar = 50 mm. Drawings by E. Enderburg and the author.

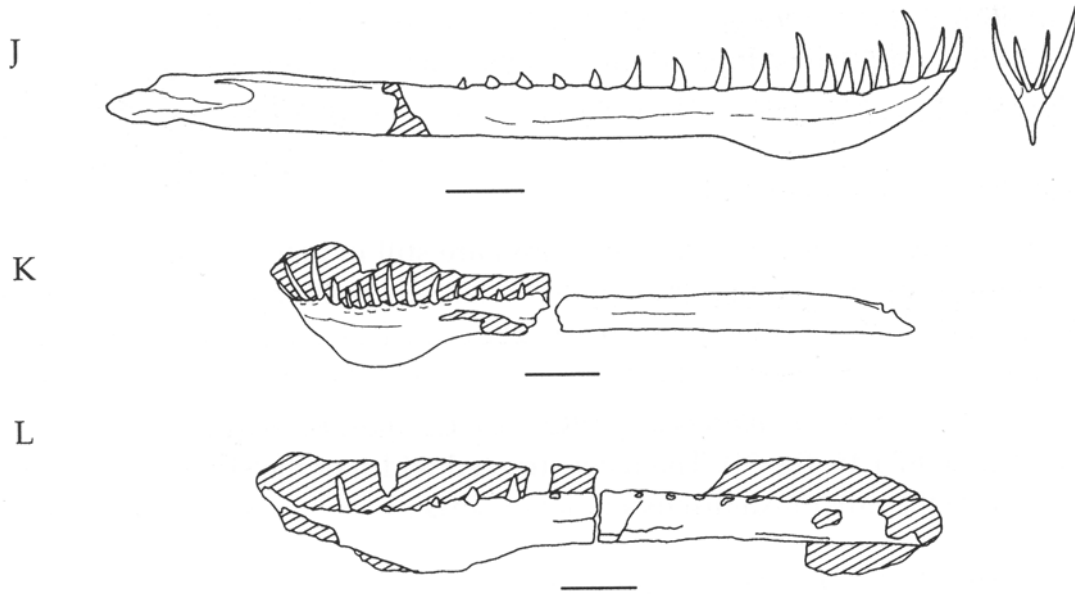


Figure 2.8. Mandibles of compared pterosaurs in various aspects. J: *Co. piscator* (reconstructed, after Kellner & Tomida, 2000: 10, 23); K: *Anhanguera* sp. indet. (SAO 200602); L: *Anhanguera* sp. indet. (AMNH 22573). Scale bar = 50 mm. Drawings by E. Endenburg and the author.

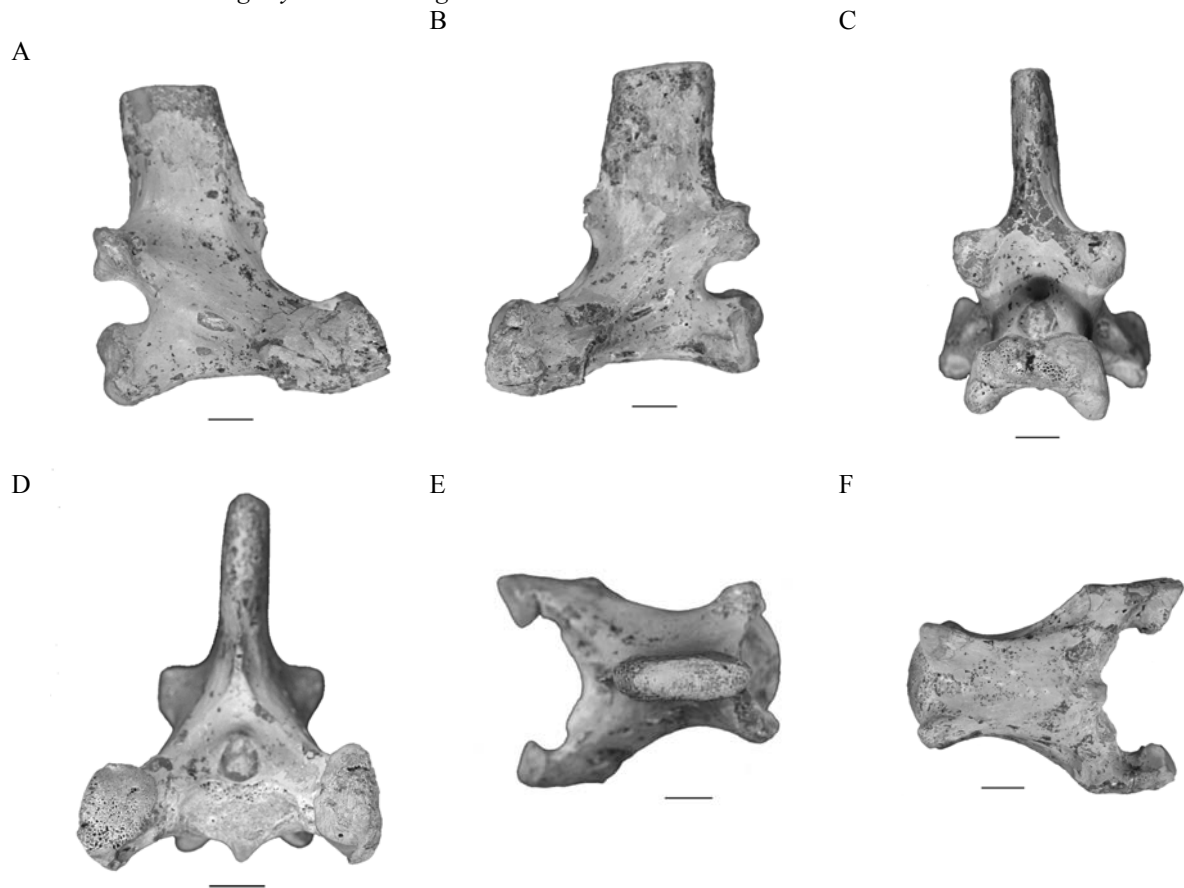


Figure 2.9A-F. *Co. spielbergi* sp. nov. (RGM 401 880), the seventh cervical in various aspects. A: right lateral; B: left lateral; C: posterior; D: anterior; E: dorsal; F: Ventral. Scale bar = 10 mm. Photographs by A. 't Hooft. Courtesy RGM, Leiden.

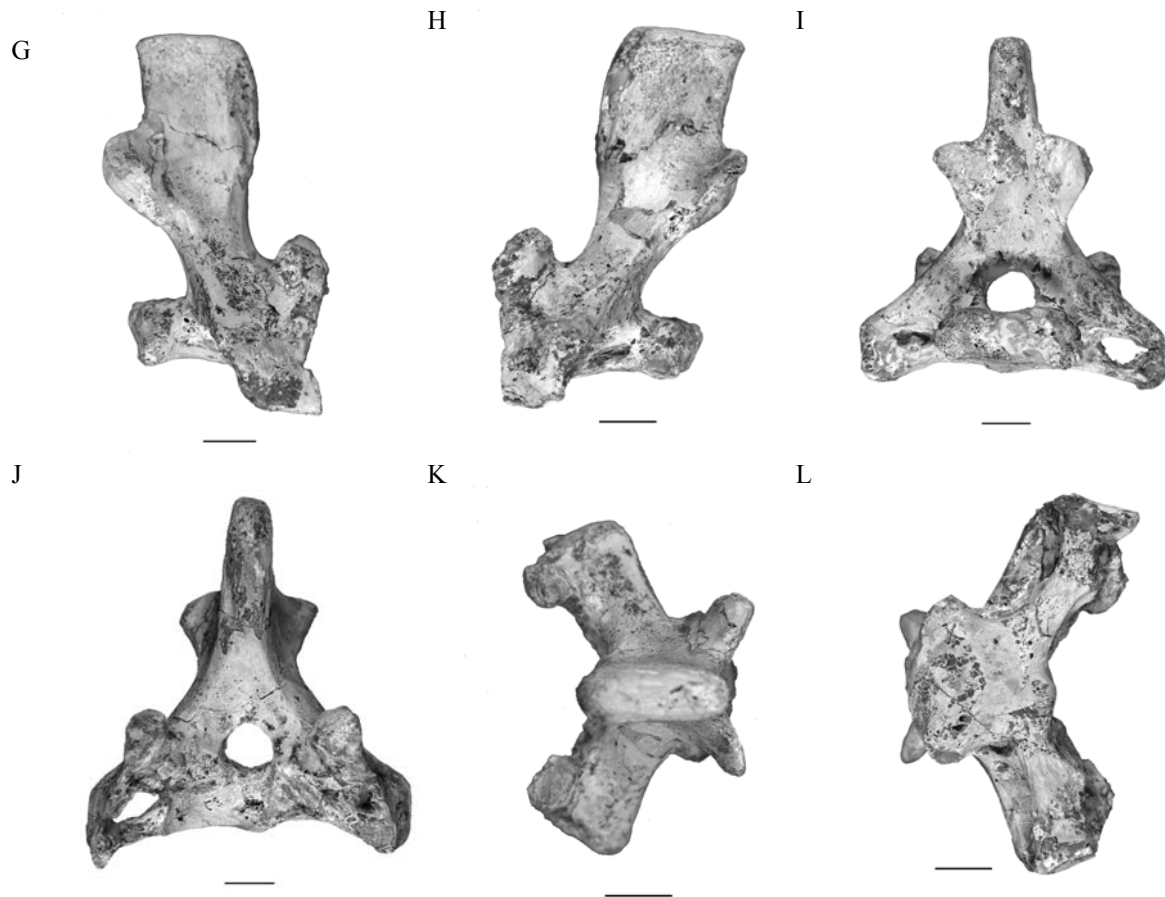


Figure 2.9G-I. *Co. spielbergi* sp. nov. (RGM 401 880), the eighth cervical in various aspects. G: right lateral; H: left lateral; I: posterior; J: anterior; K: dorsal; L: Ventral. Scale bar = 10 mm. Photographs by A. 't Hooft. Courtesy RGM, Leiden.

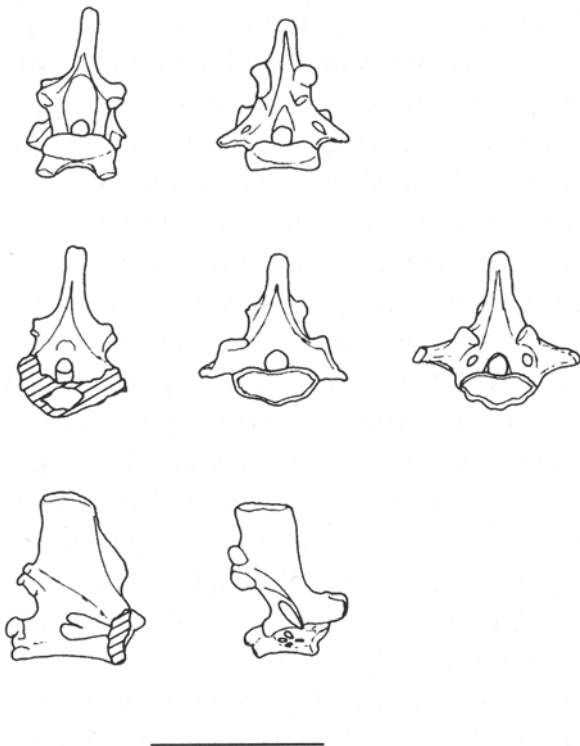


Figure 2.10. Cervicals of a compared pterosaur in various aspects. Seventh, eighth and ninth cervicals (from left to right) of *An. santanae* (AMNH 22555: after Wellnhofer, 1991b: 56-57). Scale bar = 50 mm. Drawings by E. Enderburg and the author.

A

C,
BD,
E

F



Figure 2.11. *Co. spielbergi* sp. nov. (RGM 401 880), the notarium in various aspects. A: right lateral; B: left lateral; C: anterior; D: posterior; E: dorsal; F: ventral. Scale bar = 50 mm. Photographs by A. 't Hooft. Courtesy RGM, Leiden.

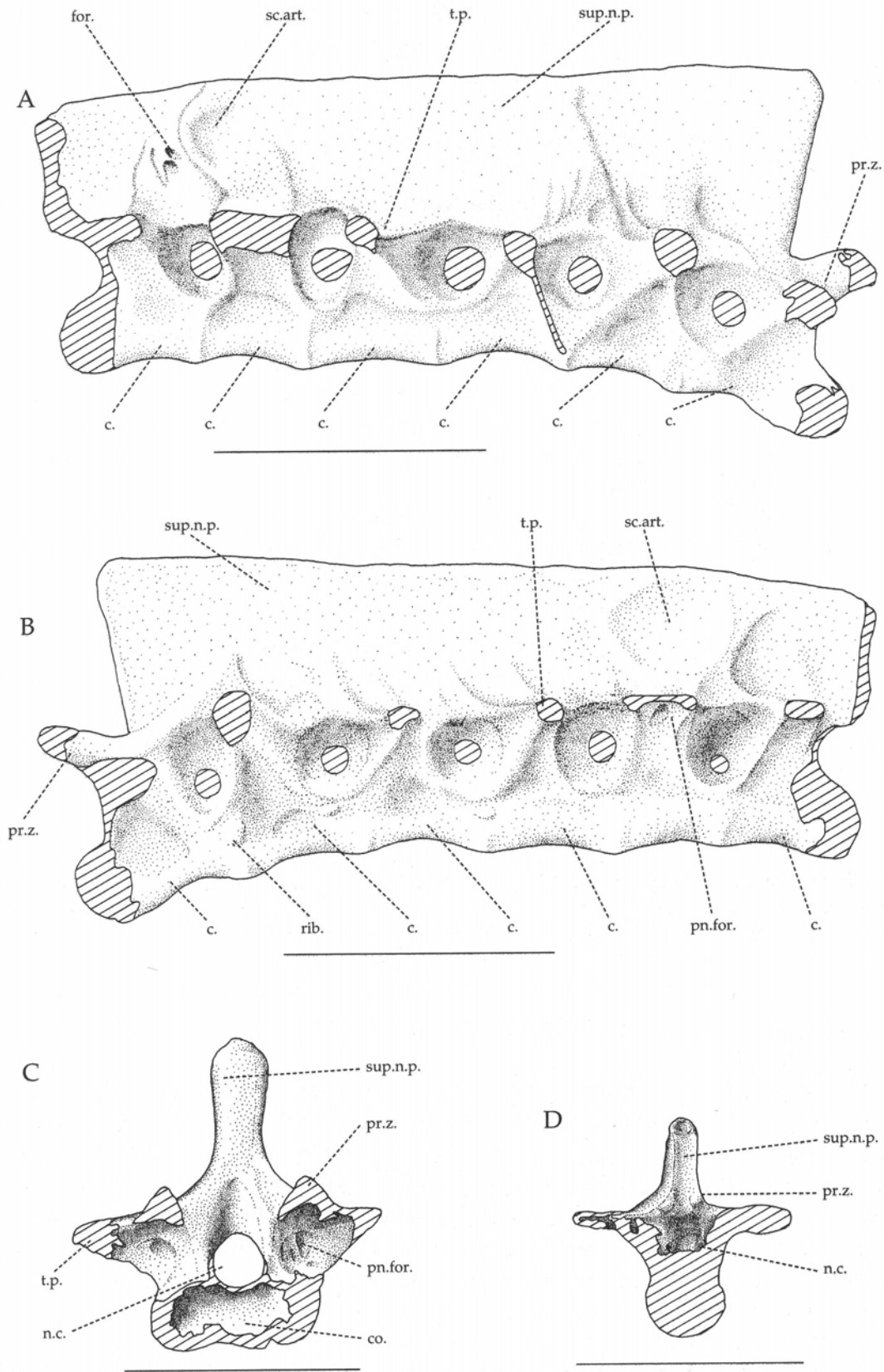


Figure 2.12. *Co. spielbergi* sp. nov. (RGM 401880), the notarium in various aspects. A: right lateral; B: left lateral; C: anterior; D: posterior. Scale bar = 50 mm. Drawings by the author.

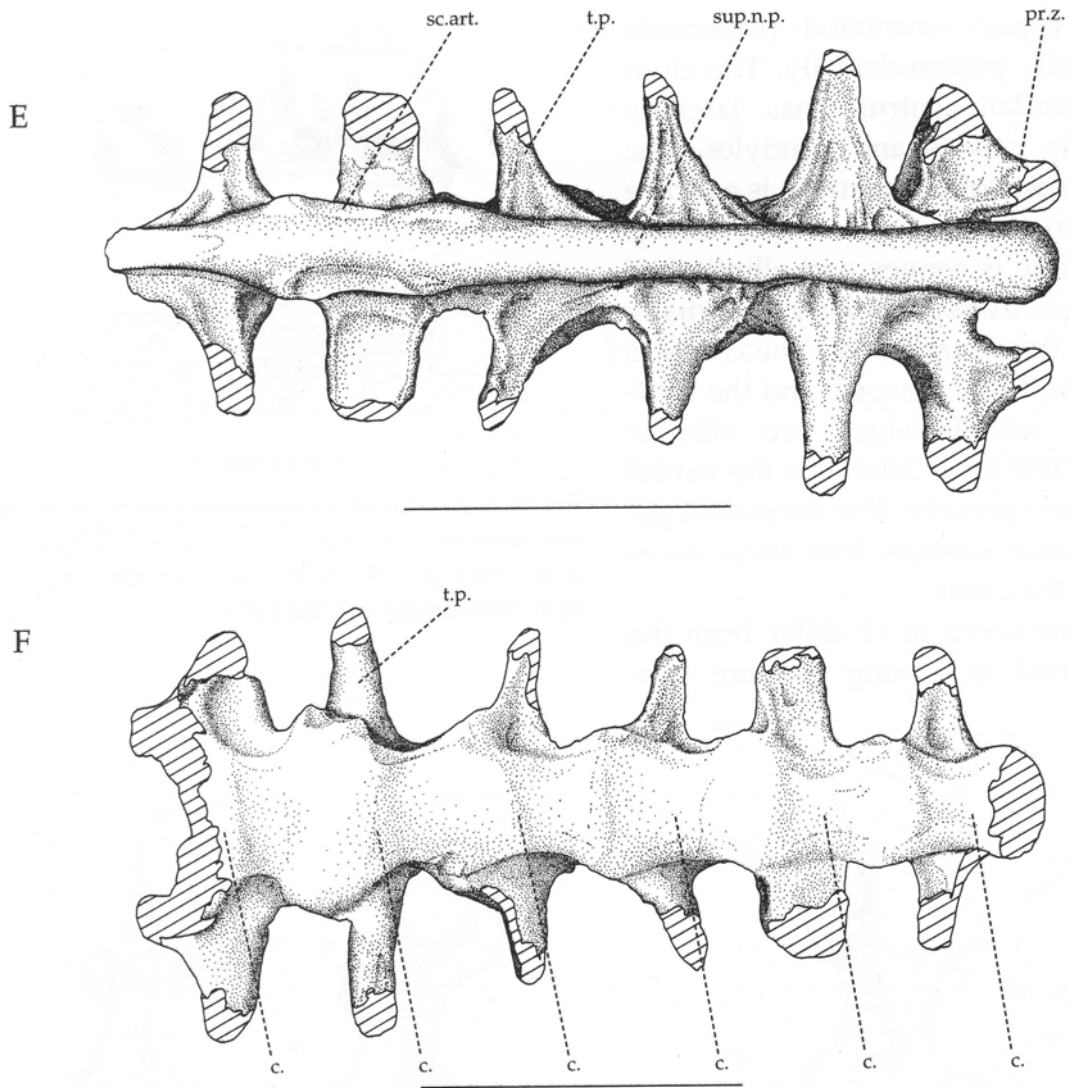


Figure 2.12. *Co. spielbergi* sp. nov. (RGM 401880), the notarium in various aspects. E: dorsal; F: ventral. (Note that only one transverse process is indicated). Scale bar = 50 mm. Drawings by the author.

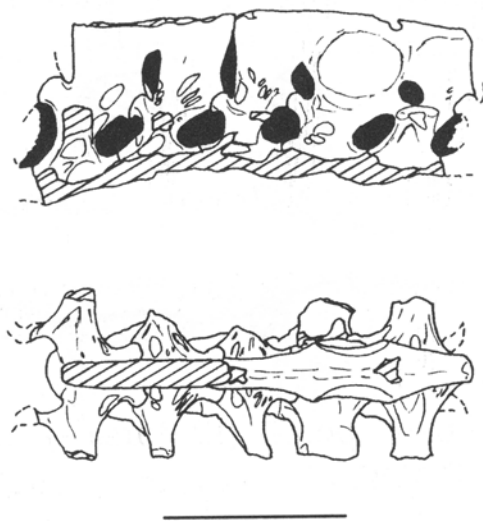


Figure 2.13. Notarium of a compared pterosaur in various aspects, *S. brasilensis* (V-201; after Wellnhofer et al., 1983: 153). Scale bar = 50 mm. Drawings by E. Endenburg and the author.

A

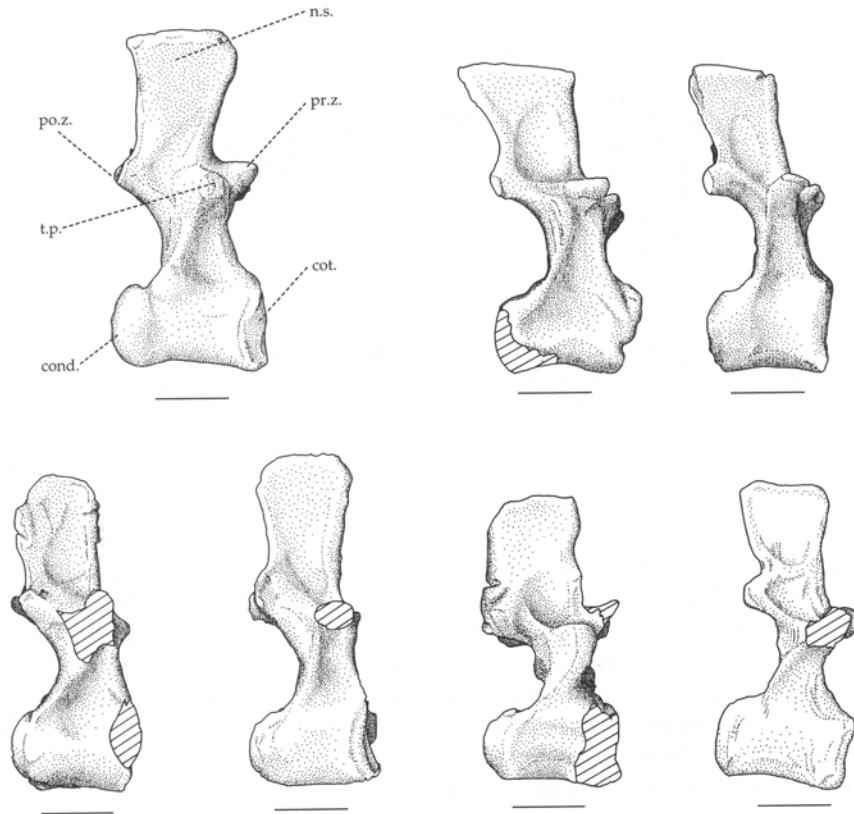


Figure 2.14A. *Co. spielbergi* sp. nov. (RGM 401880), the sixth to twelfth (from left to right, top to bottom) dorsal vertebrae in right lateral aspects.. Scale bar = 10 mm. Drawings by the author.

B

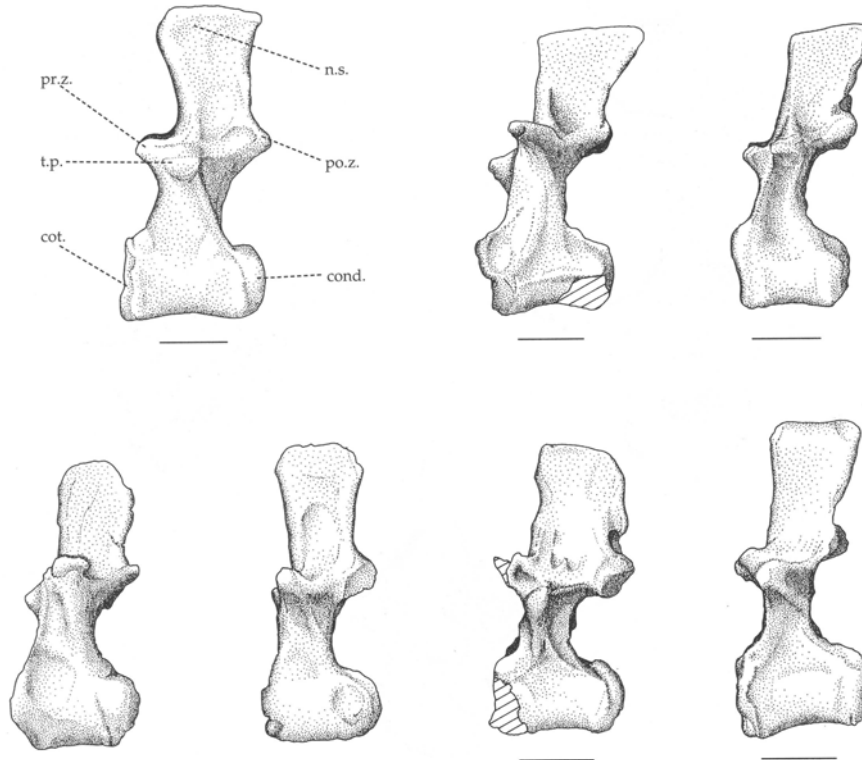


Figure 2.14B. *Co. spielbergi* sp. nov. (RGM 401880), the sixth to twelfth (from left to right, top to bottom) dorsal vertebrae in left lateral aspect. Scale bar = 10 mm. Drawings by the author.

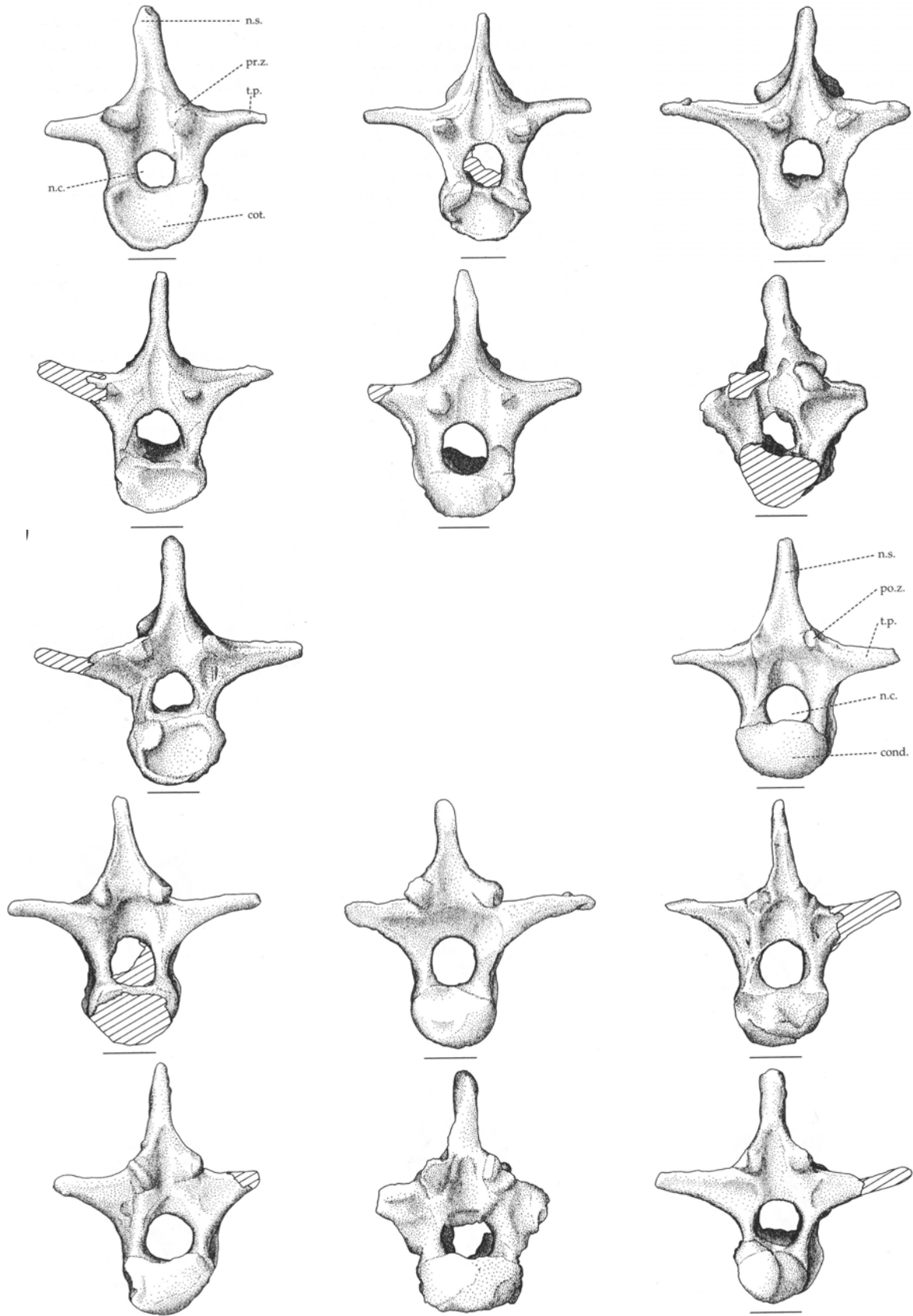


Figure 2.14C (first 7 figures). *Co. spielbergi* sp. nov. (RGM 401880), the sixth to twelfth (from left to right, top to bottom) dorsal vertebrae in anterior aspect; D: (last 7 figures) the sixth to twelfth (from left to right, top to bottom) dorsal vertebrae in posterior aspect. Scale bar = 10 mm. Drawings by the author.

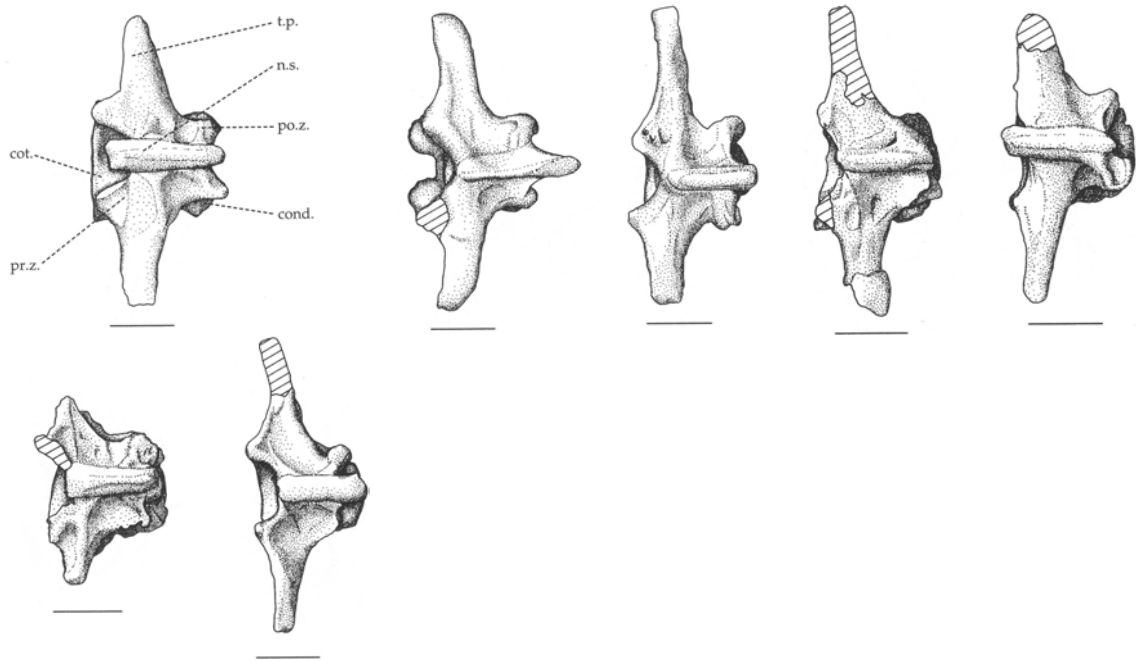


Figure 2.14E. *Co. spielbergi* sp. nov. (RGM 401880), the sixth to twelfth (from left to right, top to bottom) dorsal vertebrae in dorsal aspect. Scale bar = 10 mm. Drawings by the author.

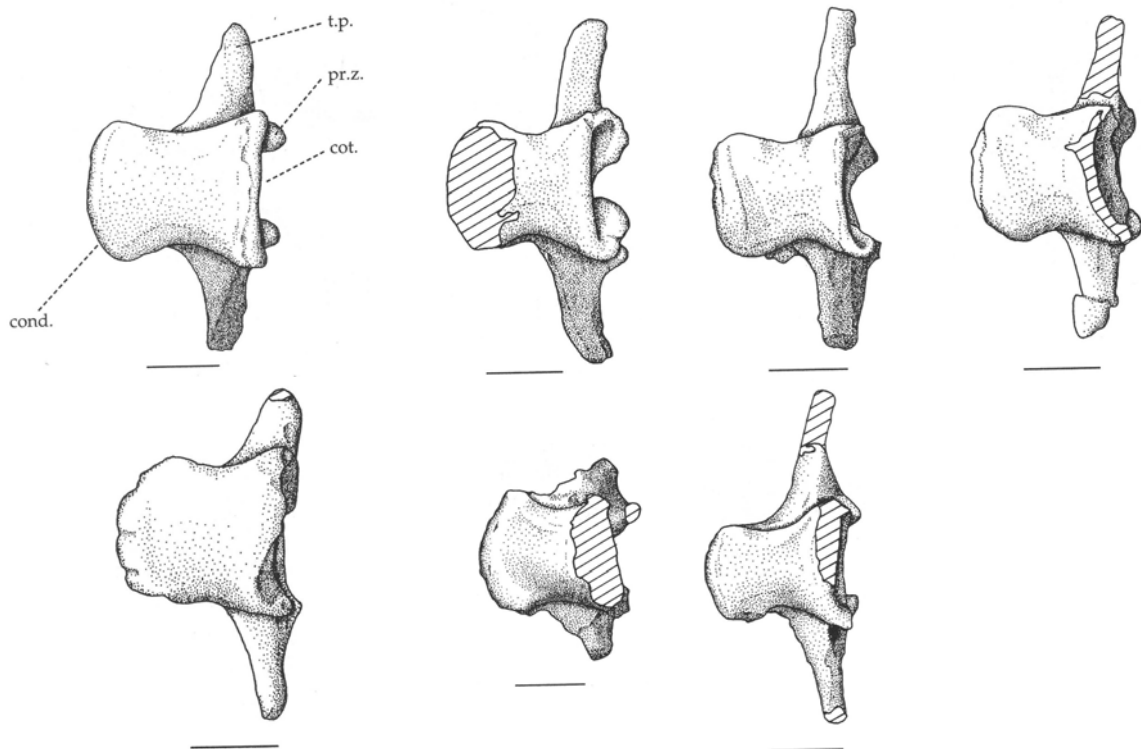


Figure 2.14F. *Co. spielbergi* sp. nov. (RGM 401880), the sixth to twelfth (from left to right, top to bottom) dorsal vertebrae in ventral aspect. Scale bar = 10 mm. Drawings by the author.

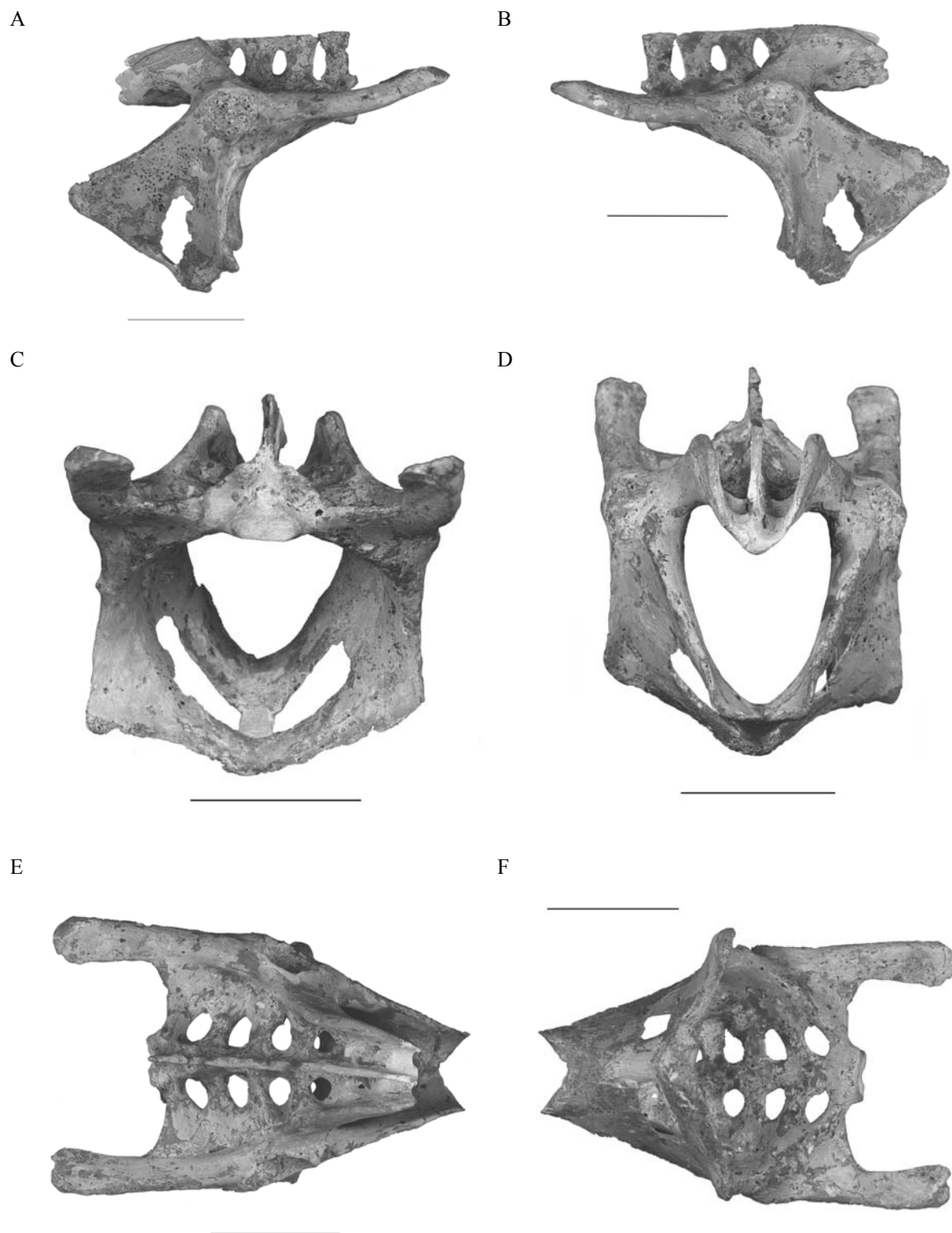


Figure 2.15. *Co. spielbergi* sp. nov. (RGM 401 880), the pelvis in various aspects. A: right lateral; B: left lateral; C: anterior; D: posterior; E: dorsal; F: ventral. Scale bar = 50 mm. Photographs by A. 't Hoof. Courtesy RGM, Leiden.

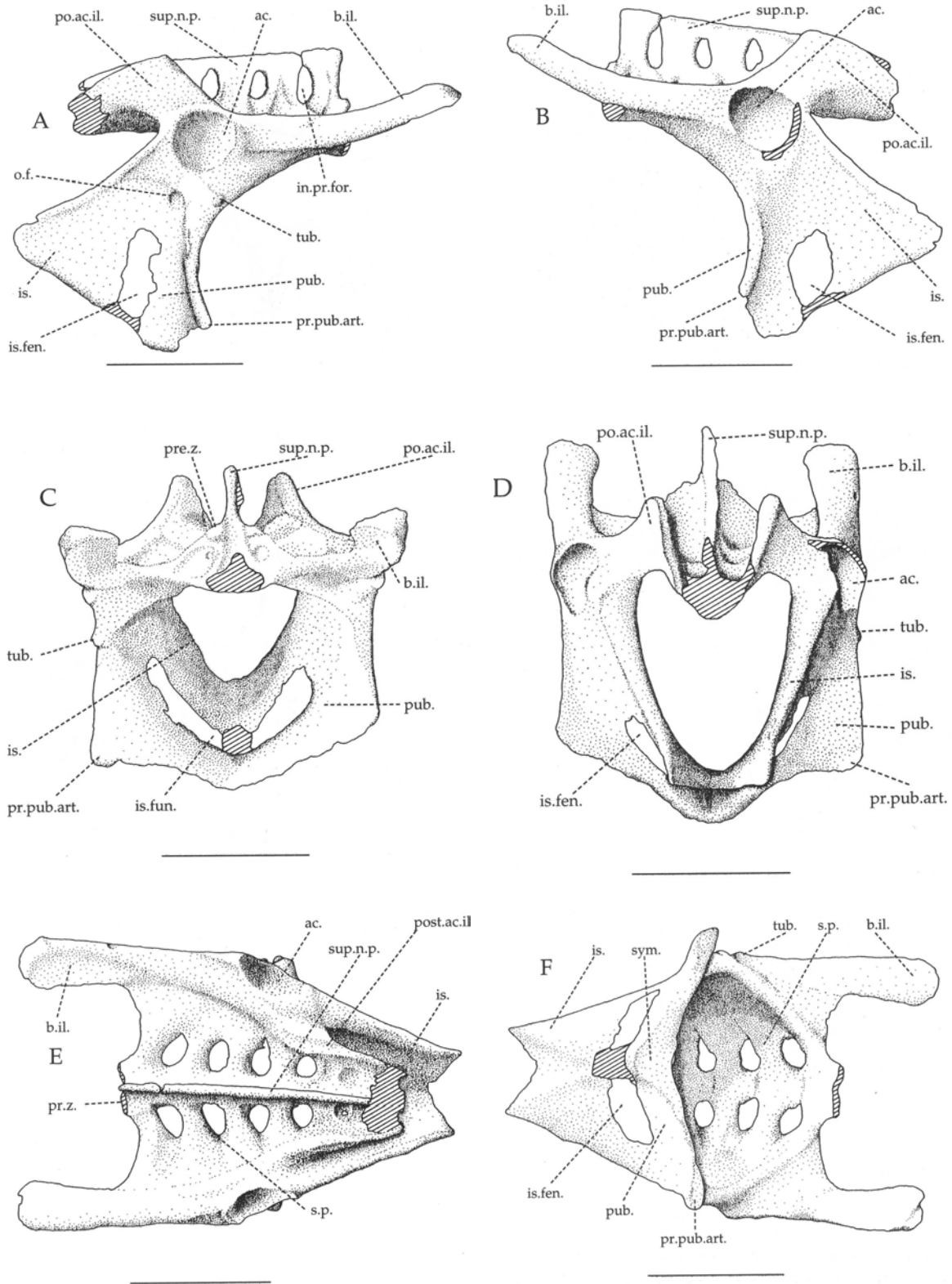


Figure 2.16. *Co. spielbergi* sp. nov. (RGM 401880), the pelvis in various aspects. A: right lateral; B: left lateral; C: anterior; D: posterior; E: dorsal; F: ventral. Scale bar = 50 mm. Drawings by the author.

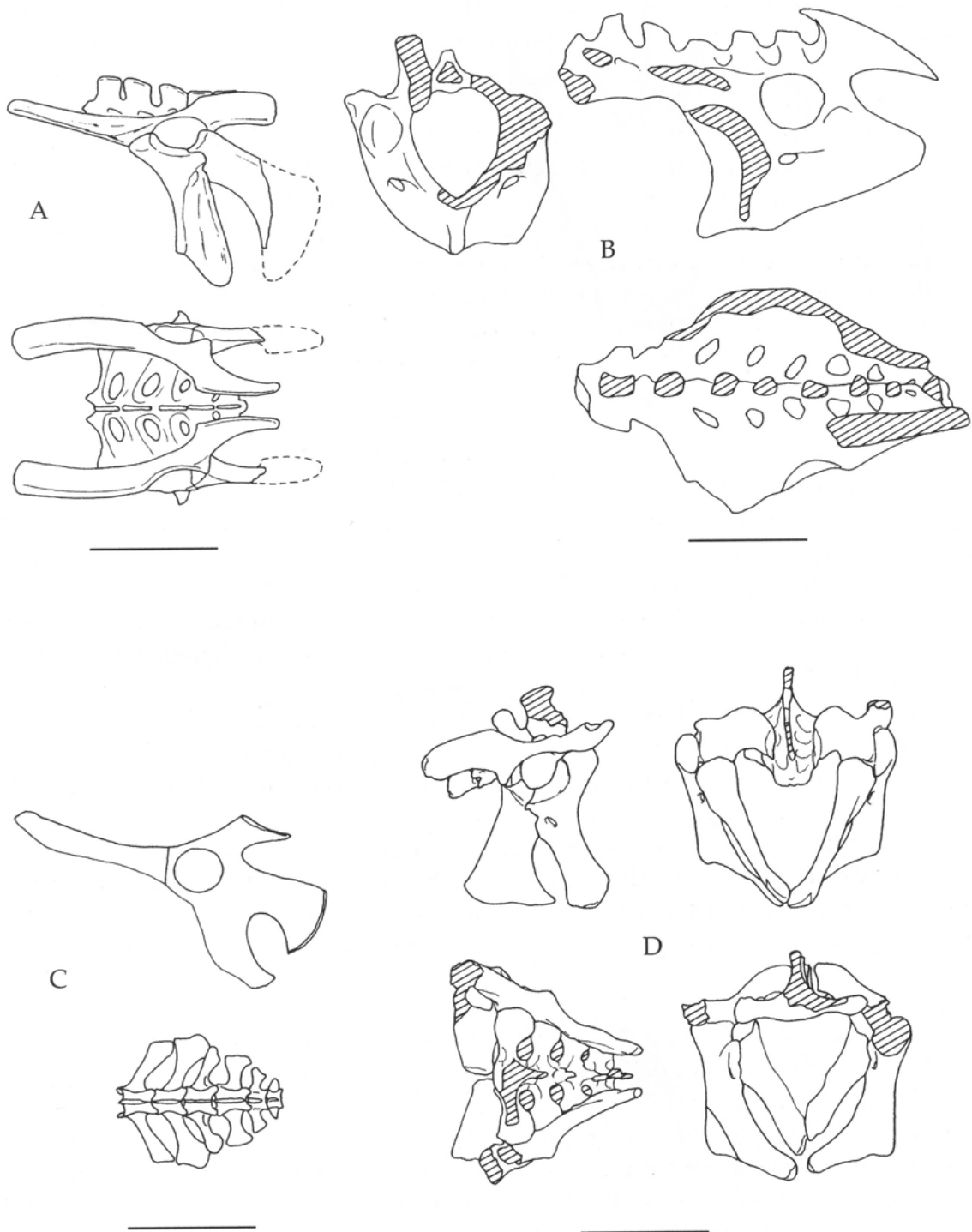


Figure 2.17. Pelves of compared pterosaurs in various aspects. A: *An. santanae* (AMNH 22555; after Wellnhofer, 1988: 10); B: AMNH 22569 (after Bennett, 1990: 81); C: reconstruction of *Ar. conandoylei* (SMNK 1132 PAL; after Frey & Martill, 1994: 393-394); D: *Co. piscator* (NSM-PV 19892; after Kellner & Tomida, 2000: 72-73). Scale bar = 50 mm. Drawings by the author.



Figure 2.18 (right). *Co. spielbergi* sp. nov. (RGM 401 880). A: four pieces of cervical rib, anterior aspect (scale bar = 20 mm); B: the first notarial rib right in various aspects. From top to bottom: lateral; medial; dorsal; ventral (scale bar = 30 mm). Photographs by A. 't Hooft. Courtesy RGM, Leiden.

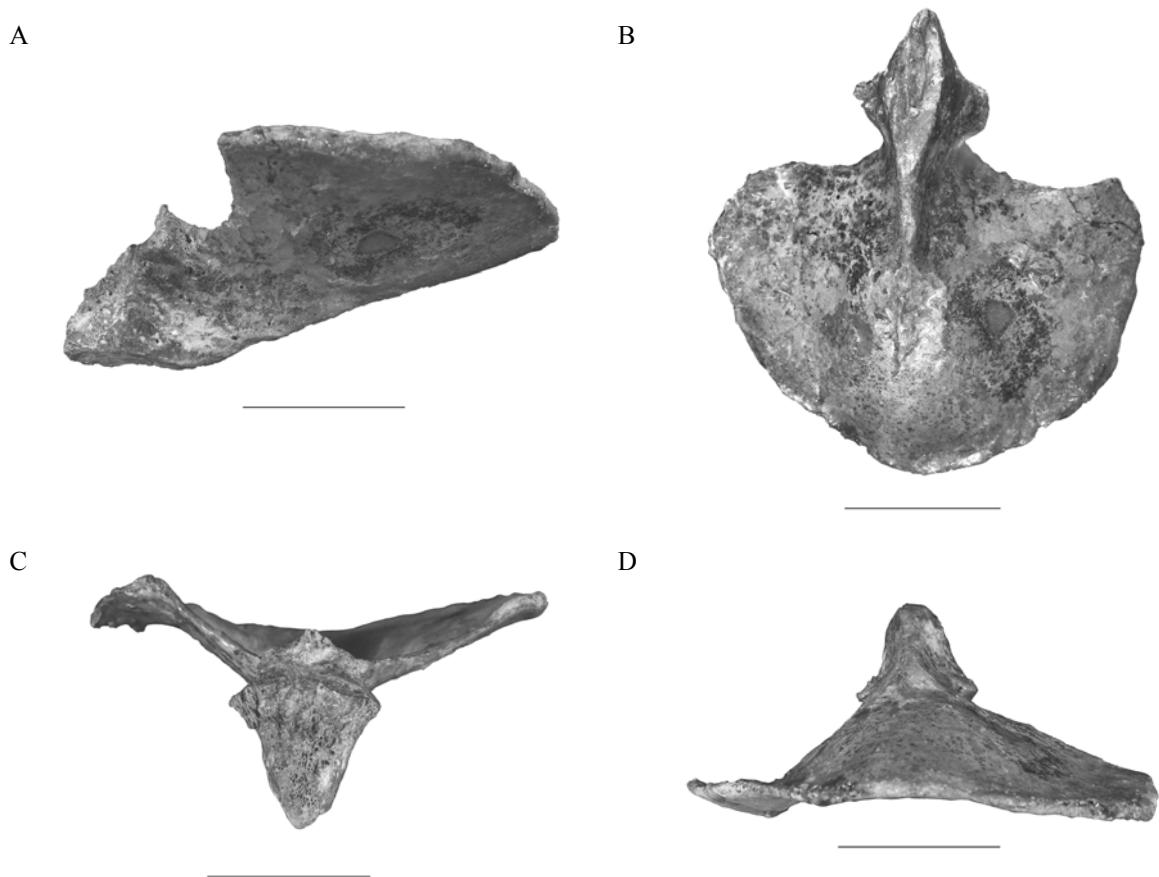


Figure 2.19. *Co. spielbergi* sp. nov. (RGM 401 880), the sternum in various aspects. A: left lateral; B: ventral; C: anterior; D: posterior. Scale bar = 50 mm. Photographs by A. 't Hooft. Courtesy RGM, Leiden.

E

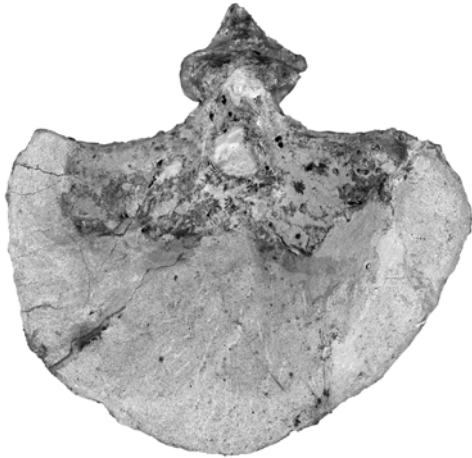
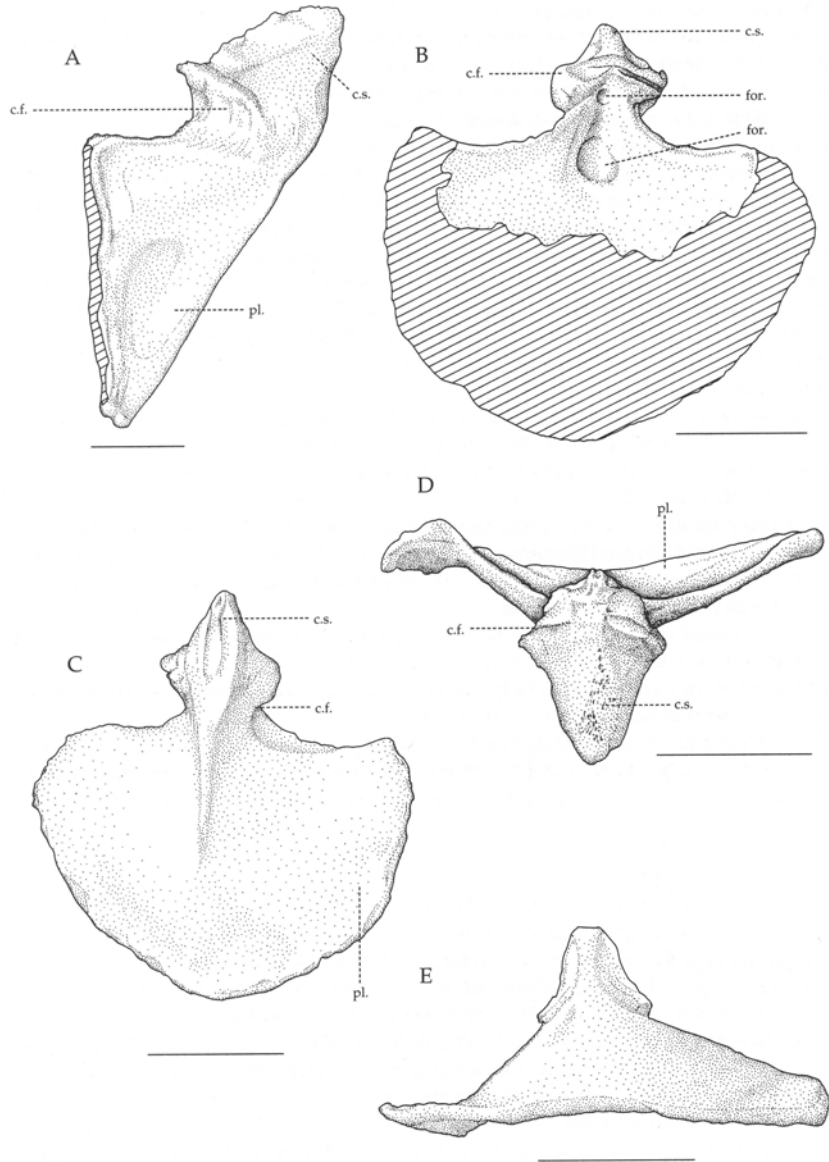


Figure 2.19E (left). *Co. spielbergi* sp. nov. (RGM 401 880), the sternum in dorsal aspect. (Note that the dorsal aspect was not included in Veldmeijer (2003a)). Scale bar = 50 mm. Photograph by A. 't Hoft. Courtesy RGM, Leiden.

Figure 2.20 (below). *Co. spielbergi* sp. Nov. (RGM 401 880), the sternum in various aspects. A: right lateral; B: dorsal; C: ventral; D: anterior; E: posterior. Scale bar = 50 mm. Drawings by the author.



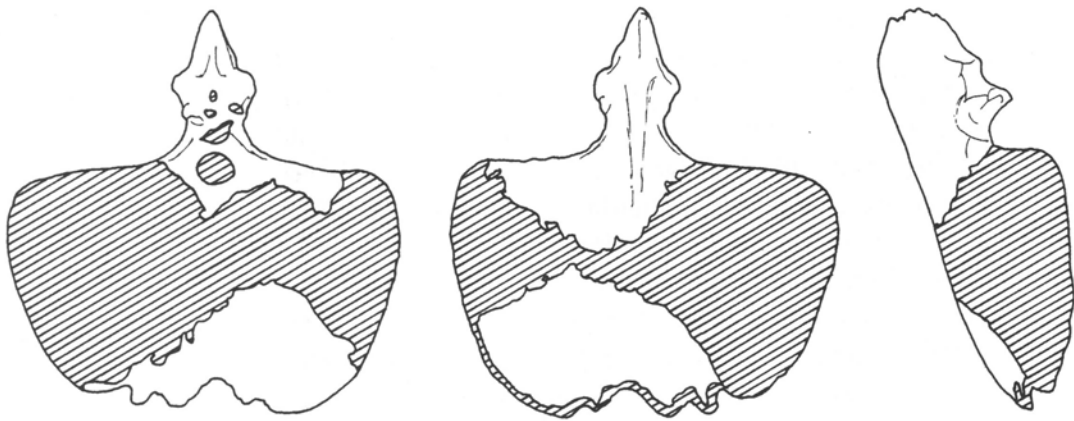


Figure 2.21 Sternum of a compared pterosaur in various aspects. *Co. piscator* (NSM-PV 19892; after Kellner & Tomida, 2000: 45, 47, 48). Scale bar = 50 mm. Drawings by the author.

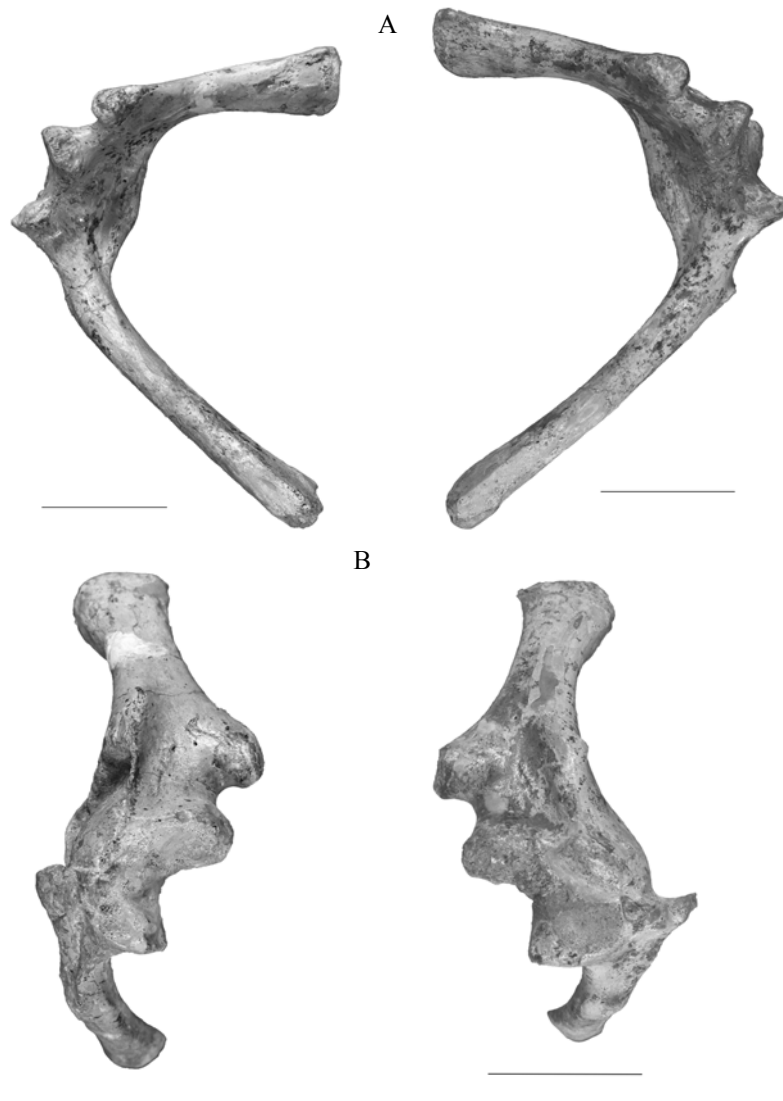


Figure 2.22. *Co. spielbergi* sp. nov. (RGM 401 880), the scapulocoracoids in A: posterior and B: lateral aspect (left and right respectively). Scale bar = 50 mm. Photographs by A. 't Hoofi. Courtesy RGM, Leiden.

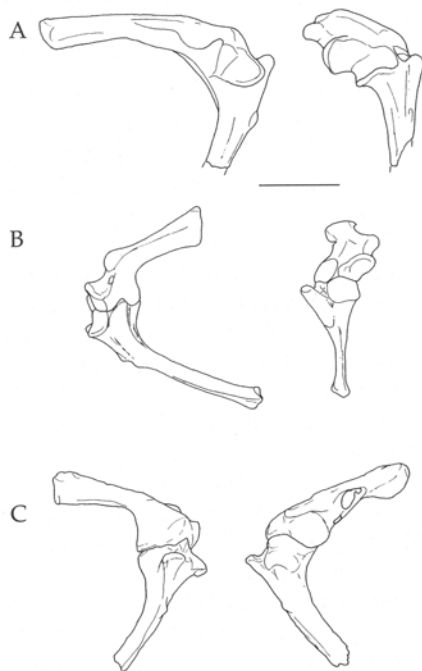
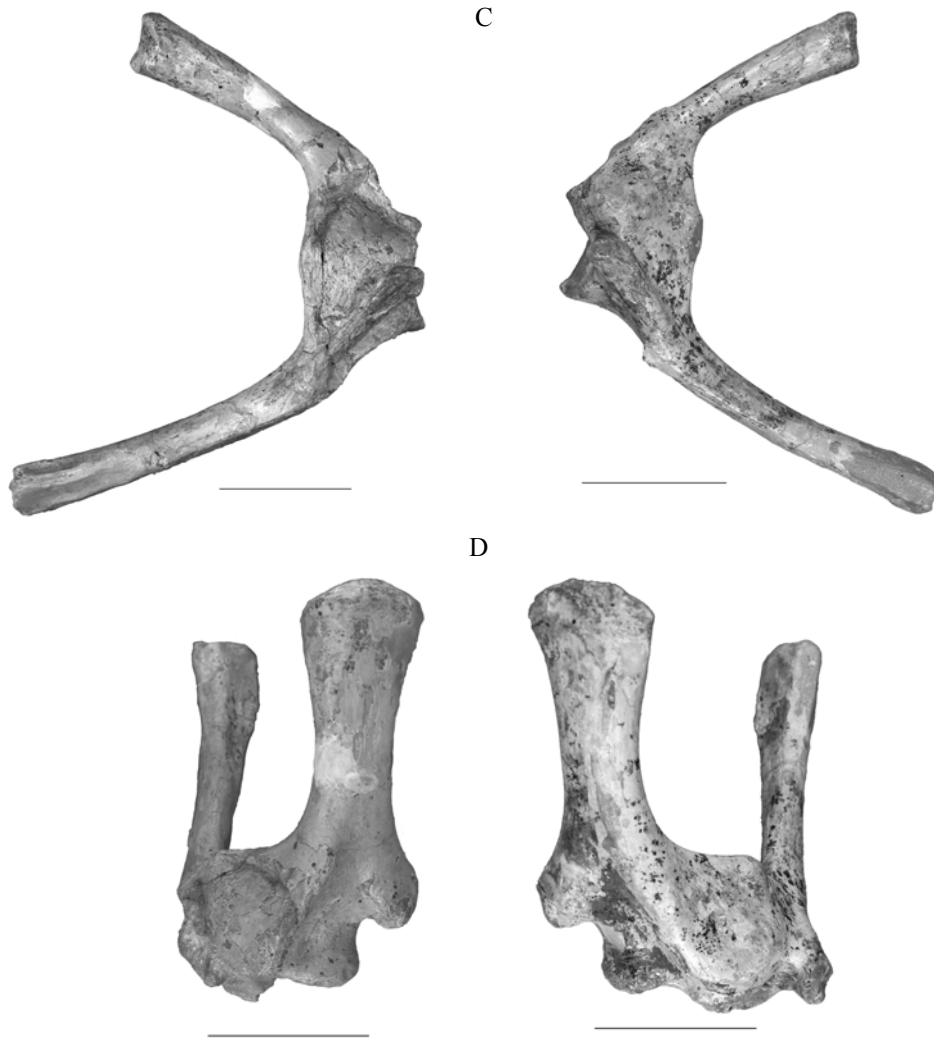


Figure 2.22 (above). *Co. spielbergi* sp. nov. (RGM 401 880), the scapulocoracoids in various aspects (left and right respectively). C: anterior; D: dorsal. Scale bar = 50 mm. Photographs by A. 't Hoof. Courtesy RGM, Leiden.

Figure 2.23 (left). Scapulocoracoids of compared pterosaurs in various aspects. A: *S. brasilensis* (BSP 1987 I 65; after Wellnhofer, 1991b: 94); B: *An. santanae* (AMNH 22555); C: *Co. piscator* (NSM-PV 19892; after Kellner & Tomida, 2000: 50-51). Drawing by the author.

A

C

D



Figure 2.24 (above and right). *Co. spielbergi* sp. nov. (RGM 401 880), the left humerus in various aspects. A: posterior; B: ventral; C: anterior; D: dorsal; E: proximal; F: distal. Scale bar = 50 mm. Photographs by A. 't Hoofst. Courtesy RGM, Leiden.

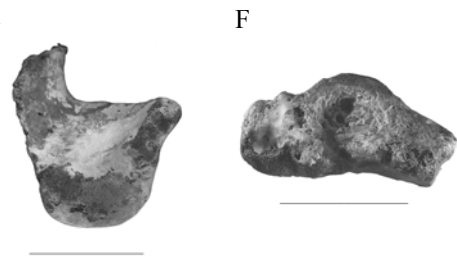


Figure 2.25 (below). *Co. spielbergi* sp. nov. (RGM 401 880), the left humerus in various aspects. A: posterior; B: ventral; C: anterior; D: dorsal; E: proximal; F: distal. Scale bar = 50 mm. Drawings by the author.

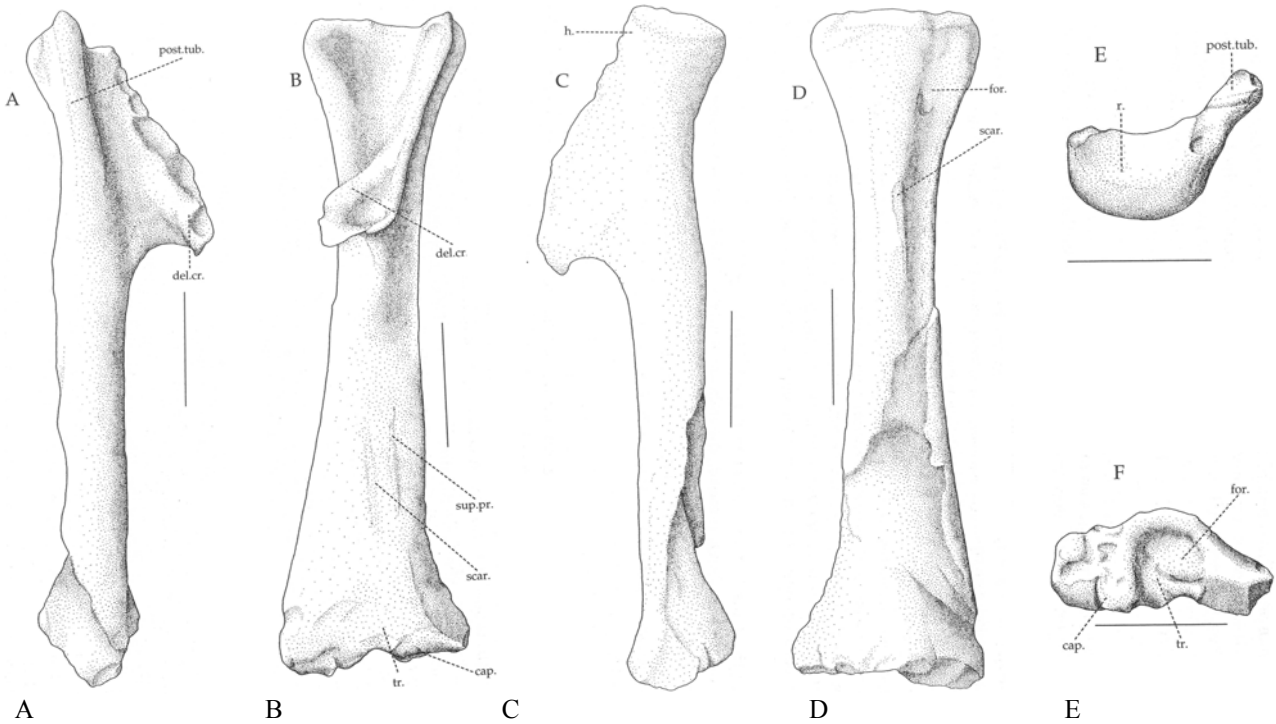




Figure 2.27. *Co. spielbergi* sp. nov. (RGM 401 880), the left ulna in various aspects. A: posterior; B: ventral; C: anterior; D: dorsal; E: proximal; F: distal. Scale bar = 50 mm. Photographs by A. 't Hooft. Courtesy RGM, Leiden.

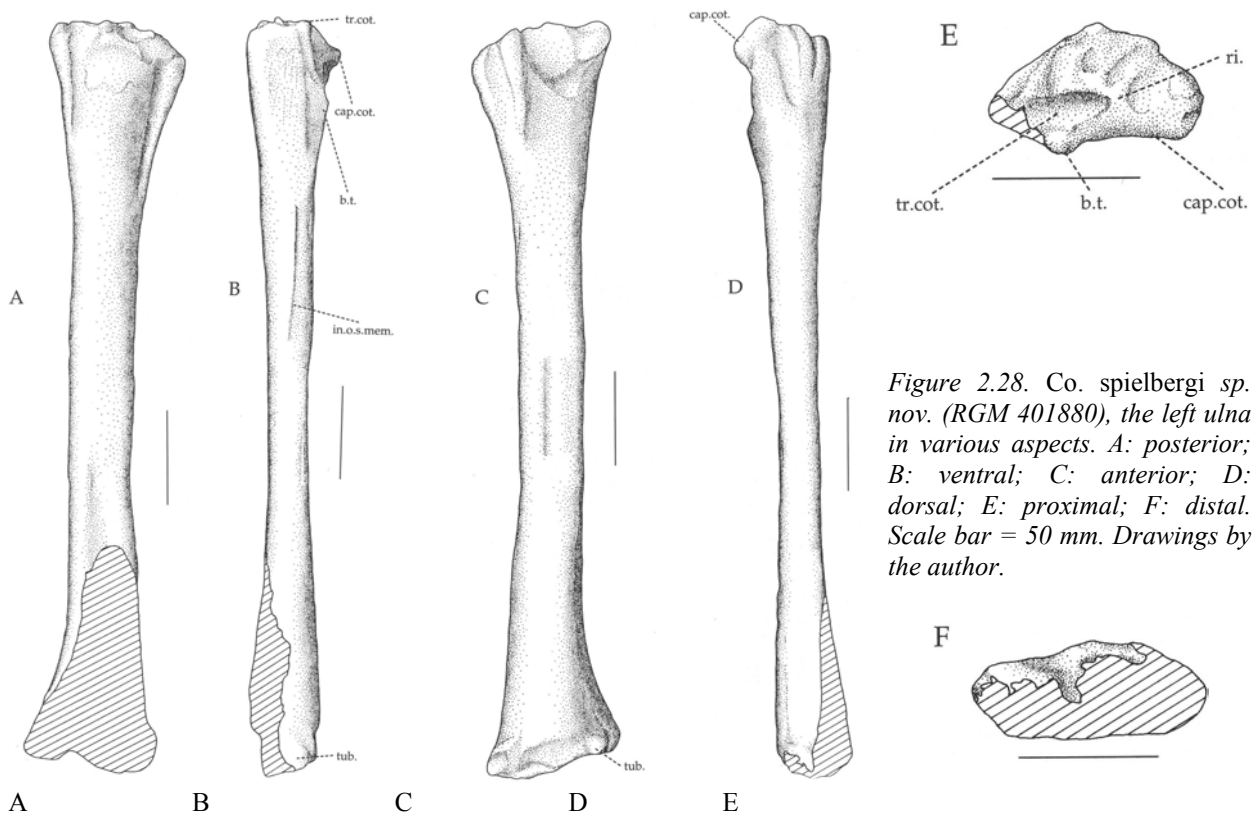


Figure 2.28. *Co. spielbergi* sp. nov. (RGM 401880), the left ulna in various aspects. A: posterior; B: ventral; C: anterior; D: dorsal; E: proximal; F: distal. Scale bar = 50 mm. Drawings by the author.

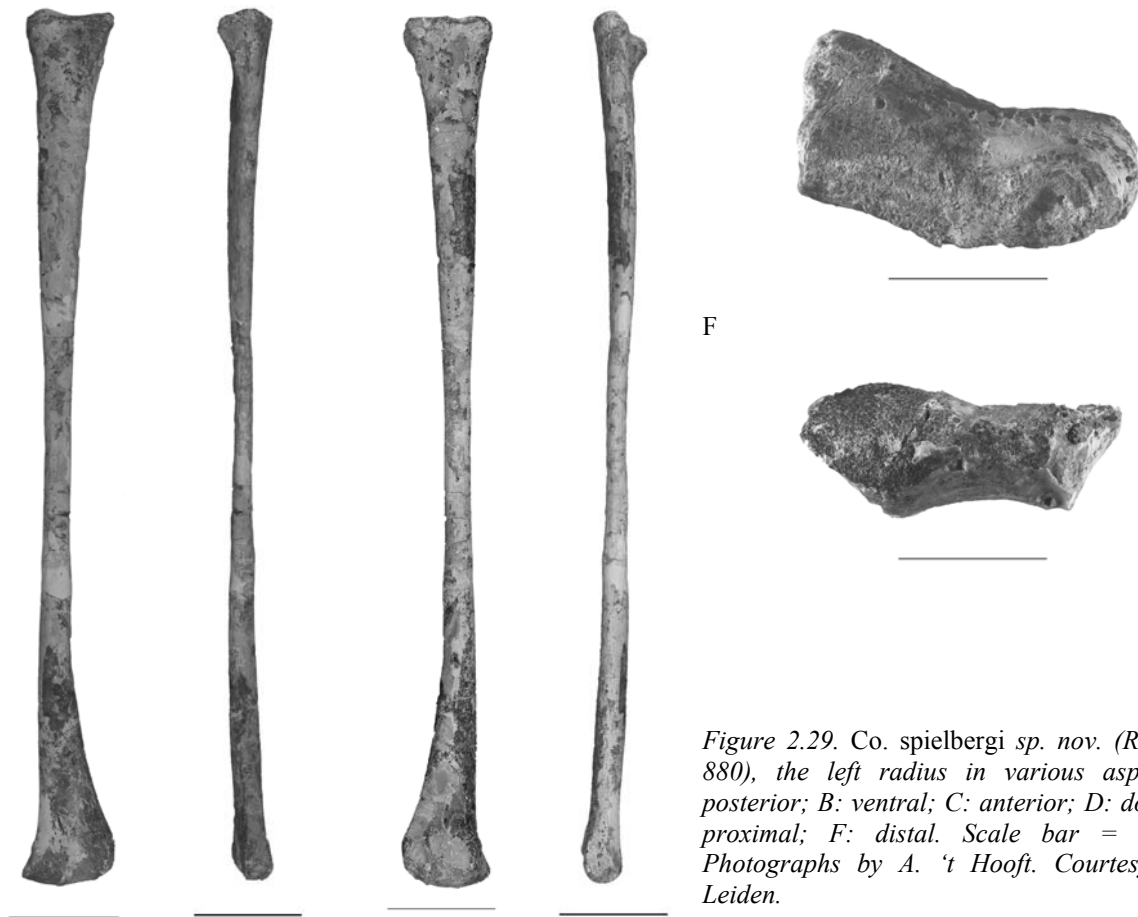


Figure 2.29. *Co. spielbergi* sp. nov. (RGM 401880), the left radius in various aspects. A: posterior; B: ventral; C: anterior; D: dorsal; E: proximal; F: distal. Scale bar = 50 mm. Photographs by A. 't Hoofst. Courtesy RGM, Leiden.

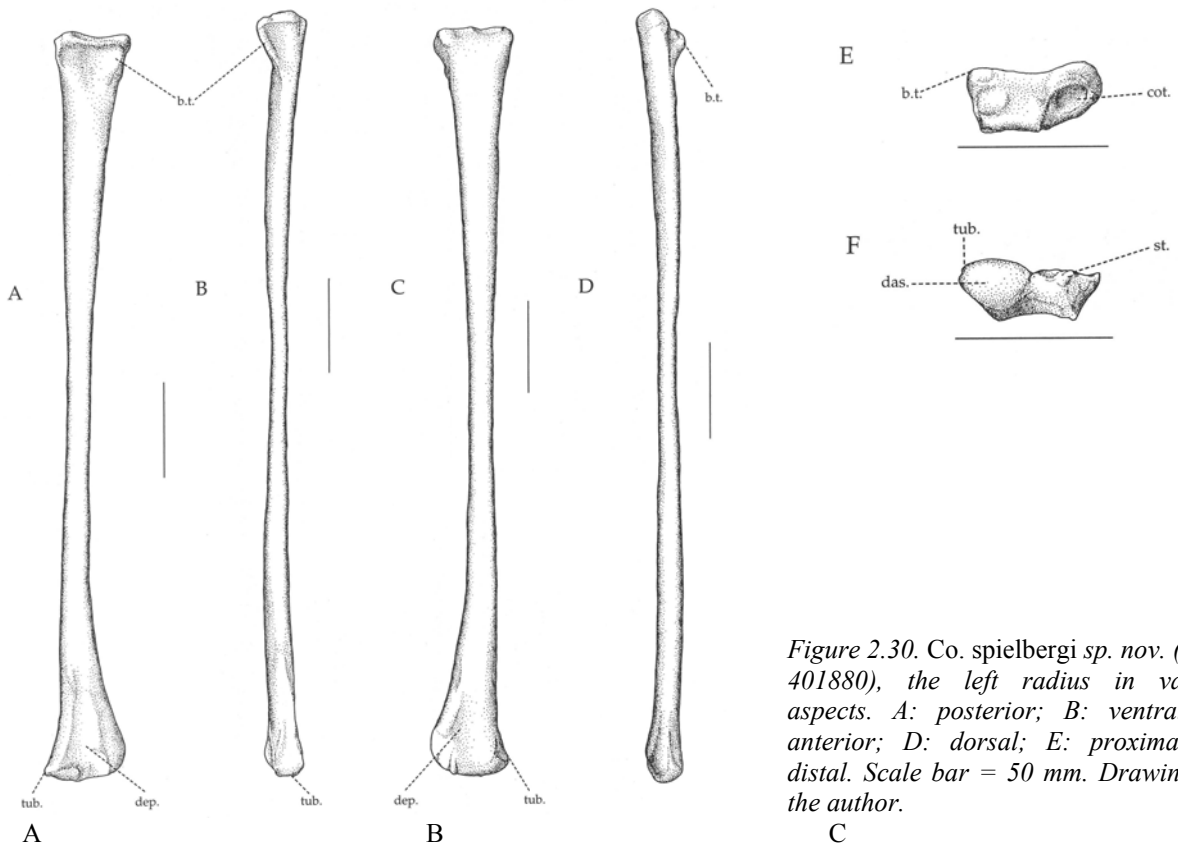


Figure 2.30. *Co. spielbergi* sp. nov. (RGM 401880), the left radius in various aspects. A: posterior; B: ventral; C: anterior; D: dorsal; E: proximal; F: distal. Scale bar = 50 mm. Drawings by the author.

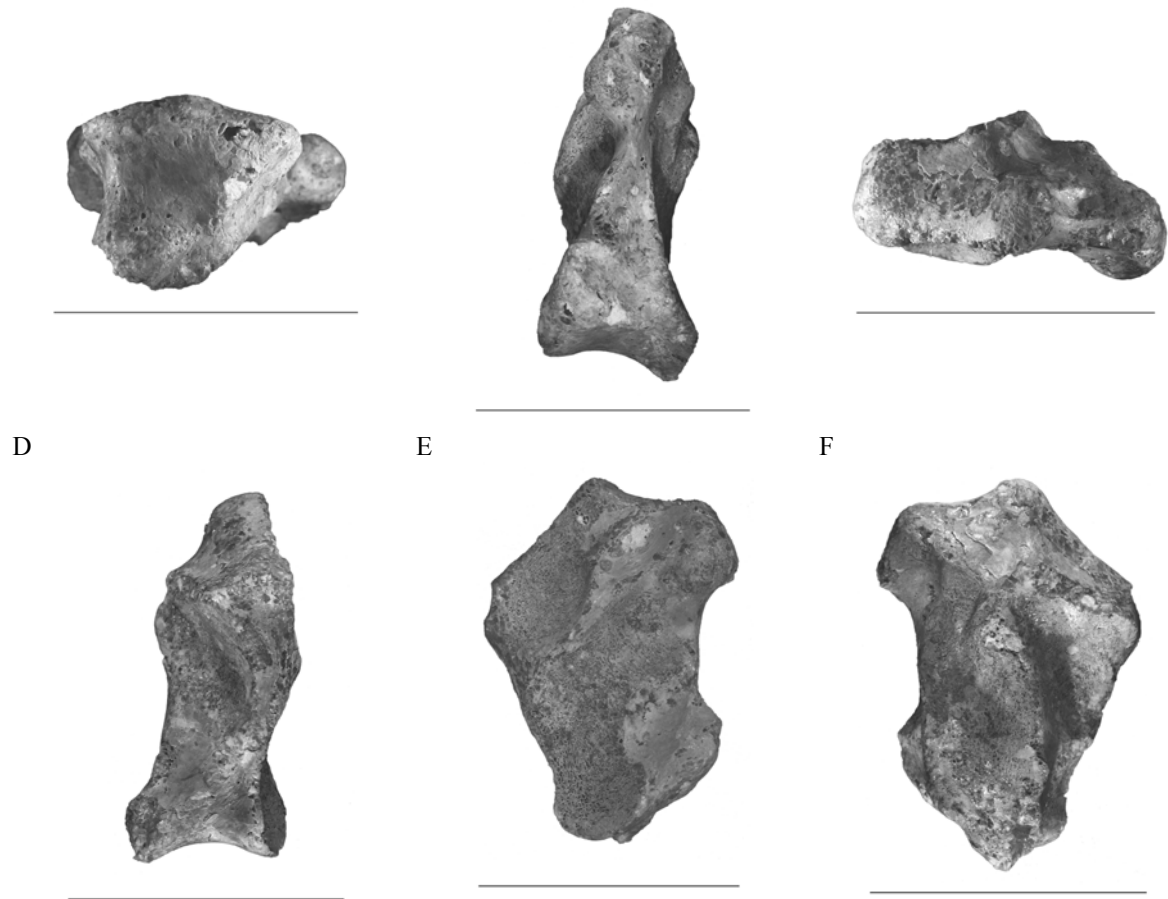


Figure 2.31. *Co. spielbergi* sp. nov. (RGM 401 880), the left proximal syncarpal in various aspects. A: posterior; B: ventral; C: anterior; D: dorsal; E: proximal; F: distal. Scale bar = 50 mm. Photographs by A. 't Hooft. Courtesy RGM, Leiden.

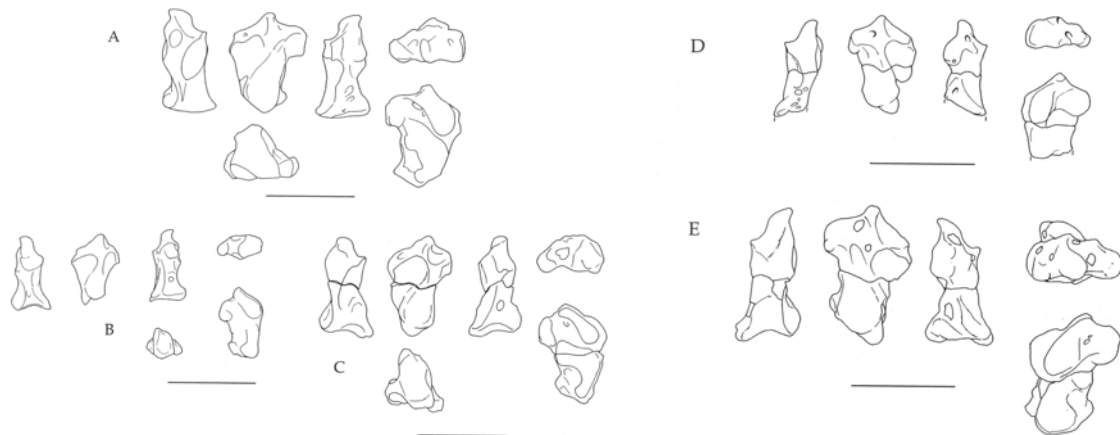


Figure 2.32. Proximal syncarpals of compared pterosaurs in various aspect. A: *Co. araripensis* (BSP 1982 I 89; after Wellnhofer, 1985: 124); B: *S. pricei* (AMNH 22552); C: *An. santanae* (BSP 1982 I 90; after Wellnhofer, 1985: 161); D: *An. santanae* (AMNH 22555); E: *Co. piscator* (NSM-PV 19892; after Kellner & Tomida 2000: 59-62). Scale bar = 50 mm. Drawings by the author.

A

B(i)

B(ii)

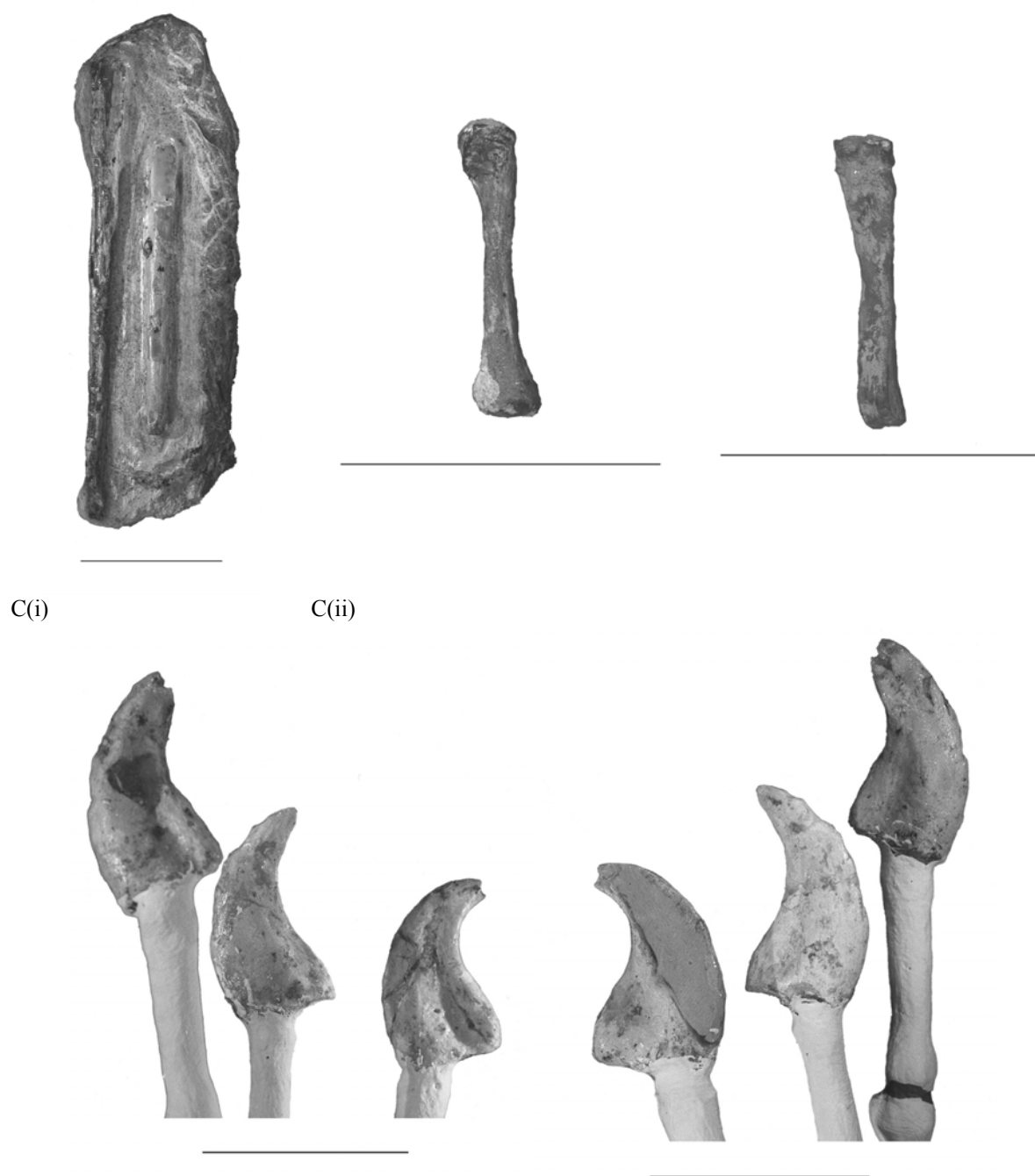


Figure 2.33. *Co. spielbergi* sp. nov. (RGM 401 880), ?metacarpals, phalanges and unguis. A: first and third ?metacarpalia; B: third phalanx with partially preserved and attached second phalanx in i) ventral and ii) anterior aspects; C: unguis in i) anterior and ii) posterior aspects. Scale bar = 30 mm. Photographs A. 't Hoof. Courtesy RGM, Leiden.



Figure 2.34. *Co. spielbergi* sp. nov. (RGM 401 880), the femora in various aspects (left and right respectively). A: posterior; B: lateral; C: anterior; D: medial; E: proximal (left) (scale bar = 30 mm); F: distal (right) (scale bar = 30 mm). Scale bar = 50 mm (unless stated otherwise). Photographs by A. 't Hoof. Courtesy RGM, Leiden.

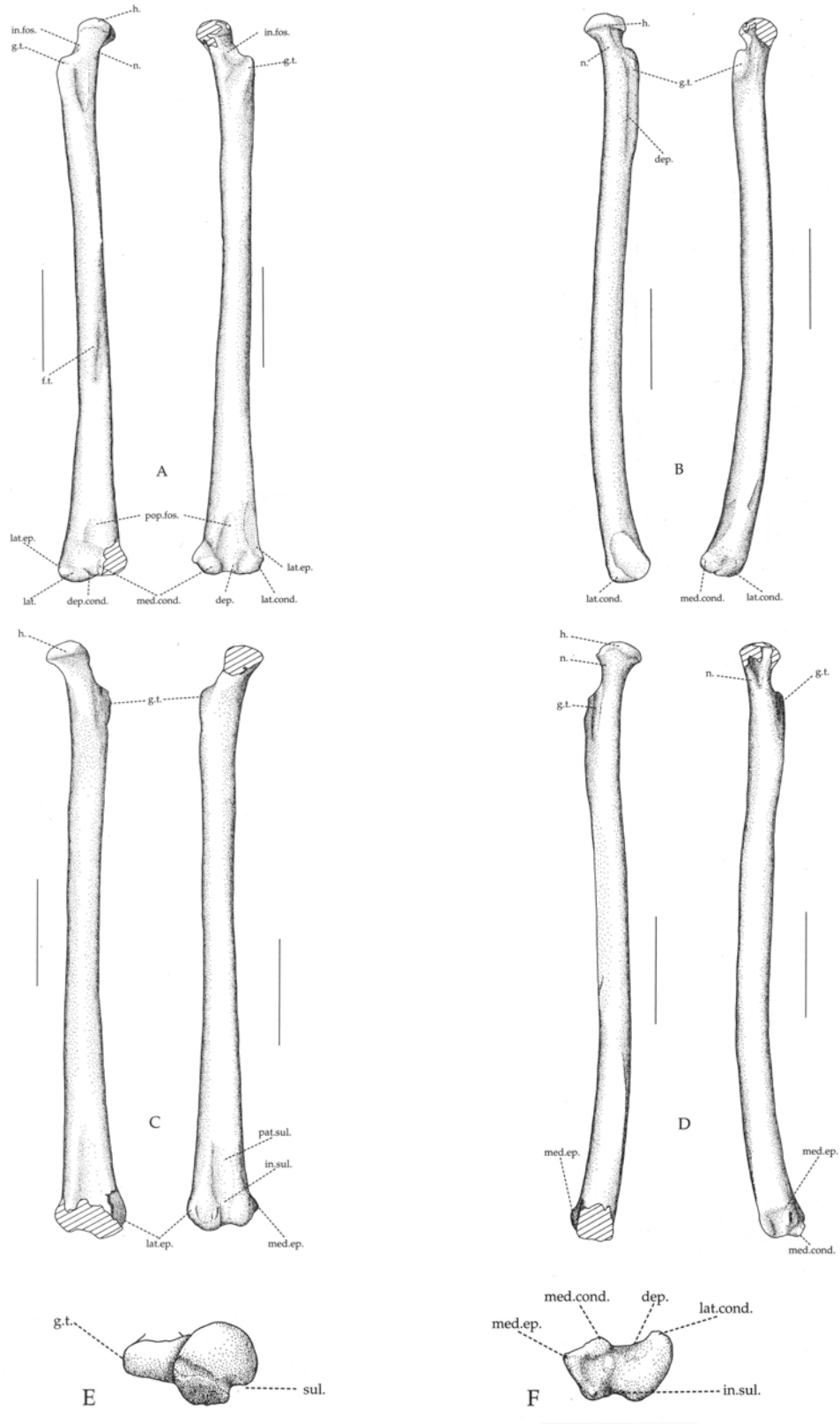


Figure 2.35. *Co. spielbergi* sp. nov. (RGM 401880), the femora in various aspects (left and right respectively). A: posterior; B: lateral; C: anterior; D: medial; E: proximal (left); F: distal (right). Scale bar = 50 mm. Drawings by the author.

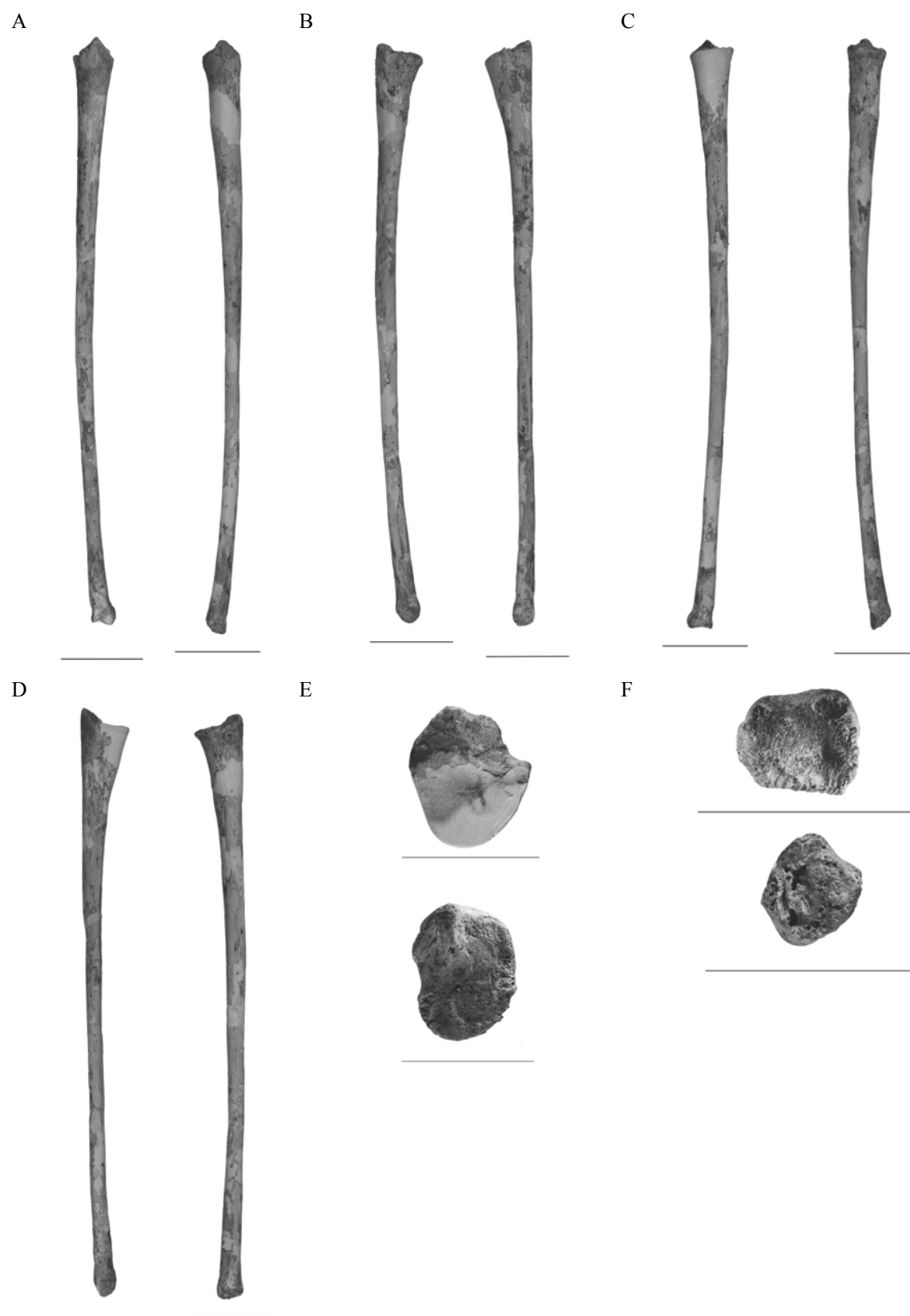


Figure 2.36. *Co. spielbergi* sp. nov. (RGM 401 880), the tibiae in various aspects (left and right respectively). A: posterior; B: lateral; C: anterior; D: medial; E: proximal (scale bar = 30 mm); F: distal (scale bar = 30 mm). Scale bar = 50 mm (unless stated otherwise). Photographs by A. 't Hooft. Courtesy RGM, Leiden.

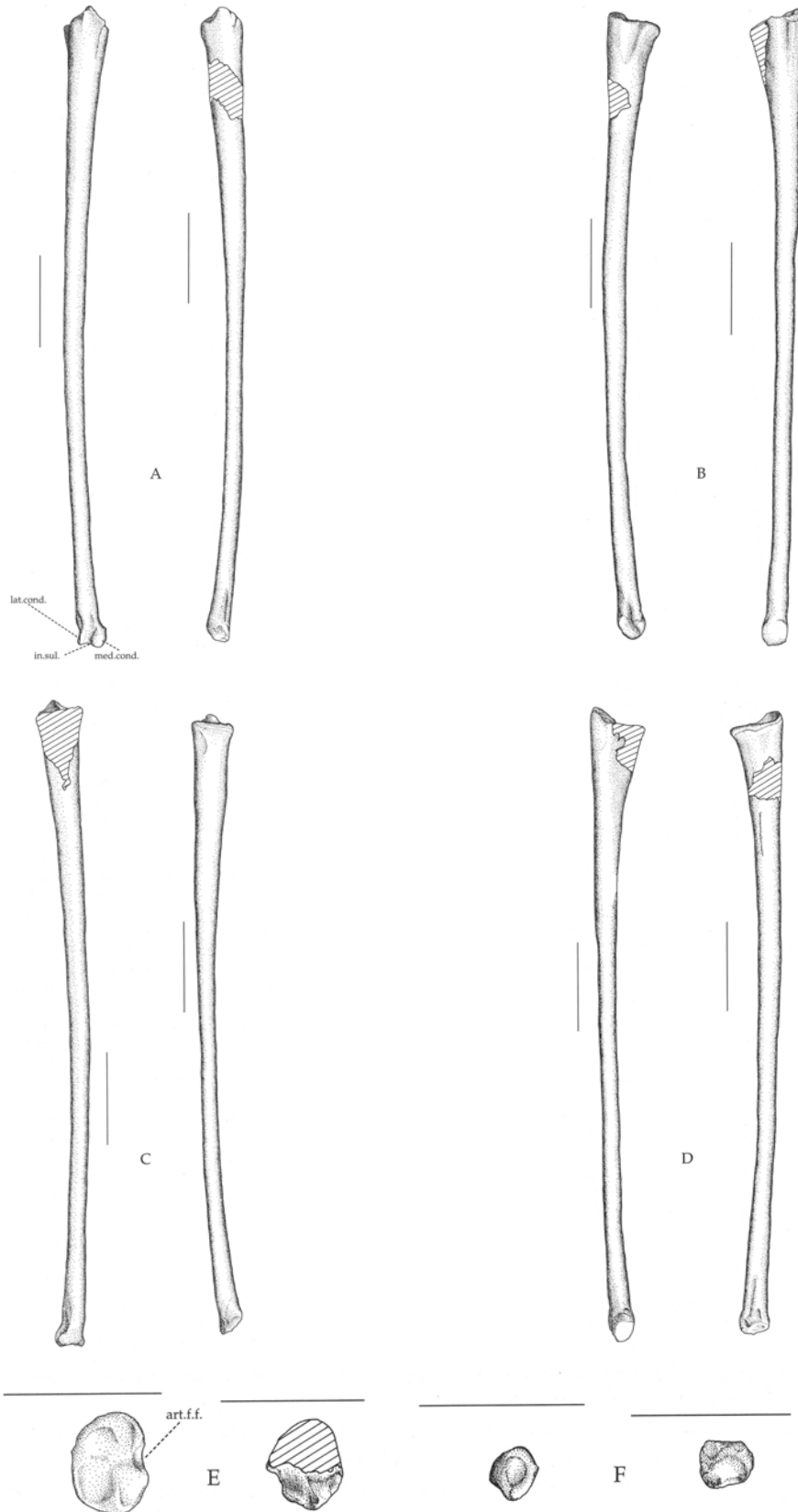


Figure 2.37. *Co. spielbergi* sp. nov. (RGM 401 880), the tibiae in various aspects (left and right respectively). A: posterior; B: lateral; C: anterior; D: medial; E: proximal (left); F: distal (right). Scale bar = 50 mm. Drawings by the author.

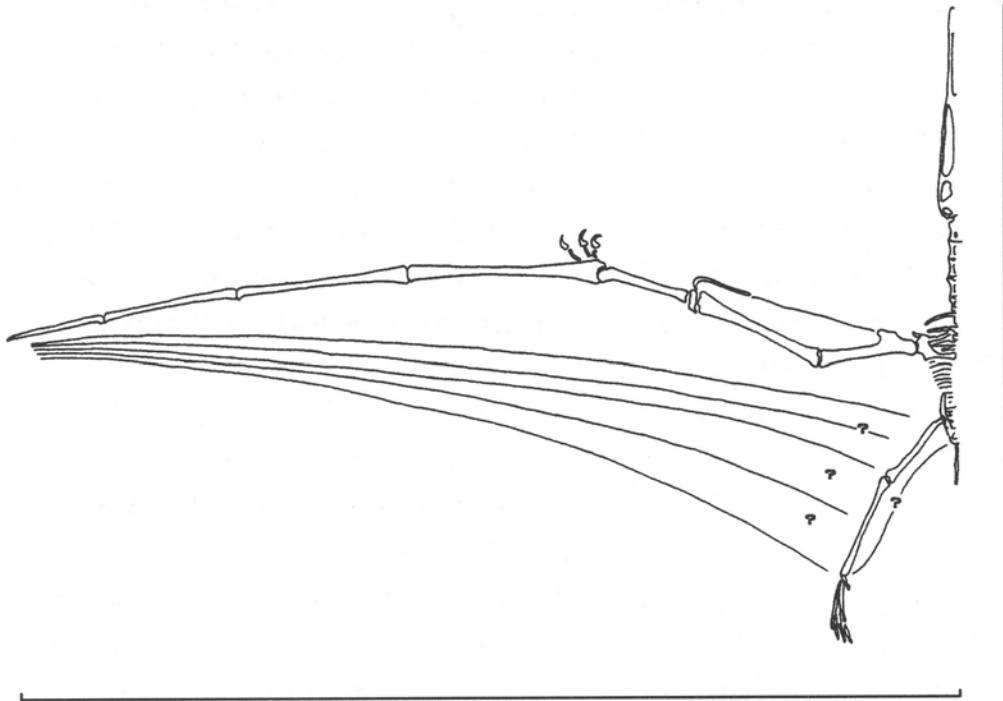


Figure 2.38. The skeleton on scale as calculated. Drawing by the author.

2.7.3. Scanning a pterosaur skull: supplement to the description of *Coloborhynchus spielbergi* in Scripta Geologica, 2003, 125: 37–139

The present sub–chapter is supplementary to the description and deals predominantly with the CT–scans. The scanning was done, because the morphology of the skull suggested the specimen to be *Coloborhynchus*. One of the most important features of *Coloborhynchus* is the first pair of teeth projecting from the rostrum at a significant higher level above the palate relative to the following teeth. However, the anterior view of the Leiden pterosaur is incomplete, although parts of the alveoli with remnants of the teeth could be observed. To be sure, however, it was decided to take CT–scans of the front part of the skull to prove the presence of such teeth. Also the back part of the skull was scanned, allowing speculation on the shape of the brains.

The full CT–scan can be seen online (homepage author). The objective of publishing this research is to provide the scientific community with a series of scans of a large Cretaceous pterosaur skull. CT–scans not only play an important role in the establishment of the morphology of the skull allowing a precise reconstruction, but can also show which parts are reconstructed. This former might be regarded as the prime motive of conducting the scanning, the latter is important because much material, especially from Chapada do Araripe, originates from fossil dealers.

Series 1_001–1_054

The first series is made of the anteriormost part of the skull until, approximately, halfway the premaxillary sagittal crest. Three mm slices were made with an increment of three mm.

As can be seen, this part of the skull is largely intact, save for the anterior aspect (see description). Internally, pyrites have been formed. There is a small reconstructed area at the right side of the premaxillary sagittal crest (figure 1_012–1_024). This is visible by the fact that this material has another, higher density than bone and shows up in the figures as darkish grey homogeneous material. Figure 1_0005–1_0010 clearly show the alveolus of the first pair of teeth, situated at the anterior surface of the skull.

Series 2_001–2_0054

This second series is directly following onto the first series and views the posterior half of the area with the premaxillary sagittal crest. Of this part, three mm slices were made with an increment of three mm as well.

Pyrites are seen here too. A larger part of the inner side is filled with a comparable material as the reconstructed parts of the crest discussed with the first series (starting with figure 2_012) but bone is always there. This rules out the possibility that the skull might be a composite (which was already proven by the X–rays taken before preparation). The height of the crest and the length however, cannot be determined precisely.

The white mass inside the jaw, visible from figure 3_013 onwards, is stone. In the latter part of the series (from figure 2_038 onwards), the matrix continues dorsal and lateral to the nasoantorbital fenestra and is not removed, apparently to give strength to the fragile skull.

Series 3_001–3_162

The third series starts with the quadrates, continuing in posterior direction and includes the eye socket for approximately three quarters. One and a half mm slices were made with an increment of 0.5 mm. It is clear that the skull is deformed towards the left side. Notice the break of the lacrimal process of the right jugal. The left quadrate is reconstructed and the material is, as seen with the previous mentioned reconstructions of the crest, grey with a high density.

Series 4_001–4_049

The last series is a continuation of the previous series and also scanned with one and a half mm slices but with an increment of 1.5 mm. It starts with the posterior quarter of the orbit, continuing in posterior direction. As

is evident from the series, the back of the skull is complete, with only minor reconstructions at the left squamosal (4_001–4_026). The brain cavity is clearly visible starting from figure 4_005 and ending with figure 4_017.

Discussion

The scans were made to prove the existence of a first pair of teeth at the anterior aspect. Furthermore, the series allow in the future the reconstruction of the brains. The reconstruction itself is beyond the scope of the present work. Brain reconstructions are known from various other skulls as well and research is in progress.

Scanning fossils can prove whether a specimen is genuine or not. Some scholars expressed their doubt regarding the Leiden *Coloborhynchus*, even though X-ray proved that the skull was embedded in total in the nodules. They wondered whether the skull was composed, because there was an interruption in bone at the posterior end of the crest. Though this was a wrong observation (they haven't seen the fossil up until now), the series published in the present work clearly shows that the crested part and the posterior part from the anterior part of the nasoantorbital fenestra onwards, belong together because there are no interruptions in bone.

1_001	206.56	2_001	368.56	3_001	749.5	3_055	776.43	3_109	803.81	4_001	837.93
1_002	209.56	2_002	371.56	3_002	750	3_056	776.93	3_110	804.37	4_002	839.43
1_003	212.5	2_003	374.56	3_003	750.43	3_057	777.37	3_111	804.81	4_003	840.93
1_004	215.56	2_004	377.56	3_004	751	3_058	777.93	3_112	805.31	4_004	842.43
1_005	218.56	2_005	380.56	3_005	751.5	3_059	778.43	3_113	805.81	4_005	843.93
1_006	221.56	2_006	383.56	3_006	751.93	3_060	778.93	3_114	806.37	4_006	845.43
1_007	224.56	2_007	386.56	3_007	752.43	3_061	779.37	3_115	806.81	4_007	846.93
1_008	227.56	2_008	389.56	3_008	753	3_062	779.87	3_116	807.31	4_008	848.37
1_009	230.56	2_009	392.56	3_009	753.5	3_063	780.43	3_117	807.81	4_009	849.93
1_010	233.5	2_010	395.56	3_010	753.93	3_064	780.93	3_118	808.37	4_010	851.37
1_011	236.56	2_011	398.56	3_011	754.5	3_065	781.37	3_119	808.81	4_011	852.87
1_012	239.56	2_012	401.56	3_012	755	3_066	781.87	3_120	809.31	4_012	854.37
1_013	242.56	2_013	404.56	3_013	755.5	2_067	782.37	3_121	809.81	4_013	855.93
1_014	245.56	2_014	407.62	3_014	755.93	3_068	782.93	3_122	810.37	4_014	857.37
1_015	248.56	2_015	410.62	3_015	756.43	3_069	783.37	3_123	810.81	4_015	858.87
1_016	251.56	2_016	413.56	3_016	757	3_070	783.87	3_124	811.31	4_016	860.37
1_017	254.56	2_017	416.62	3_017	757.5	3_071	784.37	3_125	811.81	4_017	861.87
1_018	257.56	2_018	419.56	3_018	757.93	3_072	784.93	3_126	812.37	4_018	863.37
1_019	260.56	2_019	422.62	3_019	758.43	3_073	785.37	3_127	812.81	4_019	864.87
1_020	263.56	2_020	425.56	3_020	758.93	3_074	785.87	3_128	813.31	4_020	866.37
1_021	266.56	2_021	428.62	3_021	759.5	3_075	786.37	3_129	813.81	4_021	867.87
1_022	269.56	2_022	431.62	3_022	759.93	3_076	786.93	3_130	814.31	4_022	869.37
1_023	272.56	2_023	434.56	3_023	760.43	3_077	787.37	3_131	814.81	4_023	870.87
1_024	275.56	2_024	437.62	3_024	760.93	3_078	787.87	3_132	815.31	4_024	872.37
1_025	278.62	2_025	440.62	3_025	761.5	3_079	788.37	3_133	815.81	4_025	873.81
1_026	281.56	2_026	443.62	3_026	761.93	3_080	788.87	3_134	816.31	4_026	875.37
1_027	284.56	2_027	446.62	3_027	762.43	3_081	789.37	3_135	816.81	4_027	876.87
1_028	287.56	2_028	449.62	3_028	762.93	3_082	789.87	3_136	817.31	4_028	878.31
1_029	290.62	2_029	452.62	3_029	763.5	3_083	790.37	3_137	817.81	4_029	879.81
1_030	293.56	2_030	455.62	3_030	763.93	3_084	790.87	3_138	818.31	4_030	881.37
1_031	296.56	2_031	458.62	3_031	764.43	3_085	791.37	3_139	818.81	4_031	882.81
1_032	299.62	2_032	461.62	3_032	764.93	3_086	791.87	3_140	819.31	4_032	884.31
1_033	302.56	2_033	464.62	3_033	765.43	3_087	792.37	3_141	819.81	4_033	885.81
1_034	305.62	2_034	467.62	3_034	765.93	3_088	792.87	3_142	820.31	4_034	887.31
1_035	308.56	2_035	470.62	3_035	766.43	3_089	793.37	3_143	820.81	4_035	888.81
1_036	311.62	2_036	473.62	3_036	766.93	3_090	793.87	3_144	821.31	4_036	890.31
1_037	314.62	2_037	476.62	3_037	767.43	3_091	794.37	3_145	821.81	4_037	891.81
1_038	317.56	2_038	479.62	3_038	767.93	3_092	794.87	3_146	822.31	4_038	893.31
1_039	320.62	2_039	482.62	3_039	768.43	3_093	795.31	3_147	822.81	4_039	894.81
1_040	323.56	2_040	485.68	3_040	768.93	3_094	795.87	3_148	823.31	4_040	896.31
1_041	326.62	2_041	488.62	3_041	769.43	3_095	796.37	3_149	823.81	4_041	897.81
1_042	329.56	2_042	491.62	3_042	769.93	3_096	796.87	3_150	824.31	4_042	899.25

1_043	332.62	2_043	494.62	3_043	770.43	3_097	797.31	3_151	824.75	4_043	900.81
1_044	335.62	2_044	497.62	3_044	770.93	3_098	797.87	3_152	825.31	4_044	902.31
1_045	338.62	2_045	500.62	3_045	771.43	3_099	798.37	3_153	825.81	4_045	903.75
1_046	341.62	2_046	503.62	3_046	771.93	3_100	798.87	3_154	826.31	4_046	905.25
1_047	344.62	2_047	506.68	3_047	772.43	3_101	799.37	3_155	826.75	4_047	906.75
1_048	347.62	2_048	509.62	3_048	772.93	3_102	799.87	3_156	827.31	4_048	908.31
1_049	350.62	2_049	512.62	3_049	773.43	3_103	800.37	3_157	827.81	4_049	909.75
1_050	353.62	2_050	515.62	3_050	773.87	3_104	800.87	3_158	828.25		
1_051	356.62	2_051	518.62	3_051	774.43	3_105	801.31	3_159	828.81		
1_052	359.62	2_052	521.68	3_052	774.93	3_106	802.37	3_160	829.31		
1_053	362.62	2_053	524.62	3_053	775.43	3_107	802.31	3_161	829.81		
1_054	365.82	2_054	527.68	3_054	775.93	3_108	803.31	3_162	830.5		

Appendix chapter 3: Pterosaurs from the Lower Cretaceous of Brazil in the Stuttgart Collection (and supplement)

3.5. Appendix

3.5.1. Measurements

Length, as preserved	385
Length, reconstructed	400
Height at last alveolus	23.3
Width at symphysis	34.0
Largest width of rami	98.4
Depth dentary sagittal crest, as preserved	35
Length dentary sagittal crest	118
Width at second pair of teeth	21.0
Width at third pair of teeth	22.3
Width at fourth pair of teeth	21.8
Width at fifth pair of teeth	21.7

Table 3.1. Measurements of the mandible, SMNS 56994 in mm.

SMNS 55408	Length, as preserved	138
	Diameter shaft	17*
SMNS 55409	Length	243
	Width shaft, dorsal–ventral plane	28.4
	Width shaft, anterior–posterior plane	42.9
	Width proximal aspect, dorsal–ventral plane	37.3
	Width proximal aspect, anterior–posterior plane	56.6
	Width distal aspect, dorsal–ventral plane	43.3
	Width distal aspect, anterior–posterior plane	67.7
SMNS 55883	Length, as preserved	154
	Width shaft, dorsal–ventral plane (beginning deltopectoral crest)	23.5
	Width shaft : maximum height deltopectoral crest, as preserved	56.9

Table 3.2. Measurements of isolated humeri in mm.

SMNS 55410 ulna	Length, as preserved	255
	Diameter shaft (anterior)	19.7
	Width proximal aspect, as preserved	33
	Width proximal aspect, as preserved	33
SMNS 55411 ulna	Length, as preserved	150*
	Width proximal aspect, as preserved	27 x 28*
	Diameter shaft	19
SMNS 55411 radius	Length, as preserved	150*
	Width proximal aspect, as preserved	27 x 11*
	Diameter shaft	8.3
SMNS 55413 ulna	Length	395
	Diameter shaft (anterior)	27
	Width proximal aspect	66*
	Width distal aspect	69
SMNS 82001 ulna	Length, as preserved	117
	Width proximal aspect	29*
	Diameter shaft	12 x 18

Table 3.3. Measurements of ulnae and radius in mm. *: approximate.

	Diameter ulna	Diameter radius	Ratio radius:ulna
<i>Santadactylus pricei</i> * (BSP 1980 I 122)	7.5	13.5	1:1.8
<i>Santadactylus pricei</i> (AMNH 22552)	16.3	8.5	1:1.9
SMNS 55411	8.3	19	1:2.3
<i>Coloborhynchus spielbergi</i> **	11.0	28.5	1:2.6

Table 3.4. Ratios of the diameter of ulna/radius. *: measurements from Wellnhofer (1985: 134); **: for comparative reasons a large ulna and radius (410 and 401 mm respectively).

	Length	Diameter	Ratios
Humerus	182	16.7	Diameters radius:ulna 1:2.3
Ulna	260	11.7	Diameter : length humerus 1:10.9
Radius	260	5*	Lengths humerus : ulna 1:1.4

Table 3.5. Measurements of humerus and ulna/radius, SMNS 81976 in mm. *: approximate.

SMNS 55412	Length, as preserved	40
	Width shaft (anterior–posterior)	13.6*
	Width proximal aspect	41.6*
	Width distal aspect (matrix)	22.4*
SMNS 55415	Length	446
	Width shaft (anterior–posterior)	18.1
	Width proximal aspect	41.2
	Width distal aspect (matrix)	29.3

Table 3.6. Measurements of phalanges in mm. *: approximate

	Length, as preserved	Diameter
Ulna	92.1	9.5
Radius	35.0	6.8
First phalanx fourth digit	158*	5.5x124/6.2 x 9.5**
Second phalanx fourth digit	86.8	7.8/10.7**
Fourth phalanx fourth digit	104.6	2.2/7.3**

Table 3.7. Measurements of front extremities in mm. *: approximate; **: proximal and distal measurements respectively.

3.5.2. Figures and plates



Figure 3.1. Mandible of cf. *Cr. mesembrinus* (SMNS 56994) in various aspects. A (left): anterior. Below, next page B: left lateral; C: detail crest, left; D: dorsal; E: right lateral; F: detail crest, right. Photographs by E. Enderburg and the author. Courtesy of SMS, Stuttgart.

B



C



D



E



F



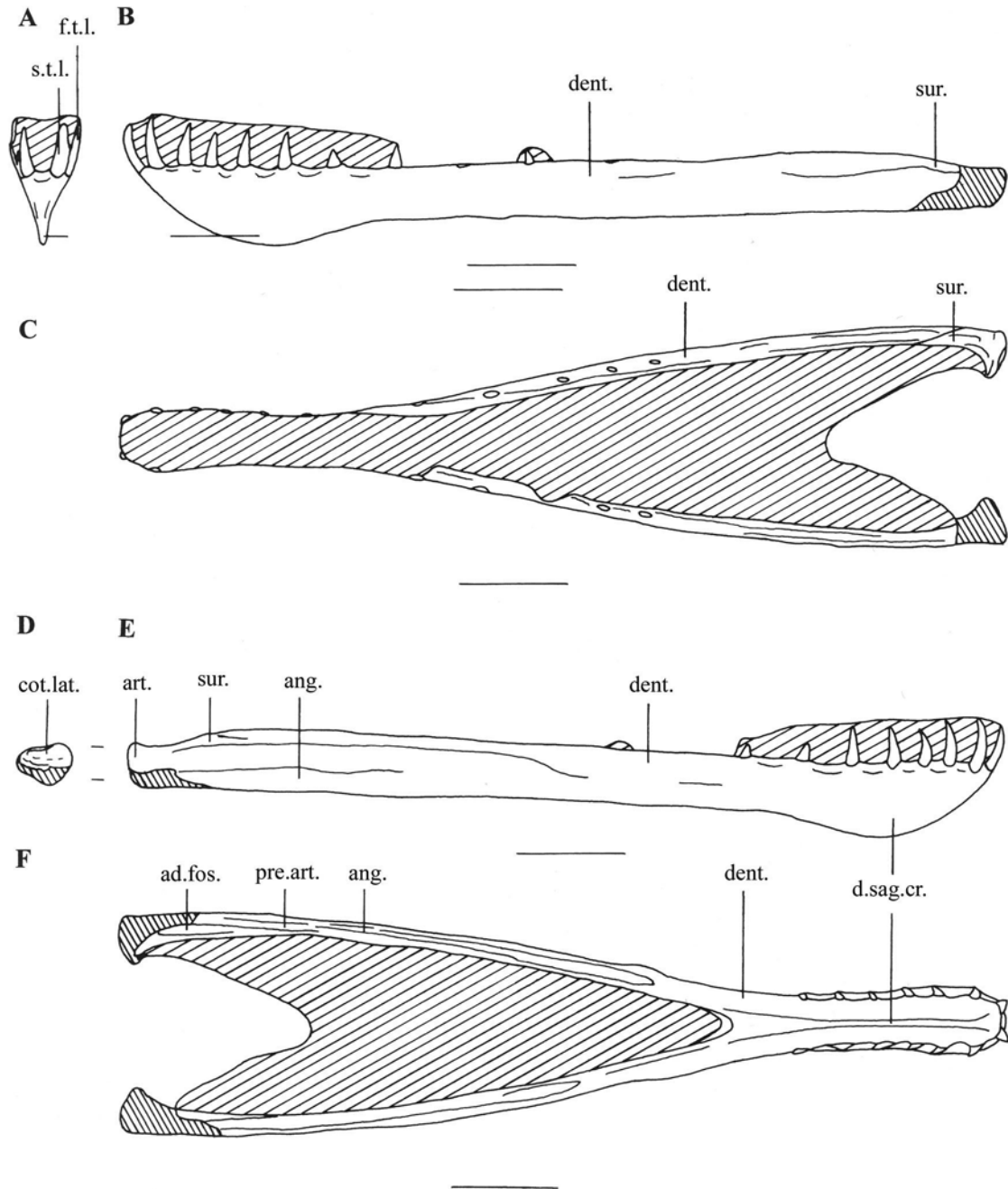


Figure 3.2. Mandible of *cf. Cr. mesembrinus* (SMNS 56994) in various aspects. A: anterior; B: left lateral; C: dorsal; D: posterior (right side); E: right lateral; F: ventral. Scale bars = 50 mm. Drawings by the author.

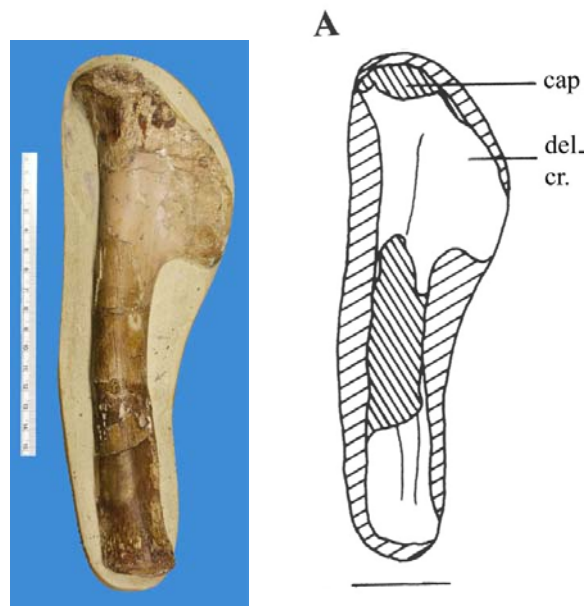


Figure 3.3A (left) and 3.4A (right). Isolated humerus SMNS 55407. Photographs and drawings by E. Endenburg and the author. Courtesy of SMS, Stuttgart.

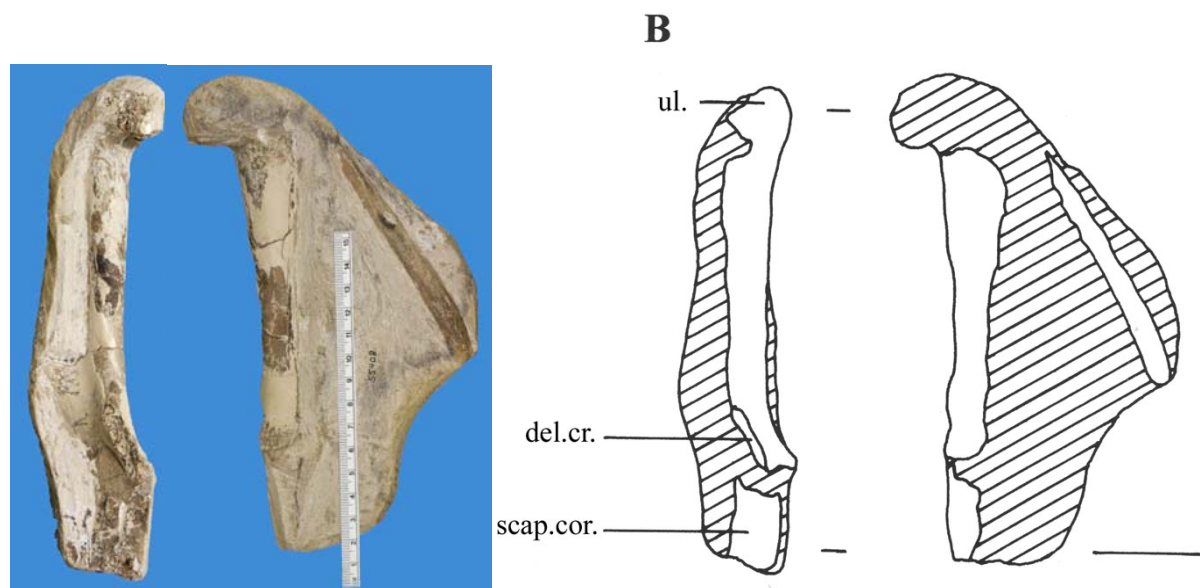


Figure 3.3B (left) and 3.4B (right). Isolated humeri SMNS 55408. Photographs and drawings by E. Endenburg and the author. Courtesy of SMS, Stuttgart.

C



Figure 3.3C (above). Isolated humerus. *Co. araripensis* (SMNS 55409) in (from top to bottom, left to right) proximal, posterior, ventral, anterior, dorsal and distal views; Photographs by E. Endenburg and the author. Courtesy of SMS, Stuttgart.

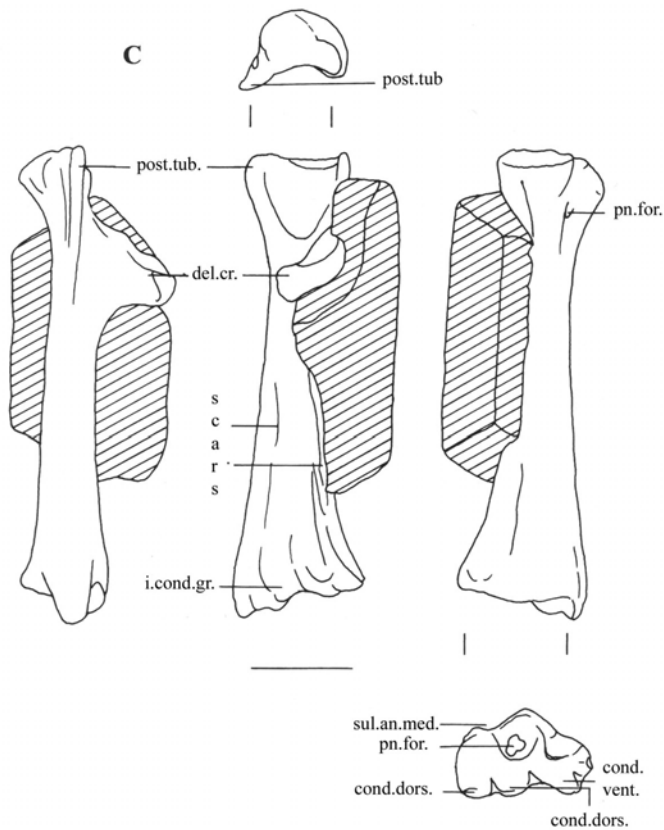


Figure 3.4C (left). Isolated humerus. *Co. araripensis* (SMNS 55409) in (from top to bottom, left to right) proximal, posterior, ventral, dorsal and distal views. Scale bar = 50 mm. Drawings by the author. Courtesy of SMS, Stuttgart.

D



D

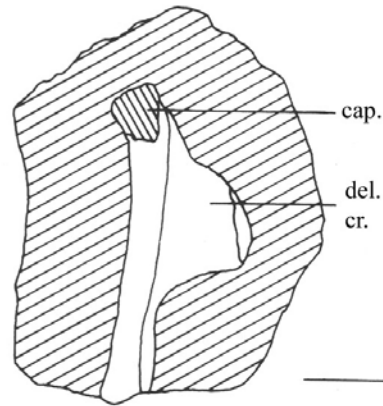


Figure 3.4D (left) and 3.5D (right). Isolated humerus. Cf. *S. pricei* (SMNS 55883). Scale bar = 50 mm. Photographs and drawings by E. Endenburg and the author. Courtesy of SMS, Stuttgart.

A



B

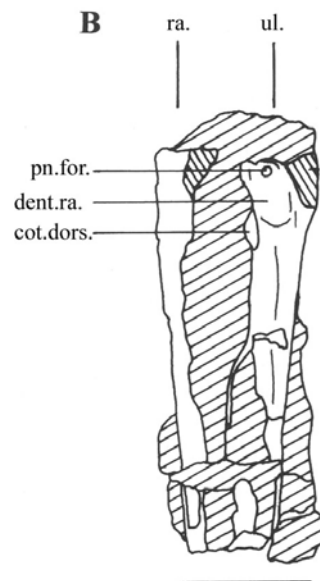
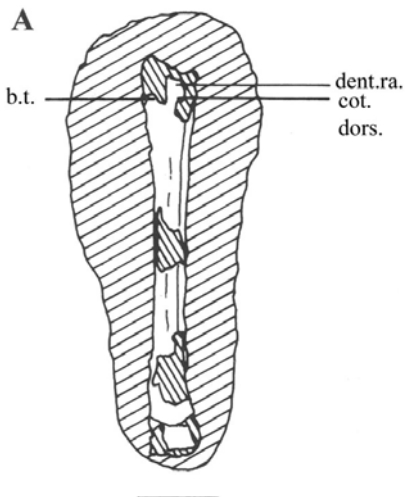


Figure 3.5 (top left and right) and 3.6 (bottom left and right). Isolated ulnae and radii. A (top left, bottom left): ulna of cf. *S. pricei* (SMNS 55410); B (top right, bottom right): ulna/radius of cf. *S. pricei* (SMNS 55411). Scale bar = 50 mm. Photographs and drawings by E. Endenburg and the author. Courtesy of SMS, Stuttgart.

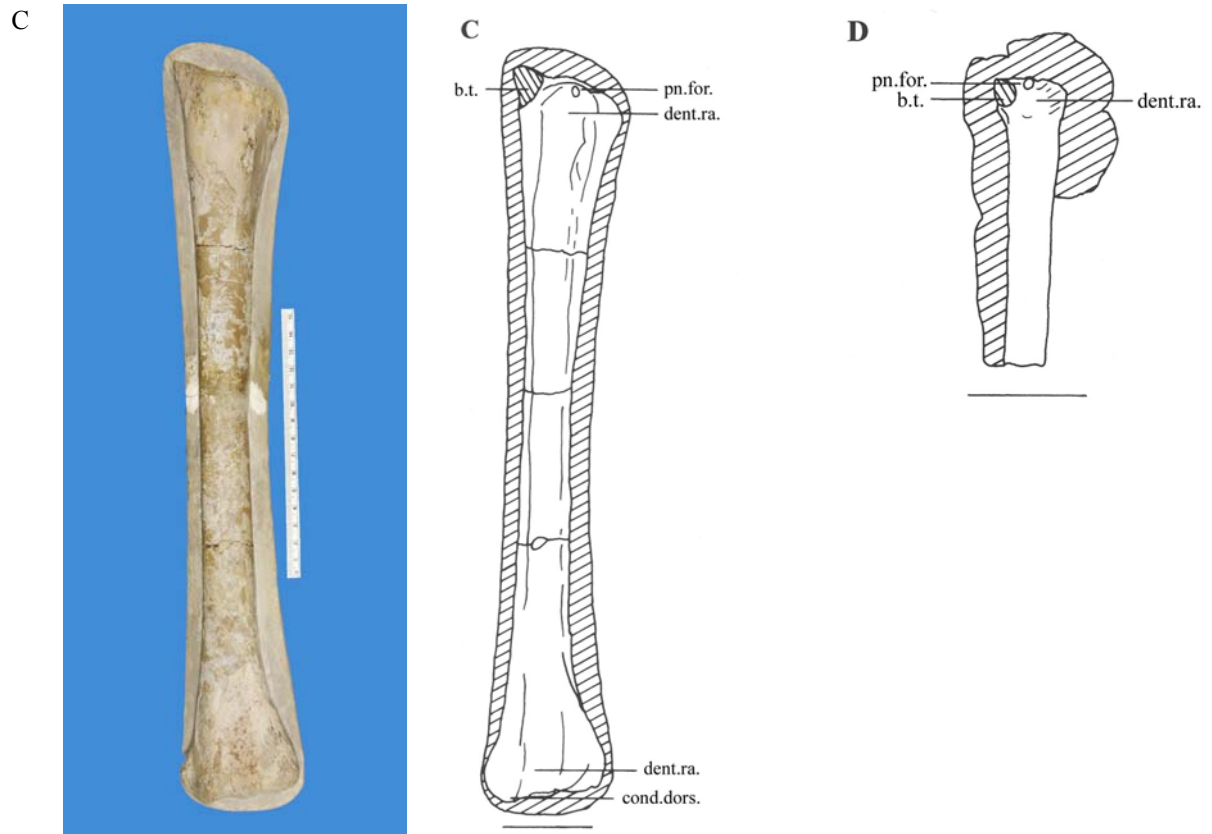


Figure 3.5 (left) and 3.6 (middle and right). Isolated ulnae and radii. Figure 3.5C (left and middle): ulna of cf. *C. spielbergi* (SMNS 55413). Figure 3.6D (right): ulna SMNS 82001. Scale bar = 50 mm. Photographs and drawings by E. Enderburg and the author. Courtesy of SMS, Stuttgart.

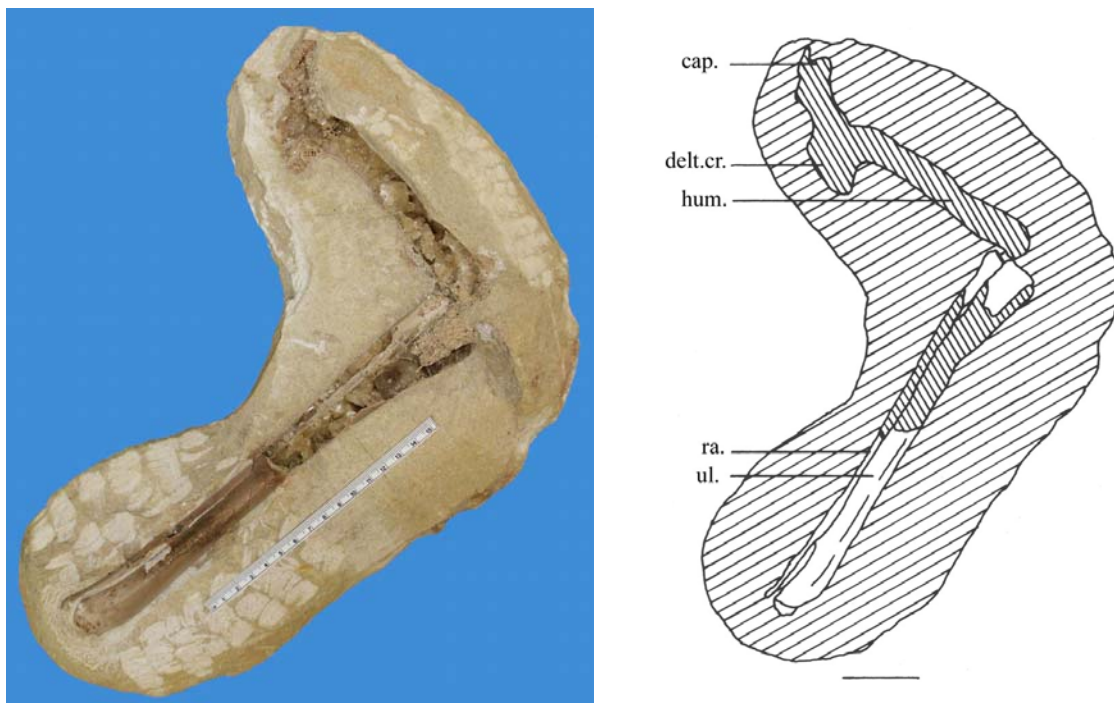


Figure 3.7 (left) and 3.8 (right). Associated humerus and ulna/radius (SMNS 81976). Scale bar = 50 mm. Photographs and drawings by E. Enderburg and the author. Courtesy of SMS, Stuttgart.



Figure 3.9. Phalanges of wing finger. A: SMNS 55412 (obverse and reverse); B: SMNS 55415. Photographs by E. Endenburg and the author. Courtesy of SMS, Stuttgart.

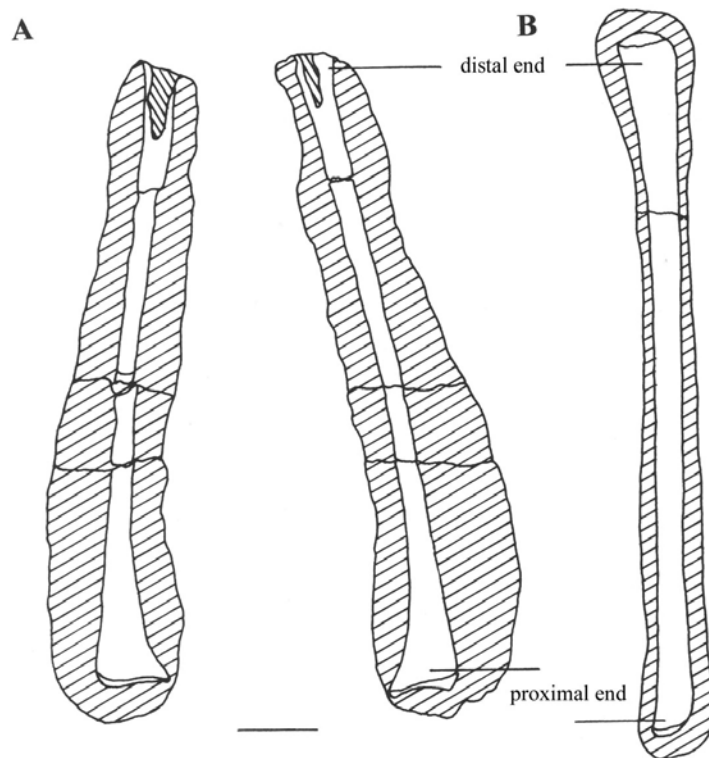


Figure 3.10. Phalanges of wing finger. A: SMNS 55412 (obverse and reverse); B: SMNS 55415. Scale bars = 50 mm. Drawings by the author.

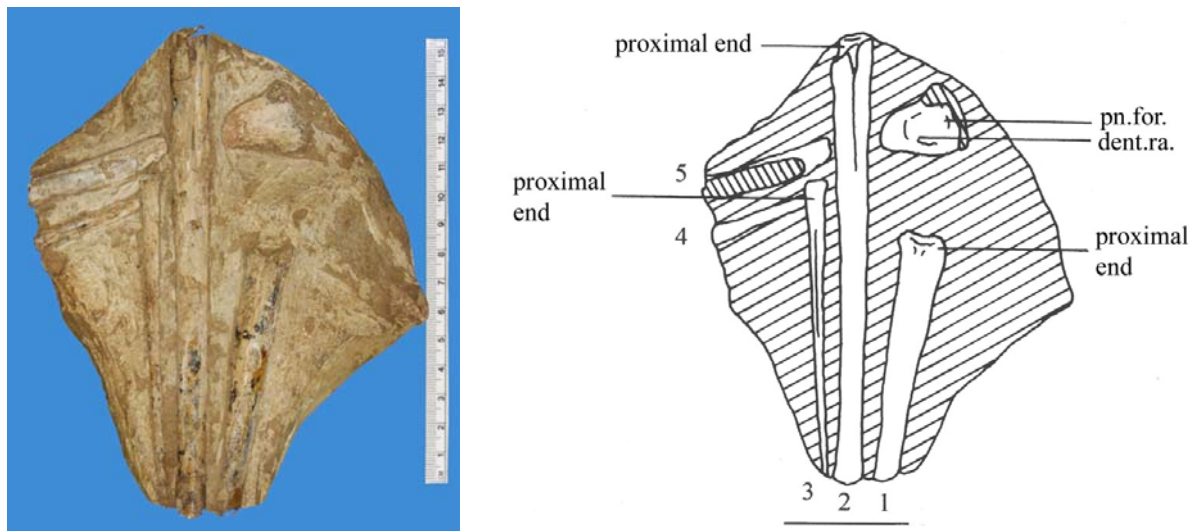


Figure 3.11 (left) and 3.12 (right). Partial front extremity (SMNS 80437). Scale bar = 50 mm. Photographs and drawings by E. Endenburg and the author. Courtesy of SMS, Stuttgart.

Appendix chapter 4: Description of two pterosaurs (Pterodactyloidea) mandibles from the Lower Cretaceous Santana Formation, Brazil

4.5. Appendix

4.5.1. Measurements

Anterior part	Length	153*
	Height anterior part, anteriormost tip	19.4
	Height anterior part, halfway length	46.8
	Height anterior part, posteriormost end	51.3
	Width anterior part, anteriormost tip	7.2
	Width anterior part, posteriormost end	31.2
	Width mandible at anteriormost end symphyseal shelf	25.1
	Width symphyseal shelf at posteriormost end	14.2
Posterior part	Length posterior part, right side	120*
	Length posterior part, left side	107*
	Height posterior part, anteriormost end	52.4
	Height posterior part, posteriormost end, right side	45.5
	Largest width posterior part, anteriormost end	32.7
	Width posterior part, anteriormost end, halfway dorsal–ventral	27.6
	Smallest width posterior part, anterior most end	9.3
	Width symphyseal shelf at anteriormost end	14.6
	Depth symphyseal shelf at posteriormost end	10.5
	Width mandibular cavity	29.4
	Height mandibular cavity	16.3
	Width right ramus, measured at one third height (from dorsal)	1.1**
	Width right ramus, measured at floor shelf	16.4**
Total	Length, as preserved, right side	273*
	Length, as preserved, left side	260*

Table 4.1. Measurements of mandible *Th. sethi* (SAO 251093) in mm. *: including the bending; **: measured medial–lateral.

Length	403
Length retroarticular process–symphysis	238
Thickness ramus (possible) last alveolus	7.2
Width expanded anterior part between alveolus 2–3 (ventrally)	20.0
Width expanded anterior part between alveolus 3–4 (ventrally)	18.5
Width expanded anterior part between alveolus 4–5 (ventrally)	15.0
Width at symphysis	37*
Width over surangular	12**
Length dentary sagittal crest	115
Maximal height dentary sagittal crest	39.7
Length ceratobranchials, including the bending	144
Width, posterior aspect (one bone)	4.0
Width, halfway (both bones)	4.0
Width, anterior aspect (both bones)	7.0

Table 4.2. Measurements of mandible *Anhanguera* sp. indet. (SAO 200602) in mm. *: approximate, because the right ramus is not preserved at this point; **: approximate, because the rami are separated from each other and the symphysis.

4.5.2. Figures and plates

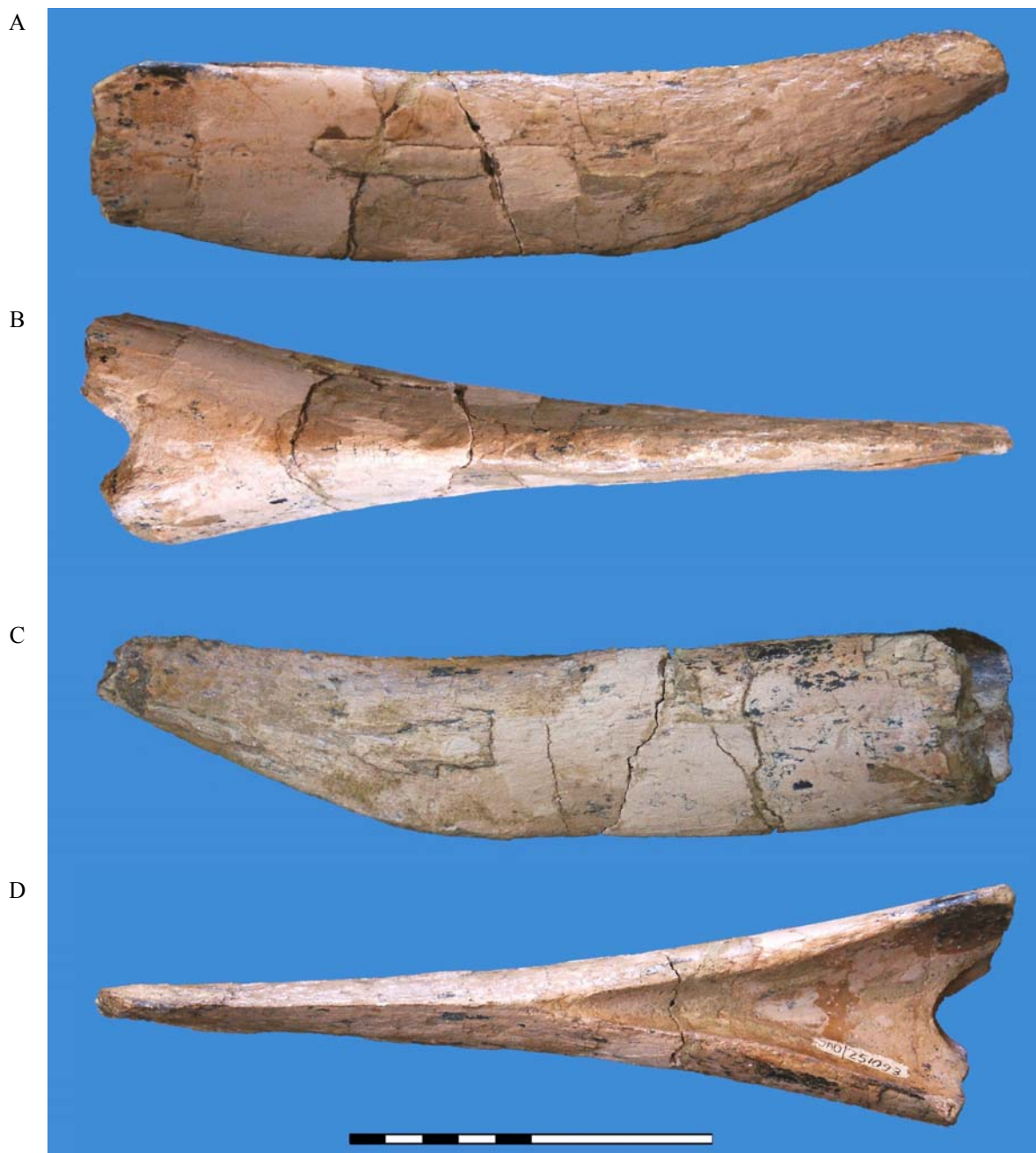


Figure 4.1. *Th. sethi* (SAO 251093) in various aspects. A: right lateral; B: ventral; C: left lateral; D: dorsal. Scale bar = 100 mm. Photographs by E. Endenburg and the author. Courtesy of U. Oberli, St. Gallen.

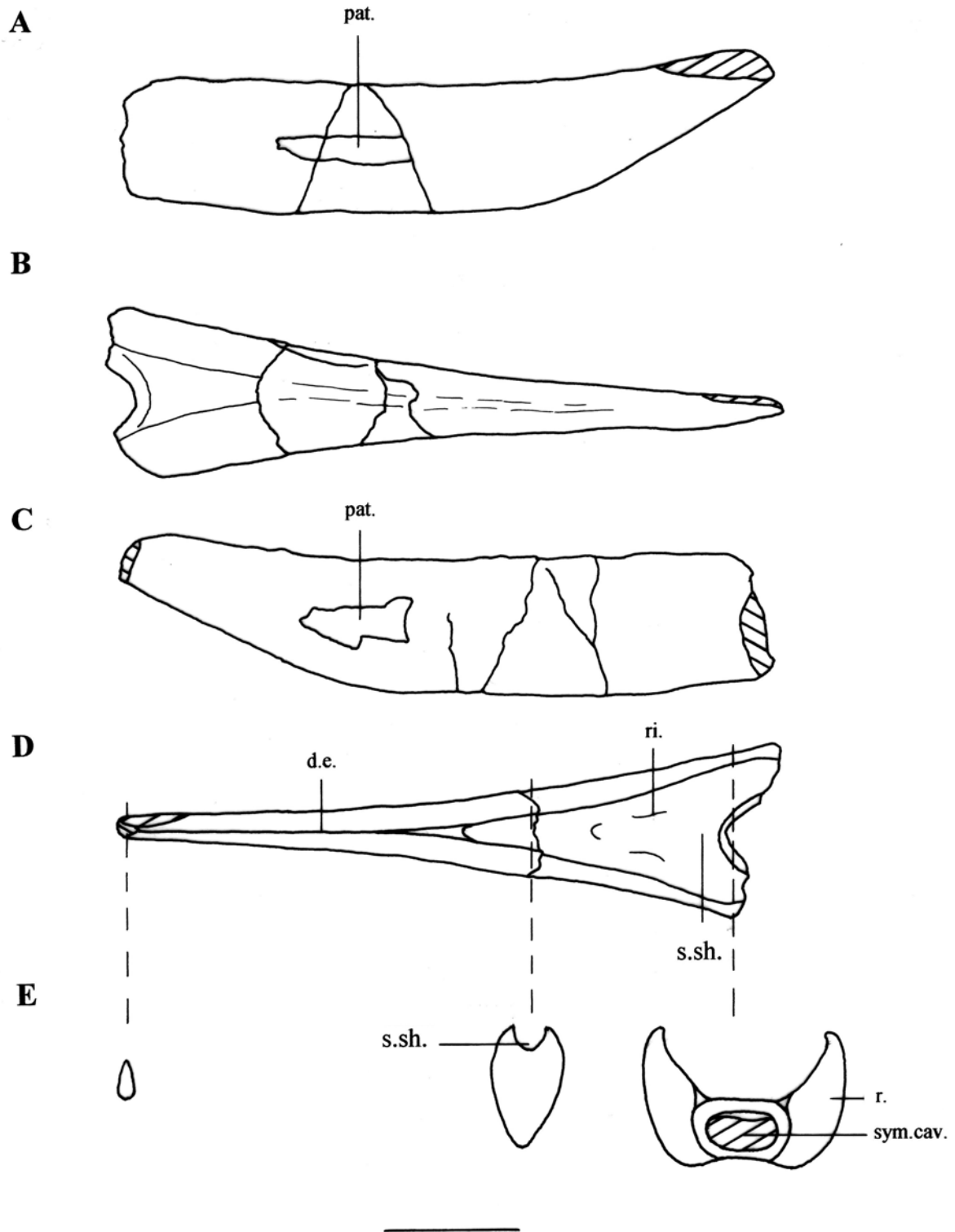


Figure 4.2. Th. sethi, mandible SAO 251093 in various aspects. A: right lateral; B: ventral; C: left lateral; D: dorsal; E: cross sections. Scale bar = 50 mm. Drawings by the author.



Figure 4.3. *Ta. wellnhoferi*. Photographs by E. Endenburg and the author. Courtesy of Iwaki Museum of Coal Mining & Fossils, Iwaki.



Figure 4.4. *Ta. navigans* (holotype SMNK 2344 PAL). Photograph by the author. Courtesy of SMN, Karlsruhe.



Figure 4.5. *Tu. leonardii*. Photographs by E. Endenburg and the author. Courtesy of Iwaki Museum of Coal Mining & Fossils, Iwaki.



Figure 4.6. *Tu. Leonardii*. Photographs by E. Endenburg and the author. Courtesy of Prefectural Museum of Natural History, Kanagawa.



Figure 4.7. *Anhanguera* sp. indet. (SAO 200602) mandible in various aspects. Symphysis in A: right lateral; B: left lateral; C ventral views. Photographs by E. Enderburg and the author. Courtesy of U. Oberli. St. Gallen.

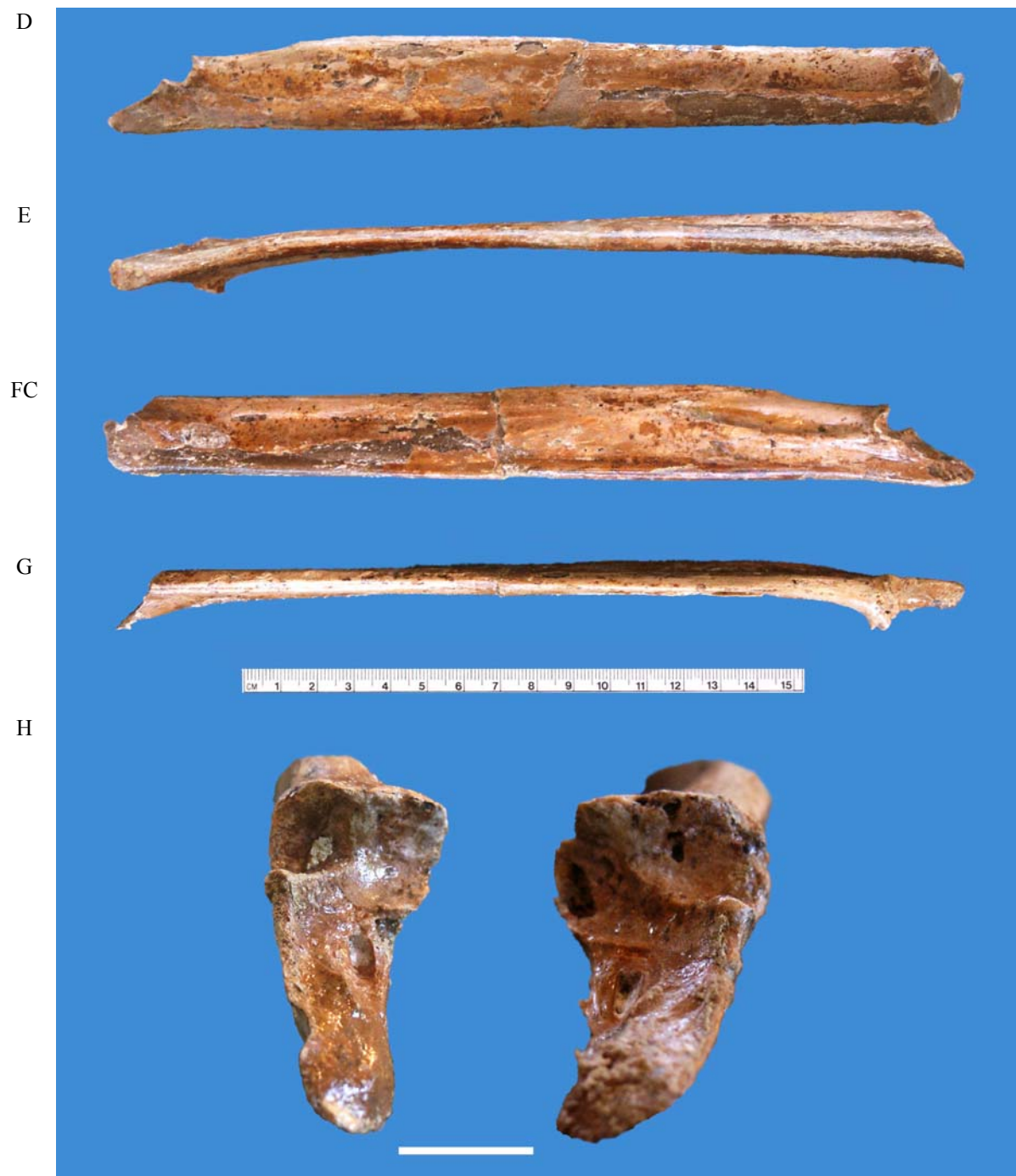


Figure 4.7. *Anhanguera sp. indet.* (SAO 200602) mandible in various aspects. Right ramus in D: lateral; E: ventral; F: medial; G: dorsal views; H: left and right posterior articular area (scale bar = 10 mm). Photographs by E. Enderburg and the author. Courtesy of U. Oberli, St. Gallen.



Figure 4.7. *Anhanguera* sp. indet. (SAO 200602) mandible in various aspects. Left ramus in I: lateral; J: ventral; K: medial; L: dorsal views. Ceratobranchials: M. Photographs by E. Enderburg and the author. Courtesy of U. Oberli, St. Gallen.

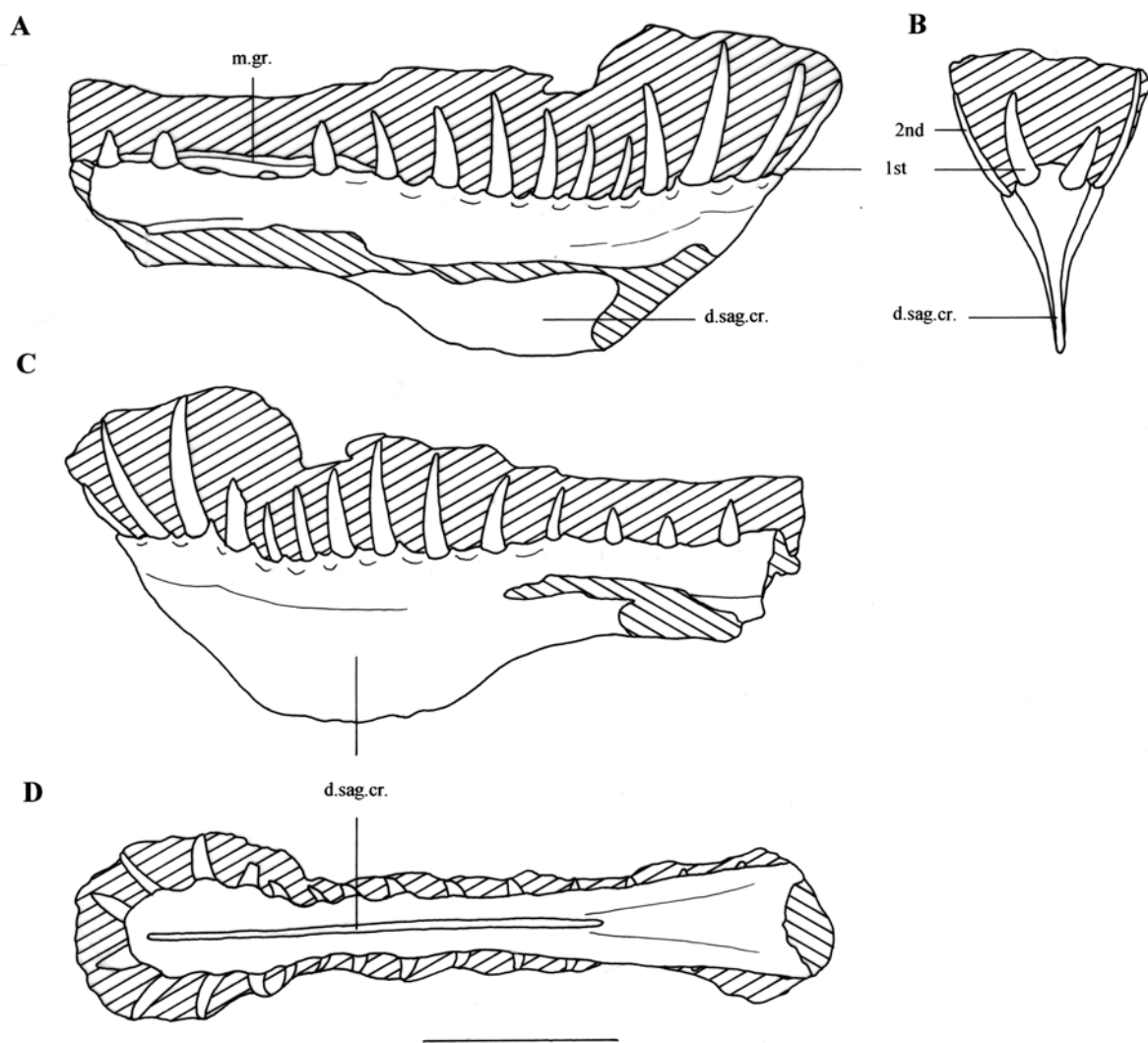


Figure 4.8. *Anhanguera* sp. indet., mandible SAO 200602 in various aspects. Symphysis in A: right lateral; B: anterior; C: left lateral; D: ventral view. Scale bar = 50 mm. Drawings by the author.

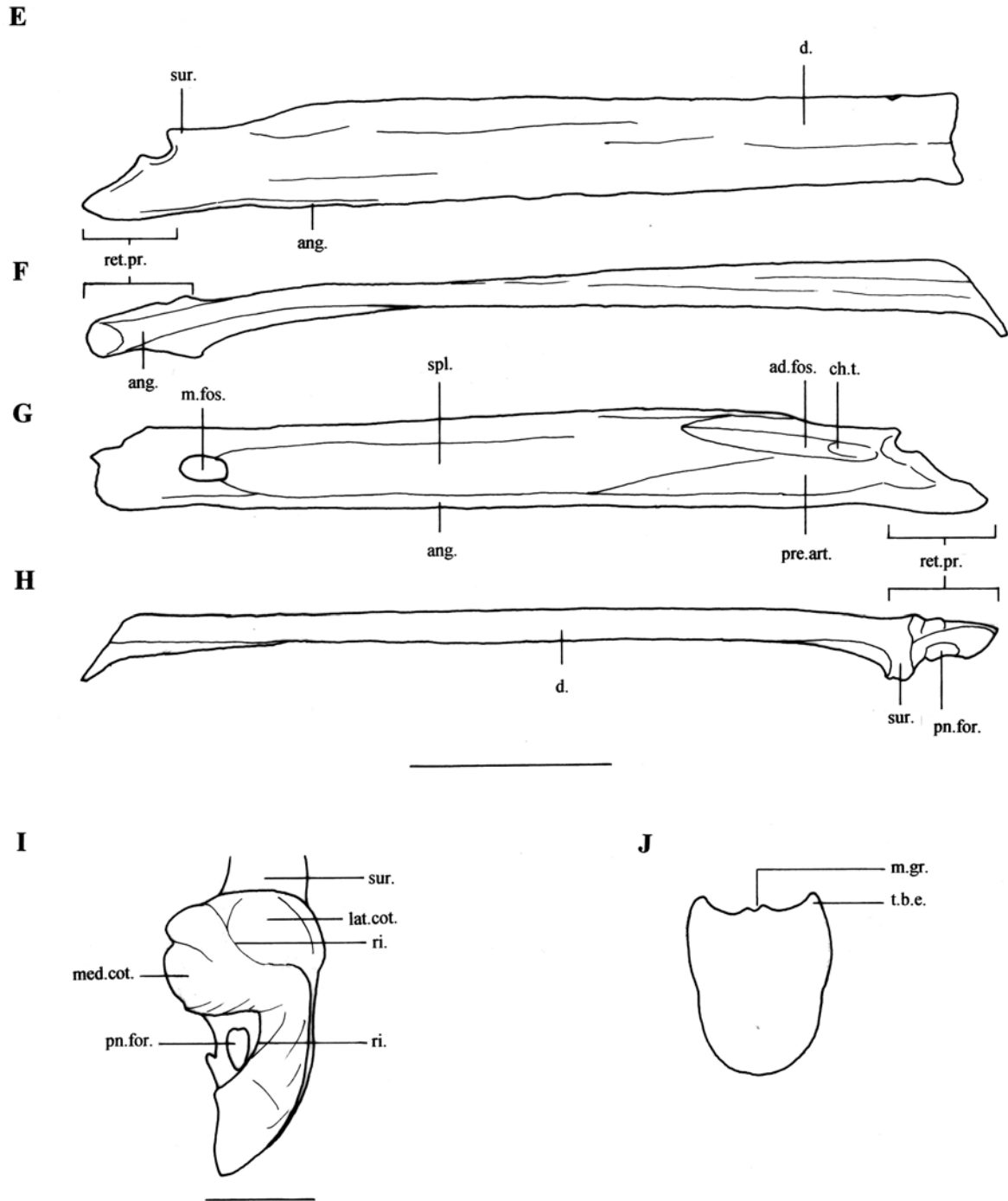


Figure 4.8. *Anhanguera* sp. indet., mandible SAO 200602 in various aspects. Right ramus in E: lateral; F: ventral; G: medial; H: dorsal views. Right retroarticular process in I: posterior view. Symphysis in cross section: J. Scale bar = 50 mm. Drawings by the author.

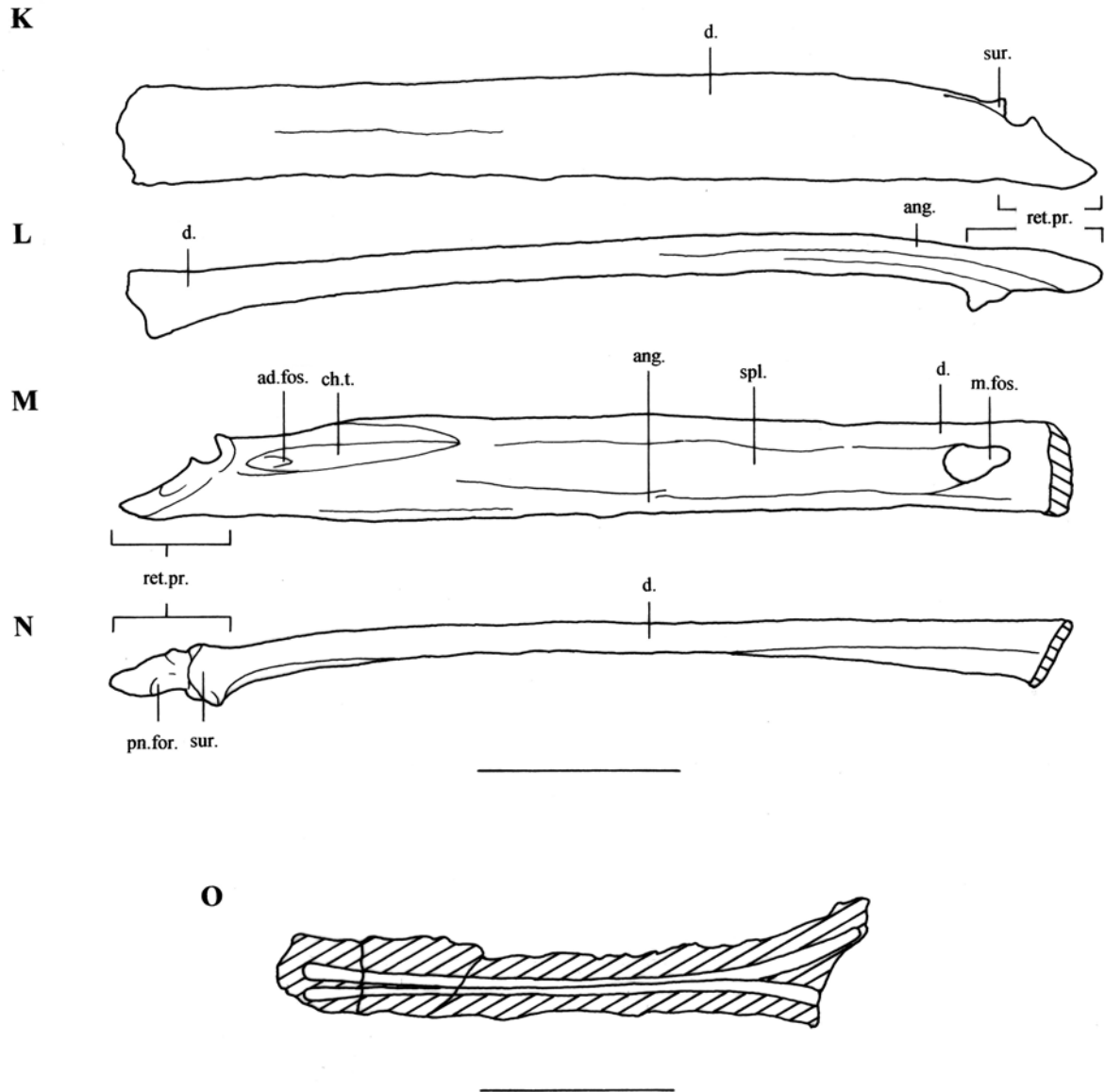


Figure 4.8. *Anhanguera sp. indet.*, mandible SAO 200602 in various aspects. Left ramus in K: lateral; L: ventral; M: medial; N: dorsal views. Ceratobranchials: O. Scale bar = 50 mm. Drawings by the author.



Figure 4.9 *An. santanae* (holotype BSP 1982 I 90), mandible in dorsal view. Scale bar = 100 mm. Photograph by E. Endenburg and the author. Courtesy of BSP, Munich.

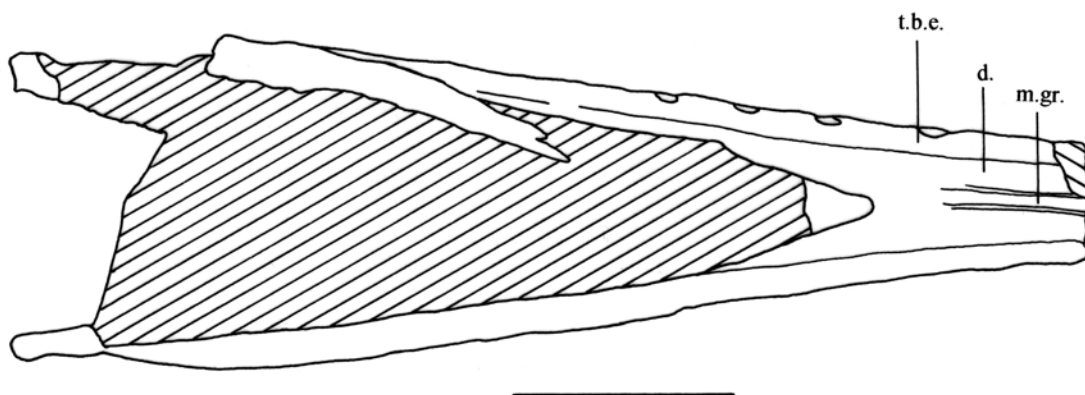


Figure 4.10 *An. santanae* (holotype BSP 1982 I 90), mandible in dorsal view. Scale bar = 50 mm. Drawing by E. Endenburg and the author.

Appendix chapter 5: Preliminary description of a skull and wing of a Brazilian Cretaceous (Santana Formation; Aptian–Albian) pterosaur (Pterodactyloidea) in the collection of the AMNH

5.6. Appendix

5.6.1. Measurements

Length	429
Right orbit (width x length)	40 x 50*
Height at quadrate	74*
Length nasoantorbital fenestra	116
Height nasoantorbital fenestra	41

Table 5.1. Measurements of the skull of *Brasileodactylus sp. indet.* (AMNH 24444) in mm. *: approximate.

Length	362*
Length retroarticular process–symphysis (posterior)	193*
Thickness ramus at last alveolus	3.5
Maximal width of symphysis (ventral)	18.7
Maximal width rami (lateral)	48.5
Minimal width symphyseal part (halfway anterior aspect)	11

Table 5.2. Measurements of the mandible of *Brasileodactylus sp. indet.* (AMNH 24444) in mm. *: approximate.

Scapulocoracoid	Length (lateral)	185*
	Length scapula	85*
	Length coracoid (as preserved)	90*
	Width supraneural plate articulation (s.n.art.)	13.0
	Smallest diameter scapular shaft	8.0
	Width distal end	15*
	Smallest diameter coracoid shaft	7.9
Ulna and radius	Length ulna	246 (66 + 180)
	Maximal width of proximal articular surface ulna	31.1
	Smallest diameter ulna	14.8 x 19.5
	Length radius	238 (70 + 168)
	Maximal width of proximal articular surface radius	11.6*
	Smallest diameter radius	6.9 x 10.5
Metacarpus	Length fourth	171 (75 + 96)
	Maximal width fourth	2.3*
	Diameter distal articular surface fourth	11.7 x 18.1
	Smallest diameter shaft fourth	11.1 x 12.3
	Thickness third	2.6
Phalanges wing finger	Length first	355 (180 + 175)
	Smallest diameter first	10.7 x 17.3
	Maximal width proximal articular surface first	42.3
	Maximal width distal articular surface first	33*
	Length second (as preserved)	86
	Width proximal articular surface second	31.2
	Diameter shaft	9.6* x 16.4

Table 5.3. Measurements of the post–cranial bones of *Brasileodactylus sp. indet.* (AMNH 24444) in mm. *: approximate.

Type specimen (except AMNH 24444) →	AMNH 24444*	<i>Anhangiera</i> * Campos & Kellner, 1985b	<i>Coloborhynchus</i> * Owen, 1874	<i>Criorhynchus</i> (Owen, 1861) See remark	<i>Brasileodactylus</i> * Kellner, 1984	<i>Cearadactylus</i> Leonardi & Borgomanero, 1985
Feature ↓						
Skull						
Premaxillary sagittal crest	no	yes, not starting at anterior aspect	yes, starting at anterior aspect	yes, starting at anterior aspect	no	no?
Anterior expansion	no (based on the mandible)	yes, slight	yes, robust	no	?	yes, slight
Tip bent upwards [§]	no	no in <i>An. blittersdorffi</i> yes in <i>An. santanae</i>)	yes	yes	no	no (type specimen)
Anterior aspect	dorso-ventrally compressed	dorso-ventrally compressed	blunt	blunt	dorso-ventrally compressed	dorso-ventrally compressed
First pair of teeth anterior	yes?	yes	yes	no in holotype); anteroventral in BSP 1987 I 46	yes	yes
First pair of teeth distinct dorsal relative to subsequent teeth	no	no	yes	no	no	no
Dentition pattern	flat	erratic	erratic	medium	flat	?
Frontoparietal crest	weak?	weak	weak	strong	?	?
Mandible						
Dentary sagittal crest	no	yes	yes	yes	no	no
Anterior expansion	no	yes, slight	yes, robust	no	yes, slight	yes, slight
Dentition pattern	flat	erratic	erratic	medium	flat	?
Anterior aspect	dorso-ventrally compressed	blunt	blunt	blunt	dorso-ventrally compressed; teeth laterally	dorso-ventrally compressed

Table 5.4. Characters of *Brasileodactylus* sp. indet. (AMNH 24444), compared with Cretaceous toothed taxa from Brazil (Romualdo Member [Albian] of the Santana Formation). Classification follows Veldmeijer, 2003a. Remark: specimens marked with * are studied first hand. It should not go without saying that BSP 1987 I 46, reclassified by Fastnacht (2001) as *Cr. mesembrinus*, has the first pair of teeth situated at the anterior aspect, contrasting the situation in the type specimen; [§]: this bending is most likely a preservational feature, rather than a morphological character.

5.6.2. Figures and plates

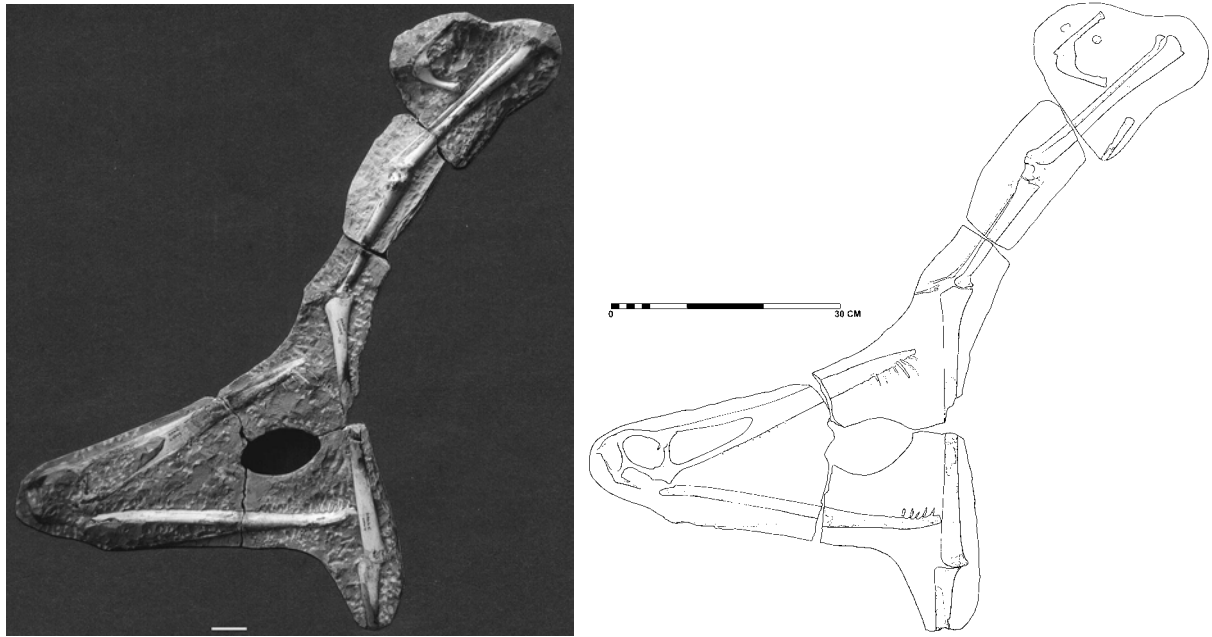


Figure 5.1 (left). *Brasileodactylus sp. indet.* (AMNH 24444), skull and partial left wing,. Scale bar = 50 mm. Photograph by the author and E. Enderburg. Courtesy of AMNH, New York.

Figure 5.2¹ (right). *Brasileodactylus sp. indet.* (AMNH 24444), skull and partial left wing,. Drawing by A.M. Hense.

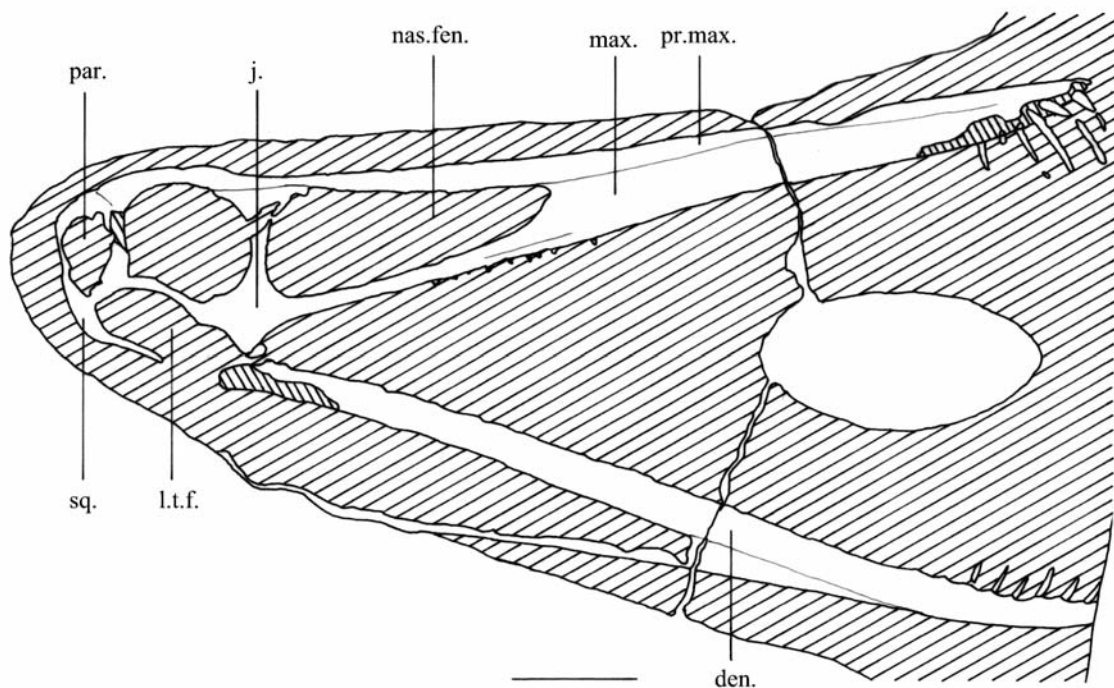


Figure 5.3. *Brasileodactylus sp. indet.* (AMNH 24444), skull and mandible. The skull is seen from right lateral; the mandible from right lateroventral. Scale bar = 50 mm. Drawing by the author.

¹ Note that this figure was not included in the original paper (Veldmeijer, 2003b). Consequently, all figures numbers differ from the original with 1.

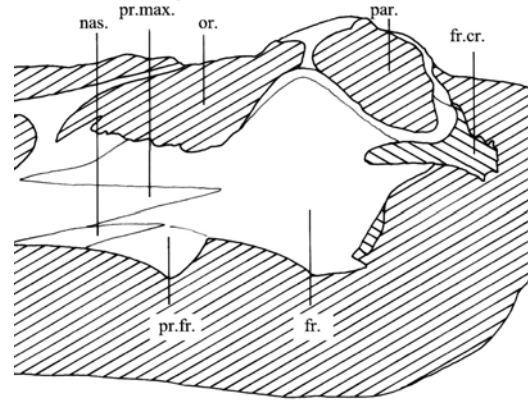
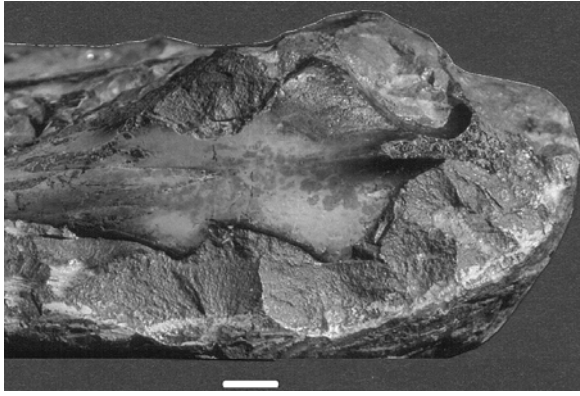


Figure 5.4 (left) and 5.5 (right). *Brasileodactylus sp. indet.* (AMNH 24444), back of skull in dorsal aspect. Scale bar = 50 mm. Photograph by the author and E. Endenburg. Drawing by the author. Courtesy of AMNH, New York.

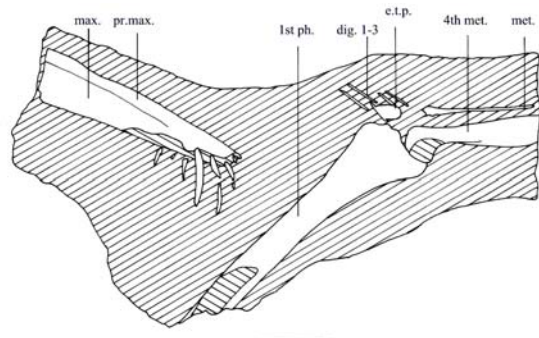
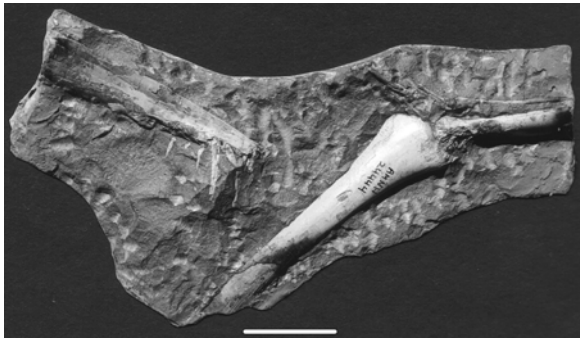


Figure 5.6 (left) and 5.7 (right). *Brasileodactylus sp. indet.* (AMNH 24444), anterior part of the skull (right lateral aspect), proximal part of the first phalanx of the left wing finger, the distal part of the left metacarpal and remnants of the three fingers left. Scale bar = 50 mm. Photograph by the author and E. Endenburg. Drawing by the author. Courtesy of AMNH, New York.

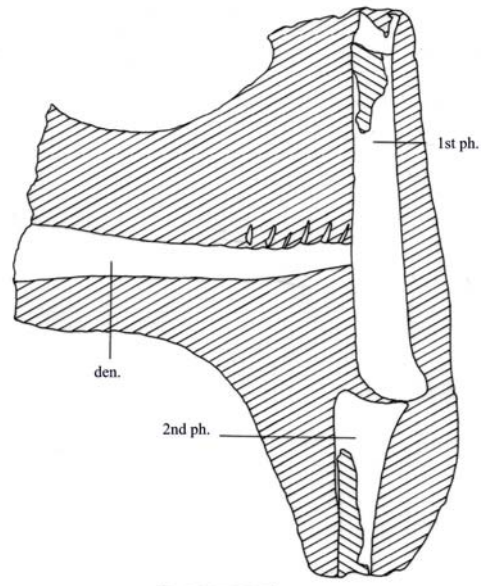
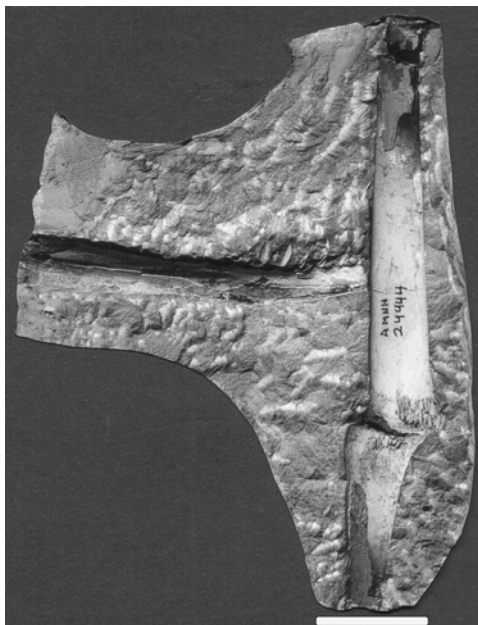


Figure 5.8 (left) and figure 5.9 (right). *Brasileodactylus sp. indet.* (AMNH 24444), anterior part of the mandible (right lateral), distal part of the first phalanx of the left wing finger and distal part of the second phalanx of the left wing finger. Scale bar = 50 mm. Photograph by the author and E. Endenburg. Drawing by the author. Courtesy of AMNH, New York.

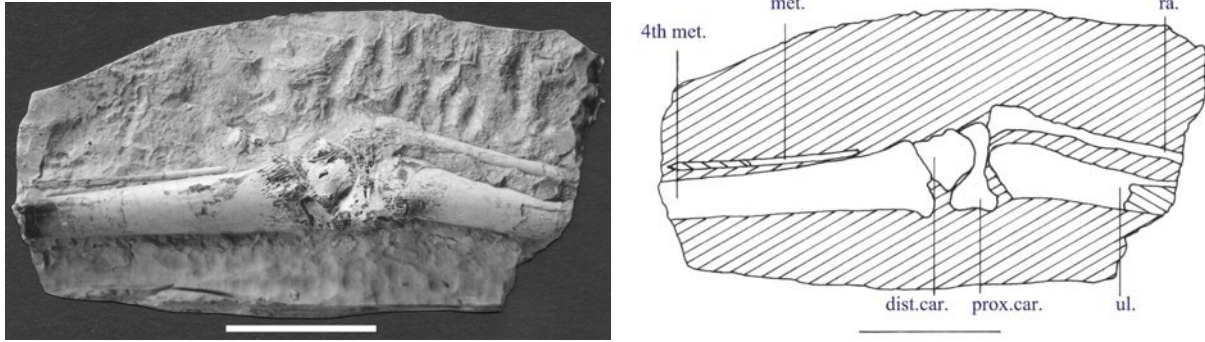


Figure 5.10 (left) and 5.11 (right). *Brasileodactylus* sp. indet. (AMNH 24444), left ulna/radius, carpus and metacarpus. Scale bar = 50 mm. Photograph by the author and E. Enderburg. Drawing by the author. Courtesy of AMNH, New York.

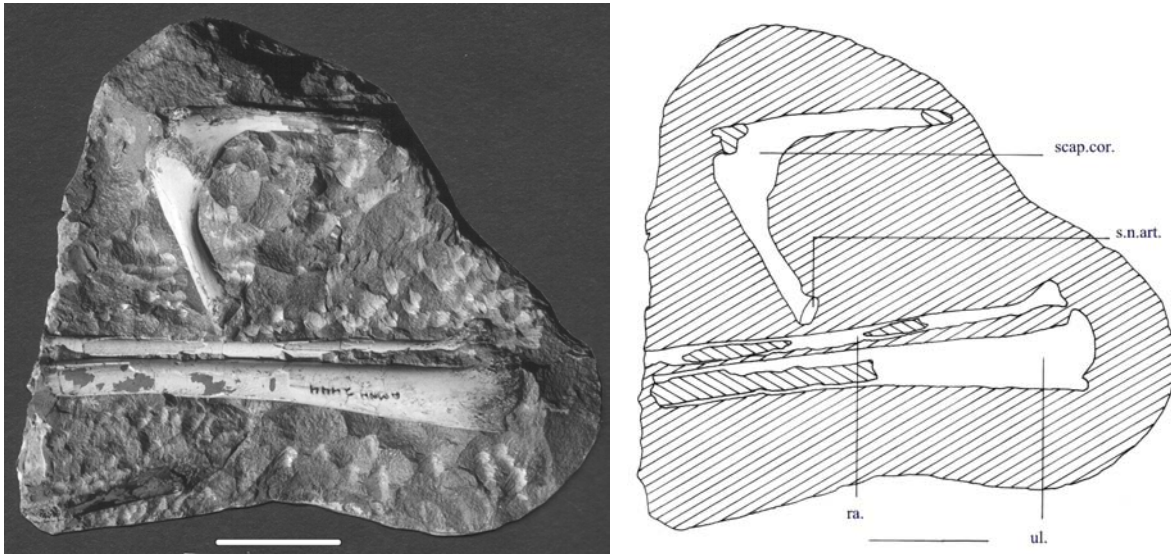


Figure 5.12 (left) and 5.13 (right). *Brasileodactylus* sp. indet. (AMNH 24444), left scapulocoracoid and distal parts of the ulna/radius. Scale bar = 50 mm. Photograph by the author and E. Enderburg. Drawing by the author. Courtesy of AMNH, New York.

**Appendix chapter 6: Description of pterosaurian
(Pterodactyloidea) remains from the Lower
Cretaceous of Brazil in various German collections**

6.6. Appendix

6.6.1. Measurements

Length, as preserved	252
Length symphysis–anterior aspect	174
Width at symphysis	20*
Width at third and sixth alveolus respectively	15*/12*
Thickness ramus	5*
Height at third/ninth alveolus respectively	11.7/19.7

Table 6.1. *B. araripensis* (SMNS 55414), measurements of mandible in mm.

Alveoli		Diastemae	
Number	Diameter	Number	Size
1	2.6*	1–2	1.3*
2	6.6	2–3	3.1
3	5.4	3–4	5.7
4	5.4	4–5	6.0
5	4.2	5–6	5.4
6	4.4	6–7	7.6
7	4.4	7–8	9.0
8	4.8	8–9	11.2
9	4.2	9–10	13.8
10	4.8	10–11	15.2*
11	2.7*		

Table 6.2. *B. araripensis* (SMNS 55414), measurements of dentition of mandible in mm. *: approximate

Length, as preserved	140
Width at anterior and posterior end respectively	21/19
Width between alveoli 3–4	20
Width between alveoli 6–7	16
Height at anterior and posterior end respectively	20*/31

Table 6.3. *Brasileodactylus sp. indet.* (BSP 1991 I 27), measurements of cranium in mm *: approximate.

Alveoli			Diastemae		
Number	Diameter left	Diameter right	Number	Size left	Size right
4	7.5*	–	4–5	3.5	–
5	5.3	5.1	5–6	6.6	6.1
6	4.1	4.5	6–7	6.0	6.5
7	5.5	5.8	7–8	8.1	7.5
8	6.9	7.5	8–9	11.4	12.6
9	7.5	6.3	9–10	15.5	16.1
10	6.5	5.9*	10–11	17.8	21.3
11	6.1	5.6			

Table 6.4. *Brasileodactylus sp. indet.* (BSP 1991 I 27), measurements of dentition of cranium in mm. *: approximate

	sixth	seventh	eighth	ninth
Length centra	47	40	25	20
Length over zygapophyses	58	50*	37	–
Width over postzygapophyses	42*	28*	21	–
Width over prezygapophyses	49	42*	33	28

Table 6.5. *Brasileodactylus sp. indet.* (BSP 1991 I 27), measurements of cervical vertebra in mm. *: approximate.

	first	second	third	fourth	fifth	sixth	seventh	eighth	ninth	tenth
Length centra	19	17	17	19	17	16	15	14	13	–
Height	41*	36	34	30*	34	31*	32	32	32*	–
Width over transverse processes	51*	36*	36*	36	40	38	29*	32*	34	30*
Width over postzygapophyses	13	11	12	13	13	12	12	12	12	13*
Width over prezygapophysis	18	14	11	12	14	13	12	13	13	13
Length neural spine	–	17*	16	24*	14*	10*	10	11*	12*	8*
Thickness neural spine (dorsalmost)	5*	4*	6	10*	5	4*	2	3	2	3*

Table 6.6. *Brasileodactylus sp. indet.* (BSP 1991 I 27), measurements of dorsal vertebra in mm. *: approximate. Remark: right transverse process of the third dorsal is complete.

ninth cervical rib, left	Length, as preserved, without bending	74
	Width over articular facets	23
first dorsal rib, right	Length, without bending	109
	Length, with bending	115
	Width over articular facets	28

Table 6.7. *Brasileodactylus sp. indet.* (BSP 1991 I 27), measurements ribs in mm.

Scapula	Length, without bending	94
	Width head	25
	Height head	17
Coracoid	Length, without bending	125
	Width head	18
	Height head	17
Scapulocoracoid	Length articulated scapulocoracoid, distal	244

Table 6.8. *Brasileodactylus sp. indet.* (BSP 1991 I 27), measurements of scapula and coracoid in mm.

Length, as preserved	95
Width head	43
Height head	29
Maximum height deltopectoral crest	60
Distance distal edge crest–head	80
Diameter shaft	25 x 27

Table 6.9. *Brasileodactylus sp. indet.* (BSP 1991 I 27), measurements of right humerus in mm.

first phalanx wing finger	Length, as preserved	130
	Width head	47
	Height head, as preserved	21
	Diameter shaft	18 x 27
second phalanx wing finger	Length, as preserved	212
	Width head	47
	Height head	22
	Diameter shaft	19 x 12

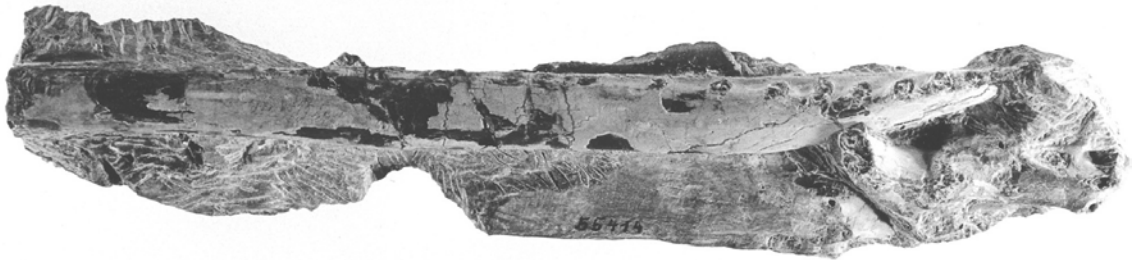
Table 6.10. *Brasileodactylus sp. indet.* (BSP 1991 I 27), measurements of first and second phanges of right wing finger in mm.

Length	52
Width, ventral	31

Table 6.11. *Brasileodactylus sp. indet.* (BSP 1991 I 27), measurements left pubis in mm.

6.6.2. Figures and plates

A



B



C

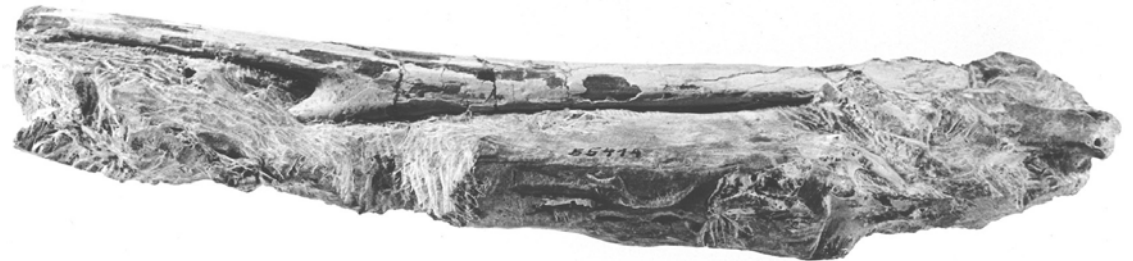


Figure 6.1. *B. araripensis* (SMNS 55414), mandible in various aspects. A: right lateral; B: dorsal; C: ventral. Photographs by R. Harling, SMN Stuttgart.

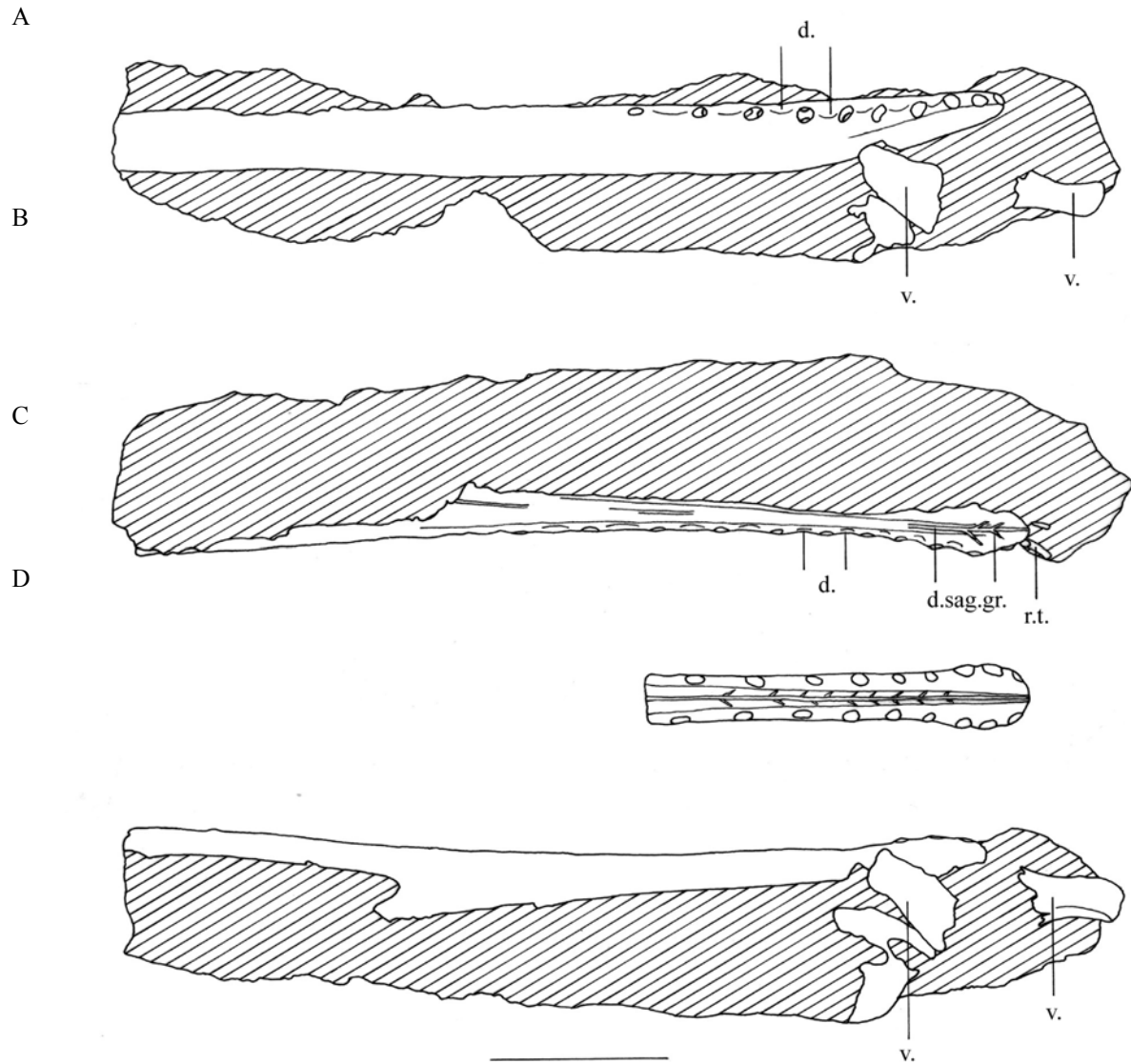


Figure 6.2. *B. araripensis* (SMNS 55414) mandible in various aspects and *B. araripensis* (holotype MN 4804-V), A: right lateral; B: dorsal; C: holotype (MN 4804-V) in dorsal aspect (redrawn after Kellner, 1984); D: ventral. Scale bar = 50 mm. Drawings by the author.

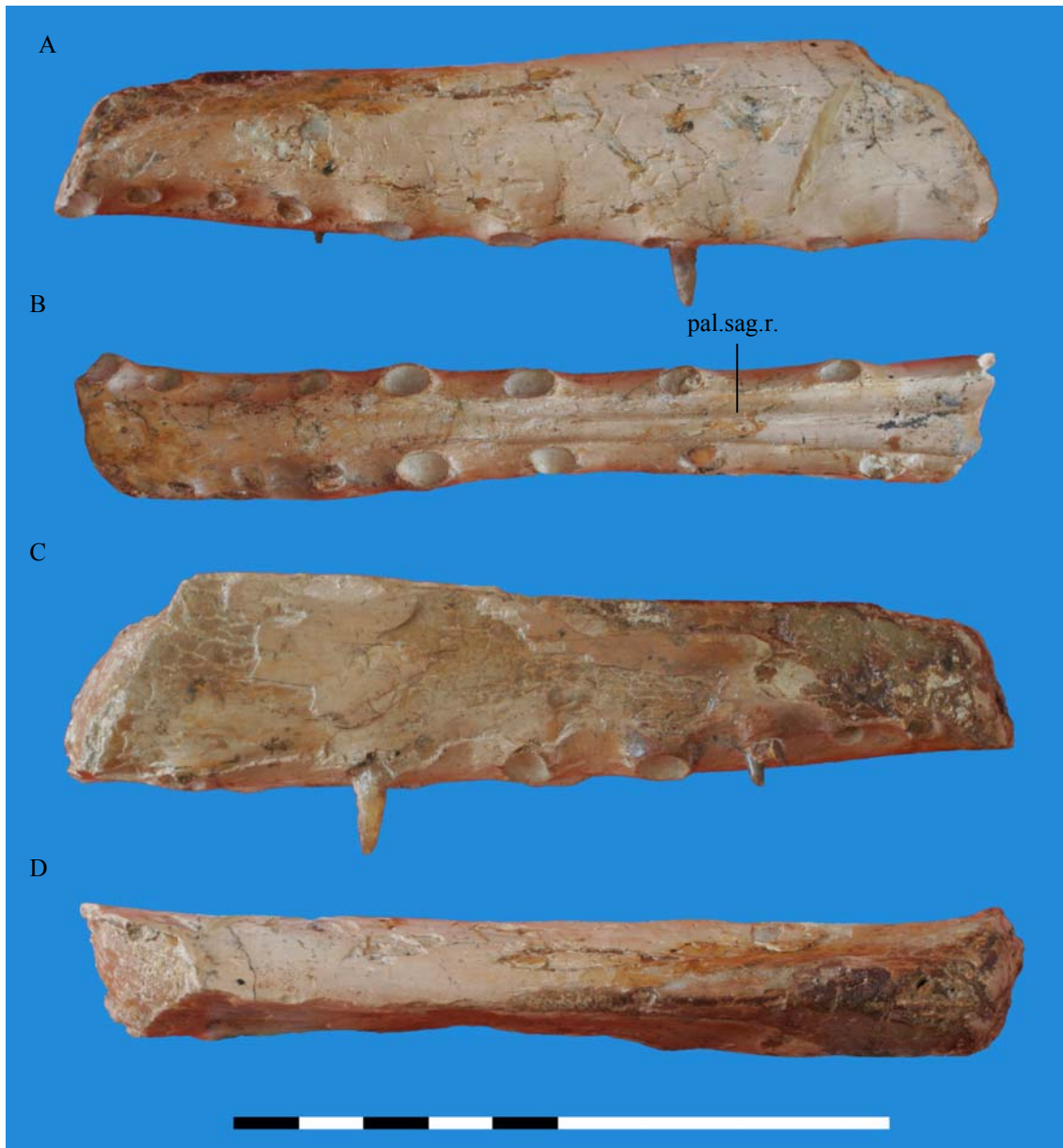


Figure 6.3. *Brasileodactylus* sp. indet. (BSP 1991 I 27), mandible in various aspects. A: left lateral; B: ventral; C: right lateral; D: dorsal. Scale bar = 10 cm. Photographs by A. 't Hooft. Courtesy of BSP, Munich.

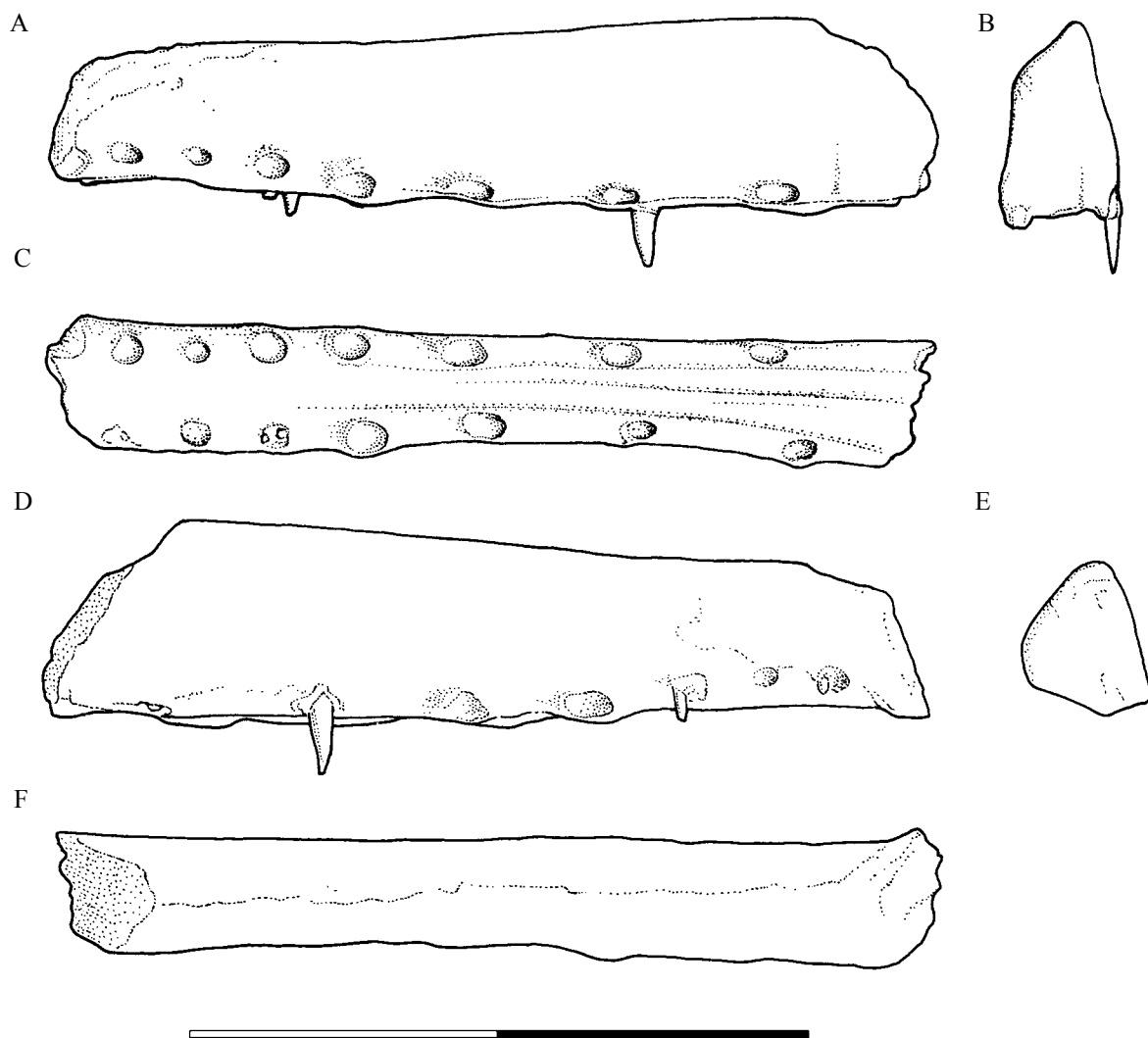


Figure 6.4. *Brasileodactylus* sp. indet. (BSP 1991 I 27), mandible in various aspects. A: left lateral; B: cross-section, posterior; C: ventral; D: right lateral; E: cross-section, anterior; F: dorsal. Scale bar = 10 cm. Drawings by A.M. Hense.

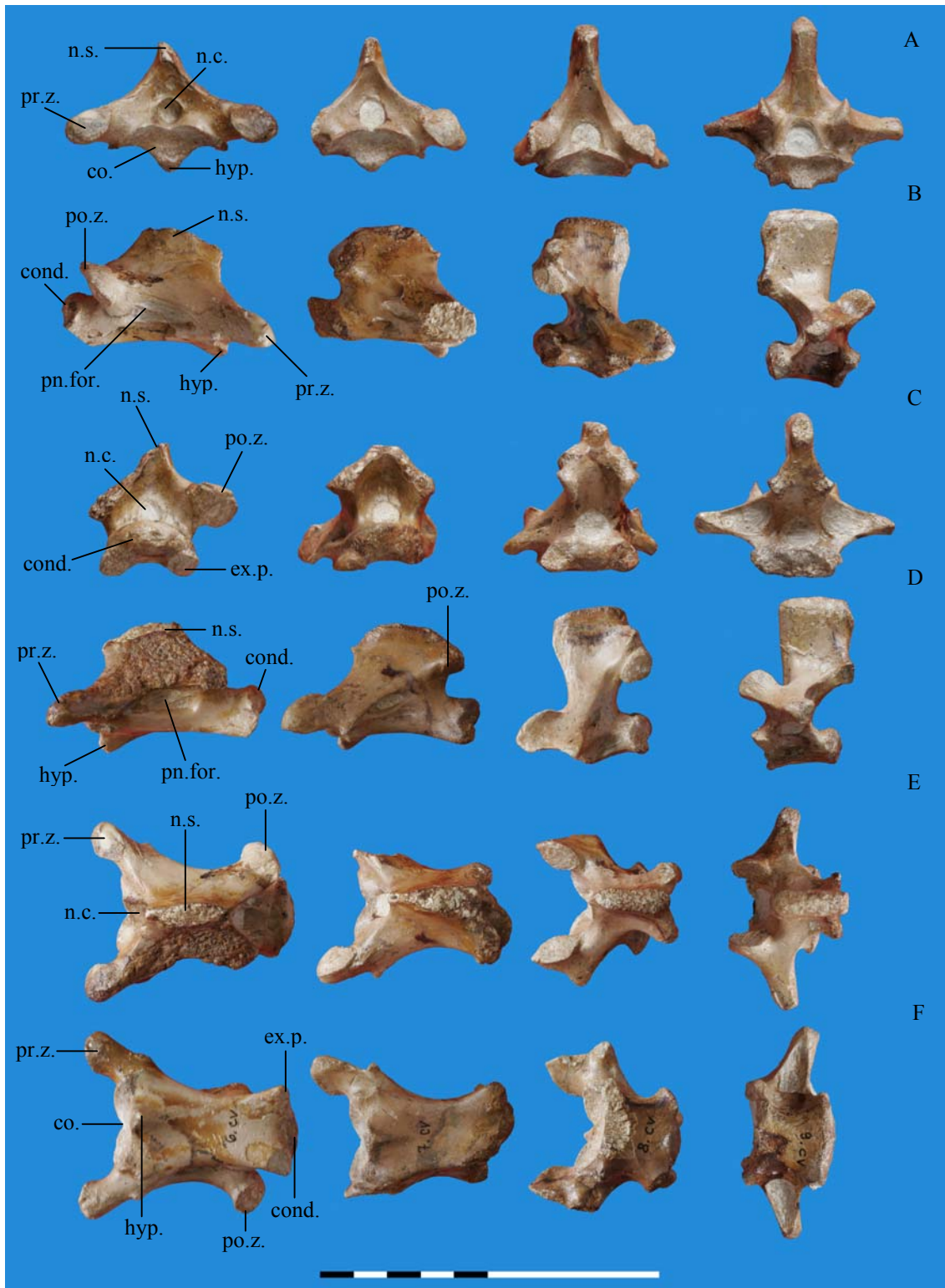


Figure 6.5. *Brasileodactylus* sp. indet. (BSP 1991 I 27), from left to right, sixth to ninth cervical vertebrae in various aspects. A: anterior; B: right lateral; C: posterior; D: left lateral; E: dorsal; F: ventral. Scale bar = 10 cm. Photographs by A. 't Hoof. Courtesy of BSP, Munich.

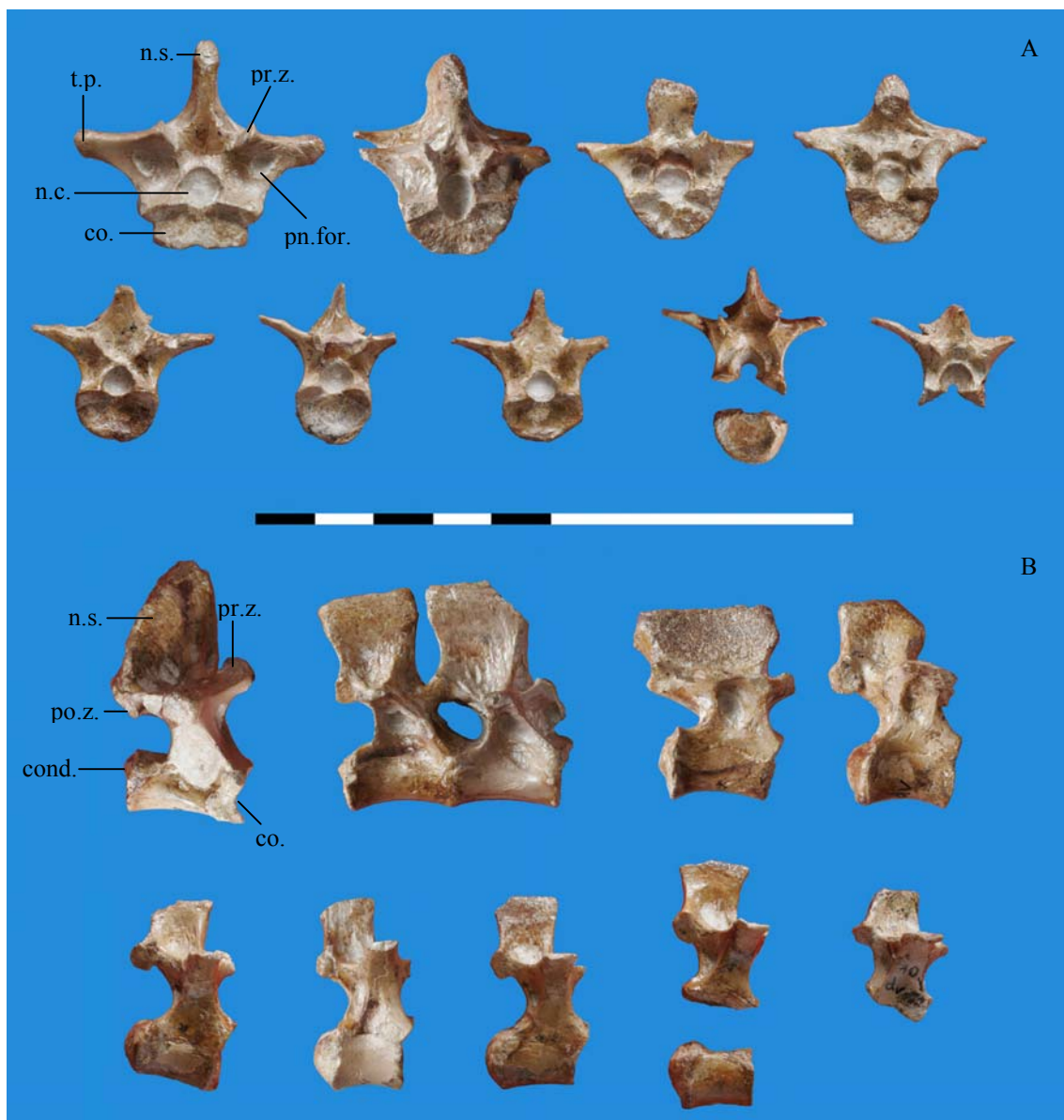


Figure 6.6. *Brasileodactylus* sp. indet. (BSP 1991 I 27), from left to right, first to tenth dorsal vertebrae in A: anterior; B: right lateral. Scale bar = 10 cm. Photographs by A. 't Hoofi. Courtesy of BSP, Munich.

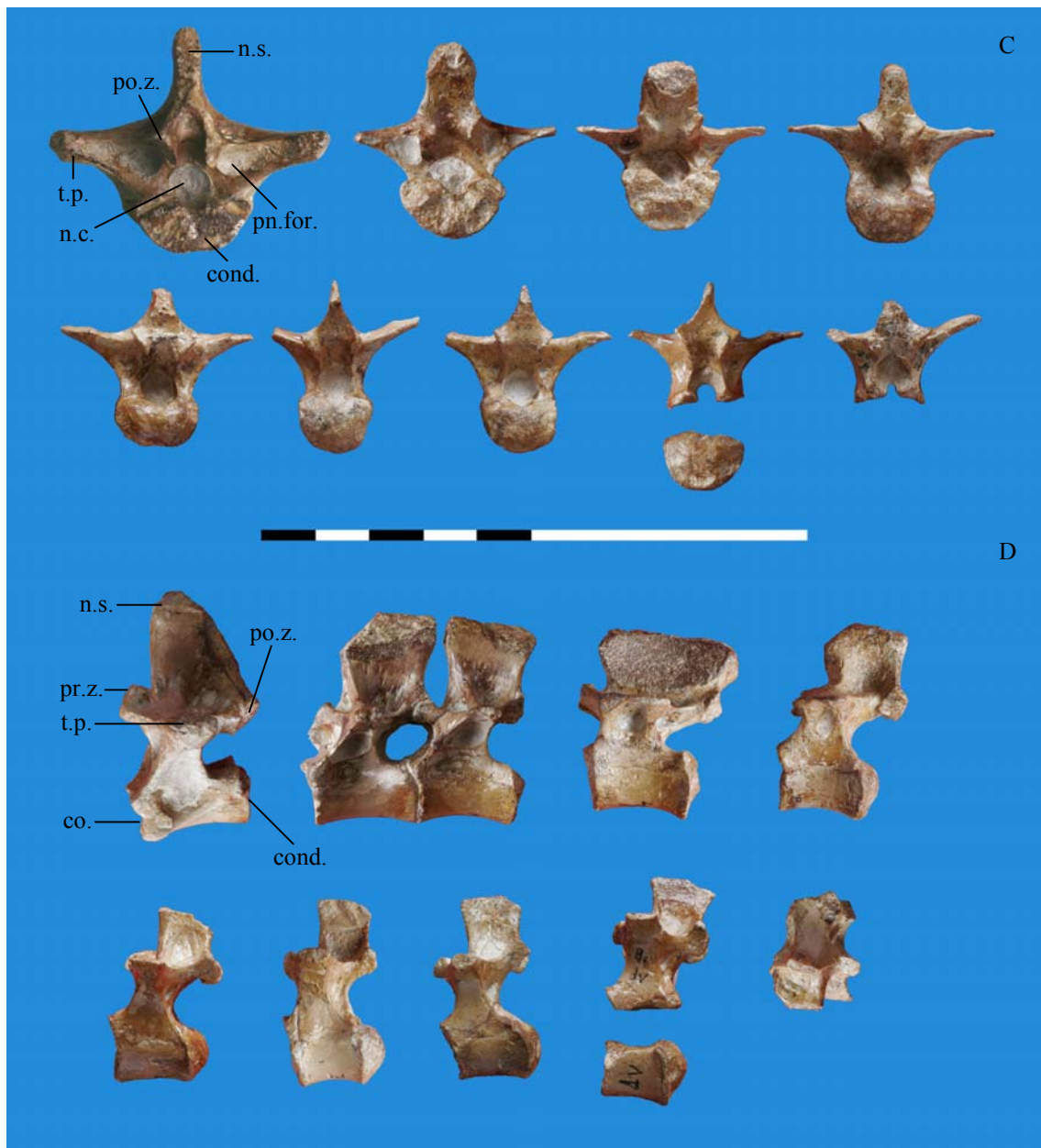


Figure 6.6. *Brasileodactylus* sp. indet. (BSP 1991 I 27), from left to right, first to tenth dorsal vertebrae in C: posterior; D: left lateral. Scale bar = 10 cm. Photographs by A. 't Hoofst. Courtesy of BSP, Munich.

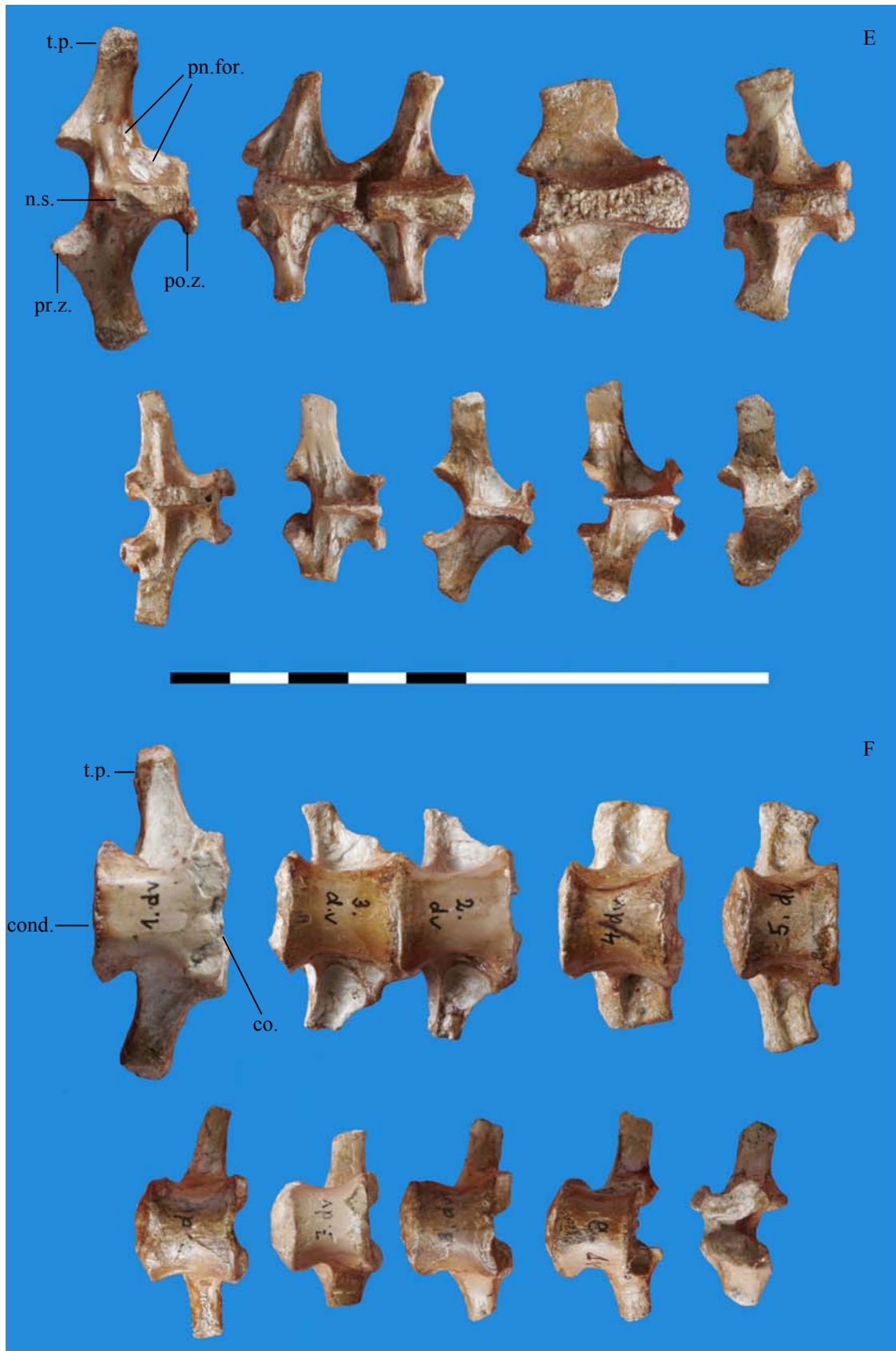


Figure 6.6. *Brasileodactylus* sp. indet. (BSP 1991 I 27), from left to right, first to tenth dorsal vertebrae in E: dorsal; F: ventral. Scale bar = 10 cm. Photographs by A. 't Hooft. Courtesy of BSP, Munich.



Figure 6.7. *Brasileodactylus* sp. indet. (BSP 1991 I 27), ribs in various aspects. A: cervical rib in posterior and anterior aspect; B: right and left dorsal rib in posterior aspect; C: right and left dorsal rib in anterior aspect. Scale bar = 10 cm. Photographs by A. 't Hoof. Courtesy of BSP, Munich.



Figure 6.8. *Brasileodactylus* sp. indet. (BSP 1991 I 27), left and right scapula in various aspects. A: dorsal; B: posterior; C: anterior; D: medial; E: ventral and F: lateral. Scale bar = 10 cm. Photographs by A. 't Hoof. Courtesy of BSP, Munich.



Figure 6.8. *Brasileodactylus* sp. indet. (BSP 1991 I 27), left and right coracoid in various aspects. G: lateral; H: ventral; I: posterior; J: dorsal; K: medial and L: anterior. Scale bar = 10 cm. Photographs by A. 't Hooft. Courtesy of BSP, Munich.

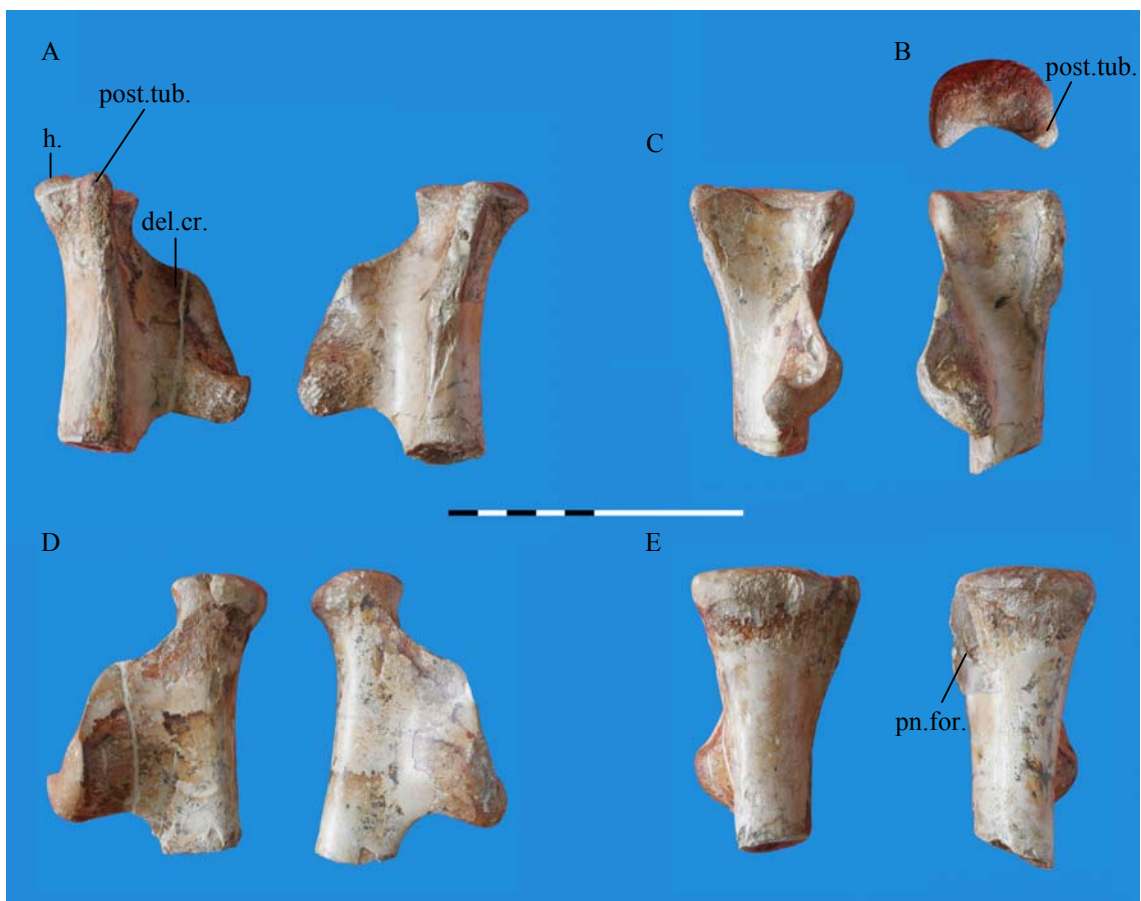


Figure 6.9. *Brasileodactylus sp. indet.* (BSP 1991 I 27), left and right humerus in various aspects. A: posterior; B: proximal; C: ventral; D: anterior and E: dorsal. Scale bar = 10 cm. Photographs by A. 't Hooft. Courtesy of BSP, Munich.



Figure 6.10. *Brasileodactylus* sp. indet. (BSP 1991 I 27), distal part of the first wing finger phalanx right in various aspects. A: dorsal; B: posterior; C: ventral; D: anterior; E: distal. Scale bar = 10 cm. Photographs by A. 't Hoofst. Courtesy of BSP, Munich.

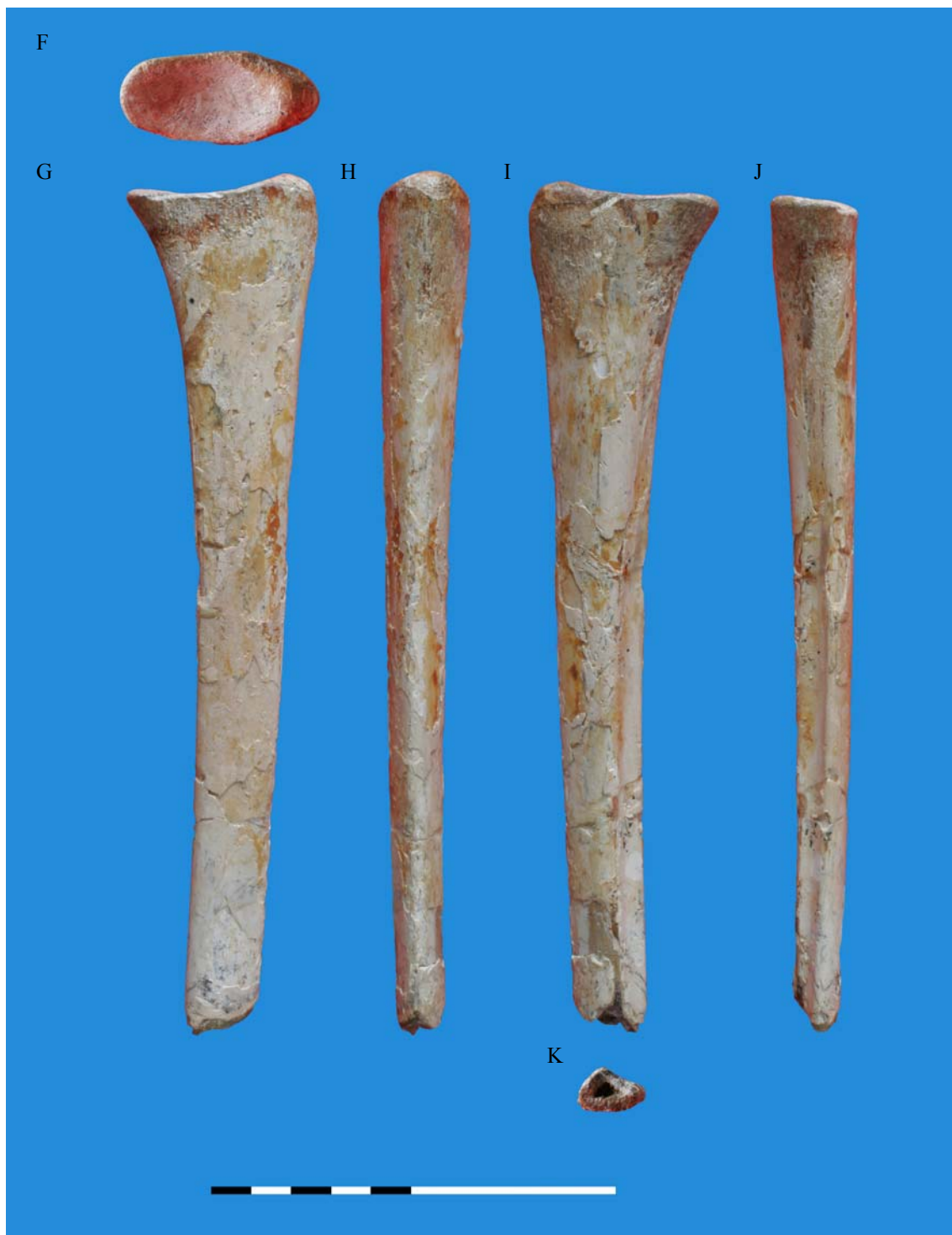


Figure 6.10. *Brasileodactylus* sp. indet. (BSP 1991 I 27), proximal part of the second wing finger phalanx right in various aspects. F: proximal; G: dorsal; H: anterior; I: ventral; J: posterior; K: distal. Scale bar = 10 cm. Photographs by A. 't Hoof. Courtesy of BSP, Munich.

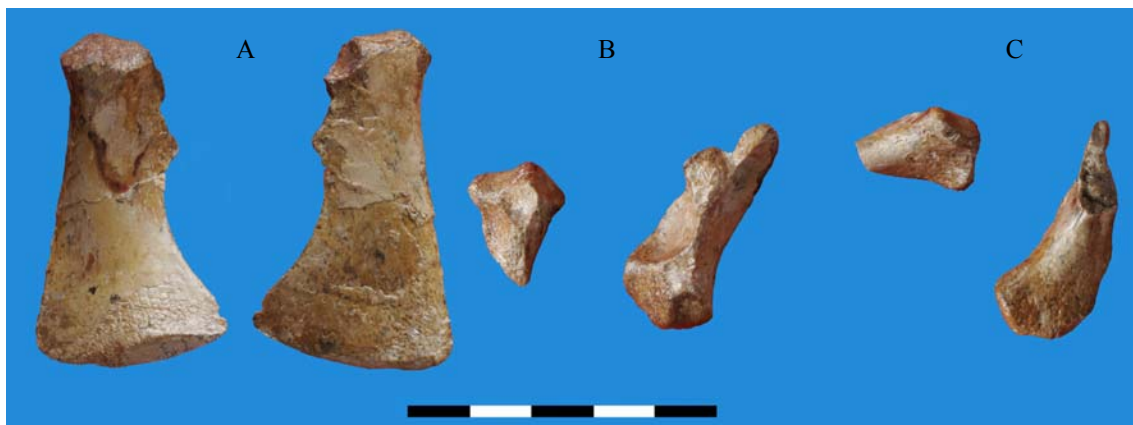


Figure 6.11. *Brasileodactylus* sp. indet. (BSP 1991 I 27), parts of the pelvis. A: left pubis; B and C: parts of the left and right ischium. Scale bar = 5 cm. Photographs by A. 't Hoofst. Courtesy of BSP, Munich.

Appendix chapter 7: Updating the toothed taxa

7.6. Appendix

7.6.1. Figures and plates



Figure 7.1. Type specimen of *Brasileodactylus* and holotype of *B. araripensis* (MN 4804-V). Scale bar = 5 cm. Photograph by E. Eendenburg and the author. Courtesy of MN, Rio de Janeiro.

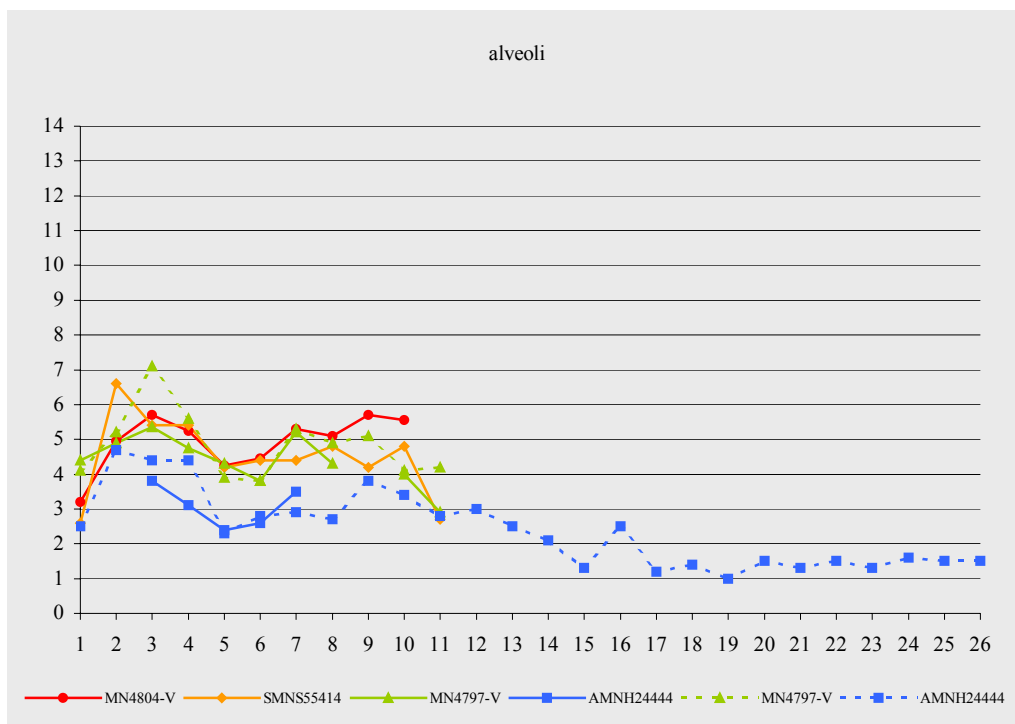


Figure 7.2. The graphs of the dentition (alveolar diameter) of the taxon *Brasileodactylus*. Vertical the diameter in mm; horizontal the number of alveolus, starting anteriorly. The interrupted line refer to the cranial dentition; the straight lines to the mandibular dentition (see appendix 11.1 for isolated graphs).



Figure 7.3. The Crato specimen of *Brasileodactylus* (MN 4797-V). Photograph by E. Endenburg and the author. Courtesy of MN, Rio de Janeiro.

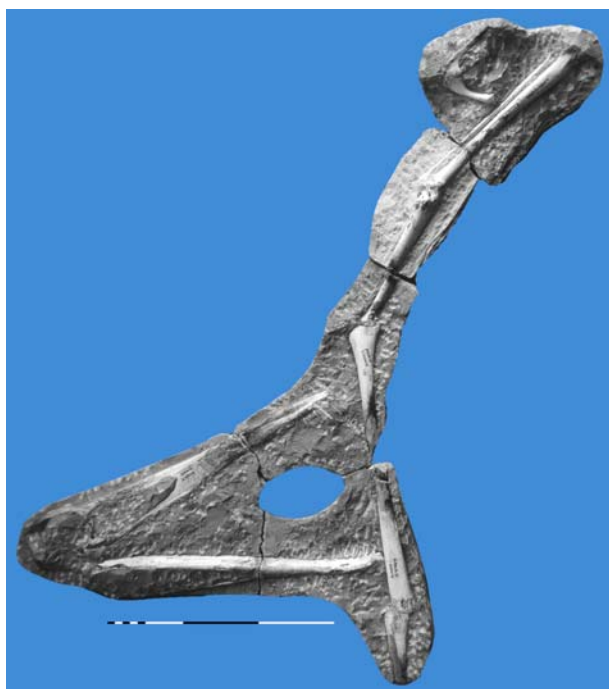


Figure 7.4. The New York specimen (AMNH 2444). Scale bar = 30 cm. Photograph by the author and E. Endenburg. Courtesy of AMNH, New York.



Figure 7.5 The Karslsruhe specimen of *Ludodactylus* (SMNK 3828 PAL). Photograph by the author. The skull has a length of about 60 cm. Courtesy of SMN, Karlsruhe.

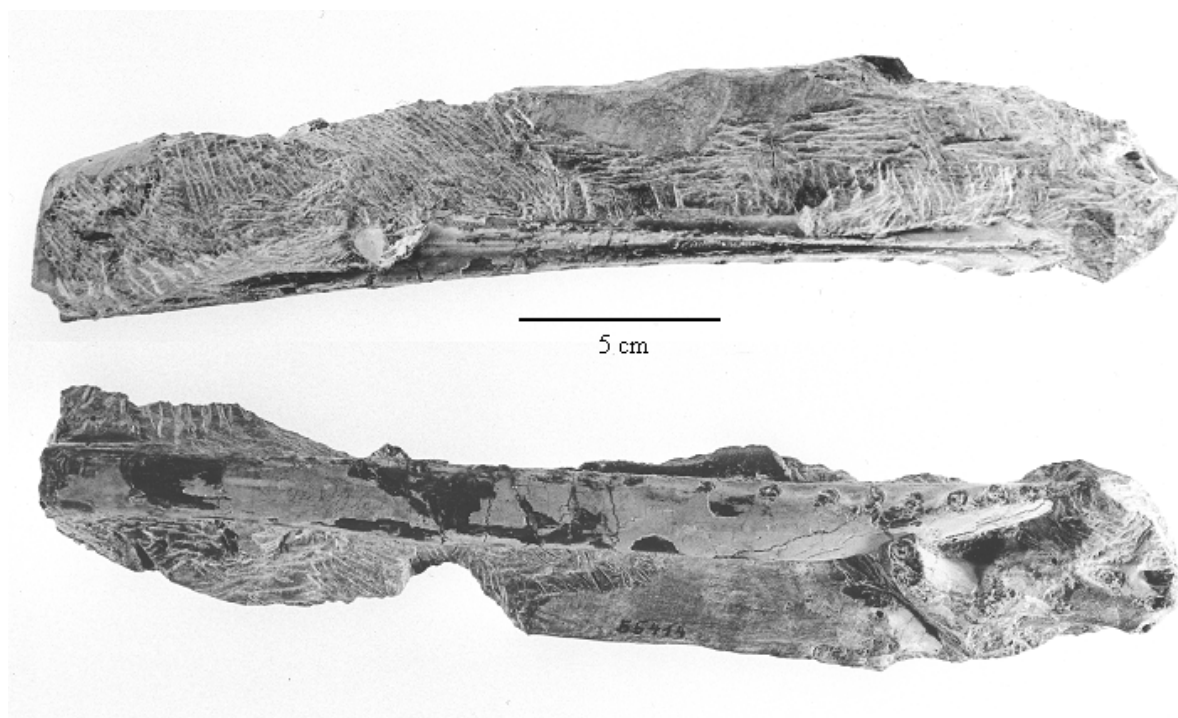


Figure 7.6. Mandible of *B. araripensis* (SMNS 55414) in dorsal and right lateral aspects. Photographs by R. Harling. Courtesy of SMN, Stuttgart.



Figure 7.7. The Munich specimen (BSP 1991 I 27), right later view. Scale bar = 5 cm. Photograph by A. 't Hooft. Courtesy of BSP, Munich.

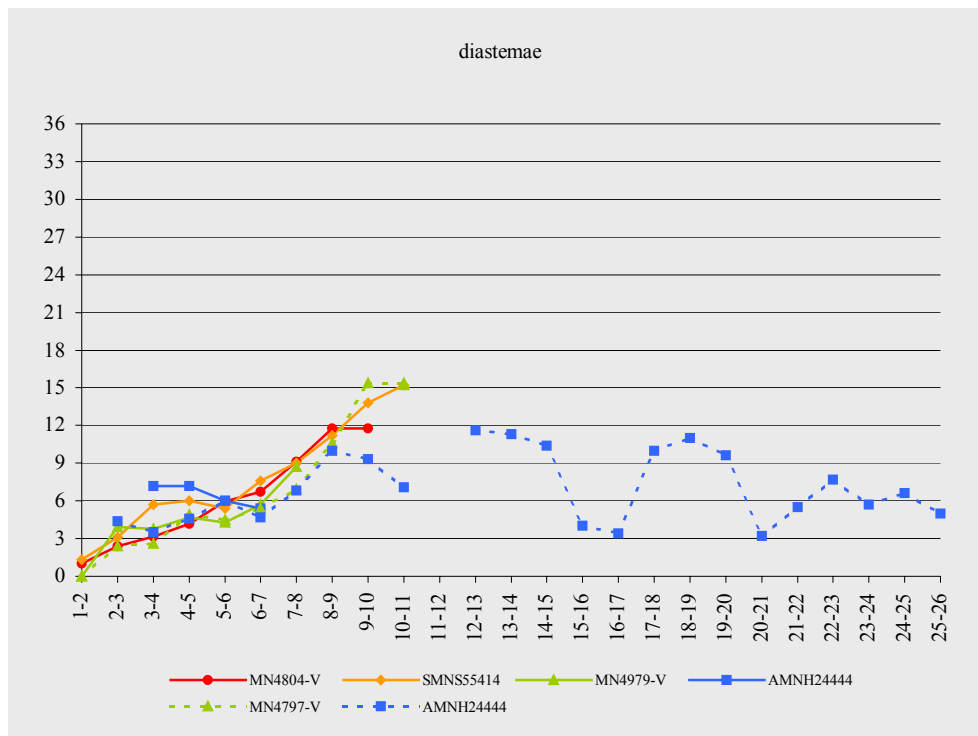


Figure 7.8. The graphs of the dentition (diastemae size) of the taxon *Brasileodactylus*. Vertical the size in mm; horizontal the number of diastema, starting anteriorly. The interrupted line refer to the cranial dentition; the straight lines to the mandibular dentition (see appendix 11.1 for isolated graphs).



Figure 7.9. Type specimen of *Coloborhynchus* and holotype of *Co. clavirostris* (BMNH 1822/BMNH 39409) in anterior, left lateral and ventral views. Photographs produced by the Natural History Museum Photographic Studio.

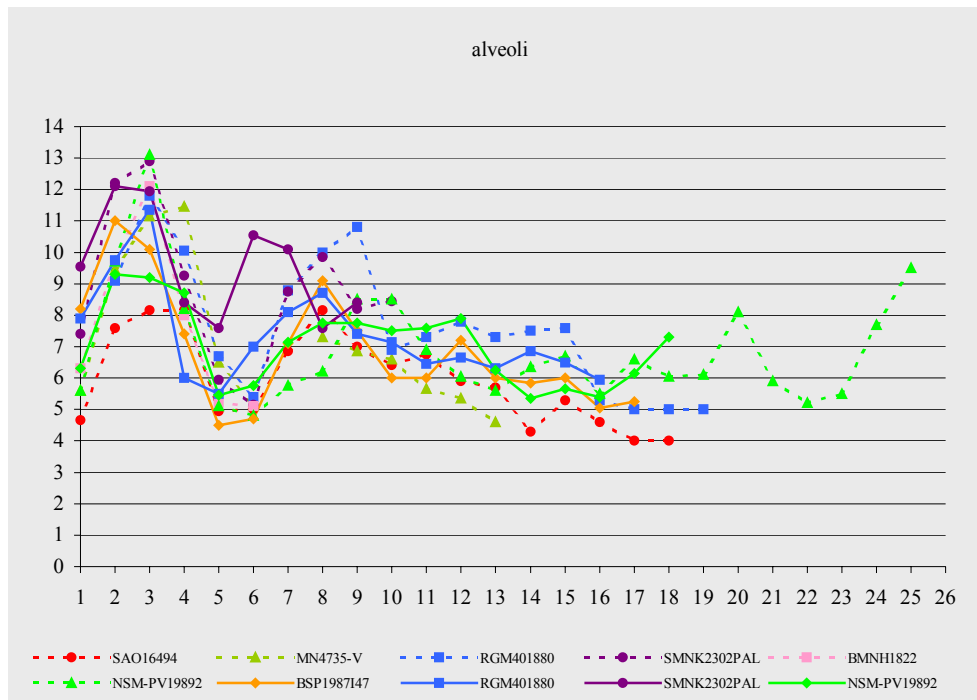


Figure 7.10. The graphs of the dentition (alveolar diameter) of the taxon *Coloborhynchus*. Vertical the diameter in mm; horizontal the number of alveolus, starting anteriorly. The interrupted line refer to the cranial dentition; the straight lines to the mandibular dentition (see appendix 11.1 for isolated graphs).



Figure 7.11. Holotype of *Co. araripensis* (BSP 1982 I 89), right lateral view. Scale bar = 5 cm. Photograph by E. Endenburg and the author. Courtesy of BSP, Munich.

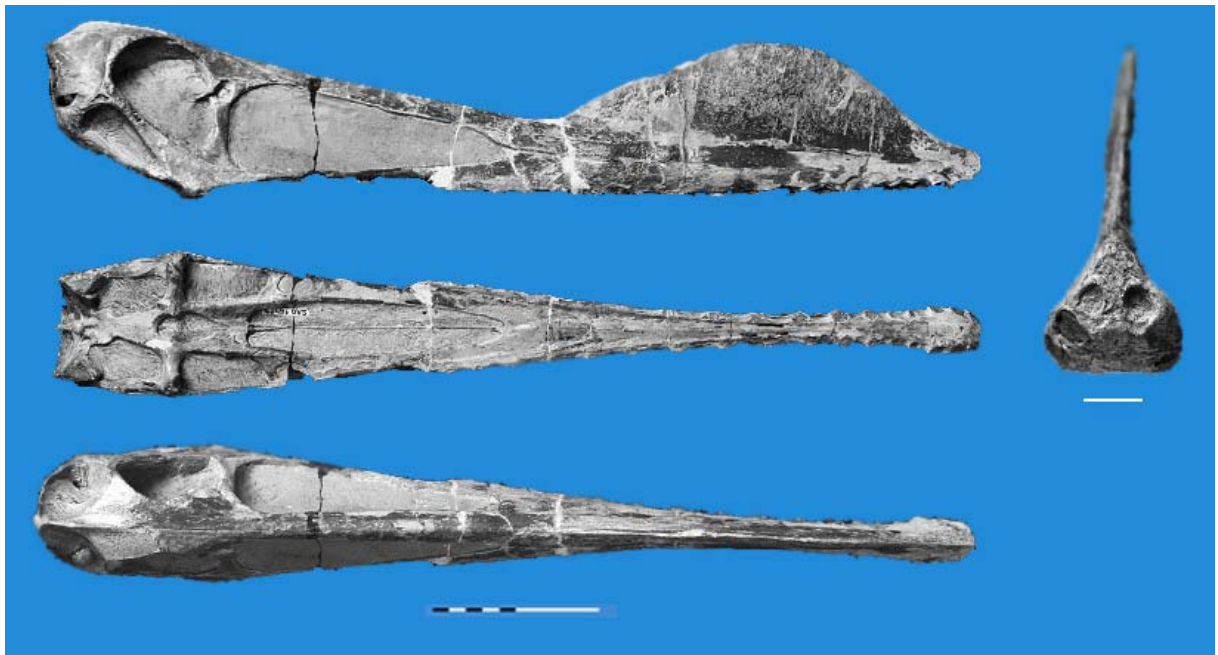


Figure 7.12. The St. Gallen specimen of *Co. araripensis* (SAO 16494). Scale bar = 10 cm (bottom) and 1 cm (right). Photograph by Naturmuseum St. Gallen. Courtesy of U. Oberli, St. Gallen.



Figure 7.13. The holotype of *Co. robustus* (BSP 1987 I 47), mandible in left lateral view. Scale bar = 10 cm. Photograph by E. Endenburg and the author. Courtesy of BSP, Munich.



Figure 7.14. The Karlsruhe specimen of *Co. robustus* (SMNK 2302 PAL). Scale bar = 10 cm. Photograph by the author and E. Endenburg. Courtesy of SMN, Karlsruhe.



Figure 7.15. *Co. piscator* (NSM-PV 19892), skull in right lateral view. Scale bar = 40 cm. Photograph by E. Endenburg and the author. Courtesy of NSM, Tokyo.

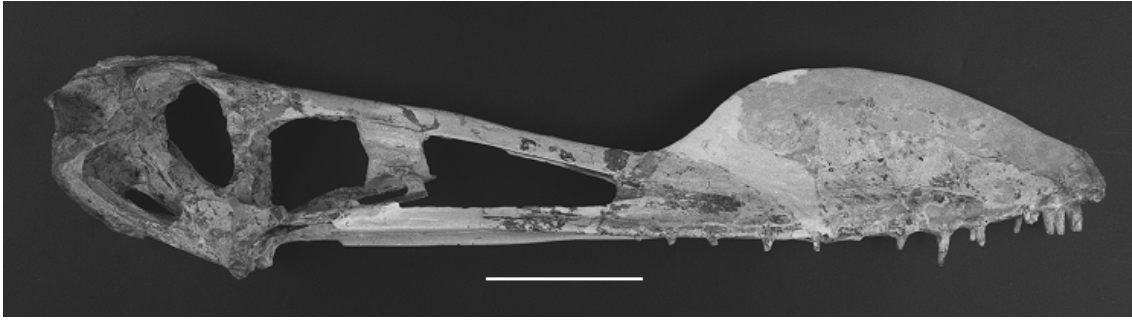


Figure 7.16. *Co. spielbergi* (RGM 401 880), skull in right lateral view. Scale bar = 10 cm. Photograph by A. 'Hooft. Courtesy of Naturalis, Leiden.

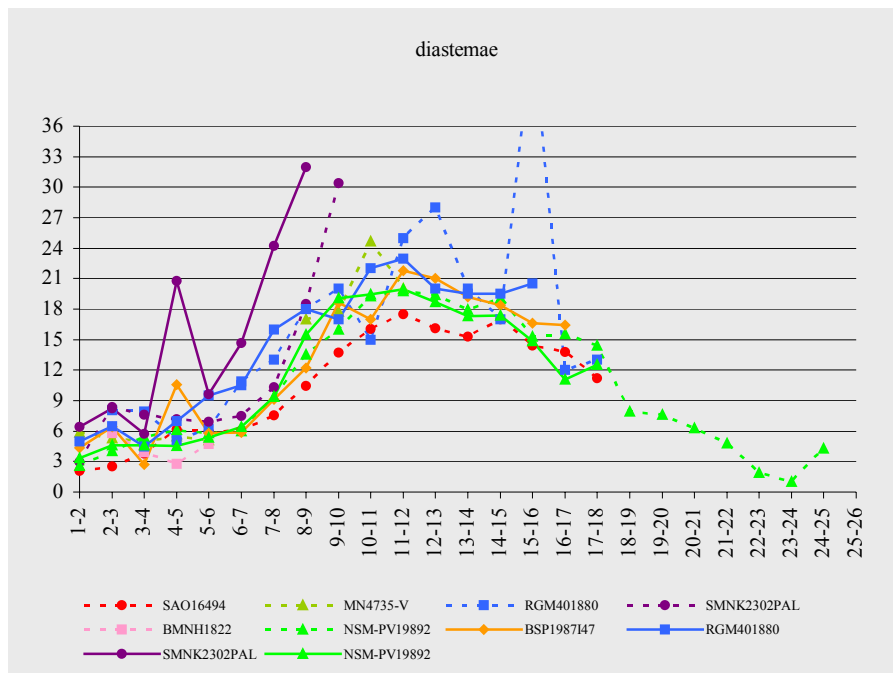


Figure 7.17. The graphs of the dentition (diastemae size) of the taxon *Coloborhynchus*. Vertical the size in mm; horizontal the number of diastema, starting anteriorly. The interrupted line refer to the cranial dentition; the straight lines to the mandibular dentition (see appendix 11.1 for isolated graphs).



Figure 7.18. Cranium of type specimen of *Anhanguera* and holotype of *An. blittersdorffi* (MN 4805-V). Scale bar = 40 cm. Photograph by E. Endenburg and the author. Courtesy of MN, Rio de Janeiro.

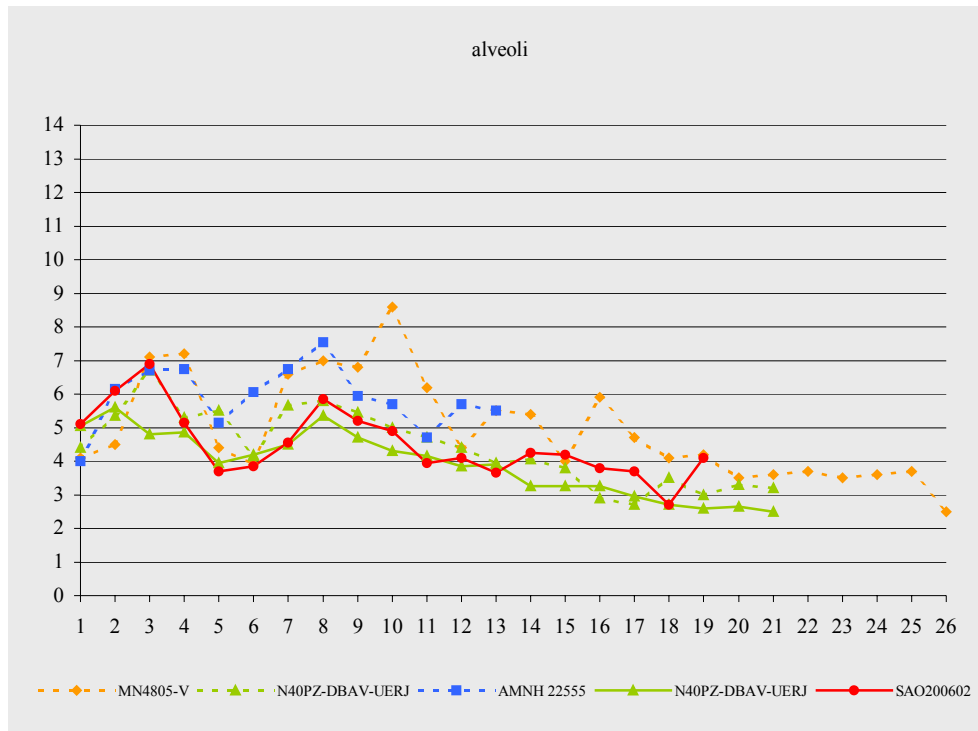


Figure 7.19. The graphs of the dentition (alveolar diameter) of the taxon *Anhanguera*. Vertical the diameter in mm; horizontal the number of alveolus, starting anteriorly. The interrupted line refer to the cranial dentition; the straight lines to the mandibular dentition (see appendix 11.1 for isolated graphs).



Figure 7.20. Cranium of the holotype of *An. santanae* (BSP 1982 I 90), left lateral view. Scale bar = 5 cm. Photograph by E. Enderburg and the author. Courtesy of BSP, Munich.



Figure 7.21. Left lateral view of the mandible of *Anhanguera sp. indet.* (SAO 200602). Photograph by E. Endenburg and the author. Courtesy of U. Oberli, St. Gallen.

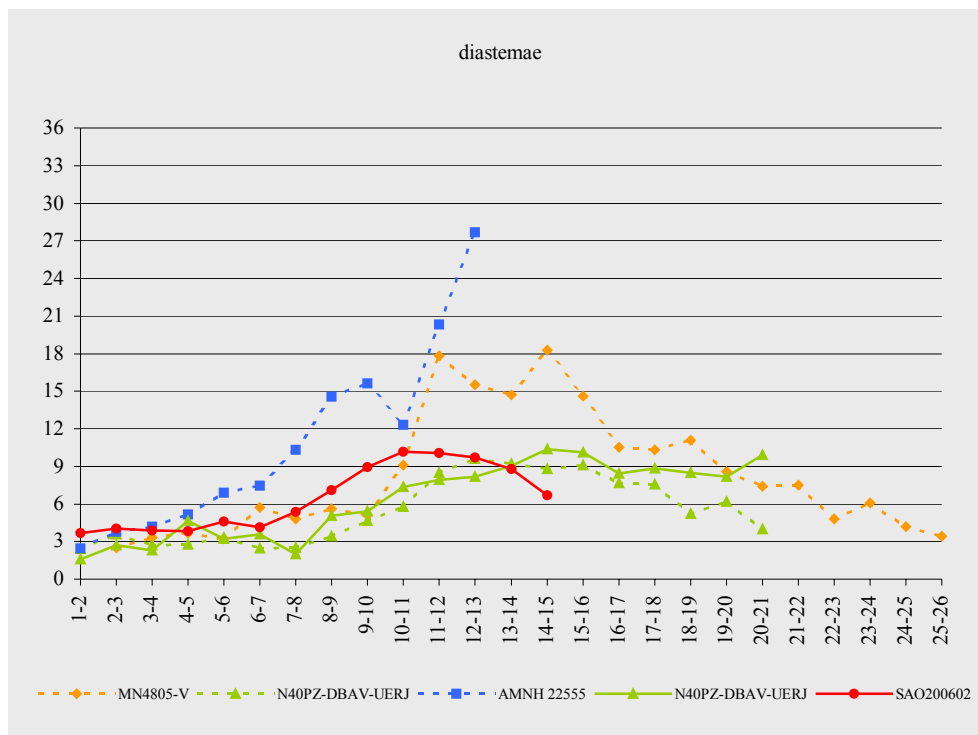


Figure 7.22. The graphs of the dentition (diastemae size) of the taxon *Anhanguera*. Vertical the size in mm; horizontal the number of diastema, starting anteriorly. The interrupted line refer to the cranial dentition; the straight lines to the mandibular dentition (see appendix 11.1 for isolated graphs).



Figure 7.23. Type specimen of *Criorhynchus* and holotype of *Cr. simus* (CAMSM B.54428), anterior, left lateral and ventral view of the anterior part of the cranium. Scale bar = 5 cm. Photograph by E. Endenburg and the author. Courtesy of SM, Cambridge.



Figure 7.24. Holotype of *Cr. mesembrinus* (BSP 1987 I 46), cranium and mandible in left lateral view. Scale bar = 10 cm. Photograph by E. Endenburg and the author. Courtesy of BSP, Munich.

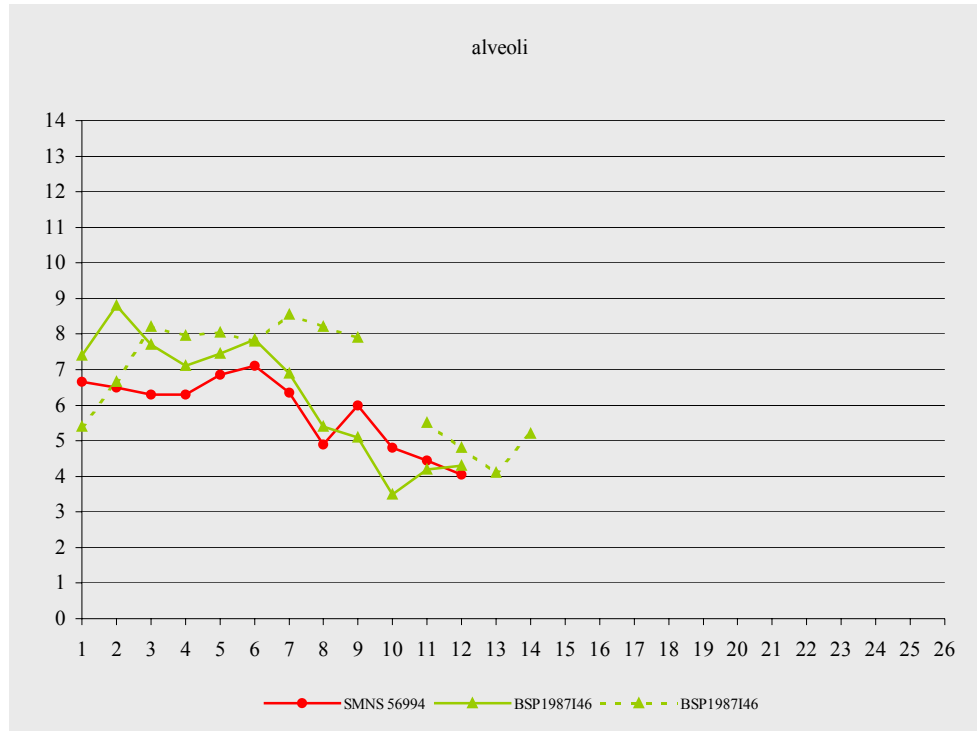


Figure 7.25. The graphs of the dentition (alveolar diameter) of the taxon *Criorhynchus*. Vertical the diameter in mm; horizontal the number of alveolus, starting anteriorly. The interrupted line refer to the cranial dentition; the straight lines to the mandibular dentition (see appendix 11.1 for isolated graphs).



Figure 7.26. Right lateral view of the mandible of cf. *Cr. mesembrinus* (SMNS 56994). Scale bar = 10 cm. Photograph by E. Endenburg and the author. Courtesy of SMN, Stuttgart.

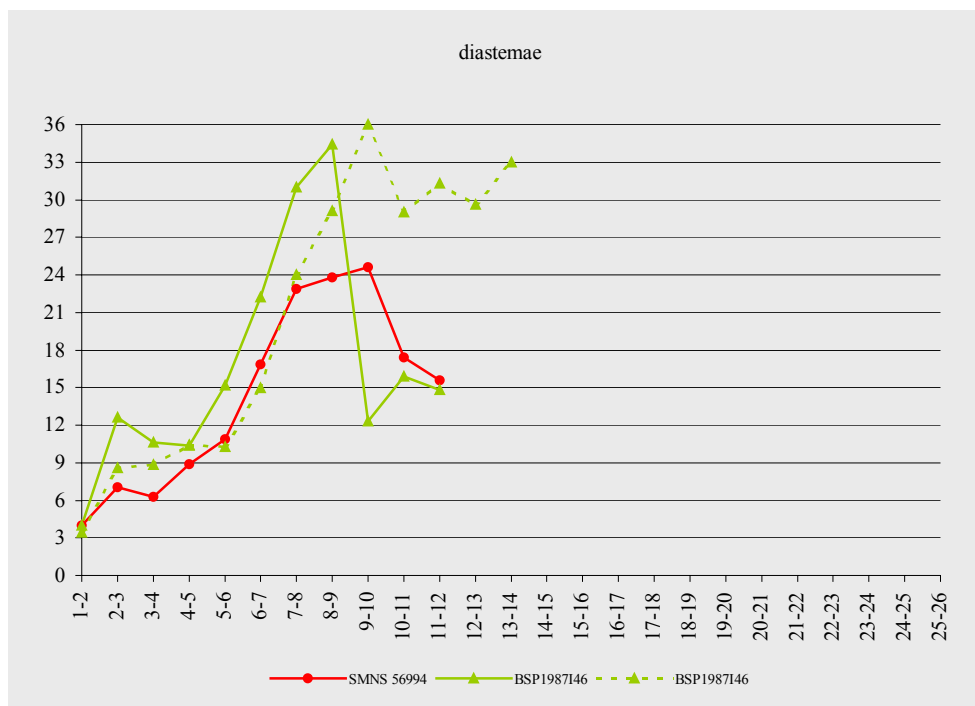


Figure 7.27. The graphs of the dentition (diastemae size) of the taxon *Criorhynchus*. Vertical the size in mm; horizontal the number of diastema, starting anteriorly. The interrupted line refer to the cranial dentition; the straight lines to the mandibular dentition (see appendix 11.1 for isolated graphs).

Appendix chapter 8: Final remarks

8.3. Appendix

8.3.1. Figures and plates



Figure 8.1. Type specimen of *Ornithocheirus* and holotype of *O. compressirostris* (BMNH 39410), photographed in the same way as illustrated in Owen (1851). Photographs produced by the Natural History Museum Photographic Studio.

